Synthetic and Biocatalytic Methods for the Chemoenzymatic Production of Novel Cryptophycin Anticancer Agents

by

Kyle Lawrence Bolduc

A dissertation submitted in partial fulfillment
of the requirements for the degree of
Doctor of Philosophy
(Medicinal Chemistry)
in the University of Michigan
2013

Doctoral Committee:

Research Professor Scott D. Larsen, Co-Chair
Professor David H. Sherman, Co-Chair
Professor John Montgomery
Professor Shaomeng Wang

DEDICATION

This dissertation is dedicated to my wife, Karoline. She has been my source of strength, my confidant, my harshest critic, my most ardent supporter, and my source of inspiration. Without her constant encouragement and unwavering faith in me the following accomplishments would never have been possible. I shall always treasure our past, delight in the present, and warmly anticipate our future together.

ACKNOWLEDGEMENTS

Many people have had a hand in helping me achieve this occasion. Not the least of which are my advisors, David and Scott. I sincerely appreciate all of the advice, guidance, criticism, and freedom you gave me. I have become a much stronger and mature independent scientist as a direct result of your mentorship. I hope that we may have many more opportunities to work together on pioneering scientific endeavors in the future. I also want to thank my committee members Dr. John Montgomery, Dr. Shaomeng Wang, Dr. Hollis Showalter, and Dr. Sylvie Garneau-Tsodikova for their direction and support.

The Department of Medicinal Chemistry provided many years of support for me and served as a home away from home during my studies. Mr. Fred W. Lyons is thanked for his generous support through a research fellowship. Finally, Rackham Graduate School kindly awarded me travel and research grants, as well as carefully steered me through the twin minefields of matriculation and graduation.

I owe my colleagues in the Sherman and Larsen labs a debt of gratitude for creating a wonderful atmosphere in which to learn and discover, particularly my rotation mentor Dr. Yousong Ding, whose help and knowledge were truly a giant's shoulders on which to stand.

TABLE OF CONTENTS

LIST OF TABLES

LIST OF FIGURES

LIST OF SCHEMES

List of Abbreviations

5-ALA	5-aminolevulinic acid
ABPP	activity based protein profiling
ACP	acyl carrier protein
AUC	area under curve
BAIB	bis(acetoxy)iodobenzene
Boc	di-tert-butyl dicarbonate
BSA	bovine serum albumin
CM	cross metathesis
DBA	dibenzylideneacetone
DBU	1,8-diazabicyclo[5.4.0]undec-7-ene
DDQ	2,3-dichloro-5,6-dicyano-1,4-benzoquinone
DIBAL-H	diisobutylaluminium hydride
DIPEA	*N,N*-diisopropylethylamine
DMAP	4-dimethylaminopyridine
DME	1,2-dimethoxyethane
DMF	*N,N*-dimethylformamide
DMSO	dimethyl sulfoxide
EDC	1-ethyl-3-(3-dimethylaminopropyl)carbodiimide
FAD	flavin adenine dinucleotide
FAS	fatty acid synthase
HOBt	1-hydroxybenzotriazole
HWE	Horner-Wadsworth-Emmons
IPTG	isopropyl β-D-1-thiogalactopyranoside
LDA	lithium diisopropylamide
MBP	maltose binding protein
MC	methylcellulose
MCD	methyl β-cyclodextrin
MTPA	α-methoxy-α-trifluoromethylphenylacetic acid
MudPIT	multidimensional protein identification technology
NADH	nicotinamide adenine dinucleotide
NADPH	nicotinamide adenine dinucleotide phosphate
NBS	*N*-bromosuccinimide
NMO	*N*-methylmorpholine *N*-oxide
NRPS	non-ribosomal peptide synthestase
OD	optical density
PCP	peptidyl carrier protein
PKS	polyketide synthase
PMB	*para*-methoxybenzyl
PPTS	pyridinium *p*-toluenesulfonate
QTOF	quantitative time-of-flight
SAR	structure activity relationship

SNAc	N-acetylcysteamine
SPE	solid phase extraction
ST	sulfotransferase
TB	terrific broth
TBAF	tetra-butylammonium fluoride
TBS	*tert*-butyldimethylsilyl
TE	thioesterase
TEMPO	(2,2,6,6-tetramethylpiperidin-1-yl)oxy
TFA	trifluoroacetic acid
THF	tetrahydrofuran
TMG	tetramethylguanidine
TPAP	tetrapropylammonium perruthenate

ABSTRACT

Synthetic and Biocatalytic Methods for the Chemoenzymatic Production of Novel Cryptophycin Anticancer Agents

by

Kyle Lawrence Bolduc

Co-chairs: David H. Sherman and Scott D. Larsen

The cryptophycin family of cyanobacterial peptolides contains exceptionally potent antimitotic anticancer agents. Active at levels significantly lower than currently approved cancer therapies, synthetic cryptophycin 52 was also effective against multi-drug resistant cancers. Phase II clinical trials revealed minor peripheral neurotoxicity, however, making synthetic derivatization a priority for the development of safe, effective cryptophycins for the treatment of cancer. Specifically, incorporation of heterocycles on unit A of cryptophycin was proposed to increase the solubility and stability, as well as reduce toxicity of the parent drugs. To this end, an efficient and divergent synthetic route to unit A analogues was developed and optimized for the production of a diverse library of heterocyclic functionality. Incorporation with units B, C, and D yielded fully elaborated, SNAc-thioester bound *seco*-cryptophycins as substrates for macrocyclization. Cryptophycin thioesterase (CrpTE) activity was reconstituted *in vitro* and used to demonstrate impressive inherent flexibility for a suite of heterocyclic substrates. CrpTE was then optimized for activity and displayed little preference for reaction temperature, buffer pH, or DMSO concentration.

Incredibly, CrpTE was active at up to 50% DMSO and in a variety of organic solvents. In fact, a novel cosolvent system of 20% diglyme with 1% MCD more than doubled CrpTE conversion with a natural substrate mimic and proved to be an effective strategy for the chemoenzymatic cyclization of the 2-pyridyl derivatized cryptophycin 500. Joined with the complementary heterocyclic substrate flexibility of cryptophycin epoxidase (CrpE), a powerful method now exists to produce unique cryptophycins in a campaign to access better anticancer agents. This chemoenzymatic method should also provide a means to construct affinity probes for mechanism of action studies and interrogation of CrpTE and CrpE active site architecture.

CHAPTER I
Introduction

1.1 Cancer Chemotherapy and Antimitotic Agents

In November 1947, Dr. Sidney Farber quietly ushered in the age of cancer chemotherapy. Leading up to his discovery, Dr. Farber was a pediatric pathologist at Harvard and Children's Medical Center, where he saw many samples from children with what was then terminal cancer.[1] His studies on these samples revealed that folic acid stimulated leukemic cell growth and enhanced disease progression, and he therefore reasoned that folic acid antagonists would inhibit the proliferation of these cancer cells.[2] Coincident with these observations, researchers at Lederle Laboratories synthesized a series of folate metabolism inhibitors (antifols) and demonstrated that they inhibited the growth of normal cells.[3] Farber took notice and requested a small amount of 4 antifols (pteroylaspartic acid, pteroyl diglutamic acid, pteroyl triglutamic acid and 4-aminopteroyl glutamic acid (aminopterin)), which were administered to 16 children with acute undifferentiated leukemia. The resulting temporary remissions, with clinical, hematological, and pathological improvement in 10 children, many of whom were terminal at the time therapy was initiated, represented the first successful clinical use of cancer chemotherapy.[4]

Much has changed in the battle against cancer over the past 65 years, and anticancer drugs now cover dozens of mechanisms of action. However, drugs that interfere with microtubule dynamics have been a particularly successful class. Microtubules (MTs) are cytoskeletal polymers

essential for cellular structure, division, and transport. MTs are nucleated and

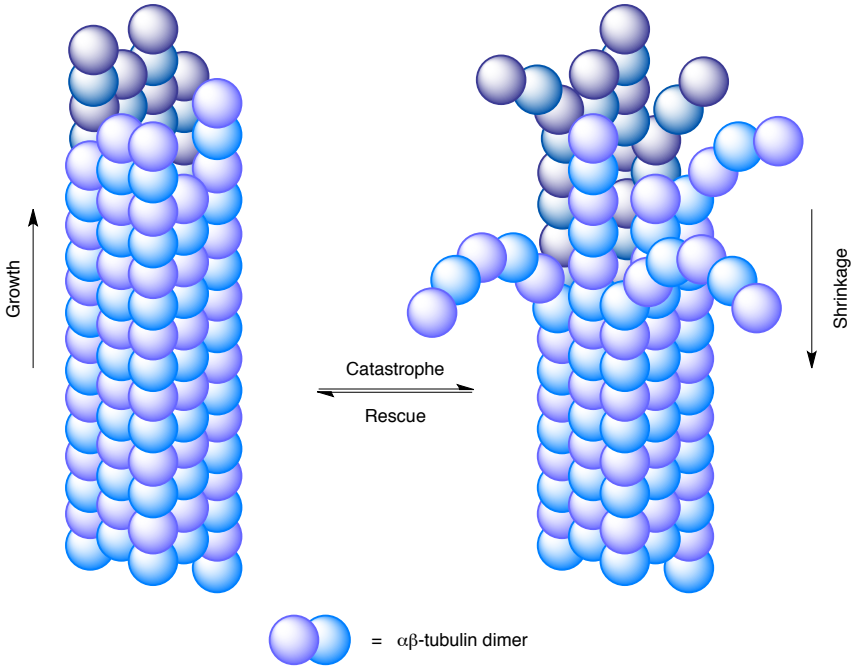

Figure 1.1: Diagram of microtubule dynamics illustrating growth and shrinkage of the polymer.

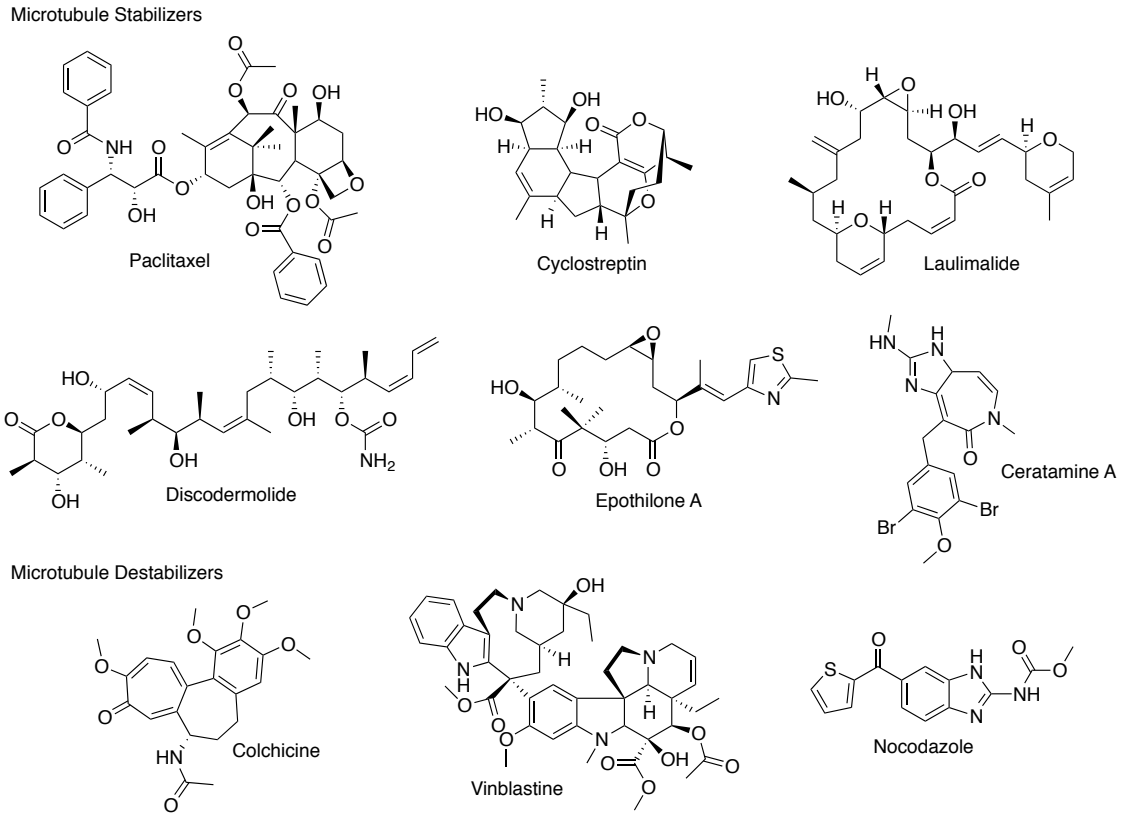

Figure 1.2: Structures of microtubule-stabilizing and destabilizing agents.

organized in microtubule organizing centers (MTOCs), such as the centrosome or the basal bodies in cilia and flagella. Contained within the MTOC is γ-tubulin, which, together with associated scaffold proteins, forms the γ-tubulin ring complex.[5] This complex acts as a scaffold for α/β-tubulin dimers to begin polymerization. MTs are also involved in cell division through the formation of mitotic spindles, which separate chromatids or genomic DNA during cell division. In addition, there are many proteins that bind to MTs, including motor proteins such as kinesin and dynein, and other proteins regulating microtubule dynamics.[6] Their dynamic instability can be described by the parameters of growth, shrinkage, and rates of catastrophe and rescue (Figure 1.1),[7,8] which are controlled by the interaction of α- and β-tubulin dimers and fueled by the hydrolysis of GTP.[9,10] MT-targeting drugs interrupt this polymer flexibility and cause affected cells to arrest at the G_2/M phase of mitosis and undergo apoptosis.[11]

Drugs that interact with MTs are structurally diverse (Figure 1.2), but can be classified into two main groups: stabilizing agents, which promote polymerization and stabilize the MT polymer, and destabilizing agents, which promote depolymerization and prevent rescue. The majority of these compounds are natural products or synthetic derivatives of natural products,

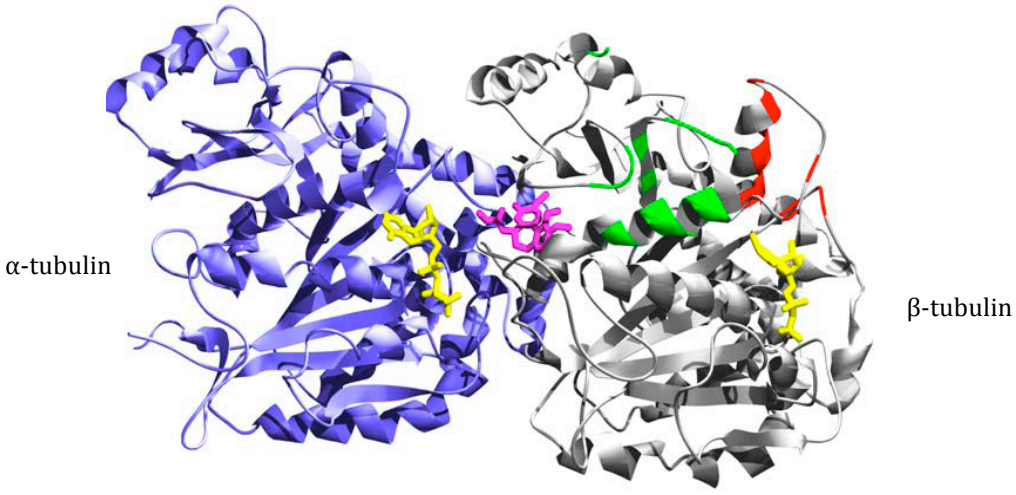

Figure 1.2: Model of the tubulin heterodimer (α in purple and β in gray) in complex with colchicine (purple) and GTP/GDP (yellow). The taxoid site is indicated in green and the "peptide" binding site in red. PDB ID: 1SA0.[12]

and most likely evolved as broad-spectrum toxins to eukaryotic predators. MT stabilizers bind to either one of the tubulin subunits (Figure 1.3) in one of two well-known binding sites: the taxoid site or the not yet fully characterized LAU site named for laulimalide.[11] Both of these sites are located externally on the β-tubulin subunit and are typically occupied in a 1:1 stoichiometry of one drug molecule per one heterodimer. MT destabilizers also have binding sites on the exterior of the heterodimer with a preference for the β-tubulin subunit. The *vinca* alkaloids are the most recognized of the destabilizers, and bind on the surface of β-tubulin overlapping the "peptide" binding site near the interface of two heterodimers.[13] Interestingly, destabilizers have been indicated to bind to microtubules in a far larger ratio of heterodimers to drug molecules. Included in the MT-stabilizer category is another class of anticancer natural products, the cryptophycins, which are the topic of this dissertation and will be discussed in detail in the next section.

1.2 The Cryptophycins

The cryptophycins and the closely related arenastatins are a family of lichen-derived cyanobacterial peptolides and are biosynthetically assembled in *Nostoc* sp. ATCC 53789 and GSV 224.[14,15] Cryptophycin 1 (Figure 1.4) is the major representative of the family containing dozens of naturally occurring analogues and is constructed from four subunits: phenyl-octenoic acid (unit A), 3-chloro-*O*-methyl-$_D$-tyrosine (unit B), methyl β-alanine (unit C), and L-leucic acid (unit D).[16] The *crp* gene cluster elucidated in the Sherman laboratory is an unusual mosaic polyketide synthase (PKS)/non-ribosomal peptide synthetase (NRPS) assembly (Figure 1.5) that has shown flexibility in using unnatural starter units to produce novel cryptophycins. Another interesting variation in the cryptophycin biosynthetic pathway is the formation of a 16-membered macrocyclic ring instead of the more common 14-membered, suggesting an unusually large thioesterase active site.

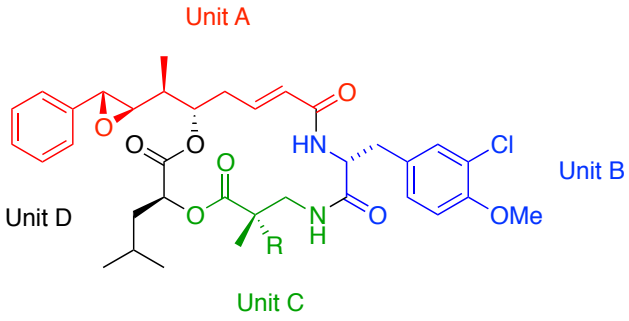

1, R = H, Cryptophycin 1
2, R = CH_3, Cryptophycin 52

Figure 1.3: Cryptophycins 1 and 52 with units A, B, C, and D highlighted.

Two key transformations in the biological assembly of the cryptophycins are the closure of the macrocyclic peptolide ring and the installation of the C2′-C3′ β-epoxide. The full-length chain intermediate is cyclized and released from the biosynthetic machinery by the terminal serine hydrolase-like cryptophycin thioesterase (CrpTE).[17] As part of the post-PKS/NRPS tailoring, the epoxide is installed regio- and stereospecifically by the cytochrome P450 cryptophycin epoxidase (CrpE).[18] Both enzymes were

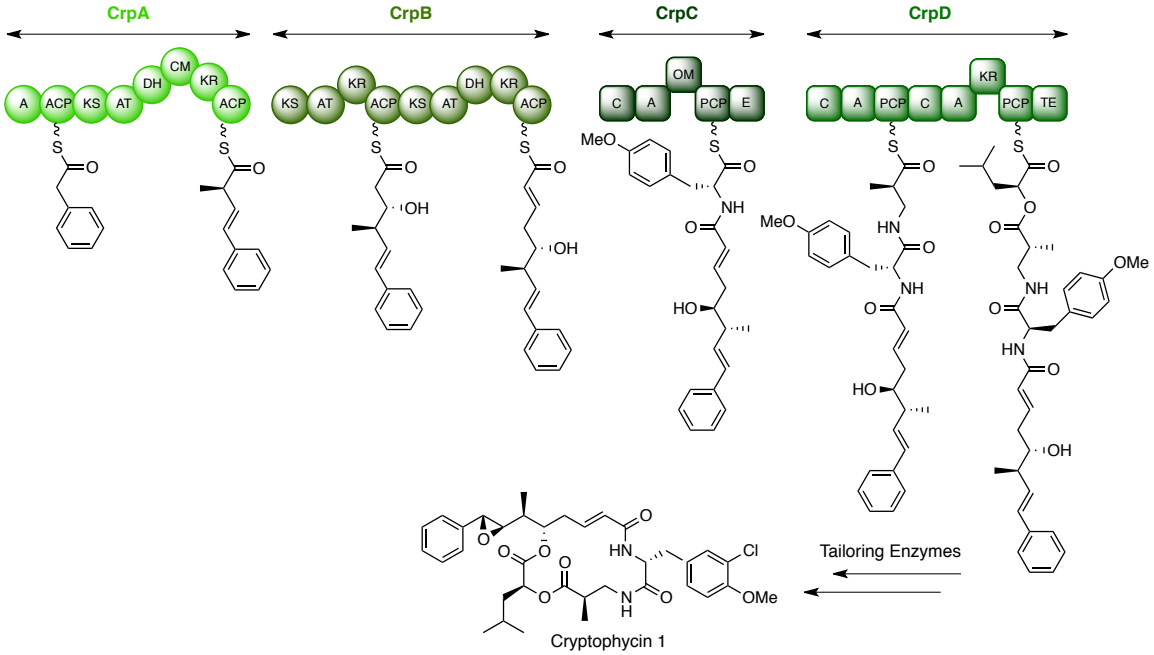

Figure 1.4: The *crp* gene cluster and the deduced PKS/NRPS assembly line. Domains within the *crp* assembly line are shown as circles (PKS) and squares (NRPS) with abbreviations (AT, acyltransferase; KS, ketosynthase; CM, C-methyltransferase; DH, dehydratase; KR, ketoreductase; ACP, acyl carrier protein; A, adenylation; C, condensation; PCP, peptidyl carrier protein; OM, O-methyltransferase; E, epimerase; TE, thioesterase).

successfully reconstituted by heterologous expression in *E. coli* and displayed remarkable *in vitro* activity and flexibility. The substrate tolerance of these enzymes will be critical to employing them as biocatalysts in the development of an efficient chemoenzymatic synthesis of novel cryptophycin compounds for the treatment of cancer.

The cryptophycins have been shown to be some of the most potent tubulin stabilizing agents discovered to date.[16,19] Initial evaluation of the cryptophycins identified this class of depsipeptides as excellent antifungal agents, especially against *Cryptococcus* fungal species. Further testing revealed that cryptophycins were exceptionally potent antiproliferative agents, active against a range of human solid tumor cell lines.[20,21] As reported by Smith *et al.*,[20] treatment with cryptophycin 52 caused marked and marginally reversible depletion of microtubules. Closer analysis of the activity of cryptophycins revealed binding to tubulin to inhibit microtubule polymerization, leading to hyperphosphorylation of Bcl-2 and triggering of the apoptotic cascade.[22-24] Cryptophycin 1 was demonstrated to depolymerize existing microtubules[25] into unique ring structures composed of only a few tubulin heterodimers[26,27] and markedly restrict microtubule dynamics at much lower concentrations than either paclitaxel or vinblastine.[22,28] Despite potent suppression of microtubule function, however, cryptophycin did not significantly decrease polymer mass, giving it an advantage over paclitaxel by avoiding increased tubulin expression to release the mitotic block. Furthermore, cryptophycin 1 was reported to complex tubulin at microtubule ends without copolymerizing with the tubulin or succumbing to cellular efflux pumps, suggesting a significant therapeutic advantage over *vinca* alkaloids in duration of intracellular retention.[22]

Even more exciting was the observation that cryptophycin 52 - a synthetic analogue of cryptophycin 1 identified as the most promising clinical candidate - was not a substrate for P-glycoprotein, an active efflux pump present in many multidrug resistant (MDR) cancer cell lines.[20,29] In

comparison studies with other widely-studied antimitotics, such as vinblastine, colchicine, and paclitaxel, cryptophycin was found to have 100- to 1,000-fold more potent growth suppression in resistant cell lines (Table 1.1).[20] However, dose-limiting peripheral neuropathy prevented cryptophycin 52 from advancing further than Phase II in clinical trials.[30-33] In a subsequent study in patients with platinum-resistant ovarian cancer, the considerable rate of disease stabilization suggested further investigation was warranted.[34] The potential for cryptophycins to become powerful and effective anti-cancer therapeutics therefore urges an in-depth study of the effects of structural modifications on pharmacology.[35] As a result, extensive medicinal chemistry efforts have been undertaken in the search for new analogues with improved therapeutic profiles.[21,36,37] Similar problems with solubility and toxicity were found and overcome for other antimitotic agents, fostering optimism about further development of these promising natural product anti-cancer agents.[38-41]

Table 1.1: Antiproliferative effects of well-known antimitotics in cultured human tumor cells and their MDR counterparts.

	IC_{50} (nM)			
Cell line	Vinblastine	Colchicine	Taxol	Cryptophycin 1
SKOV3	0.65 ± 0.25	9.0 ± 3.0	1.0 ± 0.4	0.007 ± 0.002
SKVLB1	4200 ± 1700	8000 ± 2400	8000 ± 2000	0.60 ± 0.19
resistance factor	6400	890	8000	85
MCF-7	3.0 ± 0.8	8.8 ± 3.0	2.5 ± 0.2	0.016 ± 0.002
MCF-7/ADR	183 ± 14	930 ± 280	4300 ±270	0.017 ± 0.004
resistance factor	61	106	1720	1.1

Unit A (Figure 1.4), a polyketide with a pendant phenyl ring and β-epoxide, is the most amenable subunit for synthetic derivatization, as a plethora of substituted phenyl rings maintained excellent potency.[21] The best remaining chemical space for cryptophycin unit A analogue exploration is therefore the incorporation of heterocycles in place of the endogenous

pendant phenyl ring. Heterocycle incorporation will expand current structure activity relationship (SAR) understanding and the increased number of heteroatoms will serve to decrease the hydrophobicity of the parent compounds. More hydrophilic cryptophycins (lower partition coefficients, log*P*) should have several benefits, including improved aqueous solubility for formulation purposes and decreased hydrophobicity to reduce metabolism and nonspecific protein binding,[42] hopefully mitigating the toxicity issues associated with this class of anticancer agents.

Heterocycle substitution of the cryptophycins allows a unique opportunity to explore the impact of electron demand from the ring on the vicinal epoxide. Evidence to date has suggested that cryptophycins bind tubulin tightly, but reversibly. However, the presence of a labile epoxide begs the question of potentially covalent, reversible protein interactions being responsible for the observed tubulin conformational changes and exceptionally high potency. Initial experiments measuring cryptophycin concentrations after denaturation of co-incubated tubulin found no change in drug levels, suggesting reversible, noncovalent binding.[22] Additionally, pretreatment of cryptophycin with dithiothreitol (DTT), a mimic of nucleophilic tubulin sulfhydryl groups, had no effect on cryptophycin activity in the same study. Evidence supporting the potential covalent reactivity of the epoxide was supplied in several studies on cryptophycin metabolism. Pre-clinical and solution stability studies revealed inherent reactivity of the epoxide with water leading to a diol, while clinical trials identified the glutathione conjugate as the major metabolite.[43] Solution studies with model nucleophiles like glutathione or methyl thioglycolate may therefore help deconvolute the role of epoxide ring opening in tubulin binding and cryptophycin mechanism of action.

My dissertation research under the mentorship of Professors Scott D. Larsen and David H. Sherman was designed to fuse our basic understanding of cryptophycin biosynthetic machinery with efficient and flexible synthetic methodology to achieve rapid derivatization of unit A and expand anticancer

SAR through the construction of a library of novel heterocyclic cryptophycins. The specific aims of my research included (1) the development of an efficient, flexible, divergent synthetic scheme to rapidly derivatize unit A with a suite of heterocycles, (2) attachment of these unit A analogues to endogenous units B, C, and D to construct a library of new *seco*-cryptophycins, (3) enhancing our current understanding of chemoenzymatic synthesis through optimization of CrpTE and CrpE as biocatalysts for ring closure and epoxidation, and (4) exemplification of a unique chemoenzymatic route to selected cryptophycin analogues and their implications for cancer treatment. Detailed discussion of each specific aim will be presented in the following chapters of this thesis.

LITERATURE REFERENCES

1 Mukherjee, S. *The Emperor of all Maladies: A Biography of Cancer*. (Scribner, 2010).

2 Miller, D. R. A tribute to Sidney Farber – the father of modern chemotherapy. *Brit. J. Haematol.* **134**, 20-26 (2006).

3 Hutchings, B. L. *et al.* Pteroylaspartic acid, an antagonist for pteroylglutamic acid. *J. Biol. Chem.* **170**, 323-328 (1947).

4 Farber, S., Diamond, L. K., Mercer, R. D., Sylvester, R. F. & Wolff, J. A. Temporary remissions in acute leukemia in children produced by folic acid antagonist 4-aminopteroyl-glutamic acid (aminopterin). *N. Engl. J. Med.* **238**, 787-793 (1948).

5 Desai, A. & Mitchison, T. J. Microtubule polymerization dynamics. *Annu. Rev. Cell. Dev. Biol.* **13**, 83-117 (1997).

6 Vale, R. D. The molecular motor toolbox for intracellular transport. *Cell* **112**, 467-480 (2003).

7 Browne-Anderson, H., Zanic, M., Kauer, M. & Howard, J. Microtubule dynamic instability: A new model with coupled GTP hydrolysis and multistep catastrophe. *Bioessays* **35**, 452-461 (2013).

8 Gardner, M. K., Zanic, M. & Howard, J. Microtubule catastrophe and rescue. *Curr. Opin. Cell Biol.* **25**, 14-22 (2013).

9 Weisenberg, R. C., Deery, W. J. & Dickinson, P. J. Tubulin-nucleotide interactions during the polymerization and depolymerization of microtubules. *Biochemistry* **15**, 4248-4254 (1976).

10 Mitchison, T. & Kirschner, M. Dynamic instability of microtubule growth. *Nature* **312**, 237-242 (1984).

11 Field, J. J., Diaz, J. F. & Miller, J. H. The Binding Sites of Microtubule-Stabilizing Agents. *Chem. Biol.* **20**, 301-315 (2013).

12 Ravelli, R. B. *et al.* Insight into tubulin regulation from a complex with colchicine and a stathmin-like domain. *Nature* **428**, 198-202 (2004).

13 Cormier, A., Marchand, M., Ravelli, R. B. G., Knossow, M. & Gigant, B. Structural insight into the inhibition of tubulin by vinca domain peptide ligands. *EMBO Rep.* **9**, 1101-1106 (2008).

14 Schwartz, R. E. *et al.* Pharmaceuticals from Cultured Algae. *J. Indust. Microbiol.* **5**, 113-124 (1990).

15 Hirsch, C. F., Liesch, J. M., Salvatore, M. J., Schwartz, R. E. & Sesin, D. F. Antifungal Fermentation Product and Method. U.S. patent (1990).

16 Magarvey, N. A. *et al.* Biosynthetic Characterization and Chemoenzymatic Assembly of the Cryptophycins. Potent Anticancer Agents from Nostoc Cyanobionts. *ACS Chem. Biol.* **1**, 766-779 (2006).

17 Beck, Z. Q., Aldrich, C. C., Magarvey, N. A., Georg, G. I. & Sherman, D. H. Chemoenzymatic Synthesis of Cryptophycin/Arenastatin Natural Products. *Biochemistry* **44**, 13457-13466 (2005).

18 Ding, Y., Seufert, W. H., Beck, Z. Q. & Sherman, D. H. Analysis of the Cryptophycin P450 Epoxidase Reveals Substrate Tolerance and Cooperativity. *J. Am. Chem. Soc.* **130**, 5492-5498 (2008).

19 Chaganty, S., Golakoti, T., Heltzel, C., Moore, R. E. & Yoshida, W. Y. Isolation and Structure Determination of Cryptophycins 38, 326, and 327 from the Terrestrial Cyanobacterium Nostoc sp. GSV 224. *J. Nat. Prod.* **67**, 1403-1406 (2004).

20 Smith, C. D., Zhang, X., Mooberry, S. L., Patterson, G. M. L. & Moore, R. E. Cryptophycin: A New Antimicrotubule Agent Active against Drug-resistant Cells. *Cancer Research* **54**, 3779-3784 (1994).

21 Eggen, M. & Georg, G. I. The Cryptophycins: Their Synthesis and Anticancer Activity. *Med. Chem. Rev.* **22**, 85-101 (2002).

22 Panda, D., Himes, R. H., Moore, R. E., Wilson, L. & Jordan, M. A. Mechanism of Action of the Unusually Potent Microtubule Inhibitor Cryptophycin 1. *Biochemistry* **36**, 12948-12953 (1997).
23 Panda, D. *et al.* Interaction of the Antitumor Compound Cryptophycin-52 with Tubulin. *Biochemistry* **39**, 14121 (2000).
24 Lu, K., Dempsey, J., Schultz, R. M., Shih, C. & Teicher, B. A. Cryptophycin-induced hyperphosphorylation of Bcl-2, cell cycle arrest, and growth inhibition in human H460 NSCLC cells. *Cancer Chemother. Pharmacol.* **47**, 170-178 (2001).
25 Kerksiek, K., Mejillano, M. R., Schwartz, R. E., Georg, G. I. & Himes, R. H. Interaction of Cryptophycin 1 with Tubulin and Microtubules. *FEBS Letters* **377**, 59-61 (1995).
26 Watts, N. R., Cheng, N., West, W., Steven, A. C. & Sackett, D. L. The Cryptophycin-Tubulin Ring Structure Indicates Two Points of Curvature in the Tubulin Dimer. *Biochemistry* **41**, 12662-12669 (2002).
27 Boukari, H., Sackett, D. L., Schuck, P. & Nossal, R. J. Single-Walled Tubulin Ring Polymers. *Biopolymers* **86**, 424-436 (2007).
28 Bai, R., Schwartz, R. E., Kepler, J. A., Pettit, G. R. & Hamel, E. Characterization of the Interaction of Cryptophycin 1 with Tubulin: Binding in the Vinca Domain, Competitive Inhibition of Dolastatin 10 Binding, and an Unusual Aggregation Reaction. *Cancer Research* **56**, 4398-4406 (1996).
29 Rohr, J. Cryptophycin Anticancer Drugs Revisited. *ACS Chem. Biol.* **1**, 747-750 (2006).
30 Stevenson, J. P. *et al.* Phase I Trial of the Cryptophycin Analogue LY355703 Administered as an Intravenous Infusion on a Day 1 and 8 Schedule Every 21 Days. *Clin. Cancer Res.* **8**, 2524-2529 (2002).
31 Sessa, C. *et al.* Phase I and pharmacological studies of the cryptophycin analogue LY355703 administered on a single intermittent or weekly schedule. *Eur. J. Cancer* **38**, 2388-2396 (2002).
32 Edelman, M. J. *et al.* Phase 2 study of cryptophycin 52 in patients previously treated with platinum based chemotherapy for advanced non-small cell lung cancer. *Lung Cancer* **39**, 197-199 (2003).
33 Wagner, M. M. *et al.* In vitro pharmacology of cryptophycin 52 (LY355703) in human tumor cell lines. *Cancer Chemother. Pharmacol.* **43**, 115 (1999).
34 D'Agostino, G. *et al.* A multicenter phase II study of the cryptophycin analog LY355703 in patients with platinum-resistant ovarian cancer. *Int. J. Gynecol. Cancer* **16** (2006).
35 Shih, C. & Teicher, B. A. Cryptophycins: A Novel Class of Potent Antimitotic Antitumor Depsipeptides. *Curr. Pharm. Des.* **7**, 1259-1276 (2001).
36 Eisler, S., Stonicus, A., Nahrwold, M. & Sewald, N. The synthesis of cryptophycins. *Synthesis* **22**, 3747 (2006).
37 Eggen, M. *et al.* Total Synthesis of Cryptophycin-24 (Arenastatin A) Amenable to Structural Modifications in the C16 Side Chain. *J. Org. Chem.* **65**, 7792-7799 (2000).
38 Kingston, D. G. I. The Chemistry of Taxol. *Pharmac. Ther.* **52**, 1-34 (1991).
39 Kingston, D. G. I. Taxol: the chemistry and structure-activity relationships of a novel anticancer agent. *Trends Biothechnol.* **12**, 222-227 (1994).
40 Rowinsky, E. K. The Development and Clinical Utility of the Taxane Class of Antimicrotubule Chemotherapy Agents. *Annu. Rev. Med.* **48**, 353-374 (1997).
41 Silverman, J. A. & Deitcher, S. R. Marqibo (vincristine sulfate liposome injection) improves the pharmacokinetics and pharmacodynamics of vincristine. *Cancer Chemother. Pharmacol.* **71**, 555-564 (2013).
42 Pliska, V., Testa, B. & Waterbeemd, H. v. d. *Lipophilicity in Drug Action and Toxicology*. (VCH Publishers, 2008).

43 Martinelli, M. J., Vaidyanathan, R., Khau, V. V. & Staszak, M. A. Reaction of Cryptophycin 52 with Thiols. *Tet. Lett.* **43**, 3365-3367 (2002).

CHAPTER 2

Development of an Efficient, Divergent Synthesis of Heterocyclic Unit A Analogues

2.1 Methods for the Synthesis of Cryptophycin Unit A

Of the four subunits that comprise the cryptophycins, unit A is the only subunit where significant structural modification has been previously performed with demonstrated tolerance.[1-3] As noted by Corbett and coworkers,[4] substituted phenyl ring analogues of unit A have displayed antitumor activity with promising pharmacological profiles. By going a step further and incorporating heterocycles on unit A, understanding of cryptophycin Structure Activity Relationship (SAR) will expand and the correlation between epoxide electron-deficiency and binding affinity can be determined. First, a strong correlation would be evidence for binding affinity to be due, at least in part, to reversible addition of a nucleophile to the epoxide. If cryptophycin covalently interacts with tubulin, modulation of the electronics of the epoxide should significantly affect the kinetics of addition. Second, the presence of heterocyclic unit A-bearing cryptophycins should enhance the overall pharmacology of this class of drugs, including improved aqueous solubility for formulation purposes and decreased hydrophobicity to reduce metabolism and nonspecific protein binding. Therefore, we were motivated to establish a selective, scalable, and efficient method for the production of unit A analogues varied in the phenyl region to support development of improved cryptophycins for the treatment of cancer.

Many methods exist for the construction of natural and novel unit A fragments, each with its own unique advantages and disadvantages.[5,6] The

challenge lies in choosing among these methods one which allows a rapid, selective, high-yielding synthesis but is also flexible and divergent. That is, the synthetic scheme must allow for attachment of a variety of substitutions without intensive method development for each, and it must facilitate structural diversification at or near the end to avoid multiple parallel syntheses. One of the earlier syntheses of unit A developed by Moore and coworkers installed the two stereocenters in unit A through the ring opening of an oxirane (Scheme 2.1).[7] The key steps in this route for installing the stereocenters were a Sharpless asymmetric epoxidation and regioselective nucleophilic ring opening with trimethylaluminum to give 1,2-diol **4**. While this method was high yielding and stereoselective, the ring functionality was installed at the very beginning using dihydrocinnamaldehyde and was not suitable for divergent synthesis. Another oxirane opening synthesis of unit A was developed by Furuyama and Shimizu, and relied on a Sharpless epoxidation for the introduction of the stereogenic centers.[8] The stereogenic

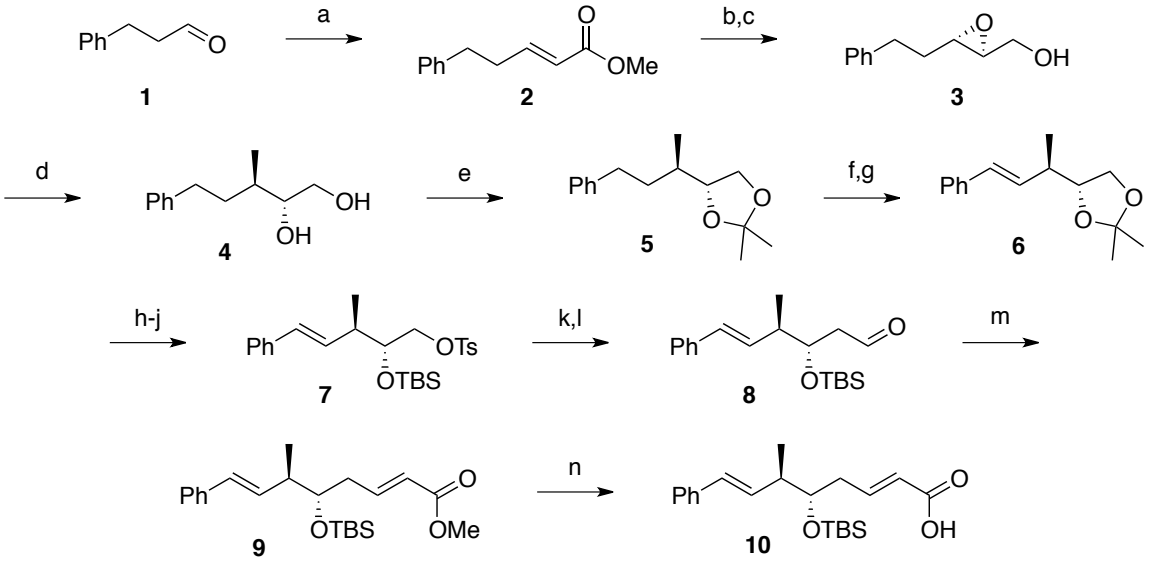

Scheme 2.1: Unit A synthesis by Moore and coworkers: regio- and stereoselective ring opening of an oxirane.[7] *Reagents and conditions*: (a) $(MeO)_2P(O)CH_2CO_2Me$, THF, TMG, -78 °C to rt (86%); (b) DIBAL-H, THF, -78 °C to rt (90%); (c) L-(+)-DET, $Ti(O\textit{i}\text{-}Pr)_4$, t-BuOOH, CH_2Cl_2, -20 °C (94%, >95% ee); (d) Me_3Al, hexane-CH_2Cl_2, 0 °C to rt (95%); (e) $(MeO)_2CMe_2$, PPTS, CH_2Cl_2, rt (97%); (f) NBS, $(MeO)_2CMe_2$, CCl_4, *hv*, rt; (g) DBU, 70 °C, (80%, f-g); (h) 1% aq. HCl-MeOH, rt (93%); (i) $Bu_2Sn(OMe)_2$, PhMe, Dean-Stark, TsCl, Et_3N, 0 °C to rt (82%); (j) TBSOTf, Et_3N, CH_2Cl_2, rt (98%); (k) KCN, DMSO, 60 °C (92%); (l) DIBAL-H, CH_2Cl_2, -78 °C to rt (95%); (m) $(MeO)_2P(O)CH_2CO_2Me$, TMG, THF, -78 °C to rt (83%); (n) LiOH, acetone, 25 °C (95%).

oxirane was then opened via palladium-catalyzed hydrogenation with isomerization of the intermediate palladium complex. This method was shorter and highly stereoselective, but the ring functionality was installed through Wittig chemistry likely to be poorly suited for a large number of analogues.

Aldol additions with chiral auxiliaries also found early success in the synthesis of cryptophycin unit A, as in the route of Maier and coworkers[9] (Scheme 2.2) that utilized chiral auxiliary **11** with known aldehyde **12**. This route employed the auxiliary to direct the aldol addition and set the two required stereocenters, while a late-stage oxidation and Wittig reaction was attractive for derivatization. A subsequent modification by the same group introduced a Julia-Kocienski olefination for aryl group attachment, but both

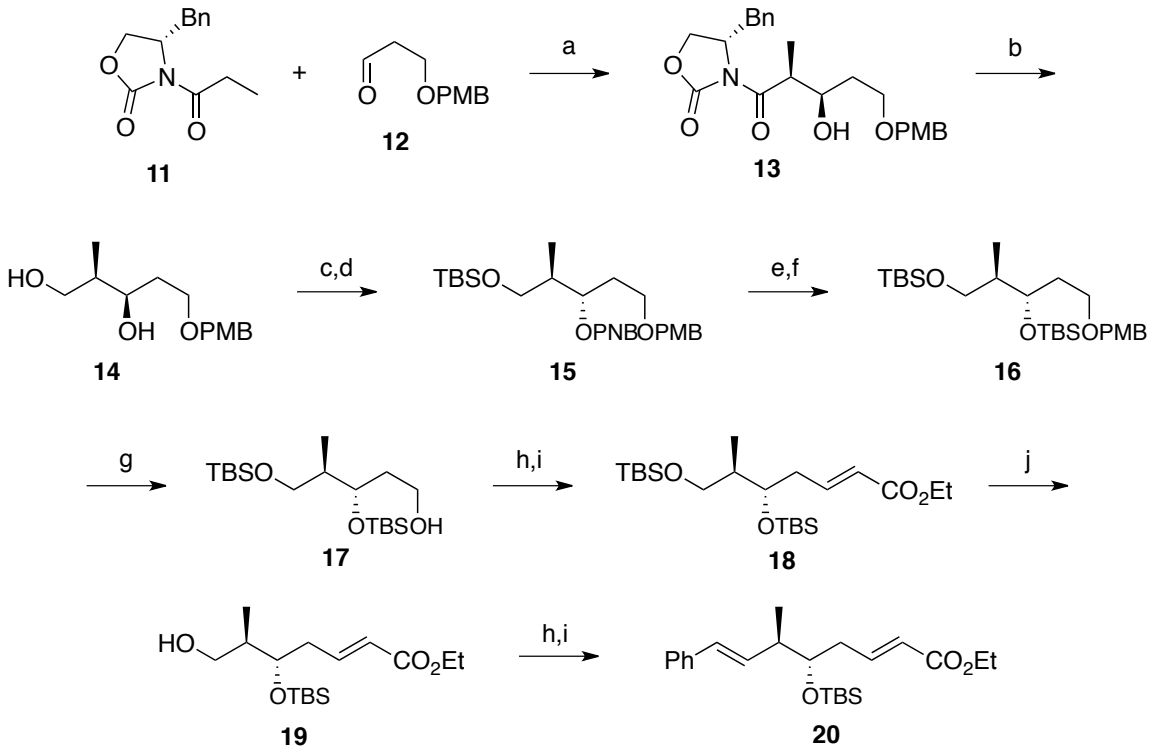

Scheme 2.2: Unit A synthesis by Maier and coworkers: aldol addition with a chiral auxiliary.[9] *Reaction conditions:* (a) Bu_2BOTf, DIPEA, CH_2Cl_2, -78 °C to rt, 2.5 h (82%); (b) $NaBH_4$, THF-H_2O (5:1), 0 °C to rt, 2 h (76%); (c) TBSCl, Et_3N, DMAP, CH_2Cl_2, 0 °C to rt, 12 h (95%); (d) Ph_3P, *i*-$PrO_2CN{=}NCO_2$*i*-Pr, 4-$O_2NC_6H_4CO_2H$, THF, 0 °C to rt, 12 h (70%); (e) NaOH, MeOH, rt, 2 h (94%); (f) TBSCl, imidazole, DMF, rt, 12 h (87%); (g) DDQ, CH_2Cl_2/H_2O (20:1), 0 °C to rt, 2.5 h (85%); (h) $(COCl)_2$, DMSO, CH_2Cl_2, -78 °C, 1 h, then Et_3N, -78 °C to 0 °C, 2 h; (i) $(EtO)_2P(O)CH_2CO_2Et$, NaH, THF, 0 °C to rt, then addition to the aldehyde, 0 °C, 1 h (95%, h-i); (j) AcOH-H_2O-THF (1:1:2), rt, 50 h (75%); (k) $(COCl)_2$, DMSO, CH_2Cl_2, -78 °C, 1 h, then Et_3N, -78 °C to 0 °C, 3 h; (l) $(EtO)_2P(O)CH_2Ph$, *n*-BuLi, THF, -78 °C, 1 h, then addition of the aldehyde, -78 °C to rt, 7 h (56%, k-l).

routes required costly epimerization of the carbon center bearing the hydroxyl group in **14**, and the olefination necessitated the use of a structurally limited pool of aryl aldehyde or aryl phosphonate coupling partners.

Chemoenzymatic approaches have also been utilized for the synthesis of unit A. For example, Sih and coworkers published the first synthesis of unit A using enzyme-catalyzed kinetic resolution of a racemate (Scheme 2.3).[10] The racemic α-methyl esters **22** were subjected to resolution using *Candida*

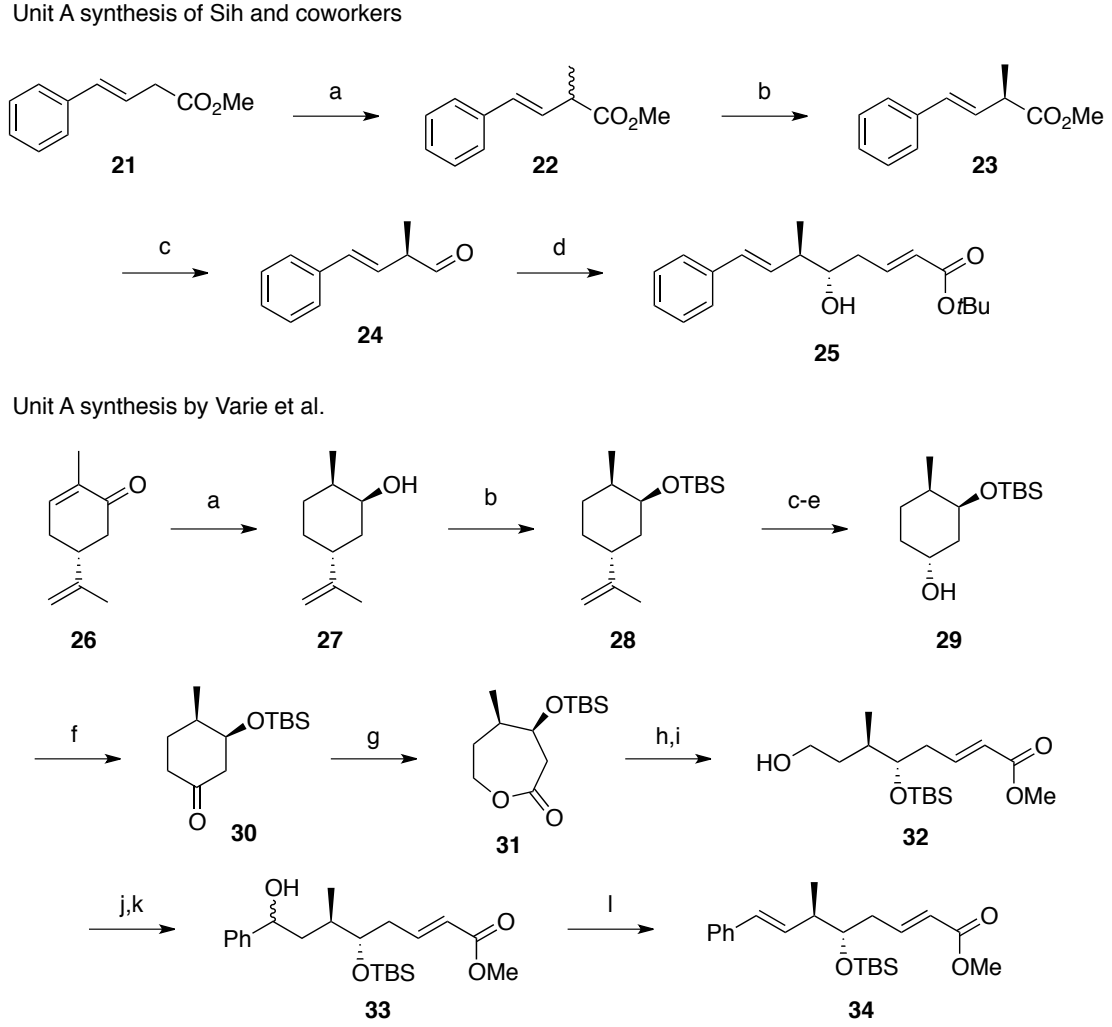

Scheme 2.3: Chemoenzymatic approaches to unit A. (Top) Sih and coworkers. *Reaction conditions*: (a) Me_2SO_4, LDA, THF, -60 °C to 5 °C (92%); (b) 2-propanol-treated *Candida rugosa* lipase, 0.2 M phosphate buffer, rt (48%, ee >96%); (c) DIBAL-H, Et_2O, -70 °C (95%); (d) *tert*-butyl 4-bromocrotonate, Zn-Pb (18%). (Bottom) Varie et al. *Reaction conditions*: (a) *Trigonopsis variabilis*, pH 7 buffer, glucose (50-62%, >98% de); (b) TBSCl, DBU, DMF (87%); (c) O_3, MeOH-CH_2Cl_2; (d) Ac_2O, DMAP; (e) NaOH, MeOH (73%, c-e); (f) NaOCl, TEMPO, CH_2Cl_2 (87%); (g) CF_3CO_2H, CH_2Cl_2, TFA, -15 °C, 2 h (83%); (h) DIBAL-H, PhMe, -78 °C; (i) $(MeO)_2P(O)CH_2CO_2Me$, TMG, THF (66%, h-i); (j) NaOCl, TEMPO; (k) PhMgBr, -78 °C (67%, j-k); (l) Ms_2O, Et_3N, DMAP, CH_2Cl_2 (53%).

rugosa lipase-catalyzed saponification to furnish the *S*-acid leaving the *R*-isomer **23** untouched. Unfortunately for this route, any phenyl ring functionality would need to be present in the starting methyl ester and be accepted as a substrate by the enzyme, while the subsequent Reformatsky rearrangement to add the terminal carboxyl using a zinc-lead couple was low yielding and offered virtually no diastereoselectivity. Varie and coworkers published another chemoenzymatic approach starting from (*R*)-(-)-carvone, which was exclusively converted to isomer **27** by *Trigonopsis variabilis* (Scheme 2.3).[11] Notably, both stereocenters were installed in a single enzyme-catalyzed step, followed by a Baeyer-Villiger oxidation and 1,2-addition of phenylmagnesium bromide to access the desired unit A fragment. While short and potentially divergent, the major drawbacks to this route were the poor structural diversity offered by the use of arylmagnesium bromides and the inefficient *in situ* β-elimination to access unit A precursor **34**.

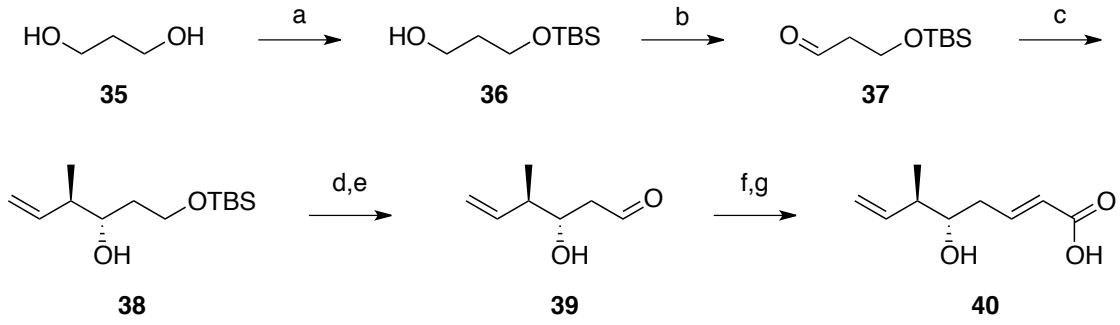

Scheme 2.4: Unit A synthesis of Martinelli and coworkers: asymmetric crotylboration. *Reaction conditions:* (a) NaH, TBSCl, THF, 0 °C (95%); (b) TEMPO, NaOCl, $NaHCO_3$, CH_2Cl_2, pH 9.0-9.2 (91%); (c) 1. di[(-)-α-pinenyl]crotylborane, Et_2O, -78 °C, 2. H_2O_2, NaOAc (67%, 99% ee, 99% de); (d) TBAF; (e) TEMPO, NaOCl, $NaHCO_3$; (f) HWE reaction; (g) saponification (85%, d-g).

Some of the more recent approaches to unit A and its analogues employed Brown crotylboration to significantly improve the introduction of the two stereocenters, as in the synthesis of unit A precursor **40** by Martinelli and coworkers.[12] This method (Scheme 2.4) relied on (*E*)-crotyl diisopinocampheylborane to carry out an enantio- and diastereoselective crotylation of aldehyde **37**. Subsequent oxidation with hydrogen peroxide provided the homoallylic alcohol **38** in over 99% enantiomeric excess and

67% overall yield. After cleavage of the TBS protecting group and oxidation, a Horner-Wadsworth-Emmons (HWE) reaction and saponification provided unsaturated acid **40** primed for introduction into the cryptophycin macrocycle or derivatization via the terminal olefin.

2.2 First Generation Unit A Synthesis

Among the available literature methods, we initially envisioned a synthetic route modelled closely on that of Eggen et al.,[13] which was attractive for utilizing Heck coupling for the late-stage installation of the phenyl ring in unit A. This coupling was ideal for derivatization of the unit A phenyl ring using diverse aryl iodides. The synthetic scheme was therefore adopted for the production of desired unit A analogues through a process that forms a terminal olefin as a common precursor to both natural unit A and analogues (Scheme 2.5). Briefly, 1,3-propanediol is utilized as the feedstock and monoprotected as the *para*-methoxybenzyl (PMB) alcohol, followed by 2,2,6,6-tetramethylpiperidine-1-oxyl (TEMPO)-mediated oxidation to aldehyde **42**. Brown crotylboration is employed to install the two stereocenters in good yield and selectivity. Once isolated, homoallylic alcohol **43** undergoes protecting group exchange to mask the secondary alcohol as the *tert*-butyldimethylsilyl (TBS) ether and expose the primary alcohol. A perruthenate oxidation affords the second aldehyde **45**, which is homologated to the critical α,β-unsaturated *tert*-butyl ester olefin **46**. This terminal olefin was envisioned to provide an excellent handle for rapid diversification to a library of heterocyclic unit A analogues. Heck coupling is then employed to append the pendant phenyl and the resulting unit A fragments are globally deprotected. Considering the divergent and flexible nature of this chemistry, efforts were focused on optimizing this scheme for large-scale production of the desired compounds (for Experimental Details, see Chapter 6).

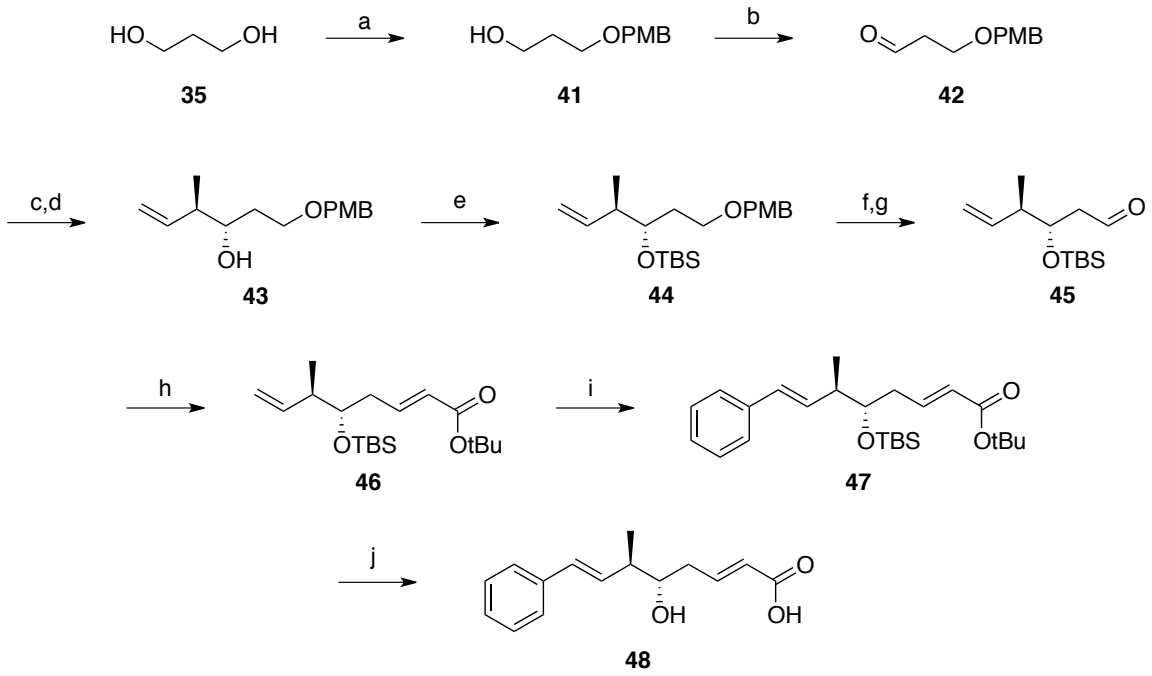

Scheme 2.5: First generation synthetic route to unit A and analogues developed from Eggen et al.[13] *Reaction Conditions:* (a) NaH, DMF, 0 °C, 1 h, then PMBCl, 0 °C to rt (81%); (b) TEMPO, NaOCl, $NaHCO_3$, KBr, CH_2Cl_2, pH 8.5-8.7 (88%); (c) *trans*-2-butene, KOtBu, nBuLi, (+)-$(ipc)_2BOMe$, BF_3-OEt_2, THF, -78 °C, 3 h; (d) ethanolamine, Et_2O, rt; (e) TBSOTf, 2,6-lutidine, CH_2Cl_2, -45 °C (32%, c-e, 90% ee, >95% de); (f) DDQ, H_2O, CH_2Cl_2; (g) TPAP, NMO, 4 Å sieves, CH_2Cl_2 (48%, f-g); (h) $(EtO)_2P(O)CH_2CO_2tBu$, DBU, LiCl, CH_2Cl_2 (74%); (i) PhI, $Pd(OAc)_2$, PPh_3, Et_3N, CH_3CN, 80 °C (63%); (j) TFA, CH_2Cl_2, 18 h, then $NaHCO_3$, MeOH, CH_2Cl_2 (23%).

Initially, the mono-protection of 1,3-propanediol was challenging given poor solvent participation and significant bis-protection. Changing from THF to DMF as the reaction solvent and using an excess of the diol afforded excellent yield of the singly PMB-protected propanol (**41**) on up to 25-gram scale.[14] The subsequent TEMPO oxidation to aldehyde **42** proceeded smoothly on small scale, but degraded upon scale-up. A method utilizing mechanical stirring to more effectively mix the two-phase reaction and adjusting of the sodium hypochlorite oxidant solution to pH 8.5 with solid sodium bicarbonate was found to be necessary for good yields on large scale.[15] Incorporation of the crotyl fragment was accomplished by the Brown aldehyde crotylation method[16] to afford **43** in excellent diastereoselectivity. Yields from crotylation using the Brown method remained low, however, despite significant optimization efforts to remove traces of moisture and strictly control stoichiometric equivalents. Subsequent silyl ether protection of

the secondary alcohol suffered from decomposition of the substrate, but proceeded to the product, as did DDQ removal of the PMB protecting group. The exposed primary alcohol was then converted to aldehyde **45** using tetrapropylammonium perruthenate (TPAP) oxidation conditions. This oxidation was variable on larger scale, but was sufficient for the task at hand. The *tert*-butyl ester moiety on **46** was then installed using a Horner-Wadsworth-Emmons (HWE) coupling with the corresponding phosphonate, which was followed by Heck coupling to introduce the terminal phenyl. Removal of the silyl ether and *tert*-butyl ester then liberated free unit A (**48**). Using the optimized synthesis described above, approximately 650 mg of natural unit A was produced with assistance from Russell Betts, PhD of Alluvium Biosciences, for use in the synthesis of several members of a cryptophycin-52 unit B library (data not shown).

Development of this route in our laboratory for higher throughput proved to be problematic. The Brown crotylboration was the most significant hindrance to large-scale synthesis, as it proceeded in poor yield with competing decomposition of aldehyde **42**. In addition, protecting group exchange was inefficient (**43** to **45**), and the second round of oxidation provided a volatile silyl ether aldehyde (**45**) whose isolation was problematic. The complexity and low-throughput (0.12% over 11 steps to **48**) of this route hindered our ability to access the desired quantities of unit A and its analogues.

2.3 Second Generation Unit A Synthesis

Recent advances in crotylation technology pioneered in the Krische laboratory[17-20] allowed significant improvements to the synthetic scheme presented above. In this scheme (Scheme 2.6), the TBS protecting group[21] was preferred to the PMB group due to improved stability and reduced side products in the Krische crotylation, which replaced the Brown crotylation to improve enantioselectivity and ease of reaction. This optimization improved

the overall yield of the reaction, and the discovery that the catalyst could be recovered and recycled dramatically improved throughput and lowered cost. Subsequent TBAF deprotection without prior purification afforded diol **51**, which was then selectively oxidized using TEMPO. The resulting aldehyde (**52**) was unstable, volatile, and prone to elimination, so great care was taken in developing buffered reaction conditions and decreasing handling during delivery of the aldehyde to the HWE conditions. The subsequent olefination proceeded smoothly to afford the required methyl ester **53** in 52% yield from the starting diol. With the desired terminal olefin **53** in hand, the remaining task was to find Heck reaction conditions suitable for appendage of both the endogenous phenyl ring and a variety of heterocycles into the unit A structure. Literature reports suggested that Jeffery conditions[22,23] would be both mild and versatile for this purpose. Further investigation found suitable conditions[24-26] using the Herrmann-Beller palladacycle (**54**) that successfully afforded the natural phenyl version of unit A (**48**), but never successfully created heterocyclic derivatives.

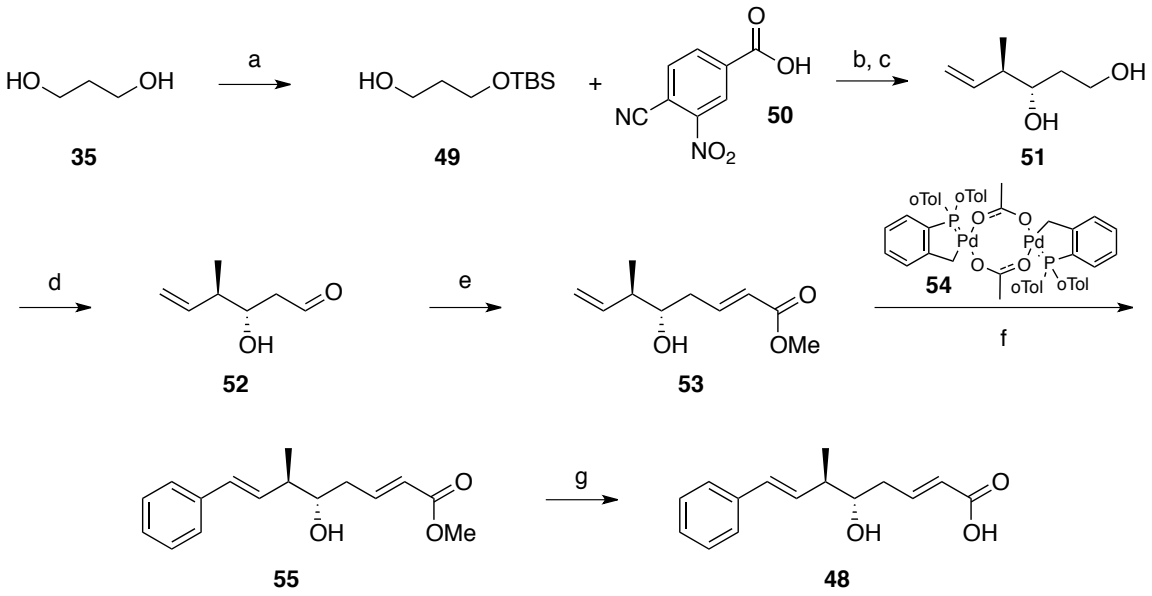

Scheme 2.6: Second generation synthetic route to unit A and analogues. *Reaction conditions:* (a) NaH, DMF, 0 °C, 1 h, then TBSCl, 0 °C to rt (81%); (b) **50**, $[Ir(cod)Cl]_2$, (*R*)-3-TUNEPHOS, α-methyl allyl acetate, Cs_2CO_3, THF, 90 °C; (c) TBAF, THF (35%, 6:1 dr, b-c); (d) TEMPO, NaOCl, $NaHCO_3$, KBr, CH_2Cl_2, pH 8.5-8.8; (e) $(EtO)_2P(O)CH_2CO_2Me$, DBU, LiCl, CH_2Cl_2 (74%, d-e); (f) **54**, PhI, K_3PO_4, TBACl, DMF, 80 °C (42%); (g) LiOH, MeOH, H_2O, THF (87%).

Facing these initial obstacles, a new route to unit A analogues was sought that was both short and enabled diversification as a terminal, divergent step. As already stated, recent advances in crotylation technology created the opportunity for a catalytic process with the potential for recovery and recycling of the expensive iridium-based reactive complex.[27] This crotylation was also highly efficient, as it eliminated the need for a separate aldehyde generation and isolation step. Significant product (**58**) decomposition challenges were overcome by preforming the iridium catalyst (**57**, Scheme 2.7), as well as running the reaction at a lower temperature with K_3PO_4 as base instead of Cs_2CO_3. Furthermore, an Eli Lilly process chemistry report[12] suggested that tedious protection and deprotection steps through the final alcohol oxidation would not be necessary, and that an *in situ* olefination could further shorten the synthetic route. Thus, analogue synthesis through olefin cross metathesis (CM), Heck coupling, and Suzuki-Miyaura cross coupling could all be pursued.

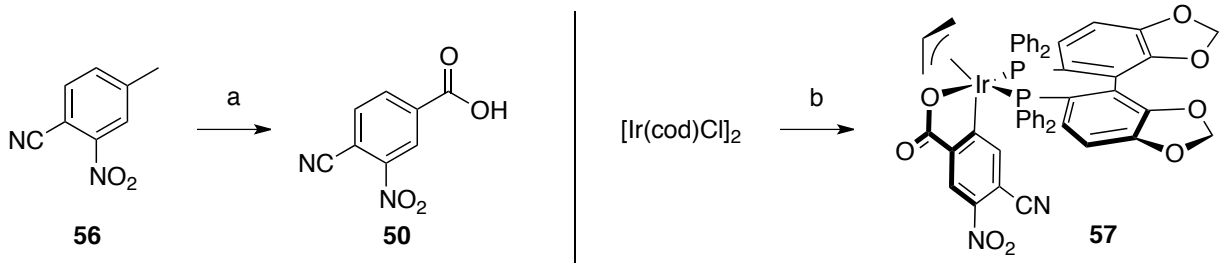

56 **50** **57**

Scheme 2.7: Synthesis of the Krische auxiliary (50) and iridium crotylation complex (57). *Reaction conditions:* (a) H_5IO_6, CrO_3, CH_3CN (52%); (b) **50**, (*R*)-(+)-SEGPHOS, 3-buten-2-yl acetate, Cs_2CO_3, THF, 80 °C (quant.).

Our final synthesis of intermediate **53**, which would serve as the common intermediate for unit A and analogues, is summarized in Scheme 2.8.[28] Starting from 1,3-propanediol, monosilylated alcohol **49** was prepared as previously reported in excellent yield.[21] Treatment of **49** with the Ir complex **57**, prepared and isolated as described,[16] in the presence of α-methyl allyl acetate afforded the expected crotyl alcohol in a 6:1 dr that was sufficiently pure to carry forward without purification. Mosher ester analysis[29,30] of the diastereomeric mixture of **58** confirmed the correct

stereochemistry (3*S*,4*R*) and revealed a 95:5 er.[‡] Precipitation with pentane and filtration allowed recovery of the catalyst, while the filtrate containing **58** was concentrated and treated with TBAF to liberate crotyl diol **51** in good yield from **49**. With **51** in hand, a one-pot oxidation/olefination sequence was employed to effect chemoselective conversion of the primary alcohol to unsaturated ester **53** (>20:1 *E*/*Z*).[31] The terminal alkene on **53** was then employed as the handle to generate unit A analogues.

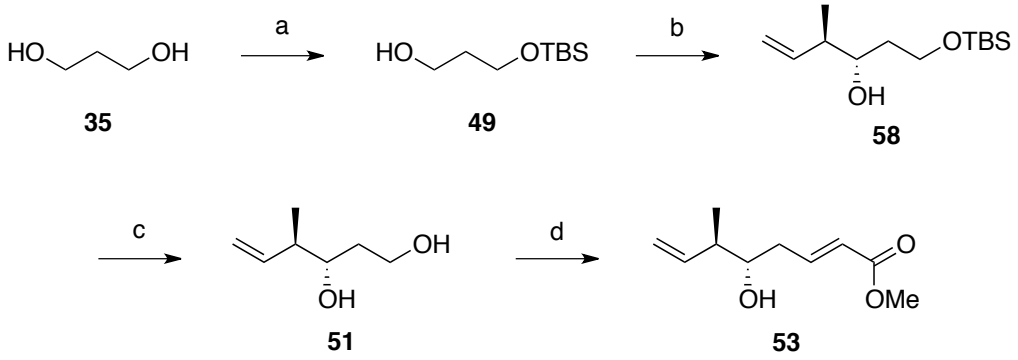

Scheme 2.8: Final efficient, divergent synthesis of key olefin intermediate 53. *Reaction conditions:* (a) NaH, THF, 0 °C, 1 h, then TBSCl, 0 °C to rt (92%); (b) **57**, 3-buten-2-yl acetate, K_3PO_4, H_2O, THF, 60 °C, 48 h; (c) TBAF, THF (52%, b-c, 6:1 dr, 95:5 er); (d) TEMPO, BAIB, CH_3CN, 4 h, then Ph_3PCHCO_2Me, 0 °C to rt (72%, >20:1 *E*/*Z*).

A series of phenyl moieties (4-H, 4-trifluoromethyl, 4-methoxy, and 4-cyano) was chosen to demonstrate the flexibility of the newly developed synthetic scheme. This series was chosen for the wide range of electron demand presented and for structural replication of non-native cryptophycins produced through precursor-directed biosynthesis.[32] As previous methods utilized Heck coupling for appending the phenyl on unit A, this was the first route explored for analogue creation (Table 2.1). Phosphine-free Pd catalysis with aryl iodides **59a-d** in acetonitrile proved to be the most versatile for reactions with the terminal olefin of **53**, but also induced reactivity with the α,β-unsaturated methyl ester.[33-35] Elimination of the secondary alcohol was also evident, likely due to extended heating times, but yields were acceptable for analogues **60a-d**.

[‡] The MTPA ester was synthesized from purified **58** using (*S*)-(+)-MTPA acid chloride in anhydrous pyridine at 60 °C for 24 h. The ^{19}F NMR spectra of esters prepared from **58** and its enantiomer (from (*S*)-(-)-**57**) were compared to determine the er (Appendix A).

Table 2.1: Heck route to unit A analogues.[a]

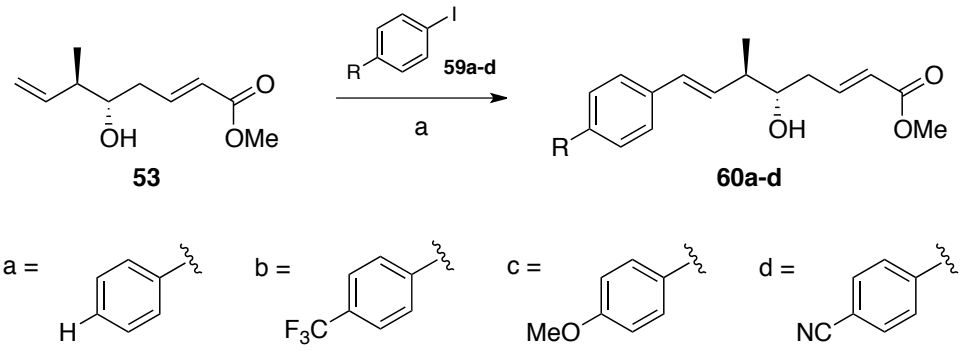

Aryl iodide	Product	Yield (%)[b]
59a	**60a**	31
59b	**60b**	28
59c	**60c**	38
59d	**60d**	30

[a]*Reaction conditions:* (a) $Pd(OAc)_2$, 1.1 eq. aryl iodide, Et_3N, CH_3CN, 85 °C, 18 h. [b]Isolated yields.

The second route investigated for flexible analogue generation was CM (Table 2.2). In this case, olefin **53** underwent metathesis in the presence of Hoveyda-Grubbs II catalyst in dichloromethane at reflux temperature with a set of *para*-substituted styrenes (**61a-d**).[36-38] CM was successful in providing the desired analogues **60a-d**, but competitive insertion of the α,β-unsaturated methyl ester prevented higher yields (Table 2.2). However, this route could potentially be further optimized to utilize the full spectrum of styryl building

Table 2.2: Cross-metathesis route to unit A analogues.[a]

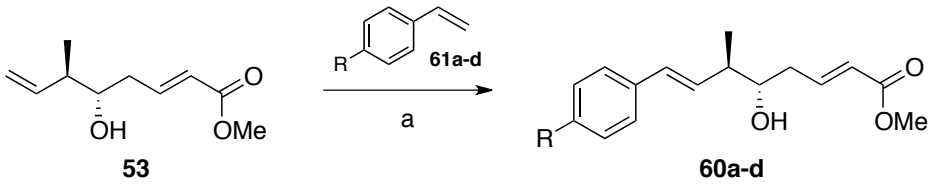

Styryl fragment	Product	Yield (%)[b]
61a	**60a**	30
61b	**60b**	23
61c	**60c**	26
61d	**60d**	8

[a]*Reaction conditions:* (a) Hoveyda-Grubbs II (5 mol%), 4.0 eq. styryl fragment, CH_2Cl_2, reflux, 2 h. [b]Isolated yield.

blocks available.

The final route developed for unit A analogue synthesis employed Suzuki-Miyaura cross coupling. For this method, the boronic ester **62** was first prepared through CM (Table 2.3).[39,40] Aryl iodides **59a-d** were then coupled with **62** using $Pd_2(dba)_3$ in a mixture of water and glyme to afford analogues **60a-d** in good yield with little apparent bias for electronics.[41] Reactivity can also potentially be achieved with aryl bromides and chlorides, thereby expanding the set of coupling partners available for this transformation.

Table 2.3: Suzuki-Miyaura cross coupling to unit A analogues.[a]

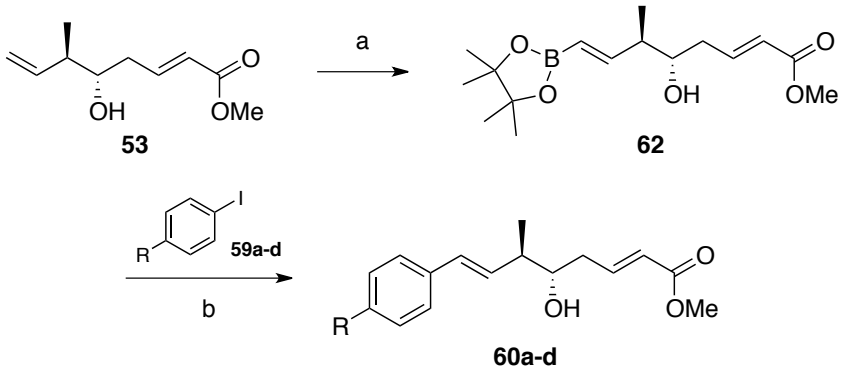

Aryl iodide	Product	Yield (%)[b]
59a	**60a**	42
59b	**60b**	55
59c	**60c**	53
59d	**60d**	63

[a]*Reaction conditions:* (a) Hoveyda-Grubbs II, vinylboronic acid pinacol ester, CH_2Cl_2, reflux (55%); (b) [$Pd_2(dba)_3$] (2 mol%), PCy_3 (4.8 mol%), K_3PO_4, DME/H_2O (2:1), 85 °C, 2 h. [b]Isolated yield.

The olefin **53** was effectively elaborated via Heck reaction, CM, and Suzuki-Miyaura coupling, but in terms of efficiency and flexibility, Suzuki coupling was clearly superior to previously reported unit A derivatization methods.[42,43] For this reason, unit A analogue library construction commenced using the boronic ester **62** under standard Suzuki conditions with aryl and heteroaryl iodides. The coupling was scaled to accommodate reactions on approximately 300 mg scale of the boronic ester to provide at least 100 mg of each of the resulting methyl esters, and first exemplified

using iodobenzene for endogenous unit A methyl ester **55** (Figure 2.1). The first set of analogues produced were the 2-, 3-, and 4-pyridyl fragments (**63**, **64**, and **65**, respectively) to explore the impact of the varying nitrogen electronics on the conjugated double bond when first installing the epoxide and then when measuring potency. In addition, the pyridine analogues were an intriguing trio of substrates for probing the tolerance of the subsequent macrocyclization by cryptophycin thioesterase (CrpTE, see Chapter 3). The methyl pyrazolyl (**66**), pyrazinyl (**67**), thiophenyl (**68**), 2-amino pyrazinyl (**72**), and imidazolyl (**73**) analogues further increased the heteroatom density on unit A to improve aqueous solubility and challenge the previous substrate boundaries of the cryptophycin biosynthetic enzymes. Analogues **69** and **70** were included in the initial library because they represented two extremes of electron-withdrawing and electron-donating character among substituted phenyls, and served as direct comparisons of the developed technology with analogues previously only produced through precursor-directed biosynthesis.[32] While not a heterocycle, aminobenzyl analogue **71** was synthesized to serve as a handle for the attachment of any number of cross-linkers,[33] fluorescent probes, targeting peptides,[44] or antibodies[45] to utilize the cryptophycins for interrogation of protein binding, biological distribution, or intracellular localization. Finally, the boronic ester **62** was also included in the analogue library because it would enable the attachment of larger and more sophisticated heterocycles, which may not be feasible CrpTE substrates, after enzymatic cyclization.

With effective elaboration of **53** via Heck reaction, CM, and Suzuki-Miyaura coupling and the successful completion of a 13-member unit A analogue library, the remaining transformation is the hydrolysis of the diverse methyl esters. This was accomplished on fragments **60a-d** and **63**, **66**, and **67** with LiOH in a 2:2:1 mixture of methanol/water/THF (Scheme 2.9) to yield the acids **74a-d**, and which should be successful for the remaining esters.

The presence of the free acid now allows attachment of these novel unit A analogues to linear depsipeptide precursors of cryptophycin.[46]

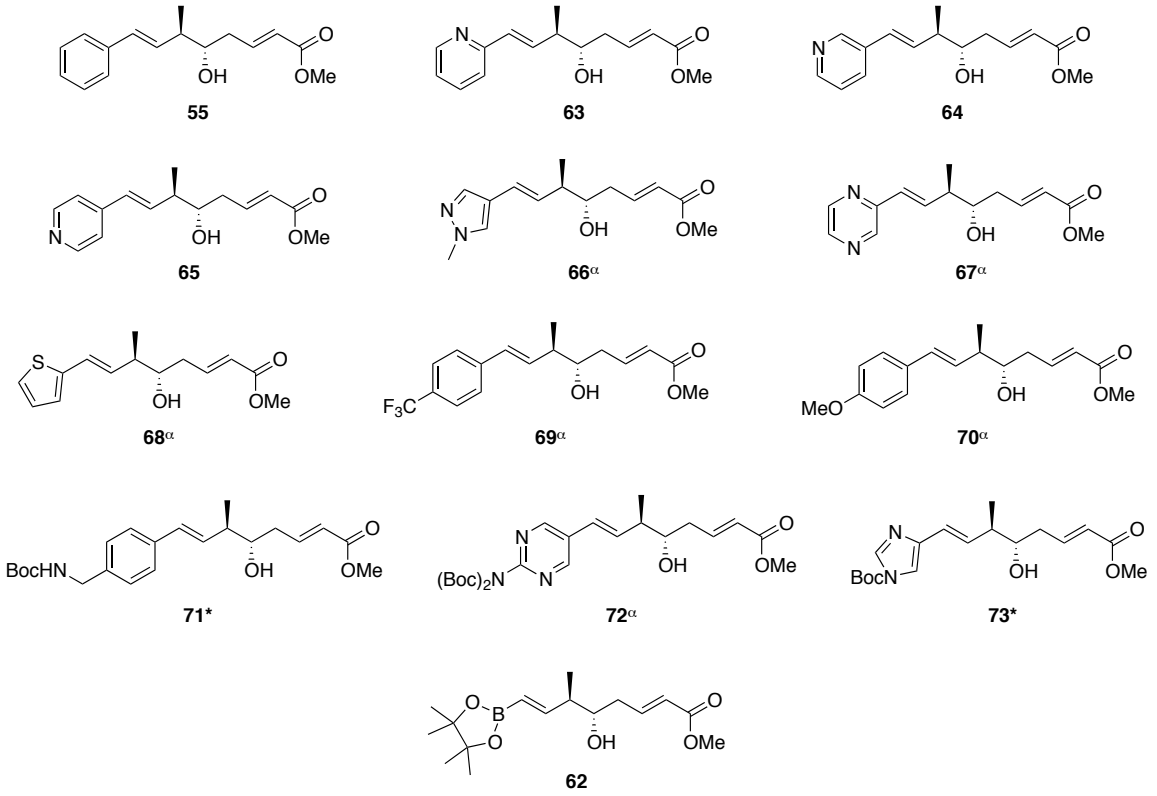

Figure 2.1: Completed unit A library containing both substituted phenyl and heterocycle analogues. [α]Synthesized on small-scale and identified by QTOF-MS; later synthesized on large scale by Jennifer Schmidt. *Synthesis and characterization performed by Jennifer Schmidt.

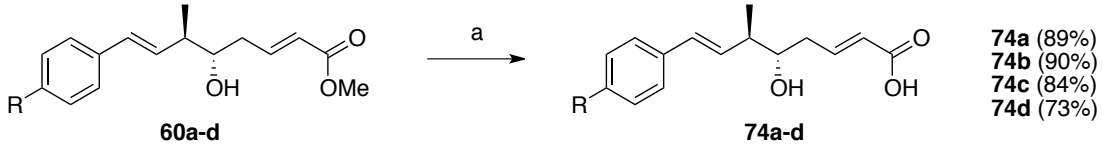

Scheme 2.9: Hydrolysis of the methyl esters 60a-d to the carboxylic acids 74a-d. *Reaction conditions:* (a) LiOH•H_2O, MeOH/H_2O/THF (2:2:1), rt.

In summary, a short and efficient synthesis has been established to intermediate **53** (4 steps, 34% overall yield) from which flexible coupling methods provide access to a broad range of phenyl or more highly functionalized aromatic and heteroaromatic moieties in the synthesis of unit A analogues. The paucity of robust synthetic routes and the surprising flexibility of the coupling chemistry merited its inclusion in a recent review of approaches to cryptophycin modifications.[47] Now with this strategy in place,

the remaining objective involves coupling of the analogues to units B, C, and D to generate *seco*-cryptophycin intermediates. Our laboratory has previously demonstrated that solid phase synthesis[48] followed by cryptophycin thioesterase and epoxidase-mediated chemoenzymatic assembly[32,49,50] enable rapid production of cryptophycin anticancer agents. The versatile unit A synthetic strategy reported here is therefore expected to open new opportunities to produce unique cryptophycin analogues for on-going drug development efforts.

LITERATURE REFERENCES

1 Patel, V. F., Andis, S. L., Kennedy, J. H., Ray, J. E. & Schultz, R. M. Novel Cryptophycin Antitumor Agents: Synthesis and Cytotoxicity of Fragment "B" Analogues. *J. Med. Chem.* **42**, 2588 (1999).

2 Varie, D. L. *et al.* Synthesis and biological evaluation of cryptophycin analogs with substitution at C-6 (fragment C region). *Bioorg. Med. Chem. Lett.* **9**, 369 (1999).

3 Shih, C. *et al.* Synthesis and biological evaluation of novel cryptophycin analogs with modification in the β-alanine region. *Bioorg. Med. Chem. Lett.* **9**, 69 (1999).

4 Al-awar, R. S. *et al.* A Convergent Approach to Cryptophycin 52 Analogues: Synthesis and Biological Evaluation of a Novel Series of Fragment A Epoxides and Chlorohydrins. *J. Med. Chem.* **46**, 2985 (2003).

5 Eisler, S., Stonicus, A., Nahrwold, M. & Sewald, N. The synthesis of cryptophycins. *Synthesis* **22**, 3747 (2006).

6 Eggen, M. & Georg, G. I. The Cryptophycins: Their Synthesis and Anticancer Activity. *Med. Chem. Rev.* **22**, 85-101 (2002).

7 Barrow, R. A. *et al.* Total Synthesis of Cryptophycins. Revision of the Structures of Cryptophycins A and C. *J. Am. Chem. Soc.* **117**, 2479-2490 (1995).

8 Furuyama, M. & Shimizu, I. A short enantioselective synthesis of a component of cryptophycin A and arenastatin A. *Tetrahedron Asymmetry* **9**, 1351-1357 (1998).

9 Phukan, P., Sasmal, S. & Maier, M. E. Flexible Routes to the 5-Hydroxy Acid Fragment of the Cryptophycins. *Eur. J. Org. Chem.*, 1733-1740 (2003).

10 Salamonczyk, G. M., Han, K., Guo, Z. & Sih, C. J. Total Synthesis of Cryptophycins via a Chemoenzymatic Approach. *J. Org. Chem.* **61**, 6893–6900 (1996).

11 Varie, D. L. *et al.* Bioreduction of (R)-carvone and regioselective Baeyer-Villiger oxidations: Application to the asymmetric synthesis of cryptophycin fragment A. *Tetrahedron Lett.* **39**, 8405–8408 (1998).

12 Dhokte, U. P., Khau, V. V., Hutchinson, D. R. & Martinelli, M. J. A novel approach for total synthesis of cryptophycins via asymmetric crotylboration protocol. *Tet. Lett.* **39**, 8771-8774 (1998).

13 Eggen, M. *et al.* Total Synthesis of Cryptophycin-24 (Arenastatin A) Amenable to Structural Modifications in the C16 Side Chain. *J. Org. Chem.* **65**, 7792-7799 (2000).

14 Urbanek, R. A., Sabes, S. F. & Forsyth, C. J. Efficient Synthesis of Okadaic Acid. 1. Convergent Assembly of the C15-C38 Domain. *J. Am. Chem. Soc.* **120**, 2523-2533 (1998).

15 Anelli, P. L., Biffi, C., Montanari, F. & Quici, S. Fast and Selective Oxidation of Primary Alcohols to Aldehydes or to Carboxylic Acids and of Secondary Alcohols to Ketones Mediated by Oxoammonium Salts under Two-Phase Conditions. *J. Org. Chem.* **52**, 2559-2562 (1987).

16 Brown, H. C. & Bhat, K. S. Enantiomeric (Z)- and (E)-Crotyldiisopinocampheylboranes. Synthesis in High Optical Purity of All Four Possible Stereoisomers of b-Methylhomoallyl Alcohols. *J. Am. Chem. Soc.* **108**, 293-294 (1986).

17 Kim, I. S., Han, S. B. & Krische, M. J. anti-Diastereo- and Enantioselective Carbonyl Crotylation from the Alcohol or Aldehyde Oxidation Level Employing a Cyclometallated Iridium Catalyst: a-Methyl Allyl Acetate as a Surrogate to Preformed Crotylmetal Reagents *J. Am. Chem. Soc.* **131**, 2514 (2009).

18 Kim, I. S., Ngai, M.-Y. & Krische, M. J. Enantioselective Iridium-Catalyzed Carbonyl Allylation from the Alcohol or Aldehyde Oxidation Level via Transfer Hydrogenative Coupling of Allyl Acetate: Departure from Chirally Modified Allyl Metal Reagents in Carbonyl Addition. *J. Am. Chem. Soc.* **130**, 14891 (2008).

19 Han, S. B., Gao, X. & Krische, M. J. Iridium Catalyzed anti-Diastereo- and Enantioselecive Carbonyl (Trimethylsilyl)allylation from the Alcohol or Aldehyde Oxidation Level *J. Am. Chem. Soc.* **132**, 9153 (2010).
20 Bechem, B., Patman, R. L., Hashmi, A. S. K. & Krische, M. J. Enantioselective Carbonyl Allylation, Crotylation, and tert-Prenylation of Furan Methanols and Furfurals via Iridium-Catalyzed Transfer Hydrogenation. *J. Org. Chem.* **75**, 1795 (2010).
21 McDougal, P. G., Rico, J. G., Oh, Y.-I. & Condon, B. D. A convenient procedure for the monosilylation of symmetric 1,n-diols. *J. Org. Chem.* **51**, 3388-3390 (1986).
22 Jeffery, T. Highly stereospecific palladium-catalysed vinylation of vinylic halides under solid-liquid phase transfer conditions. *Tet. Lett.* **26**, 2667-2670 (1985).
23 Jeffery, T. Palladium-catalysed Vinylation of Organic Halides under Solid-Liquid Phase Transfer Conditions. *J. Chem. Soc., Chem. Commun.*, 1287-1289 (1984).
24 Noel, S., Pinel, C. & Djakovitch, L. Direct synthesis of tricyclic 5H-pyrido[3,2,1-ij]quinolin-3-one by domino palladium catalyzed reaction. *Org. Biomol. Chem.* **4**, 3760-3762 (2006).
25 Noel, S., Djakovitch, L. & Pinel, C. Influence of the catalytic conditions on the selectivity of the Pd-catalyzed Heck arylation of acrolein derivatives. *Tet. Lett.* **47**, 3839-3842 (2006).
26 Battistuzzi, G., Cacchi, S. & Fabrizi, G. An Efficient Palladium-Catalyzed Synthesis of Cinnamaldehydes from Acrolein Diethyl Acetal and Aryl Iodides and Bromides. *Org. Lett.* **5**, 777-780 (2003).
27 Hassan, A. & Krische, M. J. Unlocking Hydrogenation for C-C Bond Formation: A Brief Overview of Enantioselective Methods. *Org. Process Res. Dev.* **15**, 1236 (2011).
28 Bolduc, K. L., Larsen, S. D. & Sherman, D. H. Efficient, Divergent Synthesis of Cryptophycin Unit A Analogues. *Chem. Commun.* **48**, 6414-6416 (2012).
29 Dale, J. A. & Mosher, H. S. a-Methoxy-a-trifluoromethylphenylacetic Acid, a Versatile Reagent for the Determination of Enantiomeric Composition of Alcohols and Amines. *J. Am. Chem. Soc.* **95**, 512 (1973).
30 Hoye, T. R., Jeffrey, C. S. & Shao, F. Mosher ester analysis for the determination of absolute configuration of stereogenic (chiral) carbinol carbons. *Nat. Protoc.* **2**, 2451 (2007).
31 Vatele, J.-M. One-pot selective oxidation/olefination of primary alcohols using TEMPO-BAIB system and stabilized phosphorus ylides. *Tetrahedron Lett.* **47**, 715 (2006).
32 Magarvey, N. A. *et al.* Biosynthetic Characterization and Chemoenzymatic Assembly of the Cryptophycins. Potent Anticancer Agents from Nostoc Cyanobionts. *ACS Chem. Biol.* **1**, 766-779 (2006).
33 Vidya, R., Eggen, M., Georg, G. I. & Himes, R. H. Cryptophycin Affinity Labels: Synthesis and Biological Activity of a Benziphenone Analogue of Cryptophycin-24. *Bioorg. Med. Chem. Lett.* **13**, 757-760 (2003).
34 Gurtler, C. & Buchwald, S. L. A Phosphane-Free Catalyst System for the Heck Arylation of Disubstituted Alkenes: Application to the Synthesis of Trisubstituted Olefins. *Chem. Eur. J.* **5**, 3107 (1999).
35 Kleist, W., Prockl, S. S. & Kohler, K. Heck Reactions of Aryl Chlorides Catalyzed by Ligand Free Palladium Salts. *Catal. Lett.* **125**, 197 (2008).
36 Moura-Letts, G. & Curran, D. P. *Org. Lett.* **13**, 757 (2007).
37 Funk, T. W., Efskind, J. & Grubbs, R. H. Chemoselective Construction of Substituted Conjugated Dienes Using an Olefin Cross-Metathesis Protocol. *Org. Lett.* **7**, 187 (2005).
38 Chatterjee, A. K., Choi, T.-L., Sanders, D. P. & Grubbs, R. H. A General Model for Selectivity in Olefin Cross Metathesis. *J. Am. Chem. Soc.* **125**, 11360 (2003).

39 Ghosh, A. K. & Li, J. A Stereoselective Synthesis of (+)-Herboxidiene/GEX1A. *Org. Lett.* **13**, 66 (2011).
40 Nicolaou, K. C., Li, A., Edmonds, D. J., Tria, G. S. & Ellery, S. P. Total Synthesis of Platensimycin and Related Natural Products. *J. Am. Chem. Soc.* **131**, 16905 (2009).
41 Kudo, N., Perseghini, M. & Fu, G. C. A Versatile Method for Suzuki Cross-Coupling Reactions of Nitrogen Heterocycles. *Angew. Chem. Int. Ed.* **45**, 1282 (2006).
42 Weiss, C., Bogner, T., Sammet, B. & Sewald, N. Total synthesis and biological evaluation of fluroinated cryptophycins. *Beilstein J. Org. Chem.* **8**, 2060-2066 (2012).
43 Eissler, S., Bogner, T., Nahrwold, M. & Sewald, N. Efficient Synthesis of Cryptophycin-52 and Novel para-Alkoxymethyl Unit A Analogues. *Chem. Eur. J.* **15**, 11273-11287 (2009).
44 Nahrwold, M. *et al.* Conjugates of modified cryptophycins and RGD-peptides enter target cells by endocytosis. *J. Med. Chem.* **56**, 1853-1864 (2013).
45 Bouchard, H., Brun, M.-P., Commercon, A. & Zhang, J. Novel Conjugates, Preparation Thereof, and Therapeutic Use Thereof. U.S.A. patent US 2012/0225089 A1 (2012).
46 Beck, Z. Q., Aldrich, C. C., Magarvey, N. A., Georg, G. I. & Sherman, D. H. Chemoenzymatic Synthesis of Cryptophycin/Arenastatin Natural Products. *Biochemistry* **44**, 13457-13466 (2005).
47 Weiss, C., Sammet, B. & Sewald, N. Recent approaches for the synthesis of modified cryptophycins. *Nat. Prod. Rep.* **30**, 924-940 (2013).
48 Seufert, W., Beck, Z. Q. & Sherman, D. H. Enzymatic Release and Macrolactonization of Cryptophycins from a Safety-Catch Solid Support. *Andew. Chem. Int. Ed.* **46**, 9298-9300 (2007).
49 Ding, Y., Seufert, W. H., Beck, Z. Q. & Sherman, D. H. Analysis of the Cryptophycin P450 Epoxidase Reveals Substrate Tolerance and Cooperativity. *J. Am. Chem. Soc.* **130**, 5492-5498 (2008).
50 Ding, Y., Rath, C. M., Bolduc, K. L., Hakansson, K. & Sherman, D. H. Chemoenzymatic Synthesis of Cryptophycin Anticancer Agents by an Ester Bond-Forming Non-ribosomal Peptide Synthetase Module. *J. Am. Chem. Soc.* **133**, 14492 (2011).

CHAPTER 3

Reconstitution and Optimization of Cryptophycin Thioesterase for Chemoenzymatic Macrocyclization

3.1 Introduction to Cryptophycin Thioesterase

Many polyketide synthase (PKS), nonribosomal peptide synthetase (NRPS), and fatty acid synthase (FAS) biosynthetic secondary metabolite pathways contain terminal thioesterases (TEs) to assist in product off-loading through either hydrolysis or intramolecular cyclization. These TEs typically utilize a Serine/Histidine/Aspartic acid catalytic triad, analogous to many serine proteases, to form an acyl intermediate with the Ser through general acid/base catalysis of the His and Asp residues.[1] The first step in this process is recognition and binding of the peptide or polyketide bound to its designated peptidyl (or acyl) carrier protein (P[A]CP) via a thioester with the phosphopantetheine arm (Figure 3.1). Once bound, a tetrahedral intermediate is formed between the peptide thioester and the active site serine, appropriately activated by histidine. The tetrahedral intermediate collapses to yield an acylenzyme complex that can undergo formation of a second tetrahedral intermediate with either water (hydrolysis) or an intramolecular hydroxyl (macrolactonization). Collapse of this second intermediate then liberates either the free acid or the macrocyclic natural product and regenerates the active site.

Bacteria are a rich source of natural products, and they utilize TEs within their biosynthetic machinery for one of two major transformations.[2] The first transformation is basic hydrolysis of chain elongation intermediates to liberate free acid products, such as in the case of the polyketide metabolite

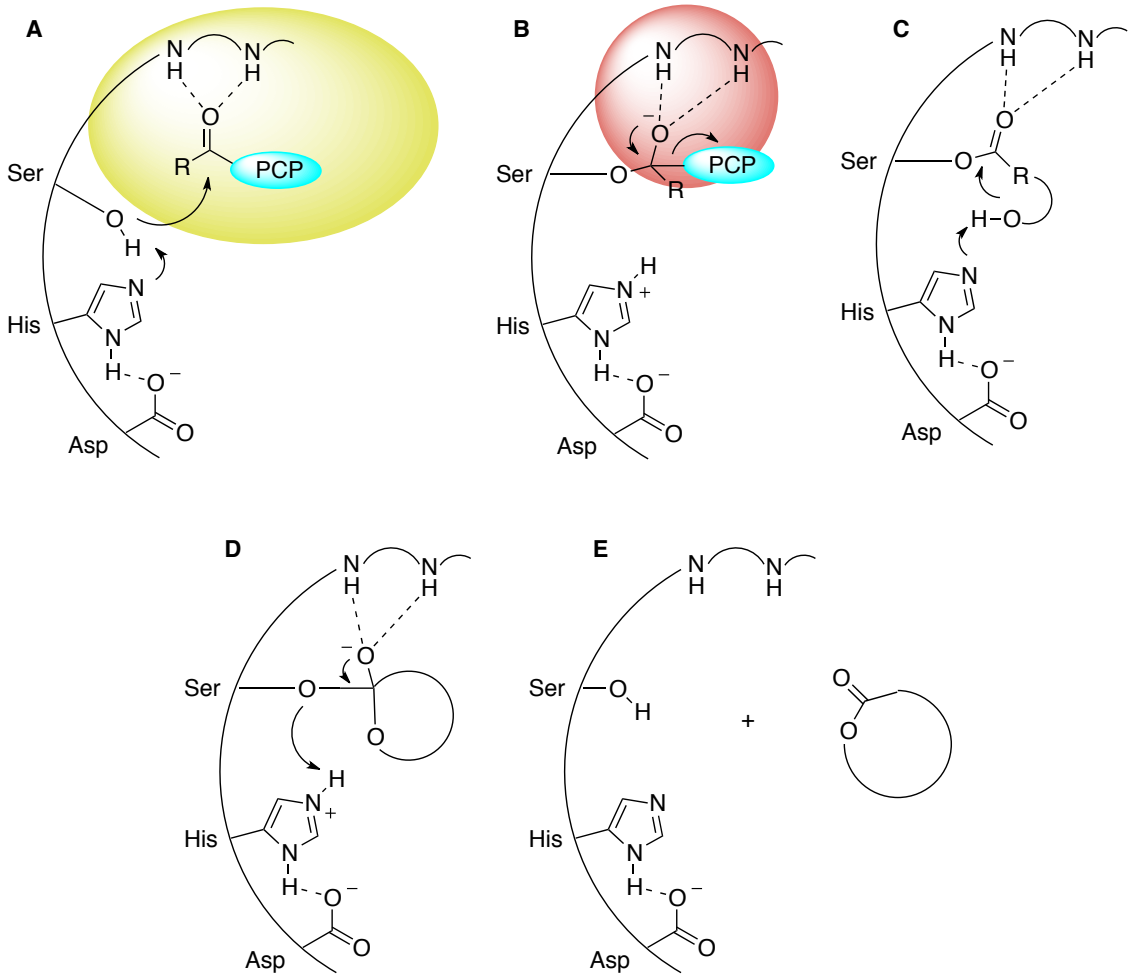

Figure 3.1: Diagram of the basic mechanism of a thioesterase. A) Recognition and binding of PCP (blue)-bound substrate in the peptide binding site (yellow). **B**) Formation of first tetrahedral intermediate with the serine and stabilization in the oxyanion hole (red). **C**) Collapse to expel the PCP and formation of second tetrahedral intermediate with intramolecular hydroxyl. **D**) Collapse of second tetrahedral intermediate. **E**) Return of active site to resting state and release of the macrolactone.

tautomycetin produced by *Streptomyces* sp. CK4412.[3] The characterized tautomycetic gene cluster *tmc* contains a dimeric α,β-hydrolase-type thioesterase similar in structure to other Type I PKS TEs. The action of the TE at the end of module 9 releases the fully extended polyketide as a carboxylic acid (Figure 3.2), and post-PKS maturation is presumed to then catalyze decarboxylative dehydration. A subtype of TE hydrolysis is then the release of a free acid that spontaneously undergoes decarboxylation to form a natural product with an unusual terminal alkene. An example of this uncommon tailoring is the tandem sulfotransferase (ST) and TE domains in the curacin A biosynthetic pathway (Figure 3.2).[4] After sulfonation of the β-

hydroxy-acyl-ACP intermediate, TE hydrolysis, decarboxylation, and sulfate elimination follow to afford the mature product.

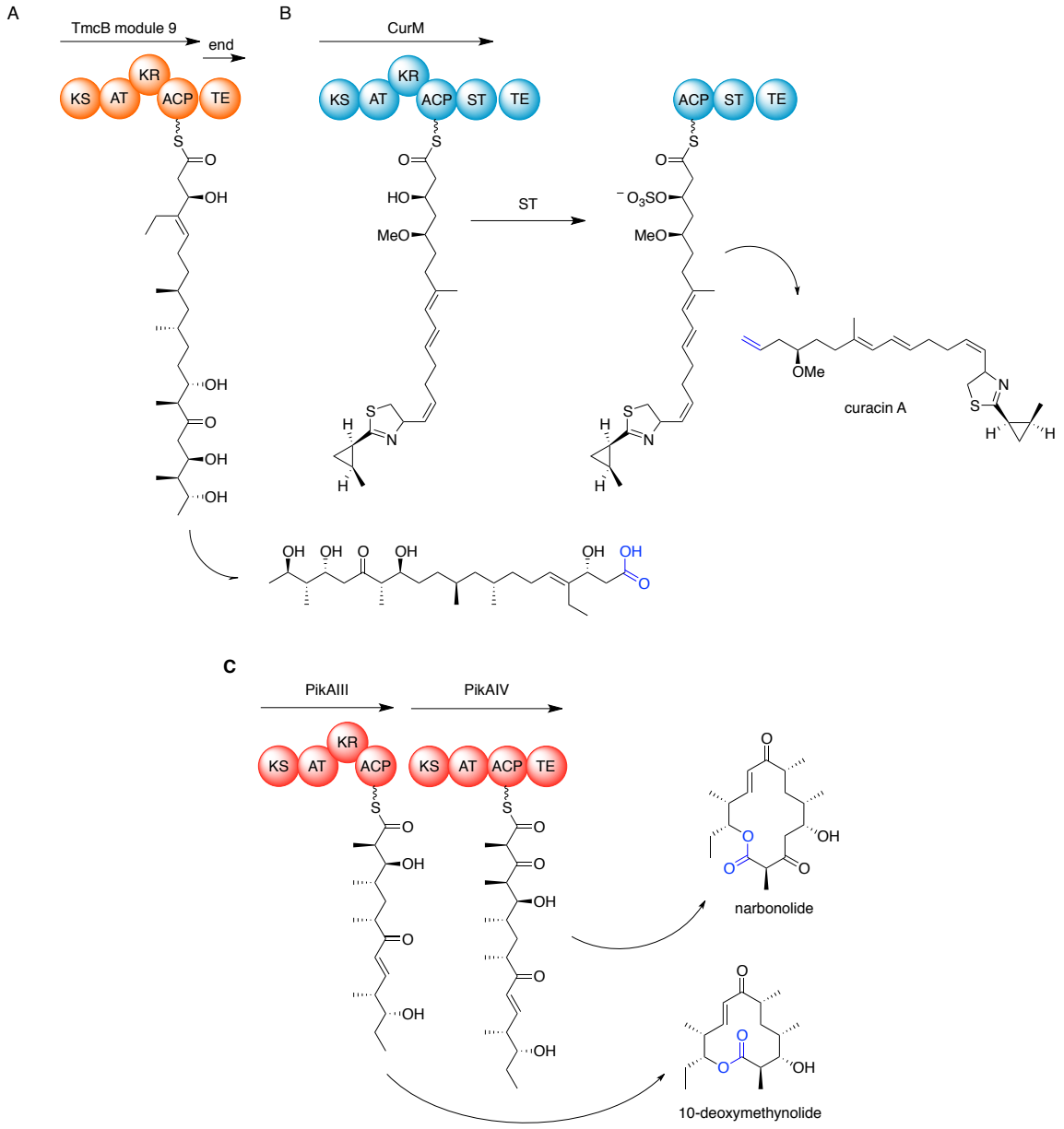

Figure 3.2: Thioesterase functions in three distinct biosynthetic pathways. A) Terminal hydrolysis of the chain elongation product of the tautomycetin pathway to yield a free acid. **B**) Off-loading of the sulfonated intermediate by the TE in CurM results in decarboxylation and sulfate elimination to produce the terminal alkene curacin A. **C**) Differential action of pikromycin TE results in the production of the 12- and 14-membered macrolactones 10-deoxymethynolide and narbonolide, respectively.

The second major type of reaction catalyzed by bacterial biosynthetic TEs is cyclization. One example of macrocyclization is the well-characterized pikromycin pathway.[5] In this context, the pikromycin TE can function

prematurely to terminate polyketide synthesis with PikAIII, yielding the 12-membered macrolactone 10-deoxymethynolide (Figure 3.2). Alternatively, continued elongation by PikAIV and then TE intervention results in the 14-membered macrolactone narbonolide. Employing a pentaketide phosphonate mimic allowed crystallization of this TE with the substrate mimic bound and revealed important structural considerations affecting ring-closure in the pikromycin pathway. A hydrophobic pocket exists close to the active site serine in the immediate vicinity that presumably functions as the substrate recognition and binding site. This chamber opens to a narrower channel that serves as a hydrophobic environment for the bound substrate. The co-crystal structure further suggests the presence of a hydrophilic barrier at the exit of the channel inducing substrates to curl back upon themselves for ring closure. This narrow hydrophobic binding pocket with an exit that induces a conformation change in the substrate enabling macrocyclization appears to be a common strategy employed by many biosynthetic TEs, including the DEBS pathway[6] and likely the cryptophycin pathway as well. While the nonspecific hydrophobic contacts within these active sites afford poor

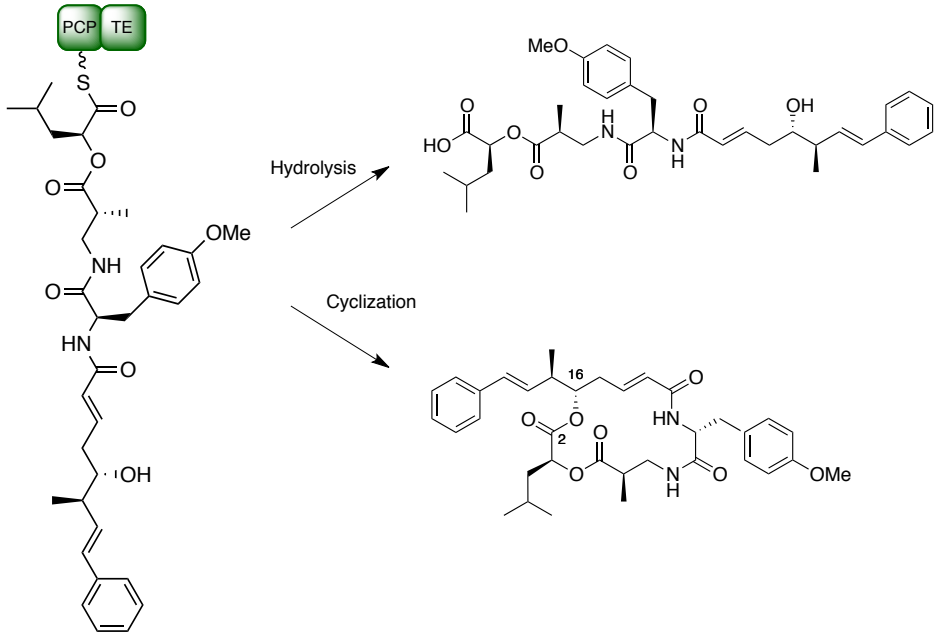

Figure 3.3: TE processing of the cryptophycin PKS/NRPS-derived chain elongation intermediate provides either the free acid through hydrolysis or the macrolactone through cyclization.

substrate specificity, they support the use of biosynthetic TEs as versatile biocatalysts for macrocyclization reactions.

The cryptophycin TE (CrpTE) mediates the termination and cyclization of the mixed PKS/NRPS-derived chain elongation intermediate to give the 16-membered macrolactone between C2 and C16, while hydrolysis to the acid is a competing side reaction (Figure 3.3). To explore the substrate tolerance first hinted at by the diverse array of products produced both naturally[7-10] and from feeding studies,[11] CrpTE was cloned and expressed in *E. coli* and used with chemically synthesized *seco*-cryptophycin *N*-acetylcysteamine (SNAc) thioester substrates.[12] Enzymatic activity for CrpTE was successfully reconstituted *in vitro* after heterologous expression and purification using Ni agarose resin, and the results from enzymatic reactions with the synthetic substrates revealed a 40-fold decrease in cyclization when the pendant phenyl ring was absent on unit A, underscoring the essential function of this ring for macrocyclization. In addition, the presence of a chlorine on the ring of unit B was not necessary for efficient cyclization, and CrpTE was insensitive to the presence or absence of methyl substituents on unit C. Compared to other macrolactone-forming TEs in the epothilone and surfactin biosynthetic pathways, CrpTE was 60 times more efficient at cyclization under comparable conditions.[12] Seufert, Beck, and Sherman[13] then demonstrated the first application of CrpTE to the macrocyclization of solid-supported acylsulfonamide substrates for the production of cryptophycins. The extraordinary tolerance and efficiency displayed by CrpTE has thus encouraged our continued efforts to develop it as a highly efficient and flexible biocatalyst for chemoenzymatic production of substantial quantities of novel cryptophycins.

3.2 SYNTHESIS OF NOVEL *SECO*-CRYPTOPHYCIN SNAC-THIOESTER SUBSTRATES

In the natural biosynthetic system, a peptidyl carrier protein (PCP)-bound substrate is shuttled between domains. This PCP anchors the chain

elongation intermediate through a phosphopantetheine arm, which must be mimicked to access CrpTE activity. Previous research revealed that SNAc was structurally identical to the terminus of the phosphopantetheine arm and an excellent stand-in for PKS and NRPS substrates.[12,14-16] Therefore, SNAc was employed here to generate synthetic *seco*-cryptophycin thioester substrates for enzymatic macrolactonization by CrpTE.

The substrates were synthesized in the reverse order of biosynthesis starting with unit D using a route previously reported in the Sherman lab[12] with minor modifications (Scheme 3.1). The original synthesis reporting direct thioesterification of (*S*)-leucic acid (**75**) using SNAc in acetone with EDC and $NaHCO_3$ was not successful, so an alternative transformation was sought. To decrease the number of protection and deprotection steps, a direct protection of the alcohol using pyridine with boc anhydride was developed to access **76**. Although the yield of **76** was low, the inexpensive, commercially available starting material allowed the reaction to be run on scale, and solvent exchange from DMF to THF simplified purification and improved the yield.

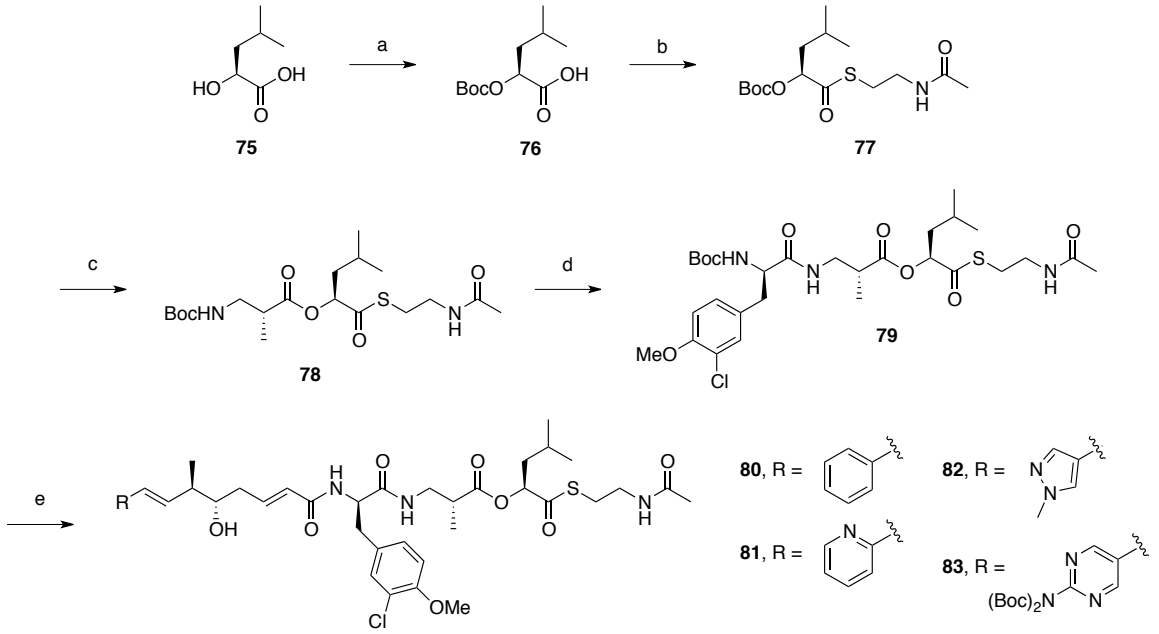

Scheme 3.1: Synthesis of seco-cryptophycin SNAc-thioester substrates for CrpTE-mediated macrocyclization. *Reaction conditions:* (a) $(Boc)_2O$, pyridine, THF, rt (27%); (b) SNAc, EDC, HOBt, DIPEA, CH_2Cl_2, rt (46%); (c) 4 N HCl/dioxane, rt, then (*R*)-3-(Boc-amino)-2-methylpropionic acid, EDC, HOBt, DIPEA, THF, rt (32%); (d) 4 N HCl/dioxane, rt, then **87**, EDC, HOBt, DIPEA, THF, rt (70%); (e) 4 N HCl/dioxane, rt, then unit A analogue (Figure 2.1), EDC, DIPEA, THF, rt (46-55%).

The thioester **77** was constructed using SNAc and the common coupling reagents EDC and HOBt. Initial attempts at this coupling using catalytic dimethylaminopyridine (DMAP) resulted in significant recovery of the free acid through aminolysis of the newly formed thioester. This decomposition pathway was confirmed when the same problem was observed using piperidine to deblock Fmoc-protected starting material. As a result, all nucleophilic amines were excluded from contact with the peptide thioester **77** and all subsequent thioester-containing intermediates.

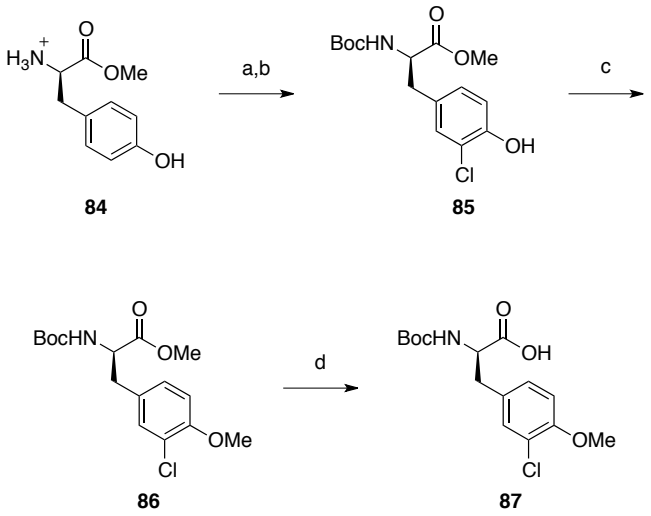

Scheme 3.2: Synthesis of unit B from D-tyrosine methyl ester. *Reaction conditions:* (a) SO_2Cl_2, AcOH, Et_2O, rt; (b) $(Boc)_2O$, $NaHCO_3$, THF/MeOH (4:1), rt (89%, a-b); (c) MeI, K_2CO_3, acetone, reflux (79%); (d) $LiOH•H_2O$, THF/H_2O (4:1), rt (quant.).

Unit C was the next subunit for incorporation and was purchased from Sigma as (*R*)-3-(Boc-amino)-2-methylpropionic acid. Deprotection of **76** with 4 N HCl in dioxane and standard coupling conditions with EDC and HOBt then afforded dipeptide thioester **78** in moderate yield. Recent studies have identified MSNT and NMI as better coupling reagents for the formation of the hindered ester, with yields of **78** as high as 61% (J. Schmidt). Then, unit B was first prepared synthetically from D-tyrosine methyl ester using the unpublished method of W. Seufert, with minor modification (Scheme 3.2). Chlorination with sulfuryl chloride followed by boc protection of the hydrochloride salt afforded chlorotyrosine **85**. Subsequent methylation and saponification then provided the desired boc-unit B acid in excellent yield for

coupling. This coupling was achieved by treating **78** with 4 N HCl/dioxane and reacting the resulting amine with **87** and EDC/HOBt. With **79** in hand, the final step to *seco*-cryptophycins was attachment of either unit A or any of the prepared analogues using identical coupling conditions. As of the time of writing this dissertation, four complete *seco*-cryptophycins had been completed: natural phenyl (**80**), 2-pyridyl (**81**), methylpyrazolyl (**82**), and 2-(boc-amino)pyrimidinyl (**83**).

Analogous chemistry exists for the synthesis of these *seco*-cryptophycins supported on solid phase,[13] but attempts to copy this procedure were unfruitful, possibly due to the lack of availability of the originally used safety-catch PEGA resin. In addition, the maximum swelling diameter of the resin was determined to be very near the lower size limit of CrpTE, which suggested poor diffusion of the enzyme into the support matrix.

3.3 Production of CrpTE and Optimization of Enzymatic Activity

The expression and purification of CrpTE was carried out as previously reported by Beck et al. as the pET28b construct in *E. coli* strain BL21 (DE3).[12] Briefly, 1 L cultures of 2XYT media containing 50 µg/mL kanamycin were inoculated with an LB starter culture and grown to OD_{600} of 0.6-0.8 at 37

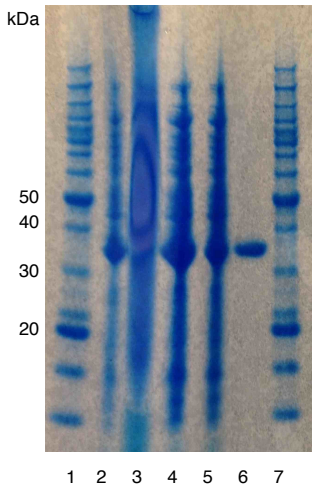

Figure 3.4: SDS-PAGE gel depicting purification of CrpTE. Lane 1, Invitrogen Benchmark™ protein ladder; lane 2, whole cell protein after induction; lane 3, insoluble lysate pellet; lane 4, lysate soluble fraction; lane 5, resin flow through; lane 6, purified CrpTE; lane 7, Invitrogen Benchmark™ protein ladder.

°C. Overexpression was induced by the addition of 100 µM IPTG at 30 °C for approximately 16 h. CrpTE was purified on Ni agarose resin to >95% purity and matched the expected average mass of 35,550 Da (Figure 3.4). A yield of approximately 6 mg protein/liter culture was obtained as calculated from a Coomassie standard curve using bovine serum albumin (BSA). Purified protein aliquots were stored in phosphate buffer, snap frozen in liquid nitrogen, and stored at -80 °C until needed.

3.3.1 Confirmation of In Vitro *Activity and Promiscuity*

Successful implementation of CrpTE as a biocatalyst in the production of cryptophycin analogues requires substantial inherent substrate promiscuity. Small-scale enzymatic reactions were therefore carried out on CrpTE with both natural and heterocycle-bearing cryptophycin substrates. The ability of CrpTE to load and cyclize cryptophycins was first tested with natural substrate after expression of *E. coli* BL21 (DE3) containing the pET28b *crpTE* plasmid. Reactions were set up in 1.7 mL Eppendorf tubes and contained 100 µM protein, 500 µM substrate (in DMSO), 5% (v/v) DMSO, and 100 mM sodium phosphate buffer, pH 7.0 in 100 µL total volume. After incubation at 28 °C for 24 h, reactions were quenched by the addition of double the volume of ethyl acetate (2 x 200 µL) and the organics were removed under a stream of nitrogen. The residues from these reactions were then used directly for the preparation of acetonitrile solutions for LC-QTOF-MS analysis. Gratifyingly, the purified CrpTE was found to convert **88** to cryptophycin 4 at levels comparable to previous reports[12] (**Cr4**, 63% conversion, Figure 3.5) and had little interbatch variability. In a separate study, addition of a second 100 µM aliquot of enzyme after 24 h followed by incubation at 28 °C for another 16 h increased conversion to the macrolactone from 40% to 60%. Moreover, crude cell lysate containing CrpTE was tested for activity and found to be approximately equal to purified enzyme, but it was not possible to quantify the

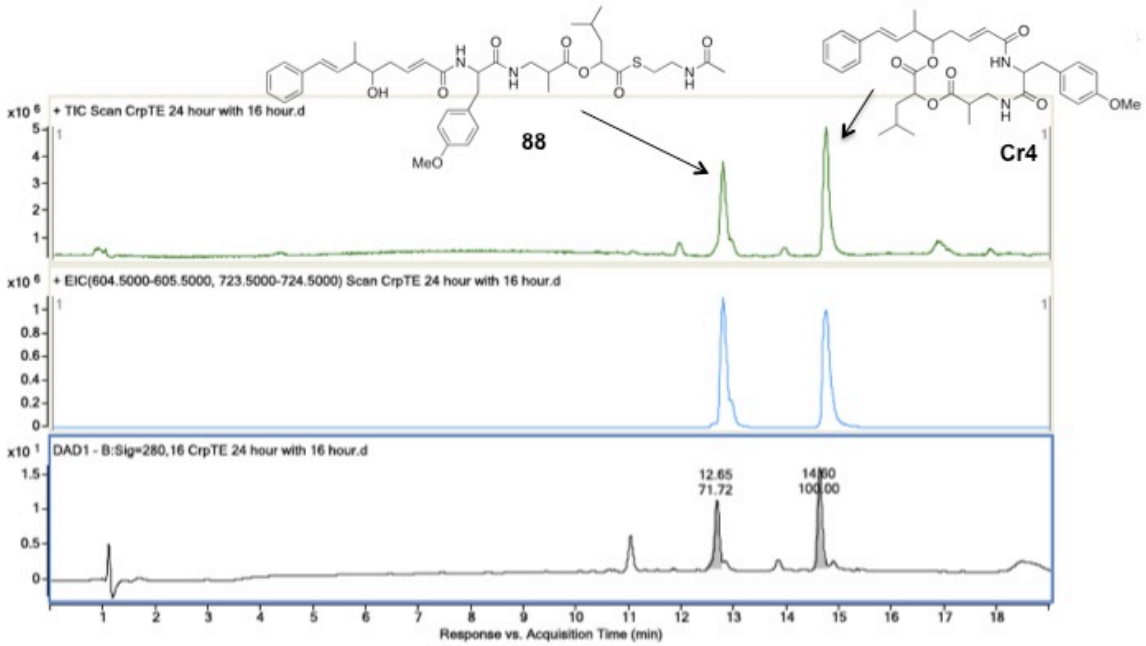

Figure 3.5: Recapitulation of CrpTE activity on natural substrate 88. Reaction contained 100 uM CrpTE and 500 uM **88** in 50 mM sodium phosphate buffer, pH 7.0 with 10% DMSO at 23 °C for 24 h. Reaction analyzed by LC-QTOF-MS using a Phenomenex HydroRP column. Top panel, TIC of LC-QTOF-MS; middle panel, EIC searching for $[M+H]^+$ of **88** and **Cr4**; bottom panel, UV absorbance at 280 nm. Conversions were calculated as the ratios of the macrocycle UV trace AUCs to remaining starting material and free acid UV trace AUCs.

amount of CrpTE in the lysate and was thus not the preferred preparation for enzymatic reactions. Nevertheless, the use of crude cell lysate would be a viable option for preparative scale reactions.

The activity of CrpTE was then expanded to unnatural cryptophycin substrates containing 2-, 3-, and 4-pyridyl rings, as well as a pinacol boronic ester, on unit A. Under the standard reaction conditions described above, CrpTE displayed remarkable flexibility in the cyclization of all of the tested heterocyclic unit A analogues (Table 3.1 and Figure 3.6) with impressive conversion. Surprisingly, the 3-pyridyl unit A substrate was cyclized with a higher efficiency than the natural substrate, suggesting a positive effect for the pyridine nitrogen in cyclization when located in the 3- position on the ring of unit A. It is possible this effect was achieved through the ring nitrogen inducing a favorable binding mode for cyclization or by associating with active site water to disfavor hydrolysis. Conversions were calculated from the ratios of the AUCs of the UV_{280} signals in the LC traces.

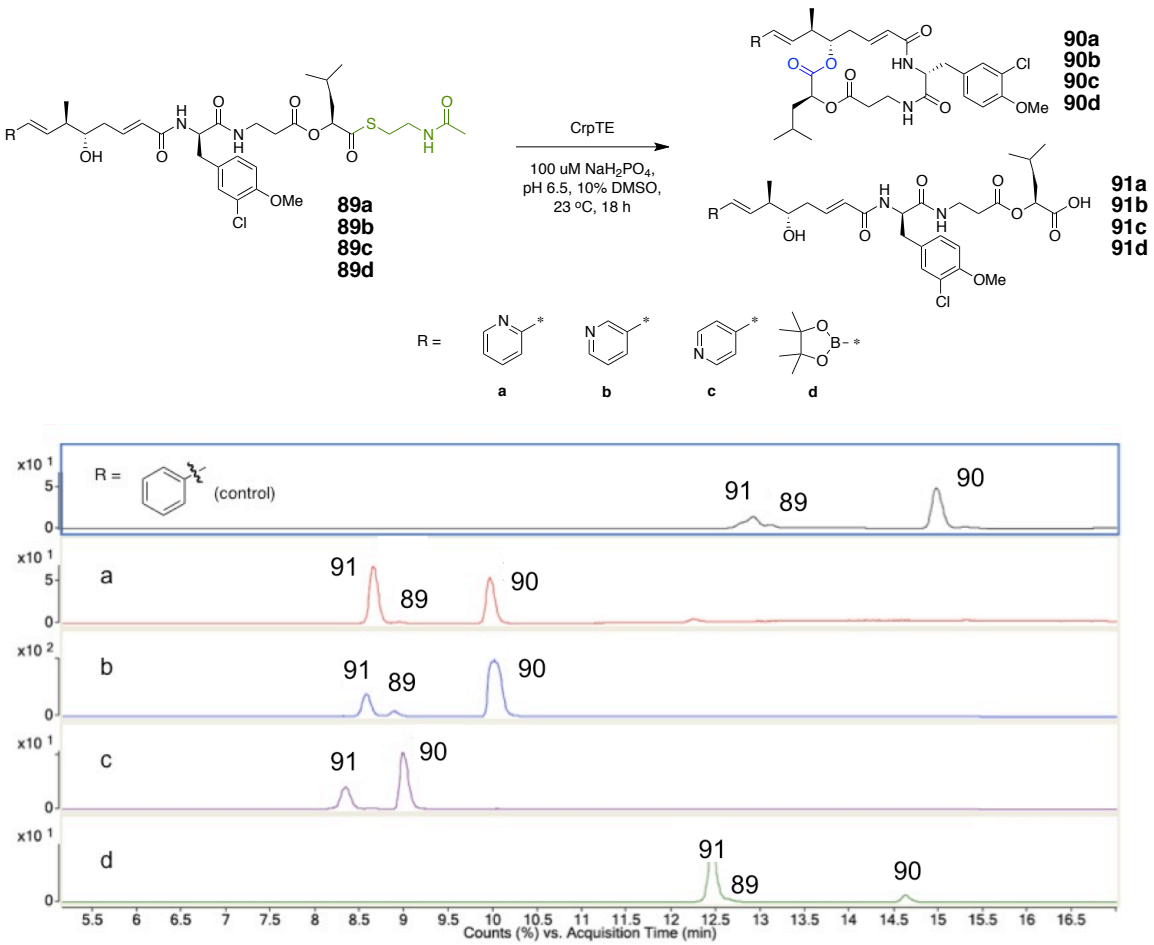

Figure 3.6: LC-QTOF-MS spectra (EIC) of CrpTE enzymatic reactions. Top panel shows reaction using natural substrate as a control with unreacted substrate (**89**), desired macrocycle (**90**), and hydrolysis side product (**91**) indicated. Subsequent panels show product distribution with a suite of unnatural heterocyclic substrates. Reaction: 100 µM CrpTE, 50 mM sodium phosphate, pH 6.5, 500 µM substrate, 10% DMSO, 23 °C, 18 h.

Table 3.1: Comparison of cyclization, hydrolysis, and no reaction of natural and heterocyclic cryptophycin substrates of CrpTE. Conversions were calculated as the ratios of the macrocycle UV trace AUCs to remaining starting material and free acid UV trace AUCs.

Substrate	*Cyclization (**90**)*	*Hydrolysis (**91**)*	*Unreacted (**89**)*
Control	63%	27%	10%
89a	37%	60%	3%
89b	73%	19%	7%
89c	61%	39%	0%
89d	18%	82%	0%

3.3.2 CrpTE Timecourse Study

Traditionally, the CrpTE reactions were allowed to proceed overnight or for up to 24 h, but literature precedent indicated that the lifetimes of the

majority of enzymes are significantly shorter. Therefore, delineating the lifetime of CrpTE in our *in vitro* reaction conditions could reduce the need for labor-intensive steps and maximize enzymatic conversion through the addition of aliquots of enzyme in regular intervals according to the lifetime of CrpTE. A simple timecourse study was thus conducted on CrpTE with substrate **88** under standard reaction conditions (Figure 3.7). As can be seen from the table, CrpTE continued to be active up to 8 h, after which negligible increases in product conversion was observed. An effective lifetime of 8 h

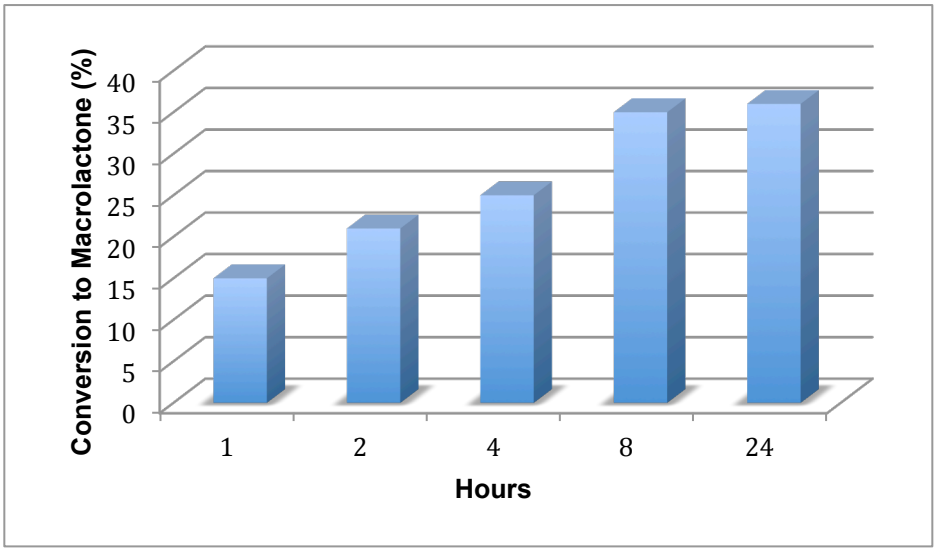

Figure 3.7: CrpTE timecourse study to determine enzyme lifetime. *Reaction conditions:* 100 μM CrpTE, 50 mM sodium phosphate, pH 7.0, 500 μM **88**, 5% DMSO, 28 °C. Conversions were calculated as the ratios of the macrocycle UV trace AUCs to remaining starting material and free acid UV trace AUCs.

was therefore determined for CrpTE, which represented a potential advancement towards developing an effective enzyme dosing regimen for future chemoenzymatic synthesis.

3.3.3 CrpTE Tolerance of Reaction Buffer pH and Temperature

The pH of the buffer in an enzymatic reaction has been demonstrated to significantly impact protein and/or substrate stability, as well as enzymatic activity, as can reaction temperature. We also speculated that pH might affect the relative rates of hydrolysis versus cyclization. Therefore, a series of enzymatic reactions was run with buffer pH values of 6.0, 6.5, or 8.0 at both

23 °C and 28 °C. pH values outside of this range would likely result in protein denaturation and were not tested. Interestingly, CrpTE activity was insensitive to pH values ranging from 6.0 to 8.0, as conversions for the 2-pyridyl substrate **89a** were all within 5% (Figure 3.8) of each other. However, as high as 11% hydrolysis of the SNAc thioester in the no enzyme control was observed when the buffer pH was 8.0 (data not shown). Furthermore, little variation was found when comparing conversions at the two temperatures tested. Considering these results, CrpTE reactions were all performed in buffer at the optimal pH values of 6.5 or 7.0 at ambient room temperature.

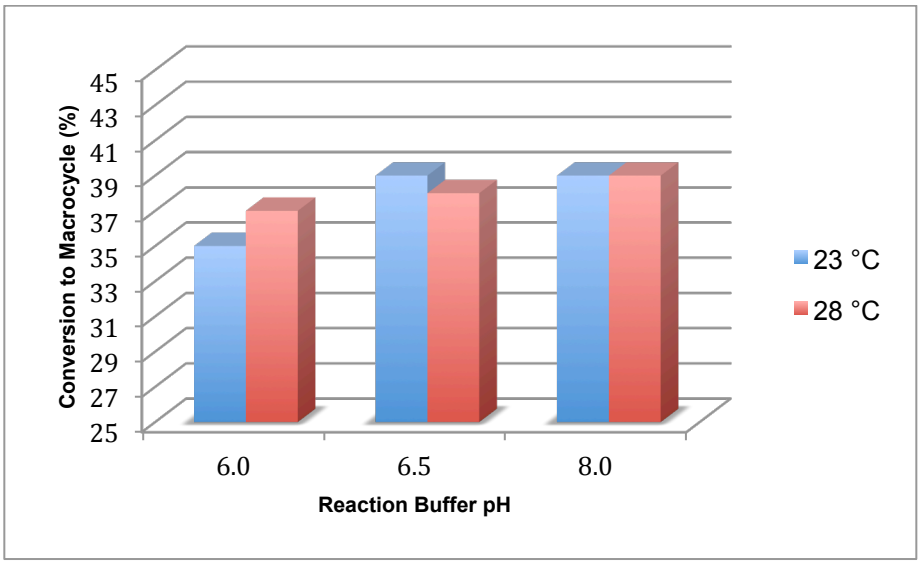

Figure 3.8: CrpTE tolerance of reaction temperature and pH. *Reaction conditions:* 100 μM CrpTE; 50 mM sodium phosphate, pH 6.0, 6.5, or 8.0; 500 μM **89a**; 10% DMSO; 23 or 28 °C. Conversions were calculated as the ratios of the macrocycle UV trace AUCs to remaining starting material and free acid UV trace AUCs.

3.4 Large-Scale Macrolactonization with CrpTE

To bring large-scale chemoenzymatic production of novel cryptophycins one step closer to reality, the enzymatic reactions must be scaled and optimized to synthetically relevant levels without needing prohibitively large volumes or amounts of enzyme. For this purpose, 20 mL solid phase extraction (SPE) reservoirs from Sigma were found to be well-suited for enzymatic reactions between 5 and 10 mL total volume. In addition, the plastic containers did not retain the cyclized cryptophycins – a possible

complication noted previously (Y. Ding, personal communication) – and a fritted bottom with an outlet port allowed precipitation and filtration of the denatured protein from the reaction. A typical large-scale CrpTE reaction was modeled on the macrocyclizations performed on solid phase[13] and contained 200 μM purified enzyme, *seco*-cryptophycin SNAc-thioester substrate, DMSO, and 100 mM sodium phosphate buffer, pH 7.0 to complete the reaction volume. Once all of the components were combined, the SPE reservoirs were tightly capped and agitated at 250 rpm at ambient room temperature. After an overnight incubation, the reactions were quenched and protein precipitated using twice the volume of ethyl acetate, then filtered though a plug of celite.

The first scale-up of the CrpTE macrocyclization aimed to maximize the quantity of natural substrate **80** exposed to the enzyme and decrease the number of discrete, parallel reactions necessary to convert all of the material on hand. Unfortunately, a final concentration of 2.5 mM in a 7% DMSO reaction found the substrate to be poorly soluble as indicated by a considerable amount of white precipitate suspended in solution. Not surprisingly, the corresponding conversion to the macrocycle cryptophycin 1 was very low in this reaction (Reaction A, Table 3.2). The observation that macrocyclization by CrpTE was possible at volumes 50 times greater than any previously attempted however was encouraging. Halving the concentration of the substrate to 1.25 mM and increasing the volume to 10 mL with 10% DMSO (Reaction B) still resulted in significant precipitation and consequently low conversion. Additional CrpTE was also added to these reactions after the initial 18 h incubation to improve conversion, but without significant results. Lacking a strong UV signal for these reactions in the LC traces it was difficult to quantify the low levels of conversion observed. Further reduction in substrate **80** concentration to 0.75 and 0.5 mM finally exhibited a response to the improved solubility as increased conversion to the macrocycle (Reactions C and D). These results strongly alluded to CrpTE activity being limited by substrate solubility. Using 0.5 mM as the maximum

tolerated substrate concentration, CrpTE was found to have little preference for total reaction volume in the SPE reservoirs (compare Reactions D and E).

Operating under the hypothesis that the introduction of heterocycles would improve cryptophycin solubility, the 2-pyridyl substrate **81** was also optimized under large-scale chemoenzymatic conditions. Encouragingly, conversion to the macrocycle **92** was acceptable at a starting concentration higher than tolerated for the natural phenyl-containing substrate (Reaction G).

Table 3.2: Optimization of large-scale CrpTE macrolactonization. *Reaction conditions:* 100 μM CrpTE, substrate **80** or **81**, 100 mM sodium phosphate, pH 7.0, DMSO, 23 °C, 18 h. Conversions were calculated as the ratios of the macrocycle UV trace AUCs to remaining starting material and free acid UV trace AUCs.

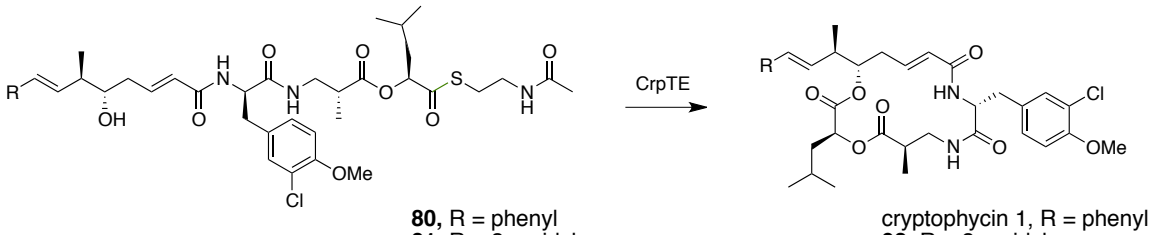

80, R = phenyl
81, R = 2-pyridyl

cryptophycin 1, R = phenyl
92, R = 2-pyridyl

Reaction	[Substrate]	~[CrpTE]	Reaction Volume	[DMSO]	Conversion
A	**80**, 2.5 mM	100 μM	5 mL	7%	<10%
B	**80**, 1.25 mM	100 μM	10 mL	10%	<10%
C	**80**, 0.75 mM	100 μM	10 mL	10%	17%
D	**80**, 0.5 mM	100 μM	5 mL	10%	28%
E	**80**, 0.5 mM	100 μM	10 mL	10%	24%
F	**80**, 0.5 mM	100 μM	5 mL	25%	31%
G	**81**, 1.25 mM	100 μM	10 mL	10%	34%
H	**81**, 0.75 mM	100 μM	5 mL	10%	33%
I	**81**, 0.5 mM	100 μM	10 mL	10%	41%
J	**81**, 0.75 mM	100 μM	5 mL	25%	52%

Decreasing the concentration of **81** again improved the conversion to almost twice that observed for the natural substrate (compare Reactions E and I), which was strong evidence that CrpTE activity was limited by the solubility of its substrate in the reaction medium.

The increasing conversions observed for substrates **80** and **81** when used at either concentrations lower than 0.75 mM or DMSO fractions higher than 7% prompted a quick test of CrpTE DMSO tolerance. Reactions with CrpTE and substrate **80** ranging from 10 to 30% DMSO were thus analyzed

for conversion to the macrocycle. Conversions were found to increase linearly with DMSO concentrations up to 30% and confirmed substrate solubility as the limiting factor in chemoenzymatic cyclization by CrpTE (Figure 3.9). Applying this newly discovered organic tolerance, large-scale reactions were repeated with **80** and **81** using 25% DMSO in the reactions. As can be seen for Reactions F and J in Table 3.2, conversion to the macrocyclic product was

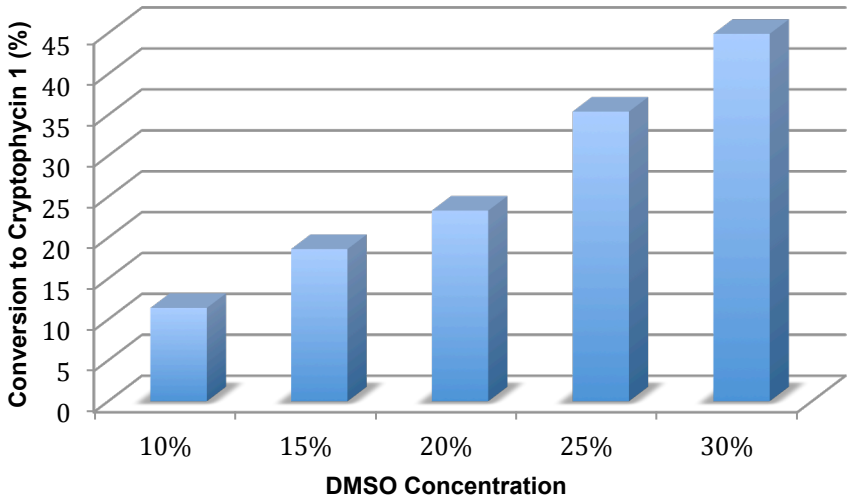

Figure 3.9: Initial analysis of CrpTE DMSO tolerance. *Reaction conditions:* ~100 μM CrpTE, 500 μM substrate **80**, 50 mM sodium phosphate, pH 6.5, 23 °C, 18 h. Conversions were calculated as the ratios of the macrocycle UV trace AUCs to remaining starting material and free acid UV trace AUCs.

significantly increased using the higher DMSO concentration, and visual inspection revealed far less precipitate suspended in the reactions. It is anticipated that using increased organic fractions with poorly soluble substrates will prove to be an excellent optimization strategy in the future.

3.5 Optimization of CrpTE Substrate Solubility with Organic Cosolvents

The limited aqueous solubility of the *seco*-cryptophycin SNAc-thioesters became apparent during optimization efforts in large-scale chemoenzymatic synthesis. The significant hindrance their hydrophobicity presented to scale-up was tackled by investigating new methods for solubilizing our synthetic substrates with CrpTE in aqueous buffer using organic solvents for maximum chemoenzymatic processing. Not only could

the application of organic solvents help to improve substrate solubility and therefore accessibility, but certain solvent systems could actually increase enzyme function and stability.[17]

Research into the use of enzymes in organic solvents has been on-going for decades,[18] and one of the more striking examples was the observation of lipase activity in organic solvent containing as little as 0.02% water.[19] In this case, it was necessary to "pH imprint" the proteins by lyophilizing them from a buffer at the optimum pH for activity and then reconstituting in the mixed organic/aqueous system. The authors further described a completely unexpected result where the lipases were only able to carry out certain functions to an appreciable extent when in organic solvent, a phenomenon termed "medium engineering".[20] However only a limited number of enzymes were active directly in organic solvent, namely lipases, but this family was expanded to include proteases when lyophilization of subtilisin with a competitive inhibitor resulted in an enzyme that was 100 times more active in organic solvent than unbound protein.[21] Incredibly, this ligand-induced "enzyme memory" extended to protein stability, affinity, and specificity as well. To expand the toolbox of enzymes for use in environments other than aqueous buffer, ionic liquids[22] and protein engineering[23] have also been investigated to improve solubility and stability.

With previous research as inspiration, using CrpTE in mixtures of water and common organic solvents was investigated for the production of cryptophycin 1. Dimethyl sulfoxide (DMSO), acetone, 1,2-dimethyoxyethane (DME), and diglyme were chosen because they were highly miscible in water, were capable of completely dissolving the *seco*-cryptophycin substrates, and lacked any potentially nucleophilic functionality that could intercept the acyl-enzyme intermediate (as previously observed with glycerol). A series of reactions were performed in which standard CrpTE conditions were followed with substrate **80** except for the addition of 10%, 20%, 30%, 40%, or 50% (v/v) organic solvent. The effects of the addition of the common solubilizing agents

methylcellulose (MC) and methyl β-cyclodextrin (MCD) to standard 10% DMSO reactions were also explored. After overnight incubation at ambient room temperature, the reactions were quenched and extracted with twice the volume of ethyl acetate (2 x 200 μL). The organic layers were combined and dried under a stream of nitrogen, and the residues were dissolved in 100 μL of acetonitrile for LC-QTOF-MS analysis.

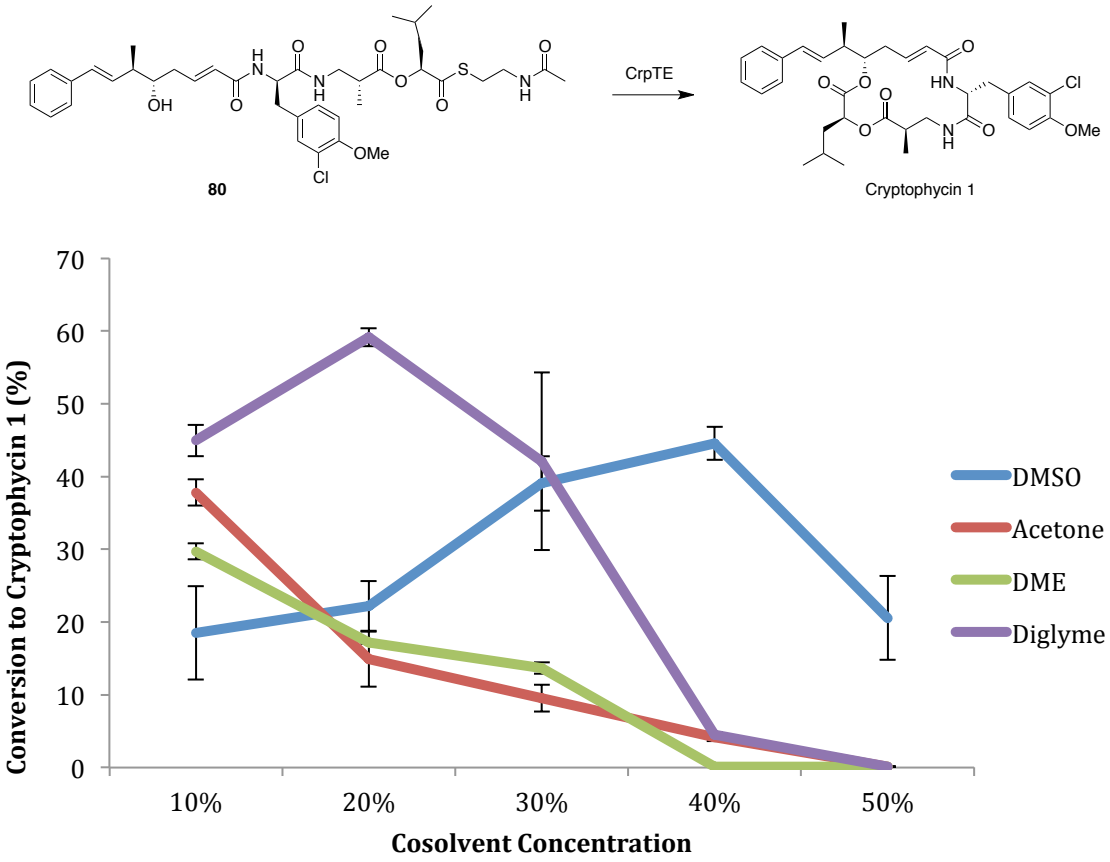

Figure 3.10: CrpTE cosolvent study for conversion of substrate 80 to cryptophycin 1. *Reaction conditions:* ~100 μM CrpTE, 500 μM substrate **80**, 50 mM sodium phosphate, selected organic solvent, pH 6.5, 23 °C, 18 h. Conversions were calculated as the ratios of the macrocycle UV trace AUCs to remaining starting material and free acid UV trace AUCs.

Comparing the results of the CrpTE cosolvent study in Figure 3.10 revealed exceptional tolerance of CrpTE to a variety of organic solvents up to 50% of the reaction volume. At 10%, DMSO surprisingly gave the lowest

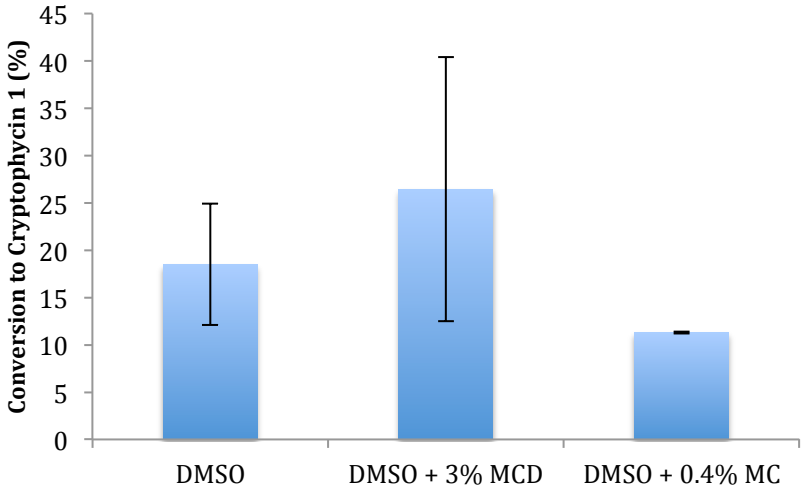

Figure 3.11: Comparison of CrpTE conversion efficiency with common solubilizing agents. *Reaction conditions:* 100 μM CrpTE, 500 μM substrate **80**, 50 mM sodium phosphate, pH 6.5, 10% DMSO, 23 °C, 18 h. Conversions were calculated as the ratios of the macrocycle UV trace AUCs to remaining starting material and free acid UV trace AUCs.

conversion, while diglyme gave nearly twice this conversion. As the organic portion was increased to 20% and then 30% of the reaction volume, conversion in acetone and DME quickly fell off. This drop was the result of significant protein precipitation observed at these concentrations. DMSO and diglyme, however, continued to show very high levels of substrate conversion. Pushing to even higher organic concentrations of 40% and 50%, DMSO maintained enzyme activity with conversions plateauing around 30%, while diglyme eventually succumbed to enzyme precipitation and loss of activity. The solubilizing agent MC, when used as a 0.4% solution in the reaction medium, appeared to have a slight negative affect on substrate conversion (Figure 3.11). By comparison, conversion in the presence of 3% MCD was more variable but could potentially improve enzymatic activity. Future work on the use of cosolvent systems with CrpTE will determine if the high organic content simply increases enzyme activity through enhanced substrate solubility or improves enzyme *efficiency* for cyclization through a modified enzyme/solvent network. A comparison of the ratios between cyclization and hydrolysis under standard and cosolvent conditions should clarify the role of high organic solvent content on CrpTE. While this cosolvent approach to

CrpTE is still relatively simple, it represents a significant improvement in conversion and *the first such use of a biosynthetic macrocycle-forming TE in high organic solvent content*. It is also an important first step in the optimization of the chemoenzymatic synthesis of novel cryptophycins.

3.5.1 Large-Scale Macrocyclizations with Organic Cosolvent

The lessons learned from the cosolvent study were applied to the optimization of large-scale macrocyclizations with CrpTE. A set of four 5 mL reactions were carried out where substrates **80** and **81**, at 500 and 750 µM, respectively, were incubated with CrpTE under either standard conditions of 10% DMSO in buffer or 20% diglyme with 1% MCD in buffer for enhanced solubility. After agitating in SPE tubes at room temperature overnight, the

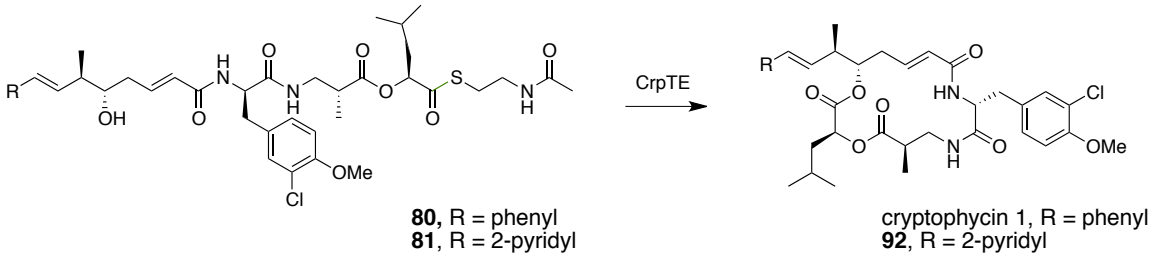

80, R = phenyl
81, R = 2-pyridyl

cryptophycin 1, R = phenyl
92, R = 2-pyridyl

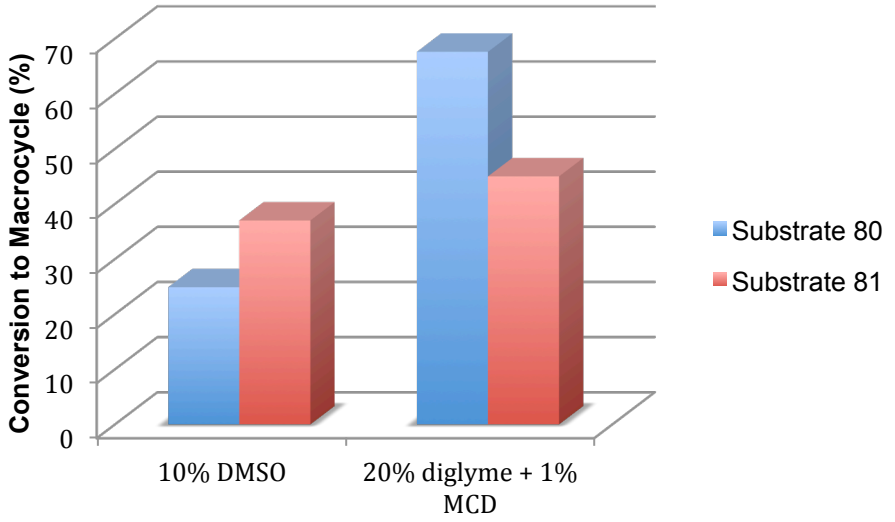

Figure 3.12: Comparison of large-scale CrpTE conversion under standard conditions and with high organic cosolvent. Reactions contained ~100 µM CrpTE, substrate **80** (500 µM) or **81** (750 µM), 100 mM sodium phosphate, pH 7.0, 23 °C, 160 rpm, 18 h. Conversions were calculated as the ratios of the macrocycle UV trace AUCs to remaining starting material and free acid UV trace AUCs.

reactions were quenched and extracted with 2 portions of 10 mL EtOAc. Small aliquots (200 µL) of the organic layers were then removed for LC-QTOF-MS analysis. Comparing the data in Figure 3.12, the reactions conducted with 20% diglyme and 1% MCD had significantly improved conversion to the macrocycle. The natural phenyl-bearing unit A substrate (**80**) in particular was responsive to the high organic conditions, with conversion increasing from 24.9% to 67.6% under otherwise identical conditions. In practice, purification of the product after CrpTE action on substrate **81** afforded a 35% yield of the new analogue cryptophycin 500 (**92**). These results indicate a major limiting factor in chemoenzymatic synthesis is substrate solubility and speak to the strongly positive effect organic cosolvents have on preparative scale CrpTE conversions.

LITERATURE REFERENCES

1 Hedstrom, L. Serine Protease Mechanism and Specificity. *Chem. Rev.* **102**, 4501-4523 (2002).

2 Burja, A. M., Banaigs, B., Abou-Mansour, E., Burgess, J. G. & Wright, P. C. Marine cyanobacterial - a prolific source of natural products. *Tetrahedron* **57**, 9347-9377 (2001).

3 Scaglione, J. B. *et al.* Biochemical and Structural Characterization of the Tautomycetin Thioesterase: Analysis of a Stereoselective Polyketide Hydrolase. *Angew. Chem. Int. Ed.* **49**, 5726-5730 (2010).

4 Gehret, J. J. *et al.* Terminal Alkene Formation by the Thioesterase of Curacin A Biosynthesis. *J. Biol. Chem.* **286**, 14445-14454 (2011).

5 Akey, D. L. *et al.* Structural basis for macrolactonization by the pikromycin thioesterase. *Nat. Chem. Biol.* **2**, 537-542 (2006).

6 Tsai, S.-C. *et al.* Crystal structure of the macrocycle-forming thioesterase domain of the erythromycin polyketide synthase: Versatility from a unique substrate channel. *Proc. Nat. Acad. Sci.* **98**, 14808-14813 (2001).

7 Schwartz, R. E. *et al.* Pharmaceuticals from Cultured Algae. *J. Indust. Microbiol.* **5**, 113-124 (1990).

8 Subbaraju, G. V., Golakoti, T., Patterson, G. M. & Moore, R. E. Three new cryptophycins from Nostoc sp. GSV 224. *J. Nat. Prod.* **60**, 302-305 (1997).

9 Chaganty, S., Golakoti, T., Heltzel, C., Moore, R. E. & Yoshida, W. Y. Isolation and Structure Determination of Cryptophycins 38, 326, and 327 from the Terrestrial Cyanobacterium Nostoc sp. GSV 224. *J. Nat. Prod.* **67**, 1403-1406 (2004).

10 Golakoti, T. *et al.* Structure determination, conformational-analysis, chemical-stability studies, and antitumor evaluation of the cryptophycins: Isolation of 18 new analogs from Nostoc sp. strain GSV-224. *J. Am. Chem. Soc.* **117**, 12030-12049 (1995).

11 Magarvey, N. A. *et al.* Biosynthetic Characterization and Chemoenzymatic Assembly of the Cryptophycins. Potent Anticancer Agents from Nostoc Cyanobionts. *ACS Chem. Biol.* **1**, 766-779 (2006).

12 Beck, Z. Q., Aldrich, C. C., Magarvey, N. A., Georg, G. I. & Sherman, D. H. Chemoenzymatic Synthesis of Cryptophycin/Arenastatin Natural Products. *Biochemistry* **44**, 13457-13466 (2005).

13 Seufert, W., Beck, Z. Q. & Sherman, D. H. Enzymatic Release and Macrolactonization of Cryptophycins from a Safety-Catch Solid Support. *Andew. Chem. Int. Ed.* **46**, 9298-9300 (2007).

14 Pohl, N. L., Gokhale, R. S., Cane, D. E. & Khosla, C. Synthesis and Incorporation of an N-Acetylcysteamine Analogue of Methylmalonyl-CoA by a Modular Polyketide Synthease. *J. Am. Chem. Soc.* **120**, 11206-11207 (1998).

15 Trauger, J. W., Kohli, R. M., Mootz, H. D., Marahiel, M. A. & Walsh, C. T. Peptide cyclization catalysed by the thioesterase domain of tyrocidine synthetase. *Nature* **407**, 215-218 (2000).

16 Hunziker, D., Wu, N., Kenoshita, K., Cane, D. E. & Khosla, C. Precursor Directed Biosynthesis of Novel 6-Deoxyerythronolide B Analogs Containing Non-natural Oxygen Substituents and Reactive Functionalities. *Tet. Lett.* **40**, 635-638 (1999).

17 Klibanov, A. M. Improving enzymes by using them in organic solvents. *Nature* **409**, 241-246 (2001).

18 Carrea, G. & Riva, S. Properties and Synthetic Applications of Enzymes in Organic Solvents. *Angew. Chem. Int. Ed.* **39**, 2226-2254 (2000).

19 Zaks, A. & Klibanov, A. M. Enzyme-catalyzed processes in organic solvents. *Proc. Nat. Acad. Sci. USA* **82**, 3192-3196 (1985).

20 Klibanov, A. M. Asymmetric Transformations Catalyzed by Enzymes in Organic Solvents. *Acc. Chem. Res.* **23**, 114-120 (1990).
21 Russell, A. J. & Klibanov, A. M. Inhibitor-induced Enzyme Activation in Organic Solvents. *J. Biol. Chem.* **263**, 11624-11626 (1988).
22 Lee, J. K. & Kim, M.-J. Ionic Liquid-Coated Enzyme for Biocatalysis in Organic Solvent. *J. Org. Chem.* **67**, 6845-6847 (2002).
23 Chen, K. & Arnold, F. H. Enzyme Engineering for Nonaqueous Solvents: Random Mutagenesis to Enhance Activity of Subtilisin E in Polar Organic Media. *Nat. Biotechnol.* **9**, 1073-1077 (1991).

CHAPTER 4

Reconstitution and Optimization of Cryptophycin P450 Epoxidase for Chemoenzymatic Epoxidation

4.1 Introduction to Cryptophycin Epoxidase

Cytochrome P450 monooxygenases (P450s) are a superfamily of heme-containing enzymes widely found in the biosynthesis of complex natural products in animals, archaea, fungi, bacteria, and plants. The reactions catalyzed by P450s depend on the consumption of NAD(P)H and O_2 to achieve many different types of modifications, including hydroxylation, demethylation, aldehyde and ketone formation, and epoxidation.[1] Bacterial secondary metabolite pathways containing epoxidases are particularly rich

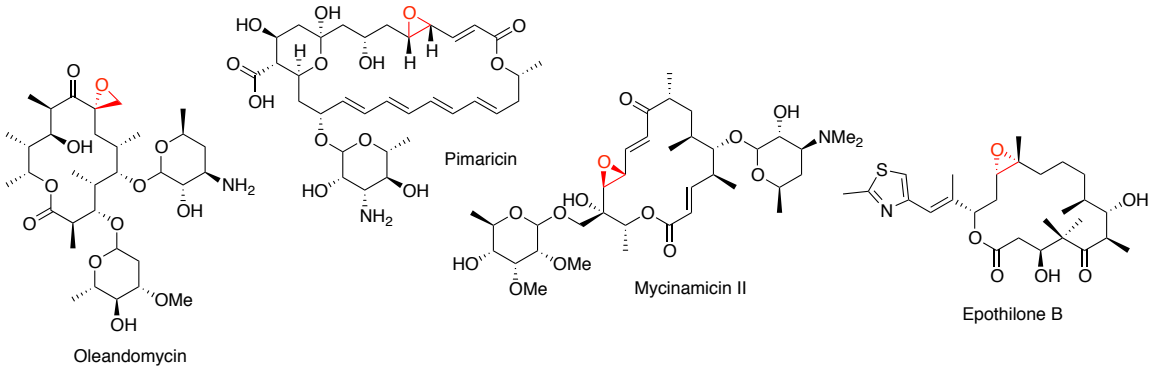

Figure 4.1: Structural diversity observed in natural products containing epoxides installed by P450s.

sources of structural diversity, and several such natural products have been isolated (Figure 4.1).[2-4] For example, the P450 epoxidase EpoK converts epothilones C and D into epothilones A and B, respectively, which are substantially more potent biological agents than their *des*-epoxy counterparts.[5,6] This increase in potency is typically seen for epoxide-

containing natural products and implies a critical biological interaction for this functionality.

More than half of the 25 cryptophycins produced by *Nostoc* sp. ATCC 53789 include a β-epoxide on subunit A of the macrolactone[7] installed during post-chain elongation tailoring by cryptophycin P450 epoxidase (CrpE). To better understand how the epoxide is installed, the *crpE* gene was previously identified in the cryptophycin biosynthetic gene cluster and cloned into a pSJ8 plasmid to create maltose binding protein (MBP)-tagged CrpE.[8] Soluble protein with the expected color of a P450 was obtained when expressed as this MBP fusion with the assistance of GroEL chaperone. The native redox partners for CrpE are not currently known, but activity was realized with spinach ferredoxin (Fdx) and ferredoxin $NADP^+$ reductase (Fdr) in conjunction with the NADPH regeneration system of glucose-6-phosphate and glucose-6-phosphate dehydrogenase. A full biochemical and kinetic characterization of CrpE was thus performed by Ding et al.[8] on the tagged protein in the presence of chaperone using spinach Fdx/Fdr and revealed exceptional substrate tolerance across units B and C of the cryptophycins. Like many human P450s,[9,10] CrpE also displayed cooperativity in substrate binding, with activity and stability of CrpE improving in the presence of high concentrations of testosterone (Y. Ding, personal communication). Considering that β-epoxy cryptophycins are 100 times more potent than the *des*-epoxy analogues,[11,12] CrpE is a critical target for optimization to make it an effective biocatalyst for the epoxidation of novel cryptophycin analogues.

4.2 Production of CrpE and Confirmation of Enzymatic Activity

Initial expression of maltose binding protein-fused CrpE (referred to as CrpE) using *E. coli* BL21 (DE3) containing a pSJ8 *crpE* plasmid with a pGro7 chaperone in LB media as previously reported afforded CrpE at a 2 μM functional concentration using gravity amylose affinity chromatography.[8] To use CrpE as a biocatalyst for the production of cryptophycins, however,

significantly higher concentrations of enzyme were needed. Optimization efforts found that TB media supplemented with 2 mM 5-ALA, 0.5 mM $Fe(NH_4)_2(SO_4)_2$, and 1 mM thiamine significantly improved yield after growing to an OD_{600} of 0.6 and inducing with 1.5 g/L arabinose and 100 µM IPTG at 18 °C. The resulting cell pellet was lysed by sonication and soluble protein was purified on amylose resin to afford CrpE at a significantly improved functional concentration of 14 µM (as assessed using CO binding assay, see Chapter 6). This concentration of MBP-CrpE was reproducible under identical conditions, and would be sufficient for chemoenzymatic epoxidation.

4.2.1 Confirmation of In Vitro *Activity and Promiscuity*

As with CrpTE, successful implementation of CrpE as a biocatalyst in the production of unnatural cryptophycin analogues requires substantial substrate flexibility. Initial experiments included small-scale enzymatic reactions conducted on CrpE with natural and heterocycle-bearing cryptophycin substrates. Activity confirmation for CrpE was obtained using

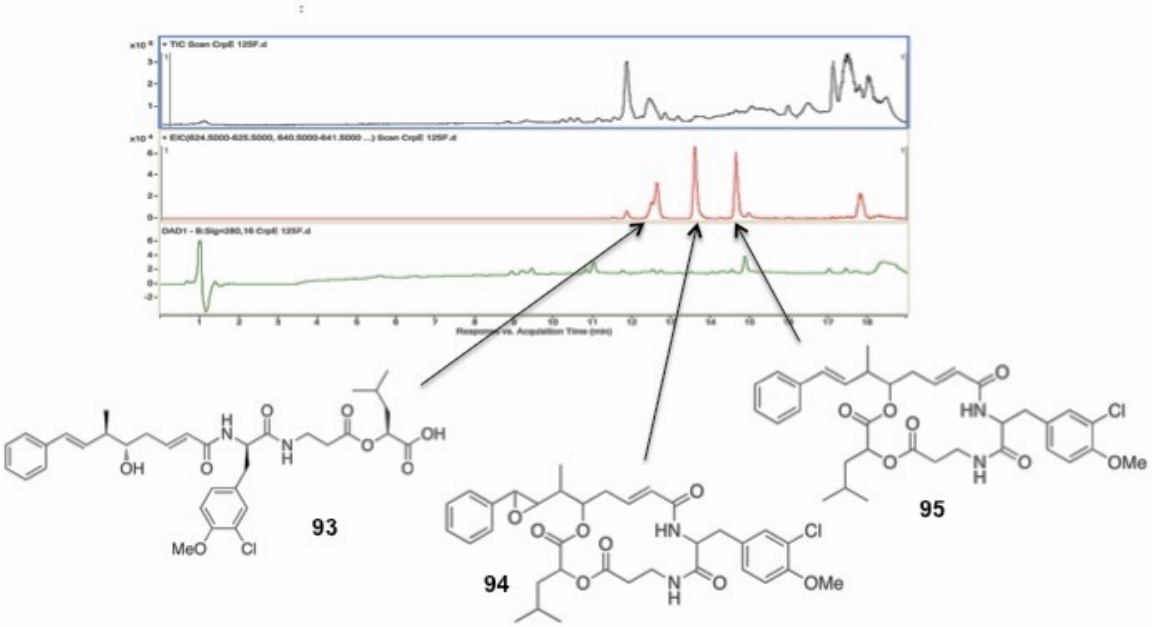

Figure 4.2: Confirmation of MBP-CrpE activity with natural substrate 95. Reaction contained 0.2 µM MBP-CrpE, 100 µg/mL spinach ferredoxin, 0.2 U/mL ferredoxin reductase, 1.4 mM NADPH, 10 mM glucose-6-phosphate, 8 U/mL glucose-6-phosphate dehydrogenase, 50 mM sodium phosphate, pH 6.4, and 5 µM **93** and **95** with 5% DMSO. Top panel, TIC of LC-QTOF-MS; middle panel, EIC for $[M+H]^+$ of **93**, **94**, and **95**; bottom panel, UV absorbance at 280 nm.

natural substrate cryptophycin 4, which was oxidized to a product with a mass matching the corresponding epoxide. When the activity of the isolated CrpE was tested against crude cryptophycin 29 (**95**) obtained from a CrpTE reaction on substrate **89**, an acceptable level of presumed epoxidation to **94** was observed in addition to the acid side product of CrpTE (Figure 4.2). These crucial pieces of data confirmed that CrpE could accept a variety of

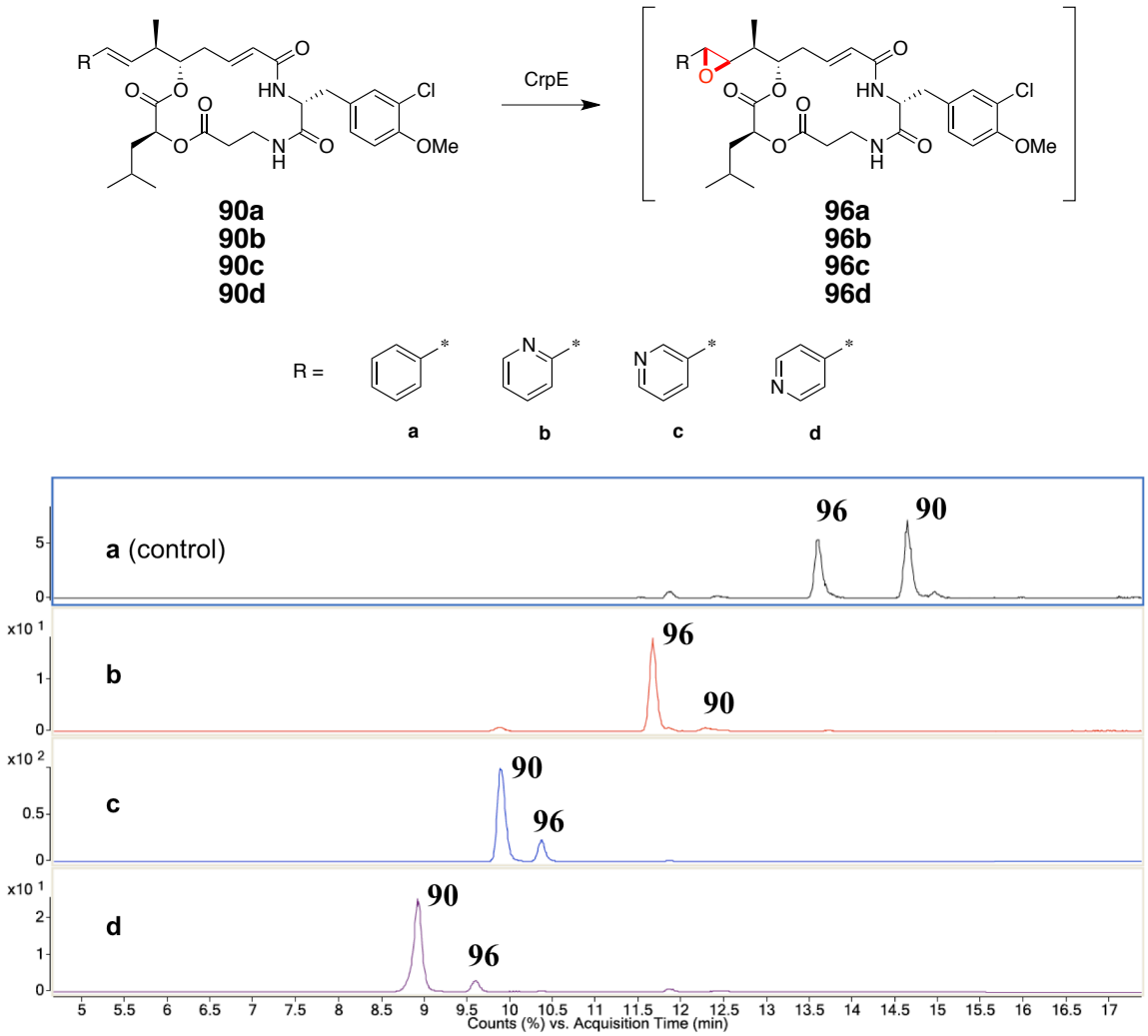

Figure 4.3: MBP-CrpE enzymatic reactions with heterocyclic cryptophycins. Top panel shows reaction using natural substrate **90** as a control with unreacted substrate (**90**) and putative epoxidated product (**96**) indicated. Subsequent panels show product distribution with a suite of unnatural heterocyclic substrates. *Reaction conditions:* 0.2 μM MBP-CrpE, 100 μg/mL Fdx, 0.2 U/mL Fdr, 1.4 mM NADPH, 10 mM glucose-6-phosphate, 8 U/mL g-6-p dehydrogenase, 50 mM NaH_2PO_4, pH 6.4, 5 μM substrate, 23 ^{o}C, 4 h. Panels are EIC traces searching for the $[M+H]^+$ mass of **90a-d** and **96a-d**.

macrocyclic cryptophycins directly from CrpTE reactions without labor- and time-intensive purification,[13] which will facilitate large-scale epoxidation reactions.

The activity of CrpE was then expanded to cryptophycin substrates containing 2-, 3-, and 4-pyridyl rings on unit A. As previously mentioned, CrpTE displayed remarkable flexibility in the cyclization of these heterocyclic unit A analogs. After workup of the CrpTE reactions and solvent removal, the residues were then used directly as substrates for CrpE to test substrate promiscuity. Remarkably, oxidation was detected for all substrates used against CrpE (Figure 4.3). Oxidation levels were found to be variable, but the 2-pyridyl substrate (**90a**) displayed a very high level of oxidation. It was possible that participation of the 2-pyridyl nitrogen in the oxidation was responsible for the observed conversion. Without significant UV absorbance in the LC traces, it was difficult to quantify the levels of conversion seen with CrpE. The enzymatic conversions for the 3- and 4-pyridyl substrates were low, but these reactions with unnatural substrates have not yet been optimized in terms of concentration, time, or solvent. The documented promiscuity is previously unknown for this particular P450 and promising for the development of CrpE into a useful biocatalyst in the epoxidation of cryptophycins. MS/MS and NMR studies are in progress to confirm the epoxides as the products of these reactions.

4.3 Design and Application of Putidaredoxin Redox Partners for CrpE

The native *Nostoc* sp. electron donor partners for CrpE are currently unknown, so alternative redox systems must be employed for catalytic turnover. Neither *E. coli* NADPH flavodoxin reductase and flavodoxin, nor rat NADPH cytochrome P450 reductase, were viable redox partners for CrpE.[8] The single component RhFRED reductase domain from *Rhodococcus* sp. NCIMB 9784, which found success with the pikromycin P450 PikC,[14,15] was fused with MBP-CrpE, but the resulting construct was poorly expressed (<1

μM functional concentration) and offered no appreciable activity increase over Fdx and Fdr. The spinach system offered therefore the best partners for CrpE, but these components are cost-prohibitive for large-scale epoxidations. To achieve optimal CrpE activity at substrate concentrations of 5 μM, 1,400 μg of Fdx and 2.8 units of Fdr would be needed for a single addition of enzyme per 50 mg of cryptophycin analogue. Having demonstrated increased conversions when the reactions were spiked with successive doses of P450 according to the lifetime of the enzyme, the cost of adding these particular redox partners could increase exponentially. Furthermore, when spread out across a dozen analogues, it became clear that an alternative redox system for catalytic turnover must be found.

The camphor oxidase system from *Pseudomonas putida* contains the P450cam monooxygenase, a FAD-containing, NADH-dependent oxidoreductase (putidaredoxin reductase or Pdr), and a 2Fe-2S ferredoxin (putidaredoxin or Pdx).[16-19] These redox partners represent a viable alternative to the expensive Fdx and Fdr in CrpE oxidation reactions because, as prokaryotic enzymes, they presumably have more efficient electron transfer interactions with CrpE, can be expressed in *E. coli* at a significant cost savings, and use inexpensive NADH instead of NADPH. Furthermore, Pdx and Pdr have demonstrated the ability to power catalytic turnover in a number of biosynthetic P450s *in vitro*.[20,21] For this purpose, the genes *camA* and *camB*, encoding for Pdr and Pdx, respectively, were obtained from the Pochapsky lab at Brandeis University.

A dual-expression system for Pdx and Pdr was designed for maximum protein yield with minimum purification to avoid decomposition of the sensitive iron-sulfur cluster in Pdx. The genes *camA* and *camB* were inserted into the commercial vector pACYCDuet-1 and the plasmid was cloned into *E. coli* BL21 (DE3) pRARE for coexpression of wild-type Pdx and Pdr. Overexpression was performed in 1 L cultures of TB media supplemented with 0.2 mM $Fe(NH_4)_2(SO_4)_2$ and 2 mM L-cysteine. Cell mass was lysed and

the clarified supernatant containing strong bands for proteins of the appropriate size (~14 kDa for Pdx and ~42 kDa for Pdr) was used without further purification. The Pdx/Pdr-containing lysate displayed functional P450 reduction with wild-type PikC for the oxidation of YC-17 (K. Chiou, personal conversation). Unfortunately, no activity was observed with CrpE for the oxidation of cryptophycin 29 when Pdx/Pdr lysate and NADH were used in place of Fdx/Fdr and NADPH.

The lack of efficient and inexpensive redox partners for CrpE remains a substantial impediment to the use of this P450 as a biocatalyst for the epoxidation of novel cryptophycins. To meet this challenge, the genome of the cryptophycin producer *Nostoc* sp. ATCC 53789 was isolated for sequencing to identify the native CrpE electron transfer partners. Once identified, the genes can be excised and subsequently expressed in *E. coli* for significantly improved CrpE epoxidation efficiency. In addition, chemical methods for epoxidation of the cryptophycins have already found use and could be employed as an alternative to enzyme-catalyzed epoxidation.[22-27] The installation of the epoxide still remains the most daunting aspect of cryptophycin synthesis, however, and new chemical methods will need to be investigated for improved yield and selectivity with heterocyclic cryptophycin analogues.[28-32]

LITERATURE REFERENCES

1 Montellano, P. R. O. d. *Cytochrome P450: Structure, Machanism, and Biochemistry*. Third edn, (Kluwer Academic/Plenum Publishers, 2005).

2 Mendes, M. V., Anton, N., Martin, J. F. & Aparicio, J. F. Characterization of the polyene macrolide P450 epoxidase from Streptomyces natalensis that converts de-epoxypimaricin into pimaricin. *Biochem. J.* **386**, 57-62 (2005).

3 Anzai, Y. *et al.* Organization of the biosynthetic gene cluster for the polyketide macrolide mycinamicin in Micromonospora griseorubida. *FEMS Microbiol. Lett.* **218** (2003).

4 Shah, S. *et al.* Cloning, characterization and heterologous expression of a polyketide synthase and P450 oxidase involved in the biosynthesis of the antibiotic oleandomycin. *J. Antibiot.* **53**, 502-508 (2000).

5 Tang, L. *et al.* Cloning and heterologous expression of the epothilone gene cluster. *Science* **287**, 640-642 (2000).

6 Molnar, I. *et al.* The biosynthetic gene cluster for the microtubule-stabilizing agents epothilones A and B from Sorangium cellulosum So ce90. *Chem. Biol.* **7**, 97-109 (2000).

7 Magarvey, N. A. *et al.* Biosynthetic Characterization and Chemoenzymatic Assembly of the Cryptophycins. Potent Anticancer Agents from Nostoc Cyanobionts. *ACS Chem. Biol.* **1**, 766-779 (2006).

8 Ding, Y., Seufert, W. H., Beck, Z. Q. & Sherman, D. H. Analysis of the Cryptophycin P450 Epoxidase Reveals Substrate Tolerance and Cooperativity. *J. Am. Chem. Soc.* **130**, 5492-5498 (2008).

9 Isin, E. M. & Guengerich, F. P. Kinetics and thermodynamics of ligand binding by cytochrome P450 3A4. *J. Biol. Chem.* **281**, 9127-9136 (2006).

10 Miller, G. P., Hanna, I. H., Nishimura, Y. & Guengerich, F. P. Oxidation of phenethylamine derivatives by cytochrome P450 2D6: the issue of substrate protonation in binding and catalysis. *Biochemistry* **40**, 14215-14223 (2001).

11 Eggen, M. & Georg, G. I. The Cryptophycins: Their Synthesis and Anticancer Activity. *Med. Chem. Rev.* **22**, 85-101 (2002).

12 Rohr, J. Cryptophycin Anticancer Drugs Revisited. *ACS Chem. Biol.* **1**, 747-750 (2006).

13 Beck, Z. Q., Aldrich, C. C., Magarvey, N. A., Georg, G. I. & Sherman, D. H. Chemoenzymatic Synthesis of Cryptophycin/Arenastatin Natural Products. *Biochemistry* **44**, 13457-13466 (2005).

14 Li, S., Podust, L. M. & Sherman, D. H. Engineering and Analysis of a Self-Sufficient Biosynthetic Cytochrome P450 PikC Fused to the RhFRED Reductase Domain. *J. Am. Chem. Soc.* **129**, 12940-12941 (2007).

15 Li, S. *et al.* Selective oxidation of carbolide C-H bonds by an engineered macrolide P450 monooxygenase. *Proc. Nat. Acad. Sci.* **106**, 18463-18468 (2009).

16 Servioukova, I. F. & Poulos, T. L. Structural biology of redox partner interactions in P450cam monooxygenase: A fresh look at an old system. *Arch. Biochem. Biophys.*, 66-74 (2011).

17 Gunsalus, I. C. & Wagner, G. C. Bacterial P450cam Methylene Monooxygenase Components: Cytochrome m, Putidaredoxin, and Putidaredoxin Reductase. *Methods Enzymol.* **17**, 166 (1978).

18 Servioukova, I. F., Garcia, C., Li, H., Bhaskar, B. & Poulos, T. L. Crystal Structure of Putidaredoxin, the [2Fe-2S] Component of the P450cam Monooxygenase System from Pseudomonas putida. *J. Mol. Biol.* **333**, 377-392 (2003).

19 Servioukova, I. F., Poulos, T. L. & Churbanova, I. Y. Crystal Structure of the Putidaredoxin Reductase-Putidaredoxin Electron Transfer Complex. *J. Biol. Chem.* **285**, 13616-13620 (2010).

20 Kudo, F., Motegi, A., Mizoue, K. & Eguchi, T. Cloning and Characterization of the Biosynthetic Gene Cluster of 16-Membered Macrolide Antibiotic FD-891: Involvement of a Dual Functional Cytochrome P450 Monooxygenase Catalyzing Epoxidation and Hydroxylation. *ChemBioChem* **11**, 1574-1582 (2010).
21 Pandey, B. P. *et al.* Screening of bacterial cytochrome P450s responsible for regiospecific hydroxylation of (iso)flavonoids. *Enzyme Microb. Tech.* **48**, 386-392 (2011).
22 Gardinier, K. M. & Leahy, J. W. Enantioselective Total Synthesis of the Potent Antitumor Macrolides Cryptophycins 1 and 8. *J. Org. Chem.* **62**, 7098-7099 (1997).
23 Al-awar, R. S. *et al.* A Convergent Approach to Cryptophycin 52 Analogues: Synthesis and Biological Evaluation of a Novel Series of Fragment A Epoxides and Chlorohydrins. *J. Med. Chem.* **46**, 2985 (2003).
24 McCubbin, J. A., Maddess, M. L. & Lautens, M. Total Synthesis of Cryptophycin Analogues via a Scaffold Approach. *Org. Lett.* **8**, 2993-2996 (2006).
25 Hoard, D. W., Moher, E. D., Martinelli, M. J. & Norman, B. H. Synthesis of Cryptophycin 52 Using the Shi Epoxidation. *Org. Lett.* **4**, 1813-1815 (2002).
26 Li, L.-H. & Tius, M. A. Stereospecific Synthesis of Cryptophycin 1. *Org. Lett.* **4**, 1637-1640 (2002).
27 Ghosh, A. K. & Bischoff, A. A Convergent Synthesis of (+)-Cryptophycin B, a Potent Antitumor Macrolide from *Nostoc* sp. Cyanobacteria. *Org. Lett.* **2**, 1573-1575 (2000).
28 Xia, Q.-H., Ge, H.-Q., Ye, C.-P., Liu, Z.-M. & Su, K.-X. Advances in Homogenous and Heterogeneous Catalytic Asymmetric Epoxidation. *Chem. Rev.* **105**, 1603-1662 (2005).
29 Shi, Y. Organocatalytic Asymmetric Epoxidation of Olefins by Chiral Ketones. *Acc. Chem. Res.* **37**, 488-496 (2004).
30 Isaacs, A. K., Xiang, C., Baubet, V., Dahmane, N. & Winkler, J. D. Studies Directed toward the Elucidation of the Pharmacophore of Steroid-Based Sonic Hedgehog Signaling Inhibitors. *Org. Lett.* **13**, 5140-5143 (2011).
31 Ottenbacher, R. V., Bryliakov, K. P. & Talsi, E. P. Non-Heme Manganese Complexes Catalyzed Asymmetric Epoxidation of Olefins by Peracetic Acid and Hydrogen Peroxide. *Adv. Synth. Catal.* **353**, 885-889 (2011).
32 Sheibani, E. & Warnmark, K. Conformationally restricted dynamic supramolecular catalysts for substrate-selective epoxidations. *Org. Biomol. Chem.* **10**, 2059-2067 (2012).

CHAPTER 5
Future Directions for the Cryptophycins

The cryptophycins are some of the most potent microtubule disrupting agents discovered to date,[1-3] and have proven to be powerful cytostatic agents capable of arresting the growth of P-glycoprotein-expressing multidrug resistant (MDR) human carcinoma cell lines.[4-6] The potential for cryptophycins to become powerful anticancer agents and the efficient, divergent unit A analogue synthesis now in place[7] demands further investigation of their structure-activity relationship (SAR), as well as interrogation of their mechanism of action through the construction of chemical probe analogues. In addition, the initial substrate tolerance[2,8,9] demonstrated by the biosynthetic enzymes CrpTE and CrpE warrants their continued development as biocatalysts in a chemoenzymatic synthesis of novel cryptophycins on an unprecedented preparative scale. Finally, we have a unique opportunity to build upon our understanding of the structural features of CrpTE and CrpE that enable flexibility to maximize analogue compatibility and engineer superior biocatalysts.

5.1 Generation of a Library of Novel Heterocyclic Unit A-Containing Cryptophycins

With the optimization of our synthetic scheme and production of heterocyclic unit A analogues, these analogues can be incorporated with units B, C, and D *via* solution phase or solid-supported peptide coupling (Figure 5.1). These linear substrates are then incubated with CrpTE to

cleave the tetra-subunit peptolide from SNAc or the solid support and catalyze the macrocyclization. Finally, CrpE or an optimized synthetic transformation will install the epoxide to generate novel cryptophycins for biological analysis. With the marriage of our chemoenzymatic technology and heterocyclic unit A synthesis, we are now poised to actively pursue a new class of cryptophycin analogues as powerful anticancer drugs.

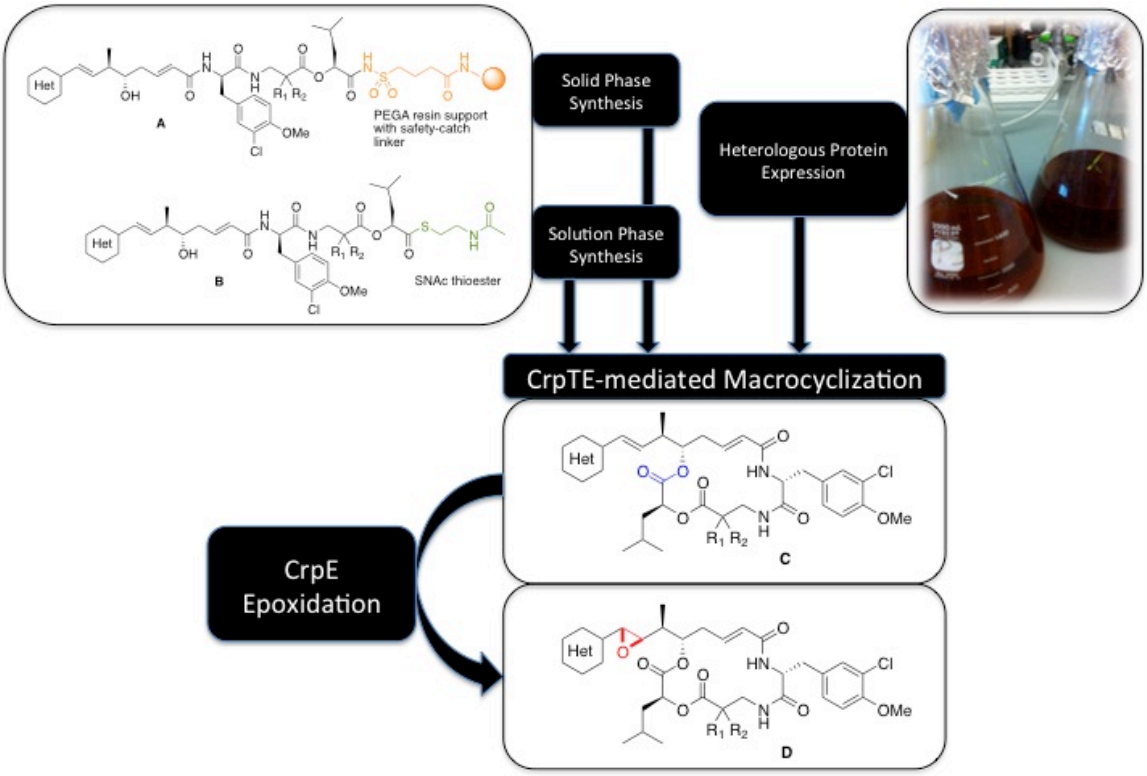

Figure 5.1: Chemoenzymatic synthesis of heterocyclic cryptophycins using CrpTE and CrpE as biocatalysts. Linear depsipeptide substrates can be produced through either solid (A) or solution phase synthesis (B). Heterologously expressed CrpTE intercepts thioester or sulfonamide to effect macrocyclization (C) and CrpE performs oxidation (D) to complete analogue synthesis.

Improving pharmacokinetic and pharmacodynamic properties *via* the incorporation of heteroatoms is possible through the lowering of CLogP and protein binding and increasing water solubility.[10,11] These modifications are expected to decrease the amount of cryptophycin necessary for an effective dose and consequently reduce the associated dose-dependent peripheral neuropathy. This dose-limiting complication can be directly predicted for any new cryptophycins using an *in vitro* single cell culture neurite inhibition assay (F. Valeriote, manuscript in preparation). In this assay, a correlation can be

drawn between neurite outgrowth & clonogenic cell survival and clinical cytotoxicity. The overall effectiveness of new cryptophycins as anticancer therapy can then be evaluated in combination with efficacy and potency studies.

5.2 Interrogation of the Interactions Between Cryptophycin and a Cellular Proteome Through the Construction of Affinity Probes

The binding site for cryptophycin on tubulin has not yet been fully characterized, nor has any significant attempt been made to identify other protein binding partners of cryptophycin. We can approach these problems in a number of ways by synthesizing valuable affinity probes based on parent cryptophycins (Figure 5.2). The first approach is to append biotin tags onto cryptophycin (**97**) to conduct pull-down assays. This method has worked well for other anticancer agents,[12,13] and involves incubating biotin-labeled cryptophycins with a cellular proteome, after which they are treated with streptavidin-coated beads to pull down proteins or complexes that bind cryptophycins. Denaturing the streptavidin beads releases any proteins associated with the probe for characterization and identification. Activity

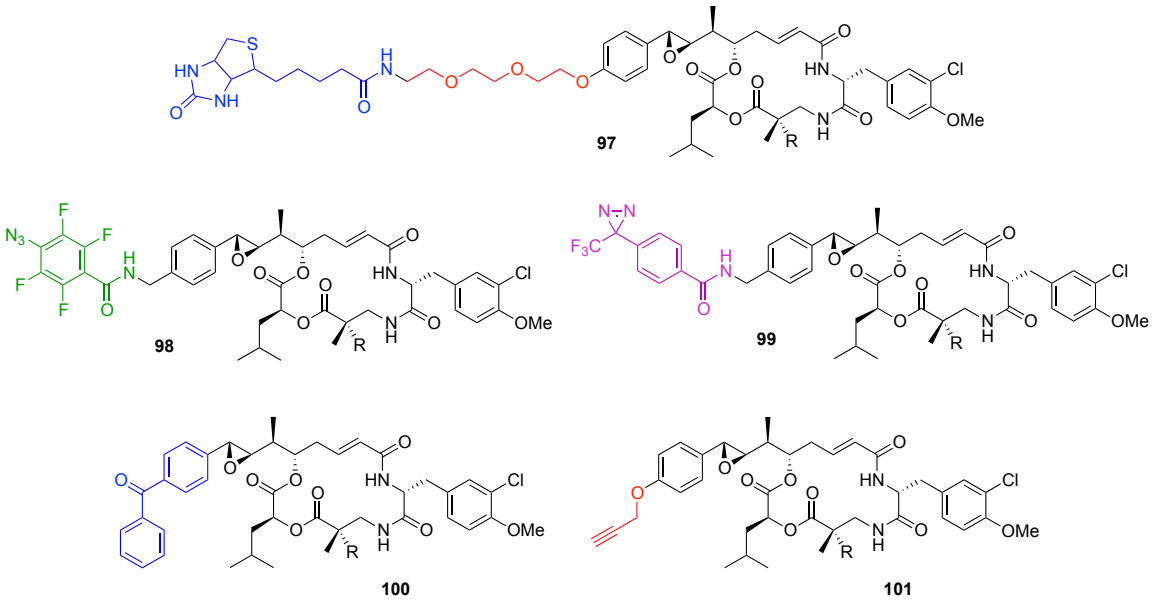

Figure 5.2: Proposed affinity probe-based cryptophycin analogues for interrogating protein binding.

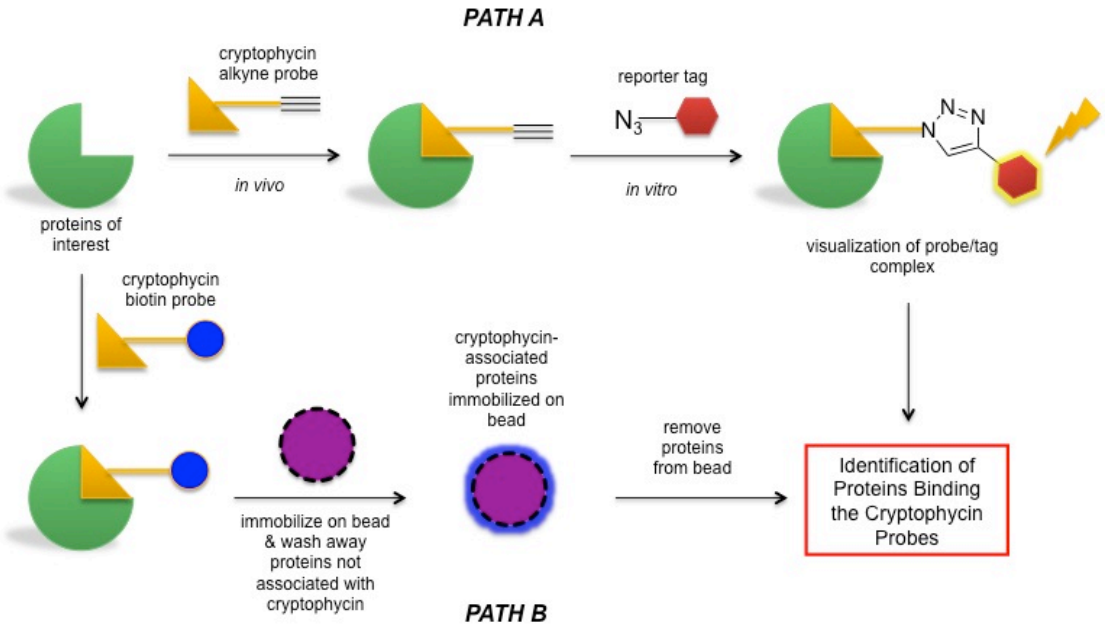

Figure 5.3: Multidimensional protein identification (MudPIT) approach for the identification of a cryptophycin interactome. Path A: an alkyne-based affinity probe is incubated in a biological environment and then fused with a reporter tag for visualization of cryptophycin localization. Path B: a biotin-coupled cryptophycin probe is incubated with a cellular proteome and immobilized on a solid support for sequence identification.

Based Protein Profiling (ABPP) and MudPIT[14-17] are even more powerful extensions of this method for the exploration of cellular binding (Figure 5.3). This technique requires the construction of cryptophycins possessing alkynes (**101**) (or azides) reactive in Cu(I)-catalyzed click chemistry.[18] After incubation with a target population of proteins *in vivo*, a reporter bearing a complementary azide (or alkyne) can flag bound proteins for visualization *in vitro* and mass spectrometric identification.[19]

Another approach to characterizing the biological interactions of cryptophycin exploits the photolabile properties of certain moieties to covalently label proteins. For this purpose, benzophenone reagents have previously been synthesized on unit A (**100**),[20] and other reagents, such as tetrafluorophenyl azide (**98**) or trifluoromethylphenyl diazirine (**99**), can also be used in the light-induced labeling of peptides for identification by mass spectrometry.[21,22] Covalent labeling of proteins will deconvolute the specific

side chains and amino acids on tubulin directly involved in cryptophycin binding.

5.2.1 Characterization of CrpTE and its Active Site

In addition to human protein interactions, cryptophycin probes may expand our understanding of the biosynthetic enzyme CrpTE. We pursued the crystallization of CrpTE with a linear cryptophycin substrate blocked in its ability to undergo cyclization (Figure 5.4) to predict enzyme flexibility around unit A. This SNAc-loaded substrate had a selective methylation on the hydroxyl that participates in the cyclization. The hypothesis was that the hydroxyl would no longer function as a nucleophile and stall the holo-CrpTE for crystallization and X-ray crystal structure analysis. In the absence of a productive macrocyclization pathway, however, hydrolysis of the acyl-enzyme intermediate predominated and only trace substrate bound protein was observed by LC-MS (see Chapter 6). Furthermore, crystallization of CrpTE as either the wild type and as a variety of mutants has so far eluded our collaborators in the Smith lab (S. Bernard) at the University of Michigan, so long-lived substrate binding may be a prerequisite for successful protein crystallization.

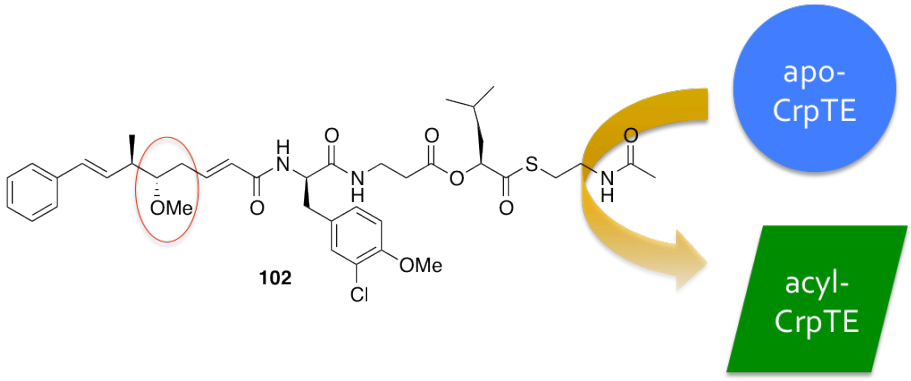

Figure 5.4: Diagram of the methylated cryptophycin depsipeptide for capture of acylated CrpTE.

In a continuing effort to map the active site of CrpTE, a phosphonate-based cryptophycin substrate could be prepared to irreversibly bind to the active site serine in CrpTE (Scheme 5.5).[23-25] Using a *seco*-cryptophycin

already on hand, the SNAc can be cleaved using piperidine and unit A protected as the silyl ether **P1**. Treatment with thionyl chloride should then furnish acid chloride **P2** ready for conversion to phosphonate **P3** under basic conditions. Deprotection with camphorsulfonic acid (CSA) liberates the covalent CrpTE substrate **P4**, which can likely be further transformed into the fluorophosphonate using diethylaminosulfur trifluoride (DAST) should the phosphonate prove ineffective. This relatively simple modification of subunit D into the phosphonate using known chemistry[26-28] should provide a linear substrate capable of being recognized

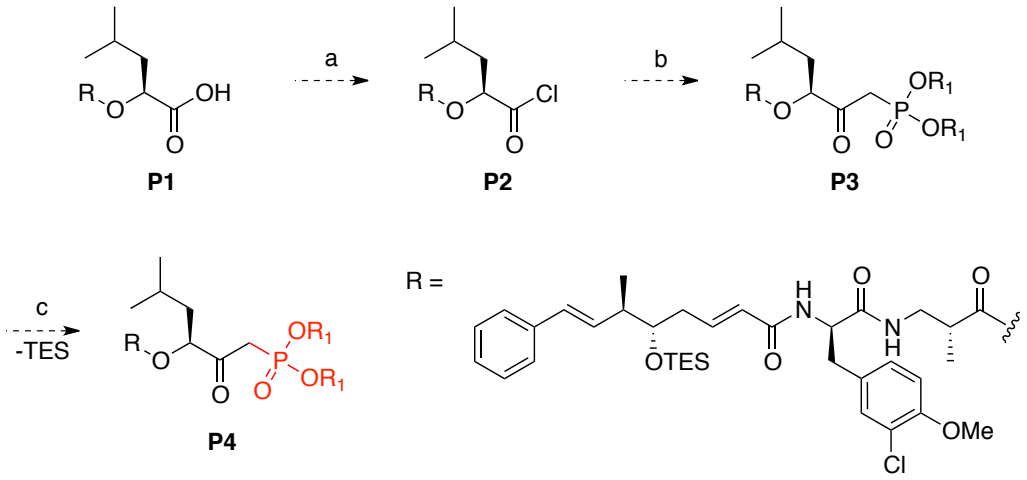

Scheme 5.5: Proposed synthesis of a phosphonate-based CrpTE acylating agent. *Reaction conditions:* (a) $SOCl_2$; (b) $(RO)_2P(O)Me$, LHMDS; (c) CSA.

by CrpTE and then irreversibly binding, hopefully allowing for crystallization of the resulting holo-TE without significant active site deformation or substrate hydrolysis. As the binding site of CrpTE becomes clear, we can begin to predict which cryptophycin analogues will be enzymatically processed. Meanwhile, site-directed mutagenesis can be employed to enhance the inherent flexibility and accommodate more sophisticated and sterically bulky unit A analogues.

5.3 CrpE Structure Determination

Understanding the active site architecture of CrpE may help us to better predict substrate flexibility and epoxidation selectivity. We currently

have an excellent protein crystallographer, Dr. Larissa Podust at UCSF, collaborating on the study of CrpE. As substrate-protein interactions become clearer, protein engineering can again be performed to enhance the inherent promiscuity of this P450. Combined with the identification of the native redox partners from the full genome sequencing of *Nostoc* sp. ATCC 53789, these advancements will help us optimize CrpE as a biocatalyst in the epoxidation of cryptophycins.

5.4 THE CRYPTOPHYCINS AS CONJUGATE THERAPIES

If the neurotoxic side effects of the cryptophycins prove to be recalcitrant to the incorporation of heterocycles in subunit A, the creation of cryptophycin conjugates may hold promise for their continued clinical development.[29] An example of this strategy is the recent FDA approval of Genentech's trastuzumab emtansine (trade name Kadcyla™), which is a novel antibody-drug conjugate of the maytansine[30] derivative mertansine and the monoclonal antibody trastuzumab.[31] Like the cryptophycins, mertansine is a cytotoxic microtubule inhibitor that binds tubulin and was found to be too toxic for monotherapy. However, when conjugated to the antibody trastuzumab, which targets Human Epidermal Growth Factor Receptor 2-positive ($HER2^+$) cancer, mertansine was released only in these cancer cells. As a result, trastuzumab emtansine improved survival by 5.8 months in comparison to other chemotherapeutic combinations in women with trastuzumab-resistant $HER2^+$ breast cancer.[31] Indeed, initial steps towards the use of cryptophycins as conjugates have been taken with the attachment of fluorescently labeled RGD peptides through unit C.[32] Fluorescence microscopy subsequently proved integrin-mediated internalization and lysosomal localization of the cryptophycin prodrug. Cryptophycin conjugates with targeting macromolecules may therefore prove to be a highly successful strategy for their continued development as powerful anticancer agents.

LITERATURE REFERENCES

1 Schwartz, R. E. *et al.* Pharmaceuticals from Cultured Algae. *J. Indust. Microbiol.* **5**, 113-124 (1990).

2 Magarvey, N. A. *et al.* Biosynthetic Characterization and Chemoenzymatic Assembly of the Cryptophycins. Potent Anticancer Agents from Nostoc Cyanobionts. *ACS Chem. Biol.* **1**, 766-779 (2006).

3 Golakoti, T. *et al.* Total structures of cryptophycins, potent antitumor depsipeptides from the blue-green alga *Nostoc* sp. strain GSV 224. *J. Am. Chem. Soc.* **116**, 4729 (1994).

4 Smith, C. D., Zhang, X., Mooberry, S. L., Patterson, G. M. L. & Moore, R. E. Cryptophycin: A New Antimicrotubule Agent Active against Drug-resistant Cells. *Cancer Research* **54**, 3779-3784 (1994).

5 Shih, C. & Teicher, B. A. Cryptophycins: A Novel Class of Potent Antimitotic Antitumor Depsipeptides. *Curr. Pharm. Des.* **7**, 1259-1276 (2001).

6 Eggen, M. & Georg, G. I. The Cryptophycins: Their Synthesis and Anticancer Activity. *Med. Chem. Rev.* **22**, 85-101 (2002).

7 Bolduc, K. L., Larsen, S. D. & Sherman, D. H. Efficient, Divergent Synthesis of Cryptophycin Unit A Analogues. *Chem. Commun.* **48**, 6414-6416 (2012).

8 Beck, Z. Q., Aldrich, C. C., Magarvey, N. A., Georg, G. I. & Sherman, D. H. Chemoenzymatic Synthesis of Cryptophycin/Arenastatin Natural Products. *Biochemistry* **44**, 13457-13466 (2005).

9 Ding, Y., Seufert, W. H., Beck, Z. Q. & Sherman, D. H. Analysis of the Cryptophycin P450 Epoxidase Reveals Substrate Tolerance and Cooperativity. *J. Am. Chem. Soc.* **130**, 5492-5498 (2008).

10 Gleeson, M. P. Generation of a Set of Simple, Interpretable ADMET Rules of Thumb. *J. Med. Chem.* **51**, 817-834 (2008).

11 Broughton, H. B. & Watson, I. A. Selection of heterocycles for drug design. *J. Mol. Graphics Modell.* **23**, 51-58 (2005).

12 Takeuchi, T. *et al.* Antitumor antibiotic fostriecin covalently binds to cysteine-269 residue of protein phosphatase 2A catalytic subunit in mammalian cells. *Bioorg. Med. Chem.* **17**, 8113-8122 (2009).

13 Yu, Y. *et al.* Withferin A targets heat shock protein 90 in pancreatic cancer cells. *Biochem. Pharmacol.* **79**, 542-551 (2010).

14 Cravatt, B. F., Wright, A. T. & Kozarich, J. W. Activity-Based Protein Profiling: From Enzyme Chemistry to Proteomic Chemistry. *Annu. Rev. Biochem.* **77**, 383 (2008).

15 Martin, B. R. & Cravatt, B. F. Large-scale profiling of protein palmitoylation in mammalian cells. *Nature Methods* **6**, 135 (2009).

16 Evans, M. J. & Cravatt, B. F. Mechanism-Based Profiling of Enzyme Families. *Chem. Rev.* **106**, 3279-3301 (2006).

17 Simon, G. M. & Cravatt, B. F. Activity-based Proteomics of Enzyme Superfamilies: Serine Hydrolases as a Case Study. *J. Biol. Chem.* **285**, 11051-11055 (2010).

18 Rostovtsev, V. V., Green, L. G., Fokin, V. V. & Sharpless, K. B. A Stepwise Huisgen Cycloaddition Process: Copper(I)-Catalyzed Regioselective "Ligation" of Azides and Terminal Alkynes. *Angew. Chem. Int. Ed.* **114**, 2708 (2002).

19 Speers, A. E. & Cravatt, B. F. Profiling Enzyme Activities In Vivo Using Click Chemistry Methods. *Chem. Biol.* **11**, 535 (2004).

20 Vidya, R., Eggen, M., Georg, G. I. & Himes, R. H. Cryptophycin Affinity Labels: Synthesis and Biological Activity of a Benziphenone Analogue of Cryptophycin-24. *Bioorg. Med. Chem. Lett.* **13**, 757-760 (2003).

21 Dorman, G. & Prestwich, G. D. Using photolabile ligands in drug discovery and development. *Trends Biothechnol.* **18**, 64-77 (2000).

22 Hatanaka, Y. & Sadakane, Y. Photoaffinity Labeling in Drug Discovery and Development: Chemical Gateway for Entering Proteomic Frontier. *Curr. Top. Med. Chem.* **2**, 271-288 (2002).
23 Patricelli, M. P., Lovato, M. A. & Cravatt, B. F. Chemical and Mutagenic Investigations of Fatty Acid Amide Hydrolase: Evidence for a Family of Serine Hydrolases with Distinct Catalytic Properties. *Biochemistry* **38**, 9804-9812 (1999).
24 Liu, Y., Patricelli, M. P. & Cravatt, B. F. Activity-based protein profiling: The serine hydrolases. *Proc. Nat. Acad. Sci.* **96**, 14694-14699 (1999).
25 Meier, J. L., Mercer, A. C. & Burkart, M. D. Fluorescent Profiling of Modular Biosynthetic Enzymes by Complementary Metabolic and Activity Based Probes. *J. Am. Chem. Soc.* **130**, 5443-5445 (2008).
26 Akey, D. L. *et al.* Structural basis for macrolactonization by the pikromycin thioesterase. *Nat. Chem. Biol.* **2**, 537-542 (2006).
27 Giraldes, J. W. *et al.* Structural and mechanistic insights into polyketide macrolactonization from polyketide-based affinity labels. *Nature Chem. Bio.* **2**, 531 (2006).
28 Martin, B. R., Wang, C., Adibekian, A., Tully, S. E. & Cravatt, B. F. Global profiling of dynamic protein palmitoylation. *Nature Methods* **9**, 84 (2012).
29 Bouchard, H., Brun, M.-P., Commercon, A. & Zhang, J. Novel Conjugates, Preparation Thereof, and Therapeutic Use Thereof. U.S.A. patent US 2012/0225089 A1 (2012).
30 Yu, T.-W. *et al.* The biosynthetic gene cluster of the maytansinoid antitumor agent ansamitocin from *Actinosynnema pretiosum*. *Proc. Nat. Acad. Sci.* **99**, 7968-7973 (2002).
31 LoRusso, P. M., Weiss, D., Guardino, E., Girish, S. & Sliwkowski, M. X. Trastuzumab Emtansine: A Unique Antibody-Drug Conjugate in Development for Human Epidermal Growth Factor Receptor 2-Positive Cancer. *Clin. Cancer Res.* **17**, 6437-6447 (2011).
32 Nahrwold, M. *et al.* Conjugates of modified cryptophycins and RGD-peptides enter target cells by endocytosis. *J. Med. Chem.* **56**, 1853-1864 (2013).

CHAPTER 6

Experimental Details

Unless otherwise stated, all reactions were performed with no extra precautions taken to exclude moisture or air. Anhydrous, inhibitor-free tetrahydrofuran (THF), 1,2-dimethoxyethane (DME), diglyme, and DMF were purchased from Sigma-Aldrich, and anhydrous acetonitrile (ACN) was purchased from Acros and used as received. Dichloromethane (DCM) was shaken with sat. aq. $NaHCO_3$, distilled from CaH_2, and degassed with three rounds of a freeze-pump-thaw procedure. All other chemicals were obtained from Sigma-Aldrich, Alfa Aesar, Strem, TCI, NovaBiochem, Advanced ChemTec, or ChemImpex and used directly unless otherwise noted.

^{1}H, ^{13}C, and ^{19}F NMR spectra were recorded on Varian 400 and 500 MHz NMRs. Proton chemical shifts are reported in ppm referenced to residual solvent in $CDCl_3$ (7.26 ppm) or CD_3OD (3.31 ppm) as the internal standard; carbon chemical shifts are reported in ppm referenced to the centerline of residual solvent in $CDCl_3$ (77.16 ppm) or CD_3OD (49.0 ppm) as the internal standard. Proton spectral data are described as follows: chemical shift, multiplicity (s = singlet, d = doublet, t = triplet, q = quartet, m = multiplet, b = broad), coupling constant (in Hz), and integration. High-resolution mass spectra were obtained on an Agilent Accurate-Mass Q-TOF 6520 using a Phenomenex Synergi 4u HydroRP (100 x 2.0 mm, 4 µm) column. Analytical thin-layer chromatography (TLC) was performed on silica gel 60 F_{254} TLC glass plates with a fluorescent indicator from EMD Chemicals. EMD Silica Gel 60 *Geduran®* (particle size 0.040 – 0.063 mm) silica gel was used for flash chromatography. Visualization was accomplished by UV fluorescence

quenching (254 nm) and by *p*-anisaldehyde, potassium permanganate, or ceric ammonium molybdate staining with heating.

6.1 First Generation Unit A Synthesis

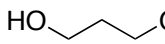

41

3-((4-methoxybenzyl)oxy)propan-1-ol (41). To a stirred solution of 1,3-propanediol (46.25 mL, 0.64 mol) in 175 mL anhydrous DMF under argon was slowly added solid NaH (9.62 g, 0.24 mol) at 0 °C. The reaction was stirred for 30 min, then treated with slow addition of PMBCl (25.0 g, 0.16 mol). The reaction was stirred for an additional 1 h and allowed to warm to room temperature overnight, then quenched with sat. aq. NH_4Cl. Reaction diluted and partitioned between water (100 mL) and ethyl acetate (EtOAc, 100 mL). Aqueous layer extracted with EtOAc (150 mL x 3) and combined organics washed with brine (250 mL) and dried with Na_2SO_4. Evaporation of the solvent and chromatographic purification (SiO_2, 2:1 hexanes:EtOAc [H:E]) afforded the desired product (**41**, 25.51 g, 81%) as a clear, colorless oil. TLC R_f = 0.15 (3:1 H:E). ^{1}H NMR ($CDCl_3$, 400 MHz) δ 7.25 (d, *J* = 8.4 Hz, 2H), 6.88 (d, *J* = 8.8 Hz, 2H), 4.45 (s, 2H), 3.80 (s, 3H), 3.77 (m, 2H), 3.63 (m, 2H), 2.49 (bs, 1H), 1.85 (m, 2H) ppm.

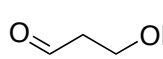

42

3-((4-methoxybenzyl)oxy)propanal (42). Sodium hypochlorite solution (47 mL, 10-15%, Sigma) was diluted 1:1 with water to an approximate concentration of 0.35 M and buffered to pH 8.5 with solid $NaHCO_3$. A separate two-phase system of KBr (303 mg, 2.55 mmol) in 50 mL water and **41** (5.0 g, 25.5 mmol) and TEMPO (40 mg, 0.25 mmol) in 100 mL of CH_2Cl_2 was cooled to 0 °C with overhead mechanical stirring. The NaOCl solution was then added quickly with vigorous stirring. After 5 min, reaction quenched by the addition of 5 mL sat. aq. $KHSO_4$ with 10% KI. Organic layer separated and washed with sat. aq. $Na_2S_2O_3$ and brine, then dried with Na_2SO_4. Evaporation of the solvent and chromatographic

purification (SiO_2, 2:1 hexanes:EtOAc [H:E]) afforded the desired product (**42**, 4.33 g, 88%) as a clear, colorless oil. TLC R_f = 0.45 (1:1 H:E). ^1H NMR ($CDCl_3$, 400 MHz) δ 9.77 (s, 1H), 7.24 (d, *J* = 8.8 Hz, 2 H), 6.87 (d, *J* = 8.8 Hz, 2H), 4.46 (s, 2H), 3.78 (m, 5H), 2.67 (dt, *J* = 2.0, 12.0, 2H) ppm.

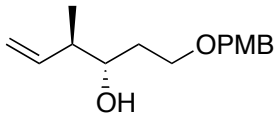

43

(3*S*,4*R*)-1-((4-methoxybenzyl)oxy)-4-methylhex-5-en-3-ol (43). A round bottom flask (RBF) was equipped with a magnetic stir bar and flame-dried under vacuum. The flask was charged with anhydrous, inhibitor-free THF (75 mL) under argon, then cooled to -78 ^oC and treated with KOtBu (49.1 mL, 1.0 M in THF, 48.46 mmol). The *trans*-2-butene was then condensed in the reaction (~11.0 g, 0.196 mol) and a 1.6 M solution of nBuLi in hexanes (30.26 mL, 48.46 mmol) was added dropwise. Reaction warmed to -45 ^oC for 10 min and then cooled back to -78 ^oC. The (+)-$(ipc)_2BOMe$ (15.48 g, 48.95 mmol) was then added to the reaction as a solution in 30 mL anhydrous THF and stirred for 30 min at -78 ^oC. The $BF_3•OEt_2$ (6.04 mL, 48.95 mmol) was then added followed by slow addition of aldehyde **42** (9.50 g, 48.95 mmol) dissolved in 10 mL anhydrous THF. Reaction stirred at -78 ^oC for 2 h, then quenched by the addition of sat. aq. NH_4Cl and warmed to room temperature. The volatiles were removed under vacuum and the residue partitioned between water and EtOAc. The organic layer was washed with water and brine and then dried with Na_2SO_4. The residue after solvent evaporation was resuspended in Et_2O, treated with ethanolamine (3.25 mL, 53.85 mmol), and stirred at room temperature overnight. Finally, the solvent was removed and the resulting residue was flash purified (4:1 H:E) to yield a mixture of crotyl alcohol **43** and isopinocampheol, which was carried through to the next step without further purification.

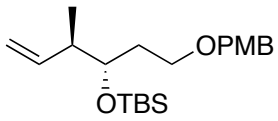

44

***tert*-butyl(((3*S*,4*R*)-1-((4-methoxybenzyl)oxy)-4-methylhex-5-en-3-yl)oxy)dimethylsilane (44).** To a stirred solution of mixed **43** in dry CH_2Cl_2 (100 mL) at -78 ^oC under argon was added 2,6-lutidine (10.74 mL, 92.22 mmol). The TBSOTf (10.59 mL, 46.11 mmol) was then added dropwise and the reaction was stirred for 3.5 h at -78 ^oC. Reaction quenched by the addition of sat. aq. NH_4Cl and warmed to room temperature. The reaction was diluted with water, and the organic layer was washed with brine and dried with Na_2SO_4. Evaporation of the solvent and chromatographic purification (SiO_2, hexanes to 10:1 H:E) afforded the desired product (**44**, 5.84 g, 32%, 2 steps) as a clear, light yellow oil. TLC R_f = 0.90 (3:1 H:E). ^1H NMR ($CDCl_3$, 400 MHz) δ 7.24 (d, *J* = 8.8 Hz, 2H), 6.87 (d, *J* = 8.7 Hz, 2H), 5.76 (m, 1H), 5.00 (s, 1H), 4.96 (d, *J* = 3.2 Hz, 1H), 4.40 (q, *J* = 11.6 Hz, 2H), 3.81 (s, 3H), 3.75 (m, 1H), 3.47 (m, 2H), 2.29 (m, 1H), 1.67 (m, 2H), 1.00 (d, *J* = 6.8 Hz, 3H), 0.88 (s, 9H), 0.03 (s, 6H) ppm.

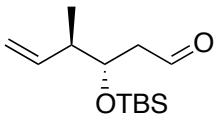

45

(3*S*,4*R*)-3-((*tert*-butyldimethylsilyl)oxy)-4-methylhex-5-enal (45). A stirred solution of **44** (2.49 g, 6.83 mmol) in CH_2Cl_2 (50 mL) at room temperature was treated with solid DDQ (1.71 g, 7.51 mmol) and water (1.84 mL, 0.10 mmol). After 1 h, reaction was quenched by the addition of sat. aq. $NaHCO_3$ and diluted with water and CH_2Cl_2. The organic layer was washed with sat. aq. $NaHCO_3$ and brine, then concentrated under vacuum. The crude residue was then dissolved in 100 mL CH_2Cl_2 containing 4 Å molecular sieves (585 mg) and NMO (961 mg, 8.20 mmol). The reaction was next treated with TPAP (120 mg, 0.342 mmol) and stirred at room temperature for 1 h. The solvent was removed under vacuum from an ice bath and the residue was flash purified (SiO_2, 10:1 H:E) to afford the desired product (**45**, 800 mg, 48%, 2 steps) as a clear, colorless oil. TLC R_f = 0.85 (3:1 H:E). ^1H NMR ($CDCl_3$, 400

MHz) δ 9.78 (s, 1H), 5.74 (m, 1H), 5.05 (m, 2H), 4.19 (m, 1H), 2.49 (m, 2H), 2.36 (m, 1H), 1.02 (d, *J* = 6.4 Hz, 3H), 0.88 (s, 9H), 0.07 (s, 6H) ppm.

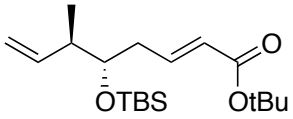

46

(5*S*,6*R*,*E*)-*tert*-butyl 5-((*tert*-butyldimethylsilyl)oxy)-6-methylocta-2,7-dienoate (46). The $(EtO)_2P(O)CH_2CO_2tBu$ (5.89 mL, 25.08 mmol), DBU (2.25 mL, 15.05 mmol), and LiCl (744 mg, 17.56 mmol) were suspended in 75 mL anhydrous ACN at room temperature and stirred vigorously for 30 min. This solution was then added dropwise to a stirred solution of **45** (3.04 g, 12.54 mmol) in 50 mL anhydrous ACN under argon at room temperature. After 2 h, the reaction was quenched by the addition of sat. aq. NH_4Cl and concentrated under vacuum. The residue was partitioned between water and EtOAc, and the organic layer was washed with sat. aq. NH_4Cl and brine, then dried with Na_2SO_4. Evaporation of the solvent and chromatographic purification (SiO_2, 20:1 H:E) afforded the desired product (**46**, 2.87 g, 74%) as a clear, light yellow oil. TLC R_f = 0.75 (9:1 H:E). ^1H NMR ($CDCl_3$, 400 MHz) δ 6.80 (m, 1H), 5.75 (m, 2H), 5.02 (m, 2H), 3.66 (m, 1H), 2.27 (m, 3H), 1.48 (s, 9H), 1.01 (d, *J* = 6.8 Hz, 3H), 0.89 (s, 9H), 0.05 (s, 6H) ppm.

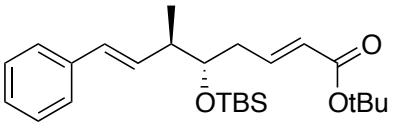

47

(2*E*,5*S*,6*R*,7*E*)-*tert*-butyl 5-((*tert*-butyldimethylsilyl)oxy)-6-methyl-8-phenylocta-2,7-dienoate (47). A solution of **46** (788 mg, 2.64 mmol), iodobenzene (330 µL, 2.90 mmol), and Et_3N (1.95 mL, 13.99 mmol) was prepared in an oven-dried pressure vessel with anhydrous, degassed ACN (10 mL). Solid $Pd(OAc)_2$ (30 mg, 0.132 mmol) and PPh_3 (69 mg, 0.26 mmol) were then added and reaction purged with argon. Reaction heated at 80 °C for 18 h and then concentrated *in vacuo*. The residue was dissolved in CH_2Cl_2 and washed with 0.5 M HCl and brine. The combined organics were dried with Na_2SO_4, and evaporation

of the solvent and chromatographic purification (50 g Biotage, SiO_2, 4:1 H:CH_2Cl_2 to 3:1 H:CH_2Cl_2, 35 mL/min) afforded the desired product (**47**, 618 mg, 63%) as a clear, yellow oil. TLC R_f = 0.60 (toluene). ^{1}H NMR ($CDCl_3$, 400 MHz) δ 7.30 (m, 4H), 7.21 (m, 1H), 6.83 (m, 1H), 6.37 (d, *J* = 16.0 Hz, 1H), 6.16 (dd, *J* = 8.0, 16.0 Hz, 1H), 5.74 (dd, *J* = 4.0, 15.6 Hz, 1H), 5.01 (m, 1H), 3.74 (m, 1H), 2.29 (m, 3H), 1.43 (s, 9H), 1.09 (d, *J* = 6.8 Hz, 3H), 0.91 (s, 9H), 0.06 (s, 6H) ppm.

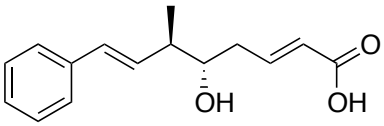

48

(2*E*,5*S*,6*R*,7*E*)-5-hydroxy-6-methyl-8-phenylocta-2,7-dienoic acid (48, unit A). A solution of **47** (380 mg, 0.91 mmol) in 10 mL CH_2Cl_2 was treated with TFA (350 µL, 4.55 mmol) and stirred at room temperature overnight. The solvent was then removed under vacuum and the residue was redissolved in 10 mL of 1:1 MeOH/CH_2Cl_2. The resulting solution was treated with solid $NaHCO_3$ (612 mg, 7.28 mmol) and stirred at room temperature overnight. The reaction was quenched by the addition of 1.0 M HCl and volatiles were removed under vacuum. The recovered residue was partitioned between water and CH_2Cl_2, and the organic layer was washed with dilute HCl and brine. Evaporation of the solvent and chromatographic purification (10 g Biotage, SiO_2, 1% MeOH/CH_2Cl_2 + 0.5% HOAc, 25 mL/min) afforded the desired product (**48**, 51 mg, 23%) as a clear, colorless oil. TLC R_f = 0.40 (5% MeOH/CH_2Cl_2 + 1% HOAc). ^{1}H and ^{13}C NMR spectra matched those previously reported.[1]

6.2 Second Generation Unit A Synthesis

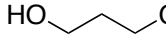

49

3-((*tert*-butyldimethylsilyl)oxy)propan-1-ol (49). To a stirred solution of 1,3-propanediol (5.0 g, 65.71 mmol) in 150 mL anhydrous DMF under argon was slowly added solid NaH (2.63 g, 65.71 mmol) at 0 °C. The reaction was stirred for 30 min, then treated with

TBSCl (9.90 g, 65.71 mmol), added portionwise. The reaction was stirred for an additional 1 hour and allowed to warm to room temperature, then quenched with sat. aq. NH_4Cl. Reaction partitioned between water (100 mL) and ethyl acetate (EtOAc, 100 mL). Aqueous layer extracted with EtOAc (150 mL x 3) and combined organics washed with brine (250 mL) and dried with Na_2SO_4. Evaporation of the solvent and chromatographic purification (SiO_2, 4:1 H:E) afforded the desired product (**49**, 9.59 g, 81%) as a clear, colorless oil. TLC R_f = 0.70 (3:1 H:E). ^1H NMR ($CDCl_3$, 400 MHz) δ 3.83 (m, 4H), 2.64 (s, 1H), 1.76 (q, *J* = 5.5 Hz, 2H), 0.89 (s, 9H), 0.05 (s, 6H) ppm; ^{13}C NMR ($CDCl_3$, 100 MHz) δ 63.06, 62.51, 34.31, 26.00, 18.29, -5.39 ppm.

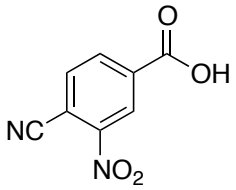

50

4-cyano-3-nitrobenzoic acid (50). Periodic acid (19.56 g, 85.82 mmol) was dissolved in anhydrous ACN (80 mL) under argon at room temperature. After 15 min, solid CrO_3 (981 mg, 9.81 mmol) and 4-methyl-2-nitro-benzonitrile (3.98 g, 24.52 mmol) were added successively and the reaction was stirred at room temperature overnight. Next, the reaction was decanted and the supernatant concentrated under vacuum. The residue was then partitioned between sat. aq. Na_2CO_3 and CH_2Cl_2. The resulting precipitate was removed by filtration and the filtrate was adjusted to pH 1 with 6 M HCl. The aqueous layer was then extracted with EtOAc and the combined organics were extracted with 1.0 M Na_2CO_3, followed by acidification to pH 1 with 6 M HCl. The resulting precipitate was collected by filtration and dried under vacuum. Recovered 2.92 g of pure **50** as a fine, yellow solid (62%). ^1H NMR (d_6-DMSO, 400 MHz) δ 8.62 (s, 1H), 8.37 (s, 1H), 8.23 (s, 1H), 3.39 (bs, 1H) ppm.

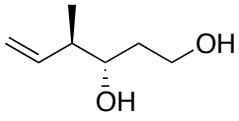

51

(3*S*,4*R*)-4-methylhex-5-ene-1,3-diol (51). To an oven-dried pressure vessel was added solid $[Ir(cod)Cl]_2$ (222 mg,

0.33 mmol), (*R*)-C3-TUNEPHOS (390 mg, 0.66 mmol), **50** (252 mg, 1.31 mmol), and Cs_2CO_3 (857 mg, 2.63 mmol) under argon. To this was added 13 mL of anhydrous, inhibitor-free THF and 3-buten-2-yl acetate (3.33 mL, 26.26 mmol). Reaction was heated at 90 °C for 30 min and then cooled to room temperature. Compound **49** (2.5 g, 13.13 mmol) was then added as a solution in a minimum amount of THF and reaction stirred at 90 °C under argon in the sealed vessel for 24 h. Next, the reaction was cooled to room temperature and diluted with pentane (~100 mL). The resulting precipitate was collected by filtration and the filtrate was concentrated under vacuum. The recovered residue was then dissolved in 75 mL of anhydrous THF under argon and treated with a 1.0 M solution of TBAF in THF (14.44 mL, 14.44 mmol). After stirring at room temperature for 1 h, reaction was concentrated under vacuum and the residue was purified (SiO_2, 1:1 H:E) to afford the desired product as a clear, light yellow oil (**51**, 586 mg, 35%, 2 steps) as a clear, colorless oil. TLC R_f = 0.25 (1:1 H:E). ^{1}H NMR ($CDCl_3$, 400 MHz) δ 5.73 (m, 1H), 5.09 (m, 2H), 3.84 (m, 2H), 3.63 (m, 1H), 2.98 (bs, 1H), 2.68 (bs, 1H), 2.23 (m, 1H), 1.68 (m, 2H), 1.02 (d, *J* = 5.0 Hz, 3H) ppm.

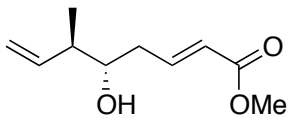

53

(5*S*,6*R*,*E*)-methyl 5-hydroxy-6-methylocta-2,7-dienoate (53). A stirred solution of **51** (67 mg, 0.51 mmol) in ACN (700 µL) and PBS buffer, pH 7.5 (300 µL) at 0 °C was treated with solid TEMPO (4 mg, 0.026 mmol) and BAIB (180 mg, 0.56 mmol). After 3 h, the reaction was warmed to room temperature, quenched with sat. aq. $Na_2S_2O_3$, and diluted with water and CH_2Cl_2. The organic layer was washed with sat. aq. $NaHCO_3$ and dried with Na_2SO_4, then concentrated under vacuum. In a separate flask, a stirred suspension of LiCl (13 mg, 0.31 mmol) in 1.5 mL anhydrous ACN at room temperature was treated with $(EtO)_2P(O)CH_2CO_2Me$ (52 µL, 0.29 mmol) and DBU (46 µL, 0.31 mmol). This reaction was stirred for 10 min and then a solution of crude **52** in 1.0 mL anhydrous ACN was added dropwise. After 1 h,

the reaction was quenched with sat. aq. NH_4Cl and diluted with water (10 mL) and CH_2Cl_2 (10 mL). The organic layer was washed with water and brine, then dried with Na_2SO_4. Evaporation of the solvent and chromatographic purification (SiO_2, 2:1 H:MTBE) afforded the desired product (**53**, 37 mg, 39%) as a clear, colorless oil. TLC R_f = 0.50 (1:1 H:MTBE). ^1H NMR ($CDCl_3$, 400 MHz) δ 7.03 (m, 1H), 5.92 (d, *J* = 15.6 Hz, 1H), 5.74 (m, 1H), 5.14 (m, 2H), 3.73 (s, 3H), 3.56 (m, 1H), 2.44 (m, 1H), 2.36-2.22 (m, 2H), 1.84 (s, 1H), 1.06 (d, *J* = 6.8 Hz, 3H) ppm.

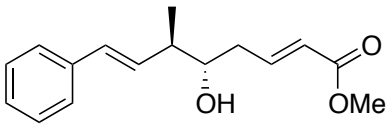

55

(2*E*,5*S*,6*R*,7*E*)-methyl 5-hydroxy-6-methyl-8-phenylocta-2,7-dienoate (55). The cataCXium® (**54**, 8 mg, 0.008 mmol), TBACl (45 mg, 0.163 mmol), and K_3PO_4 (70 mg, 0.33 mmol) were added to a dry, screw top vial and purged with argon. The iodobenzene (22 µL, 0.20 mmol) and a solution of **53** (30 mg, 0.163 mmol) in 1.0 mL of anhydrous DMF were then added and the sealed reaction stirred at 80 °C overnight. The reaction was next cooled to room temperature and partitioned between dilute NH_4Cl and CH_2Cl_2. The combined organic layers were then washed with brine and dried with Na_2SO_4. Evaporation of the solvent and chromatographic purification (SiO_2, 4:1 H:E + 0.1% Et_3N) afforded the desired product (**55**, 18 mg, 42%) as a clear, colorless oil. TLC R_f = 0.50 (1:1 H:MTBE). ^1H NMR ($CDCl_3$, 400 MHz) δ 7.36-7.25 (m, 4H), 7.20 (m, 1H), 7.04 (m, 1H), 6.44 (dd, *J* = 9.2, 15.6 Hz, 1H), 6.11 (m, 1H), 5.90 (m, 1H), 3.71 (s, 3H), 3.66 (m, 1H), 2.50-2.31 (m, 3H), 1.14 (d, *J* = 6.8 Hz, 3H) ppm.

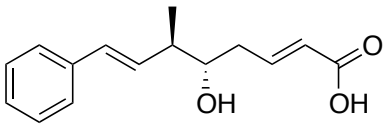

48

(2*E*,5*S*,6*R*,7*E*)-5-hydroxy-6-methyl-8-phenylocta-2,7-dienoic acid (48, unit A). A solution of **55** (94 mg, 0.036 mmol) in a 1:1:0.5 mixture of methanol/water/THF (1.5 mL) was treated with a 3 M solution of LiOH (1.8 mL) and stirred at room temperature

overnight. Reaction then quenched with 2.0 M HCl and diluted with water (2 mL) and EtOAc (2 mL). Aqueous layer extracted with EtOAc (2 mL x 2) and combined organics washed with brine and dried with Na_2SO_4. Solvent removed *in vacuo* and residue purified by flash chromatography (SiO_2, 5:95 MeOH:CH_2Cl_2 + 0.1% HOAc) to afford **48** as a clear, light yellow oil (77 mg, 87%). TLC R_f = 0.25 (5:95 MeOH:CH_2Cl_2 + 1% HOAc). ^1H and ^{13}C NMR spectra matched those previously reported.[1]

6.3 Final, Divergent Synthesis of Unit A and Analogues

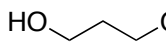

49

3-((*tert*-butyldimethylsilyl)oxy)propan-1-ol (49). To a stirred solution of 1,3-propanediol (5.0 g, 65.71 mmol) in 250 mL anhydrous THF under argon was slowly added solid NaH (2.63 g, 65.71 mmol) at 0 ^oC. The reaction was stirred for 30 min, then treated with slow addition of TBSCl (9.90 g, 65.71 mmol) dissolved in minimal THF. The reaction was stirred for an additional 1 hour and allowed to warm to room temperature, then quenched with sat. aq. NH_4Cl. Solvent removed by rotary evaporation and residue partitioned between water (100 mL) and ethyl acetate (EtOAc, 100 mL). Aqueous layer extracted with EtOAc (150 mL x 3) and combined organics washed with brine (250 mL) and dried with Na_2SO_4. Evaporation of the solvent and chromatographic purification (SiO_2, 4:1 hexanes:EtOAc [H:E]) afforded the desired product (**4**, 11.56 g, 92%) as a clear, colorless oil. TLC R_f = 0.30 (4:1 H:E). ^1H NMR ($CDCl_3$, 400 MHz) δ 3.81 (m, 4H), 2.65 (s, 1H), 1.76 (q, J = 5.5 Hz, 2H), 0.89 (s, 9H), 0.07 (s, 6H) ppm; ^{13}C NMR ($CDCl_3$, 100 MHz) δ 63.01, 62.49, 34.34, 26.01, 18.31, -5.36 ppm; HRMS (ESI+) 191.1462 *m/z* $[M+H]^+$ ($C_9H_{23}O_2Si$ requires 191.1467).

Krische crotylation complex (57). To an over-dried sealed flask was added $[Ir(cod)Cl]_2$ (500 mg, 0.74 mmol), (R)-(+)-SEGPHOS (910 mg, 1.49 mmol), **50** (427 mg, 2.22 mmol), and Cs_2CO_3 (723 mg, 2.22 mmol) under argon. The

solids were suspended in anhydrous THF (7.5 mL) and treated with 3-buten-2-yl acetate (375 µL, 2.96 mmol). The reaction was stirred at room temperature for 30 min and then at 80 °C for 2 h. Once the reaction had cooled to room temperature, it was filtered, washing with THF (10 mL). The filtrate was then diluted with pentane (100 mL) and the precipitate was recovered by filtration and dried under vacuum to yield the crotylation complex **57** as a fine, orange powder (1.76 g, quant.).

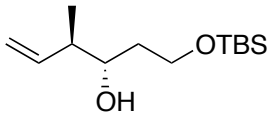

58

(3*S*,4*R*)-1-((*tert*-butyldimethylsilyl)oxy)-4-methylhex-5-en-3-ol (58). To an oven-dried, 100 mL RBF under argon was added **57**[*] (2.45 g, 2.34 mmol), K_3PO_4 (4.96 g, 23.37 mmol), anhydrous THF (25 mL), and water (2.10 mL, 116.85 mmol). The 3-buten-2-yl acetate (5.93 mL, 46.74 mmol) and **49** (4.45 g, 23.37 mmol) were then added and reaction stirred at room temp for 30 min. The reaction was then warmed to 70 °C and stirred under argon for 24 h. Next, the reaction was cooled to room temp and filtered, washing with THF. The filtrate was concentrated *in vacuo* and diluted into pentane (150 mL). Solids removed (or recovered to recycle the catalyst)[†] by filtration and eluent concentrated by rotary evaporation to afford crude **58** as a 6:1 diastereomeric mixture. This residue was used without further purification. TLC R_f = 0.45 (10:1 H:MTBE x2). ^{1}H NMR ($CDCl_3$, 500 MHz) δ 5.82 (m, 1H), 5.04 (m, 2H), 3.86 (m, 1H), 3.79 (m, 1H), 3.67 (m, 1H), 3.33 (*minor*, d, *J* = 2.5 Hz), 3.17 (*major*, d, *J* = 2.5 Hz, 1H) 2.23 (m, 1H), 1.61 (m, 2H), 1.02 (d, *J* = 7.0 Hz, 3H), 0.88 (s, 9H), -0.05 (s, 6H) ppm; ^{13}C NMR ($CDCl_3$, 125 MHz) δ 140.71, 115.10, 75.03, 62.77, 43.94, 35.52, 25.87, 18.15, 15.74, -5.55 ppm; HRMS (ESI+) 245.1931 *m/z* $[M+H]^+$ ($C_{13}H_{29}O_2Si$ requires 245.1937).

[*] Flash chromatography of the catalyst did not give significantly higher yield or selectivity, so purification was omitted.

[†] Recycling the catalyst more than once led to significant erosion of the dr and er in the crotylation.

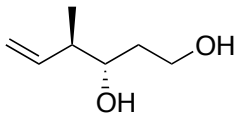

51

(3*S*,4*R*)-4-methylhex-5-ene-1,3-diol (51). The residue from above was dissolved in anhydrous THF (~95 mL) under argon, slowly treated with TBAF (1.0 M in THF, 23.0 mL, 23.37 mmol), and stirred for 1 h at room temperature. Reaction then quenched with sat. aq. NH_4Cl (50 mL) and THF removed by rotary evaporation. Residue partitioned between water (100 mL) and EtOAc (100 mL). The aqueous layer was washed with EtOAc (100 mL x 3) and combined organics dried with Na_2SO_4 and concentrated. Residue purified by chromatography (50 g Biotage® KP-SIL column, 1:1 H:E, 45 mL/min) on a CombiFlash Retrieve® system to afford the desired product (**51**, 1.60 g, 52% [2 steps]) as a clear, light orange oil. TLC R_f = 0.20 (1:1 H:E). ^1H NMR ($CDCl_3$, 500 MHz) δ 5.73 (m, 1H), 5.09 (m, 2H), 3.84 (m, 2H), 3.63 (m, 1H), 2.98 (bs, 1H), 2.68 (bs, 1H), 2.23 (m, 1H), 1.68 (m, 2H), 1.02 (d, *J* = 5.0 Hz, 3H) ppm; ^{13}C NMR ($CDCl_3$, 125 MHz) δ 140.28, 116.53, 75.00, 61.73, 44.68, 35.38, 15.99 ppm; HRMS (ESI+) 153.0885 *m/z* $[M+Na]^+$ ($C_7H_{14}NaO_2$ requires 153.0891).

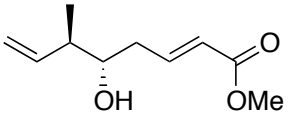

53

(5*S*,6*R*,*E*)-methyl 5-hydroxy-6-methylocta-2,7-dienoate (53). A solution of **51** (920 mg, 7.07 mmol) and TEMPO (110 mg, 0.707 mmol) in ACN (75 mL) was treated with solid [bis(acetoxy)iodo]benzene (BAIB, 2.62 g, 8.13 mmol) and stirred at room temperature for 2 h. Reaction cooled to 0 °C and treated with solid methyl(triphenylphosphoranylidene) acetate (3.07 g, 9.19 mmol). Reaction stirred for an additional hour, allowing it to warm to room temperature. Reaction then quenched with sat. aq. $Na_2S_2O_3$ and solvent removed *in vacuo*. Recovered material partitioned between water (200 mL) and DCM (200 mL). The aqueous layer was extracted with DCM (100 mL x 2) and combined organics washed with brine and dried with Na_2SO_4. Solvent removed by rotary evaporation and residue flash purified (SiO_2, 4:1 H:E) to afford 937 mg of pure **53** (72%) as a clear, faint yellow oil. TLC R_f = 0.35 (4:1

H:E). ^{1}H NMR ($CDCl_3$, 500 MHz) δ 7.01 (m, 1H), 5.91 (d, *J* = 15 Hz, 1H), 5.73 (m, 1H), 5.13 (m, 2H), 3.72 (s, 3H), 3.56 (m, 1H), 2.43 (m, 1H), 2.24 (m, 2H), 1.81 (bs, 1H), 1.05 (d, *J* = 5.0 Hz, 3H) ppm; ^{13}C NMR ($CDCl_3$, 125 MHz) δ 166.92, 145.96, 139.65, 123.32, 117.10, 73.49, 51.61, 44.01, 37.18, 16.32 ppm; HRMS (ESI+) 207.0995 *m/z* $[M+Na]^+$ ($C_{10}H_{16}NaO_3$ requires 207.0997).

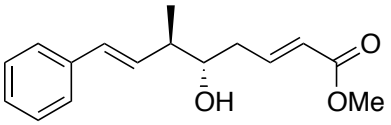

60a

(2*E*,5*S*,6*R*,7*E*)-methyl 5-hydroxy-6-methyl-8-phenylocta-2,7-dienoate (60a). Heck Reaction: $Pd(OAc)_2$ (2 mg, 0.0089 mmol) was added to a flame-dried, screw top vial under argon (solid aryl iodides were also added at this step) and dissolved in a solution of **53** (34 mg, 0.185 mmol) in anhydrous ACN (1.8 mL). The iodobenzene (23 µL, 0.203 mmol) was then added, followed by Et_3N (258 µL, 1.85 mmol). Reaction stirred at 85 ^{o}C for 18 h and then cooled to room temperature. Reaction was concentrated *in vacuo* and residue flash purified (SiO_2, 2:1 H:MTBE) to afford 13 mg of **60a** (31%) as a clear, colorless oil. TLC R_f = 0.60 (1:1 H:MTBE). Compounds **60b**, **60c**, and **60d** prepared through Heck reaction were accessed in an analogous manner. Compound **60a**: ^{1}H NMR ($CDCl_3$, 500 MHz) δ 7.38 (m, 2H), 7.31 (m, 2H), 7.24 (m, 1H), 7.05 (m, 1H), 6.48 (d, *J* = 15.9 Hz, 1H), 6.13 (dd, *J* = 8.7, 15.9 Hz, 1H), 5.92 (d, *J* = 15.8 Hz, 1H), 3.74 (s, 3H), 3.66 (m, 1H), 2.41 (m, 3H), 1.74 (d, *J* = 3.9 Hz, 1H), 1.16 (d, *J* = 6.8 Hz, 3H) ppm; ^{13}C NMR ($CDCl_3$, 125 MHz) δ 166.89, 145.81, 137.09, 132.27, 130.99, 128.73, 127.62, 126.29, 123.45, 73.95, 51.64, 43.51, 37.43, 16.96 ppm; HRMS (ESI+) 283.1305 *m/z* $[M+Na]^+$ ($C_{16}H_{20}NaO_3$ requires 283.1310).

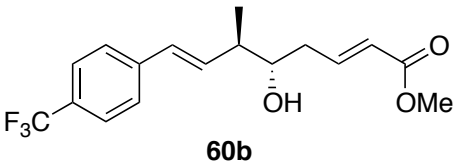

60b

(2*E*,5*S*,6*R*,7*E*)-methyl 5-hydroxy-6-methyl-8-(4-(trifluoromethyl)phenyl) octa-2,7-dienoate (60b): 28%; TLC R_f = 0.60 (1:1 H:MTBE). ^{1}H NMR ($CDCl_3$, 500 MHz) δ 7.56 (d, *J* = 8.2 Hz, 2H), 7.46 (d, *J* = 8.1 Hz, 2H), 7.03 (dt, *J* = 7.0, 14.9 Hz, 1H), 6.49 (d, *J* = 16.0 Hz,

1H), 6.26 (dd, *J* = 8.6, 16.0 Hz, 1H), 5.93 (d, *J* = 15.7 Hz, 1H), 3.73 (s, 3H), 3.70 (m, 1H), 2.45 (m, 3H), 1.71 (d, *J* = 3.9 Hz, 1H), 1.17 (d, *J* = 4.6 Hz, 3H) ppm; ^{13}C NMR ($CDCl_3$, 125 MHz) δ 166.83, 145.48, 140.62, 133.93, 130.76, 126.48, 126.44, 125.66 (q, *J* = 3.8 Hz), 123.67, 73.89, 51.68, 43.45, 37.63, 16.95 ppm; HRMS (ESI+) 351.1186 *m/z* $[M+Na]^+$ ($C_{17}H_{19}F_3NaO_3$ requires 351.1184).

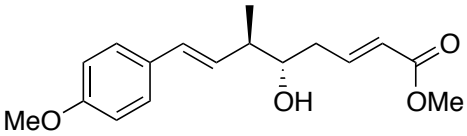

60c

(2*E*,5*S*,6*R*,7*E*)-methyl 5-hydroxy-8-(4-methoxyphenyl)-6-methylocta-2,7-dienoate (60c): 38%; TLC R_f = 0.55 (1:1 H:MTBE). ^{1}H NMR ($CDCl_3$, 500 MHz) δ 7.30 (d, *J* = 6.7 Hz, 2H), 7.06 (m, 1H), 6.86 (d, *J* = 8.7 Hz, 2H), 5.94 (m, 2H), 3.81 (s, 3H), 3.73 (s, 3H), 2.37 (m, 3H), 1.77 (d, *J* = 3.7 Hz, 1H), 1.13 (d, *J* = 6.8 Hz, 3H) ppm; ^{13}C NMR ($CDCl_3$, 125 MHz) δ 166.92, 159.27, 145.93, 131.74, 128.69, 127.49, 123.37, 114.13, 112.94, 73.96, 55.47, 51.64, 43.52, 37.37, 17.03 ppm; HRMS (ESI+) 313.1416 *m/z* $[M+Na]^+$ ($C_{17}H_{22}NaO_4$ requires 313.1416).

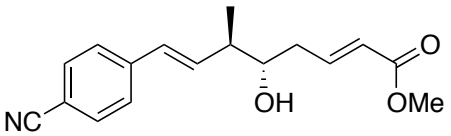

60d

(2*E*,5*S*,6*R*,7*E*)-methyl 8-(4-cyanophenyl)-5-hydroxy-6-methylocta-2,7-dienoate (60d): 30%; TLC R_f = 0.40 (1:1 H:MTBE). ^{1}H NMR ($CDCl_3$, 500 MHz) δ 7.59 (d, *J* = 8.3 Hz, 2H), 7.44 (d, *J* = 8.4 Hz, 2H), 7.01 (m, 1H), 6.46 (d, *J* = 15.9 Hz, 1H), 6.32 (dd, *J* = 8.6, 16.0 Hz, 1H), 5.92 (d, *J* = 15.7 Hz, 1H), 3.73 (s, 3H), 3.71 (m, 1H), 2.46 (m, 2H), 2.38 (m, 1H), 1.70 (d, *J* = 4.0 Hz, 1H), 1.17 (d, *J* = 6.9 Hz, 3H) ppm; ^{13}C NMR ($CDCl_3$, 125 MHz) δ 166.54, 145.06, 141.40, 135.17, 132.31, 130.15, 126.58, 123.52, 118.86, 110.48, 73.60, 51.46, 43.19, 37.48, 16.71 ppm; HRMS (ESI+) 308.1266 *m/z* $[M+Na]^+$ ($C_{17}H_{19}NNaO_3$ requires 308.1263).

Cross metathesis. Solid Hoveyda-Grubbs II (9 mg, 0.015 mmol) was added to a flame-dried, screw top vial and the atmosphere was exchanged for argon.

The catalyst was dissolved in a solution of **53** (54 mg, 0.293 mmol) in anhydrous, degassed DCM (1.17 mL). Styrene (134 µL, 1.17 mmol) was then added via syringe and reaction stirred at reflux temperature for 4 h. Reaction cooled to room temperature, treated with 50 eq. of DMSO, and stirred at room temperature for 12 h. The reaction was then concentrated *in vacuo* and purified by flash chromatography (SiO_2, 2:1 H:MTBE) to afford **60a** (23 mg, 30%) as a clear, colorless oil. Spectra were identical to those collected for **60a** above. Compounds **60b**, **60c**, and **60d** prepared through cross metathesis were accessed in an analogous manner and had spectra identical to those reported above. Compound **60b**: clear, light yellow oil (23%). Compound **60c**: clear, colorless oil (26%). Compound **60d**: clear, light yellow oil (8%).

Suzuki-Miyaura cross coupling. $[Pd_2(dba)_3]$ (2 mg, 0.0018 mmol), tricyclohexylphosphine (1 mg, 0.0043 mmol), and K_3PO_4 (32 mg, 0.153 mmol) were added to a flame-dried screw top vial under argon and suspended in a solution of **62** (28 mg, 0.090 mmol) in anhydrous DME (240 µL). Water that had been degassed under vacuum in a sonicator (120 µL) and iodobenzene (12 µL, 0.108 mmol) were then added and reaction stirred at 85 ^{o}C for 2 h. Reaction cooled to room temperature and diluted with water (5 mL) and EtOAc (5 mL). The aqueous layer was extracted with EtOAc (5 mL x 3) and combined organics washed with brine (10 mL) and dried with Na_2SO_4. Solvent removed *in vacuo* and residue flash purified (SiO_2, 2:1 H:MTBE) to afford **60a** (10 mg, 42%) as a clear, colorless oil. Spectra were identical to those collected for **60a** above. Compounds **60b**, **60c**, and **60d** prepared through Suzuki-Miyaura coupling were accessed in an analogous manner and had spectra identical to those reported above. Compound **60b**: clear, light yellow oil (55%). Compound **60c**: clear, colorless oil (53%). Compound **60d**: clear, light yellow oil (63%).

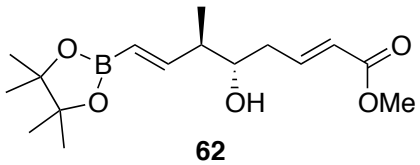

62

(2*E*,5*S*,6*R*,7*E*)-methyl 5-hydroxy-6-methyl-8-(4,4,5,5-tetramethyl-1,3,2-dioxaborolan-2-yl)octa-2,7-dienoate (12). Solid Hoveyda-Grubbs II (190 mg, 0.304 mmol) was added to a flame-dried 2-neck flask equipped with a reflux condenser under argon and dissolved in anhydrous, degassed DCM (20 mL). A solution of **53** (1.12 g, 6.08 mmol) in 10 mL DCM was then added to the flask. Vinylboronic acid pinacol ester (2.06 mL, 12.16 mmol) was passed through a plug of activated charcoal immediately prior to use and added via syringe to the stirring reaction mixture. Reaction heated at reflux temperature for 4 h, then cooled to room temperature and treated with 50 eq. of DMSO, stirring overnight, to allow removal of colored ruthenium byproducts upon silica purification.[2] Reaction concentrated and residue purified by flash chromatography (SiO_2, 3:1 pentane:EtOAc) to afford 934 mg of **62** as a clear, light tan oil (50%). ^{1}H NMR ($CDCl_3$, 500 MHz) δ 7.01 (m, 1H), 6.52 (dd, *J* = 7.9, 18.1 Hz, 1H), 5.91 (d, *J* = 15.8 Hz, 1H), 5.53 (d, *J* = 18.1 Hz, 1H), 3.73 (s, 3H), 3.62 (m, 1H), 2.37 (m, 3H), 1.66 (d, *J* = 4.2 Hz, 1H), 1.27 (s, 12H), 1.06 (d, *J* = 6.9 Hz, 3H) ppm; ^{13}C NMR ($CDCl_3$, 125 MHz) δ 166.89, 154.28, 145.89, 123.53, 83.44, 73.45, 51.63, 45.74, 37.13, 24.97, 24.93, 15.78 ppm; HRMS (ESI+) 333.1858 *m/z* $[M+Na]^+$ ($C_{16}H_{27}BNaO_5$ requires 333.1849).

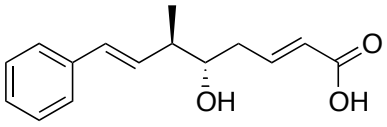

74a

(2*E*,5*S*,6*R*,7*E*)-5-hydroxy-6-methyl-8-phenylocta-2,7-dienoic acid (unit A, 74a). A solution of **60a** (10 mg, 0.038 mmol) in a 1:1:0.5 mixture of methanol/water/THF (385 µL) was treated with solid LiOH□H_2O (5 mg, 0.115 mmol) and stirred at room temperature for 2 h. Reaction then quenched with 0.1 M HCl and diluted with water (2 mL) and EtOAc (2 mL). Aqueous layer extracted with EtOAc (2 mL x 2) and combined organics washed with brine and dried with Na_2SO_4. Solvent removed *in vacuo* and residue purified by flash chromatography (SiO_2, 5:95 MeOH:DCM + 0.1%

HOAc) to afford **74a** as a clear, light yellow oil (8.5 mg, 89%). TLC R_f = 0.50 (5:95 MeOH:DCM + 0.1% HOAc). Compounds **74b**, **74c**, and **74d** were hydrolyzed using an identical procedure. Compound **74a**: ^{1}H and ^{13}C NMR spectra matched those previously reported[1]; HRMS (ESI+) 269.1149 *m/z* $[M+Na]^+$ ($C_{15}H_{18}NaO_3$ requires 269.1154).

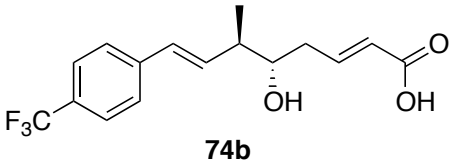

74b

(2*E*,5*S*,6*R*,7*E*)-5-hydroxy-6-methyl-8-(4-(trifluoromethyl)phenyl)octa-2,7-dienoic acid (74b). 90%; TLC R_f = 0.50 (5:95 MeOH:DCM + 0.1% HOAc). ^{1}H NMR ($CDCl_3$, 500 MHz) δ 7.55 (d, *J* = 8.2 Hz, 2H), 7.45 (d, *J* = 8.2 Hz, 2H), 7.15 (dt, *J* = 7.4, 15.7 Hz, 1H), 6.50 (d, *J* = 15.9 Hz, 1H), 6.24 (dd, *J* = 8.7, 16.0 Hz, 1H), 5.93 (d, *J* = 15.7 Hz, 1H), 3.72 (m, 1H), 2.48 (m, 3H), 1.17 (d, *J* = 6.8 Hz, 3H) ppm; ^{13}C NMR ($CDCl_3$, 125 MHz) δ 170.88, 148.57, 140.52, 133.68, 130.98, 126.50, 126.45, 125.70 (q, *J* = 3.8 Hz), 122.96, 73.91, 43.57, 37.60, 16.89 ppm; HRMS (ESI+) 337.1027 *m/z* $[M+Na]^+$ ($C_{16}H_{17}F_3NaO_3$ requires 337.1027).

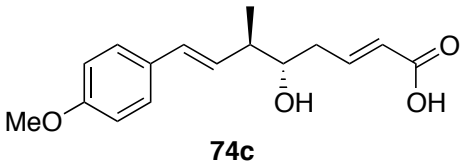

74c

(2*E*,5*S*,6*R*,7*E*)-5-hydroxy-8-(4-methoxyphenyl)-6-methylocta-2,7-dienoic acid (74c). 84%; TLC R_f = 0.45 (5:95 MeOH:DCM + 0.1% HOAc). ^{1}H NMR ($CDCl_3$, 500 MHz) δ 7.30 (d, *J* = 8.7 Hz, 2H), 7.16 (dt, *J* = 7.3, 15.6 Hz, 1H), 6.85 (d, *J* = 8.7 Hz, 2H), 6.42 (d, *J* = 15.8 Hz, 1H), 5.95 (m, 2H), 3.81 (s, 3H), 3.65 (m, 1H), 2.51 (m, 1H), 2.38 (m, 2H), 1.13 (d, *J* = 9.1 Hz, 3H) ppm; ^{13}C NMR ($CDCl_3$, 125 MHz) δ 170.87, 159.30, 148.70, 131.88, 129.83, 128.54, 127.51, 122.83, 114.15, 73.96, 55.47, 43.62, 37.41, 17.00 ppm; HRMS (ESI+) 299.1260 *m/z* $[M+Na]^+$ ($C_{16}H_{20}NaO_4$ requires 299.1259).

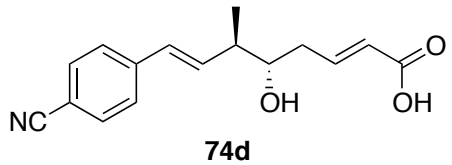

74d

(2*E*,5*S*,6*R*,7*E*)-8-(4-cyanophenyl)-5-hydroxy-6-methylocta-2,7-dienoic acid (74d). 73%; TLC R_f = 0.35 (5:95 MeOH:DCM + 0.1% HOAc). ^{1}H NMR ($CDCl_3$, 500 MHz) δ 7.59 (d, *J* = 8.3 Hz, 2H), 7.44 (d, *J* = 8.4 Hz, 2H), 7.16 (dt, *J* = 7.3, 15.6 Hz, 1H), 6.48 (d, *J* = 15.9 Hz, 1H), 6.31 (dd, *J* = 8.6, 16.0 Hz, 1H), 5.94 (d, *J* = 15.7 Hz, 1H), 3.75 (m, 1H), 2.47 (m, 3H), 1.18 (d, *J* = 6.8 Hz, 3H) ppm; ^{13}C NMR ($CDCl_3$, 125 MHz) δ 170.74, 148.84, 141.57, 135.15, 132.60, 130.67, 126.93, 126.85, 122.81, 119.05, 73.88, 43.61, 37.73, 16.90 ppm; HRMS (ESI+) 294.1102 *m/z* $[M+Na]^+$ ($C_{16}H_{17}NNaO_3$ requires 294.1106).

6.4 Mosher Ester Analysis

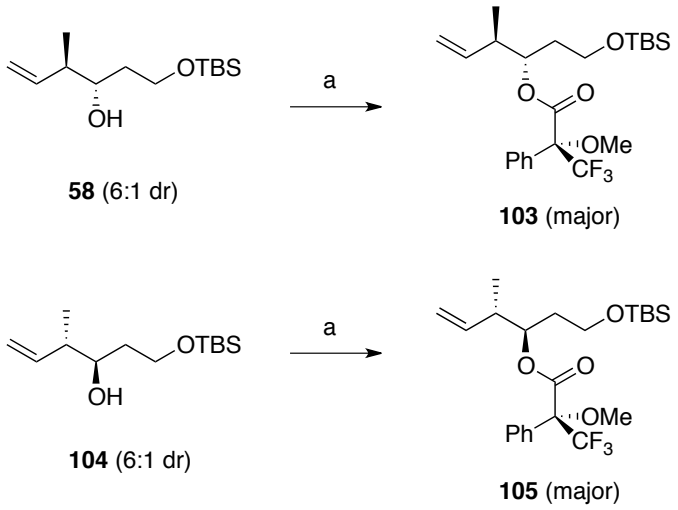

Scheme 6.1: Synthesis of Mosher ester derivatives 103 and 105. *Reaction conditions:* (a) (*S*)-MTPACl, pyridine, 60 °C, 24 h (**103**, 71%; **105**, 70%).

(*R*)-(3*S*,4*R*)-1-((*tert*-butyldimethylsilyl)oxy)-4-methylhex-5-en-3-yl 3,3,3-trifluoro-2-methoxy-2-phenylpropanoate (103). A solution of **58** (6 mg, 0.025 mmol) in anhydrous pyridine (50 µL) was treated with fresh (*S*)-(+)-α-methoxy-α-trifluoromethylphenylacetyl chloride (*S*-MTPACl, 14 µL, 0.074 mmol) and stirred at 60 °C under argon for 24 h. Reaction then cooled to room temperature, concentrated under vacuum, and purified by flash chromatography (SiO_2, 12:1 H:MTBE) to afford 8 mg of **103** (71%). TLC R_f =

0.90 (10:1 H:MTBE). ^{1}H NMR ($CDCl_3$, 500 MHz) δ 7.55 (m, 2H), 7.40 (m, 3H), 5.67 (m, 1H), 5.24 (m, 1H), 5.05 (m, 2H), 3.61 (m, 2H), 3.54 (s, 3H), 2.54 (m, 1H), 1.80 (m, 2H), 0.94 (d, *J* = 7.1 Hz, 3H), 0.88 (s, 9H), 0.02 (s, 6H) ppm; ^{13}C NMR ($CDCl_3$, 125 MHz) δ 166.24, 138.60, 132.45, 129.68, 127.60, 124.71, 122.42, 116.42, 77.30, 59.40, 55.53, 41.07, 33.89, 26.01, 18.37, 15.37, -5.28 ppm; ^{19}F NMR ($CDCl_3$, 470 MHz) δ -71.19 (*minor*), -71.23 (*major*) ppm; HRMS (ESI+) 483.2159 *m/z* $[M+Na]^+$ ($C_{23}H_{35}F_3NaO_4Si$ requires 483.2154). Compound **104** was prepared from **49** and (*S*)-(-)-**57**, the Mosher ester of which (**105**) was used for ^{19}F NMR comparison purposes.

Compound **104**: 72%; TLC R_f = 0.45 (10:1 H:MTBE x2). ^{1}H NMR ($CDCl_3$, 400 MHz) δ 5.80 (m, 1H), 5.04 (m, 2H), 3.83 (m, 2H), 3.68 (m, 1H), 3.36 (*minor*, d, *J* = 2.2 Hz), 3.21 (*major*, d, *J* = 2.2 Hz, 1H), 2.23 (m, 1H), 1.63 (m, 2H), 1.03 (d, *J* = 6.9 Hz, 3H), 0.89 (s, 9H), 0.06 (s, 6H) ppm; ^{13}C NMR ($CDCl_3$, 100 MHz) δ 142.20, 110.32, 75.00, 65.65, 43.95, 35.53, 25.88, 18.16, 15.21, -5.51 ppm; HRMS (ESI+) 245.1935 *m/z* $[M+H]^+$ ($C_{13}H_{29}O_2Si$ requires 245.1937).

Compound **105**: 70%; TLC R_f = 0.90 (10:1 H:MTBE). ^{1}H NMR ($CDCl_3$, 500 MHz) δ 7.55 (m, 2H), 7.39 (m, 3H), 5.72 (m, 1H), 5.24 (m, 1H), 5.06 (m, 2H), 3.54 (s, 3H), 3.50 (m, 2H), 2.57 (m, 1H), 1.74 (m, 2H), 1.03 (d, *J* = 7.0 Hz, 3H), 0.87 (s, 9H), 0.01 (s, 6H) ppm; ^{13}C NMR ($CDCl_3$, 125 MHz) δ 166.30, 138.85, 132.40, 129.69, 128.48, 127.63, 124.69, 122.40, 116.40, 77.37, 59.20, 55.57, 41.27, 33.84, 26.00, 18.33, 15.62, -5.29 ppm; ^{19}F NMR ($CDCl_3$, 470 MHz) δ -71.20 (*major*), -71.23 (*minor*) ppm; HRMS (ESI+) 483.2157 *m/z* $[M+Na]^+$ ($C_{23}H_{35}F_3NaO_4Si$ requires 483.2154).

6.5 Synthesis of Novel *seco*-Cryptophycin SNAc-Thioester Substrates

The SNAc-thioester CrpTE substrates were synthesized as previously reported with minor modifications as follows.[3]

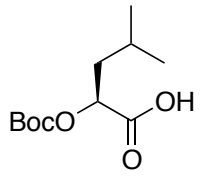

76

(*S*)-2-((*tert*-butoxycarbonyl)oxy)-4-methylpentanoic acid (76). The *S*-2-hydroxy-4-methylvaleric acid (1.0 g, 7.57 mmol) was flame-dried under vacuum and then suspended in 15 mL of anhydrous DMF. This suspension was treated with pyridine (3.06 mL, 37.85 mmol) and di-*tert*-butyl dicarbonate (3.48 mL, 15.13 mmol) and stirred at room temperature under argon overnight. The reaction was then acidified with 1.0 M HCl and diluted with water (100 mL) and EtOAc (100 mL). The aqueous layer was extracted with additional EtOAc (2 x 50 mL) and the combined organics were washed with brine and dried with Na_2SO_4. Evaporation of the solvent and chromatographic purification (SiO_2, 1:1:1 H:E:CH_2Cl_2 + 0.1% HOAc) afforded the desired product (**76**, 462 mg, 27%) as a clear, light yellow oil. TLC R_f = 0.40 (2:1 H:E + 1% HOAc). ^{1}H NMR ($CDCl_3$, 400 MHz) δ 4.90 (m, 1H), 1.85 (m, 2H), 1.66 (m, 1H), 1.47 (s, 9H), 0.95 (dd, *J* = 4.6, 6.1 Hz, 6H) ppm.

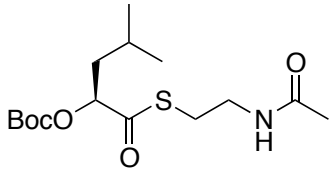

77

(*S*)-*S*-(2-acetamidoethyl) 2-((*tert*-butoxycarbonyl)oxy)-4-methylpentanethioate (77). A solution of **76** (2.06 g, 8.87 mmol) in CH_2Cl_2 (45 mL) was treated with solid EDC•HCl (3.40 g, 17.74 mmol), HOBt hydrate (2.72 g, 17.74 mmol), and DIPEA (3.40 mL, 19.51 mmol). Reaction stirred at room temperature for 10 min and then treated with N-acetylcysteamine (SNAc, 1.70 mL, 15.96 mmol). After stirring at room temperature overnight, the reaction was diluted with CH_2Cl_2 (50 mL) and sat. aq. $NaHCO_3$ (50 mL). The aqueous layer was extracted with additional CH_2Cl_2 (2 x 50 mL) and the combined organics were washed with 1.0 M HCl and brine, then dried with Na_2SO_4. Evaporation of the solvent and chromatographic purification (SiO_2 + top $CuSO_4$-impregnated SiO_2 layer, 2:1 CH_2Cl_2:E) afforded the desired product (**77**, 1.36 g, 46%) as a clear, colorless oil. TLC R_f = 0.30 (2:1 CH_2Cl_2:E). ^{1}H NMR ($CDCl_3$, 400 MHz) δ 5.82 (bs, 1H),

5.01 (dd, *J* = 3.9, 10.0 Hz, 1H), 3.42 (m, 2H), 3.06 (m, 2H), 2.03 (s, 3H), 1.78 (m, 2H), 1.58 (m, 1H), 1.48 (s, 9H), 0.94 (dd, *J* = 3.1, 6.3 Hz, 6H) ppm.

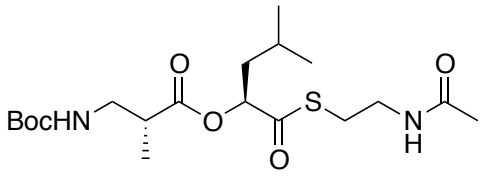

78

(*R*)-(*S*)-1-((2-acetamidoethyl)thio)-4-methyl-1-oxopentan-2-yl 3-((*tert*-butoxycarbonyl)amino)-2-methylpropanoate (78). A solution of **77** (392 mg, 0.943 mmol) in 4 N HCl/dioxane (2 mL) was stirred at room temperature for 2 h and then thoroughly dried under vacuum. The residue was dissolved in anhydrous THF (1.0 mL) and added to a stirred solution of (*R*)-3-(Boc-amino)-2-methylpropionic acid (230 mg, 1.13 mmol), EDC•HCl (217 mg, 1.13 mmol), HOBt hydrate (173 mg, 1.13 mmol), and DIPEA (360 µL, 2.08 mmol) in 5.0 mL anhydrous THF. The reaction was stirred at room temperature overnight and then concentrated *in vacuo*. The reside was partitioned between dilute NH_4Cl (50 mL) and CH_2Cl_2 (50 mL), and the aqueous layer was extracted with additional CH_2Cl_2 (2 x 50 mL). The combined organics were washed with brine and dried with Na_2SO_4. Evaporation of the solvent and chromatographic purification (SiO_2, 3:97 MeOH:CH_2Cl_2 to 5:95 MeOH:CH_2Cl_2) afforded the desired product (**78**, 126 mg, 32% [51% brsm]) as a clear, colorless resin. TLC R_f = 0.65 (5:95 MeOH:CH_2Cl_2 + 1% NH_4OH). ^1H NMR (CD_3OD, 400 MHz) δ 8.13 (bs, 1H), 6.69 (bs, 1H), 5.22 (dd, *J* = 3.8, 9.5 Hz, 1H), 3.22 (m, 2H), 3.01 (m, 2H), 1.92 (s, 3H), 1.77 (m, 2H), 1.64 (m, 1H), 1.42 (s, 9H), 1.20 (d, *J* = 7.1 Hz, 3H), 0.95 (dd, *J* = 6.4, 13.1 Hz, 6H) ppm.

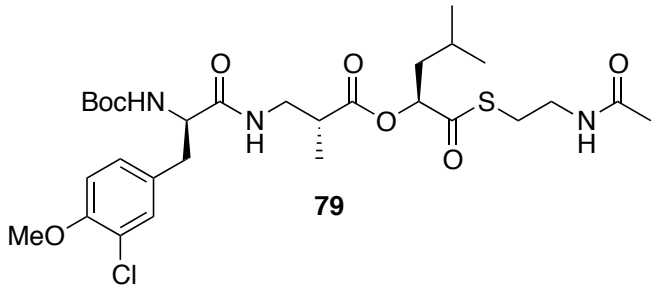

79

(*R*)-(*S*)-1-((2-acetamidoethyl)thio)-4-methyl-1-oxopentan-2-yl 3-((*R*)-2-((*tert*-butoxycarbonyl)amino)-3-(3-chloro-4-methoxyphenyl) propanamido)-2-methylpropanoate (79). Compound **78** (621 mg, 1.48 mmol) was dissolved in 4 N HCl/dioxane (7 mL) and stirred at room temperature for 30 min, then dried thoroughly under vacuum. The residue was dissolved in 5 mL anhydrous THF and added to a stirred solution of **87** (1.66 mmol), EDC•HCl (339 mg, 1.77 mmol), HOBt hydrate (271 mg, 1.77 mmol), and DIPEA (773 µL, 4.44 mmol) in 13 mL anhydrous THF. Reaction stirred at room temperature overnight and then concentrated under vacuum. The residue was partitioned between dilute NH_4Cl (50 mL) and CH_2Cl_2 (50 mL), and the aqueous layer was extracted with additional CH_2Cl_2 (2 x 50 mL). The combined organics were washed with brine and dried with Na_2SO_4. Evaporation of the solvent and chromatographic purification (SiO_2, 3:97 MeOH:CH_2Cl_2) afforded the desired product (**79**, 656 mg, 70%) as a white foam. TLC R_f = 0.70 (5:95 MeOH:CH_2Cl_2). ^{1}H NMR (CD_3OD, 400 MHz) δ 7.24 (s, 1H), 7.12 (dd, *J* = 2.1, 8.4 Hz, 1H), 6.97 (d, *J* = 8.4 Hz, 1H), 5.22 (dd, *J* = 3.9, 9.5 Hz, 1H), 4.19 (m, 1H), 3.84 (s, 3H), 3.49 (m, 1H), 3.27 (m, 2H), 3.00 (m, 3H), 2.73 (m, 2H), 1.90 (s, 3H), 1.75 (m, 2H), 1.63 (m, 1H), 1.36 (s, 9H), 1.13 (d, *J* = 7.1 Hz, 3H), 0.94 (dd, *J* = 6.4, 13.6 Hz, 6H) ppm.

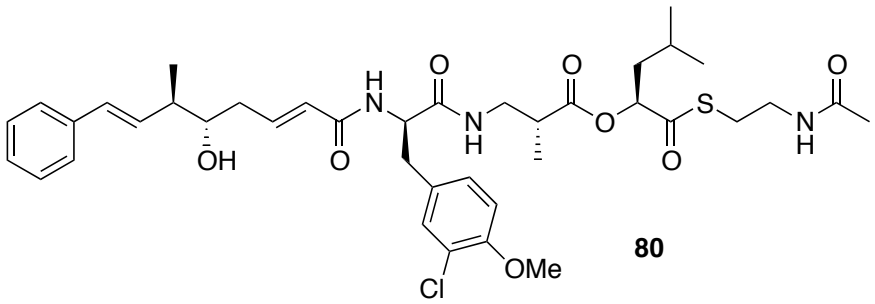

80

(*R*)-(*S*)-1-((2-acetamidoethyl)thio)-4-methyl-1-oxopentan-2-yl 3-((*R*)-3-(3-chloro-4-methoxyphenyl)-2-((2*E*,5*S*,6*R*,7*E*)-5-hydroxy-6-methyl-8-phenylocta-2,7-dienamido)propanamido)-2-methylpropanoate (80). Compound **79** (130 mg, 0.206 mmol) was dissolved in 2 mL of 4 N HCl/dioxane and stirred at room temperature for 30 min, after which the reaction was thoroughly dried under vacuum. The residue was dissolved in 1 mL anhydrous THF and added to a stirred solution of **48** (89 mg, 0.361 mmol), EDC•HCl (69 mg, 0.361 mmol), HOBt hydrate (55 mg, 0.361 mmol), and DIPEA (108 µL, 0.618 mmol). The reaction was stirred at room temperature overnight and then concentrated under a stream of nitrogen. The residue was partitioned between dilute NH_4Cl (10 mL) and EtOAc (10 mL). The aqueous layer was extracted with additional EtOAc (2 x 10 mL) and the combined organics were washed with brine and dried with Na_2SO_4. Evaporation of the solvent and chromatographic purification (SiO_2, 3:97 MeOH:CH_2Cl_2) afforded the desired product (**80**, 86 mg, 55%) as a clear, faint yellow oil. TLC R_f = 0.55 (5:95 MeOH:CH_2Cl_2). Compounds **81**, **82**, and **83** were accessed in an analogous manner. Compound **80**: ^{1}H NMR (CD_3OD, 500 MHz) δ 7.36 (d, *J* = 7.6 Hz, 2H), 7.26 (m, 3H), 7.14 (m, 2H), 6.96 (d, *J* = 6.8 Hz, 1H), 6.80 (dd, *J* = 7.6, 15.2 Hz, 1H), 6.41 (d, *J* = 15.9 Hz, 1H), 6.23 (dd, *J* = 8.6, 15.9 Hz, 1H), 6.00 (d, *J* = 15.4 Hz, 1H), 5.21 (m, 1H), 4.56 (m, 1H), 3.83 (s, 3H), 3.64 (m, 1H), 3.48 (dd, *J* = 6.5, 13.4 Hz, 1H), 3.18 (dd, *J* = 7.0, 13.5 Hz, 1H), 3.01 (m, 3H), 2.83 (m, 1H), 2.68 (m, 1H), 2.40-2.30 (m, 3H), 1.74 (m, 2H), 1.62 (m, 1H), 1.14 (d, *J* = 6.9 Hz, 3H), 1.09 (d, *J* = 7.1 Hz, 3H), 0.93 (dd, *J* = 5.2, 11.6 Hz, 6H) ppm. ^{13}C NMR (CD_3OD, 125 MHz) δ 198.92, 173.63, 172.07, 166.64,

153.96, 142.08, 137.61, 131.05, 130.67, 130.47, 130.05, 128.41, 128.05, 126.61, 125.70, 124.64, 111.90, 77.19, 73.90, 55.13, 54.82, 42.79, 41.29, 40.52, 39.14, 38.42, 37.40, 37.38, 36.64, 27.13, 24.31, 22.05, 21.10, 20.52, 16.11, 13.43 ppm.

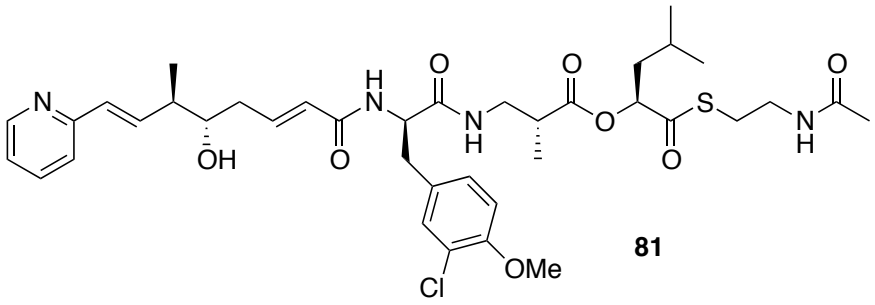

81

(*R*)-(*S*)-1-((2-acetamidoethyl)thio)-4-methyl-1-oxopentan-2-yl 3-((*R*)-3-(3-chloro-4-methoxyphenyl)-2-((2*E*,5*S*,6*R*,7*E*)-5-hydroxy-6-methyl-8-(pyridin-2-yl)octa-2,7-dienamido)propanamido)-2-methylpropanoate (81): 47%; TLC R_f = 0.35 (5:95 MeOH:CH_2Cl_2). ^{1}H NMR (CD_3OD, 500 MHz) δ 8.43 (m, 1H), 7.76 (m, 1H), 7.51 (d, *J* = 8.0 Hz, 1H), 7.23 (m, 2H), 7.13 (dd, *J* = 2.2, 8.4 Hz, 1H), 6.96 (d, *J* = 8.5 Hz, 1H), 6.80 (m, 1H), 6.66 (dd, *J* = 8.4, 16.0 Hz, 1H), 6.51 (d, *J* = 16.0 Hz, 1H), 6.02 (d, *J* = 15.4 Hz, 1H), 5.20 (m, 1H), 4.58 (m, 1H), 3.82 (s, 3H), 3.67 (m, 1H), 3.48 (dd, *J* = 6.6, 13.5 Hz, 1H), 3.19 (dd, *J* = 7.1, 13.5 Hz, 1H), 3.01 (m, 3H), 2.84 (m, 1H), 2.69 (m, 1H), 2.47-2.32 (m, 3H), 1.90 (s, 3H), 1.73 (m, 2H), 1.62 (m, 1H), 1.17 (d, *J* = 6.9 Hz, 3H), 1.09 (d, *J* = 7.1 Hz, 3H), 0.92 (dd, *J* = 6.4, 14.2 Hz, 6H) ppm. ^{13}C NMR (CD_3OD, 125 MHz) δ 198.91, 173.64, 172.06, 171.99, 166.60, 155.83, 153.97, 148.26, 141.86, 137.31, 137.21, 130.48, 128.43, 124.83, 120.90, 111.92, 77.20, 73.67, 55.15, 54.82, 42.65, 41.31, 40.53, 39.14, 38.43, 37.34, 36.67, 29.25, 27.15, 24.32, 22.05, 21.11, 20.54, 15.70, 13.45 ppm.

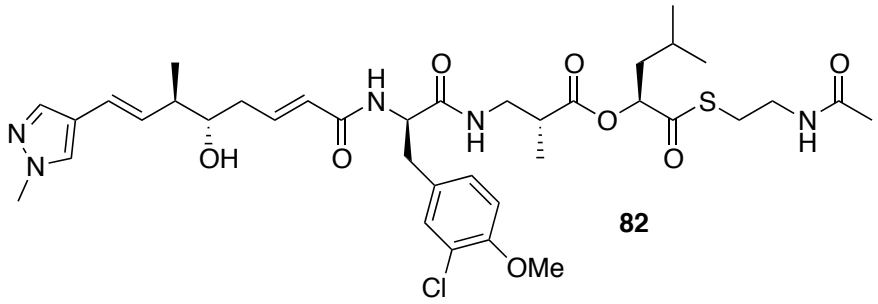

82

(*R*)-(*S*)-1-((2-acetamidoethyl)thio)-4-methyl-1-oxopentan-2-yl 3-((*R*)-3-(3-chloro-4-methoxyphenyl)-2-((2*E*,5*S*,6*R*,7*E*)-5-hydroxy-6-methyl-8-(1-methyl-1*H*-pyrazol-4-yl)octa-2,7-dienamido)propanamido)-2-methylpropanoate (82). *J. Schmidt*

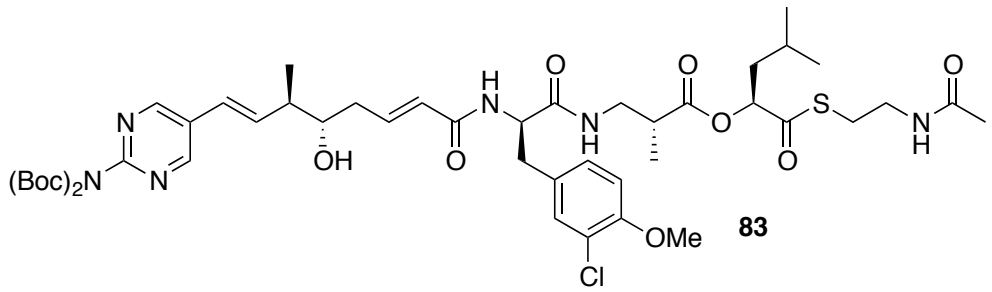

83

(*R*)-(*S*)-1-((2-acetamidoethyl)thio)-4-methyl-1-oxopentan-2-yl 3-((*R*)-3-(3-chloro-4-methoxyphenyl)-2-((2*E*,5*S*,6*R*,7*E*)-5-hydroxy-6-methyl-8-(1-methyl-2-aminopyrimidinyl-4-yl)octa-2,7-dienamido)propanamido)-2-methylpropanoate (83). *J. Schmidt*

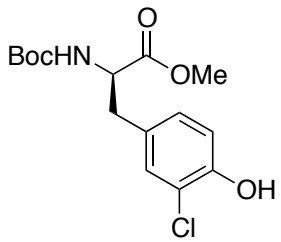

85

(*R*)-methyl 2-((*tert*-butoxycarbonyl)amino)-3-(3-chloro-4-hydroxyphenyl)propanoate (85). A suspension of H-D-Tyr-OMe•HCl (**84**, 10.0 g, 43.16 mmol) in glacial acetic acid (86 mL) was stirred vigorously and cooled to 0 °C in an ice bath. Sulfuryl chloride (4.2 mL 51.79 mmol) was then added dropwise and reaction stirred while warming to room temperature over 1 h. The reaction was then diluted with Et_2O (86 mL) and stirred for an additional 30 min at room temperature. The resulting white precipitate was collected by filtration, washed with Et_2O,

dried under vacuum, and suspended with $NaHCO_3$ (750 mg, 8.93 mmol) in 28 mL of a 4:1 mixture of THF and MeOH. This suspension was next treated with $(Boc)_2O$ (1.07 mL, 4.67 mmol) and stirred at room temperature for 4 h. The reaction was then concentrated and partitioned between 1.0 M HCl (50 mL) and CH_2Cl_2 (50 mL). The aqueous layer was extracted with additional CH_2Cl_2 (2 x 50 mL) and combined organics washed with brine (100 mL) and dried with Na_2SO_4. Purification completed by J. Schmidt for an 89% yield over 2 steps.

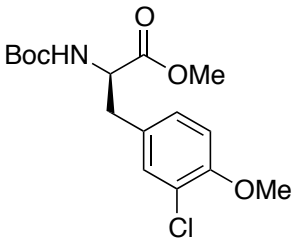

86

(*R*)-methyl 2-((*tert*-butoxycarbonyl)amino)-3-(3-chloro-4-methoxyphenyl)propanoate (86). Compound **85** was suspended with K_2CO_3 (1.29 g, 9.35 mmol) and iodomethane (582 µL, 9.35 mmol) in 22 mL of acetone dried over Na_2SO_4 and stirred at reflux temperature for 2 h. The reaction was then cooled to room temperature and concentrated under vacuum. The residue was partitioned between CH_2Cl_2 (50 mL) and dilute NH_4Cl (50 mL), and the aqueous layer was extracted with additional CH_2Cl_2 (2 x 50 mL). The combined organics were washed with brine (100 mL) and dried with Na_2SO_4. Evaporation of the solvent and chromatographic purification (SiO_2, 2:1 H:E) afforded the desired product (**86**, 1.30 g, 89%) as a clear, colorless oil. TLC R_f = 0.90 (1:1 H:E). ^1H NMR ($CDCl_3$, 500 MHz) δ 7.12 (s, 1H), 6.98 (d, *J* = 8.4 Hz, 1H), 6.84 (d, *J* = 8.0 Hz, 1H), 4.99 (m, 1H), 4.52 (m, 1H), 3.87 (s, 3H), 3.71 (s, 3H), 2.99 (dt, *J* = 5.5, 14.0 Hz, 2H), 1.42 (s, 9H) ppm.

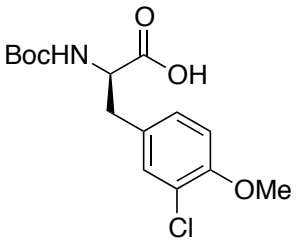

87

(*R*)-2-((*tert*-butoxycarbonyl)amino)-3-(3-chloro-4-methoxyphenyl)propanoic acid (87). A solution of **86** (570 mg, 1.66 mmol) in 8 mL of a 4:1 mixture of THF and water was treated with solid $LiOH•H_2O$ (139 mg,

3.32 mmol) and stirred at room temperature for 1 h. The reaction was judged to be complete after 1 h by TLC and then concentrated under vacuum. The resulting residue was partitioned between water and CH_2Cl_2, with the aqueous layer adjusted to pH ~3 with HCl. The aqueous layer was then extracted with additional CH_2Cl_2 and the combined organics were washed with brine and dried with Na_2SO_4. The solvent was evaporated under vacuum and the resulting residue used for coupling without further purification.

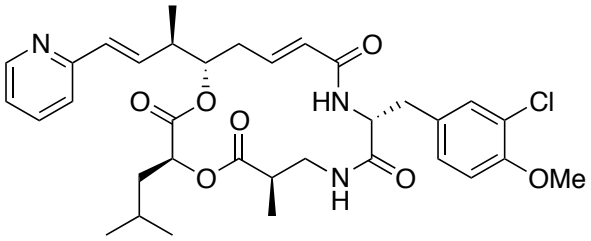

Cryptophycin 500

Cryptophycin 500. A 20 mL SPE tube equipped with a bottom frit was charged with 2.834 mL of 100 mM sodium phosphate buffer, pH 6.5, 925 µL diglyme, 166 µL of 30% aqueous methyl β-cyclodextrin, and 75 µL of **81** (50 mM in DMSO). CrpTE was then thawed on ice, 1 mL of purified protein was added to the SPE tube, and the tubes were tightly capped. The reaction was mixed by gently swirling the tube and then incubated at room temperature overnight on a rotary agitated set to 250 rpm. After overnight incubation, an equal volume with EtOAc was added to the tube and the reaction was shaken vigorously. The two-phase mixture was filtered though a packed column of celite - washing with water and EtOAc - transferred to a separatory funnel, and the aqueous layer was extracted with additional EtOAc (2 x 50 mL). The combined organic layers were washed with brine and dried with Na_2SO_4. Evaporation of the solvent and chromatographic purification (SiO_2, 3:97 MeOH:CH_2Cl_2) afforded the desired product (**Crp 500**, 3.4 mg, 35%) as a clear, colorless oil. TLC R_f = 0.55 (5:95 MeOH:CH_2Cl_2). Cryptophycin 500: ^{1}H NMR (CD_3OD, 400 MHz) δ 8.44 (dd, *J* = 5.0, 8.1 Hz, 1H), 7.76 (dt, *J* = 1.7, 7.6 Hz, 2H), 7.47 (d, *J* = 7.8 Hz, 1H), 7.24 (m, 2H), 7.15 (dd, *J* = 2.2, 8.5 Hz, 1H), 6.96 (d, *J* = 8.5 Hz, 1H), 6.69 (ddd, *J* = 3.9, 11.1, 15.0 Hz, 1H), 6.56 (m, 2H), 5.90 (d, *J* = 15.1 Hz, 1H), 5.10 (s, 1H), 5.06 (m, 1H), 4.91 (dd, *J* = 3.7, 9.9 Hz, 1H), 4.50 (dd, *J* = 3.8,

11.2 Hz, 1H), 3.82 (s, 3H), 3.57 (m, 2H), 3.32 (s, 3H), 3.24 (m, 1H), 3.16 (dd, *J* = 3.7, 14.6 Hz, 1H), 2.69 (m, 4H), 2.37 (m, 2H), 2.19 (m, 2H), 2.01 (m, 1H), 1.58 (m, 4H), 1.17 (s, 3H), 1.15 (s, 3H), 0.87 (d, *J* = 7.2 Hz, 3H), 0.70 (dd, *J* = 6.4, 14.3 Hz, 6H) ppm. ^{13}C NMR (CD_3OD, 100 MHz) δ 196.1, 179.3, 176.1, 172.6, 170.8, 166.9, 166.7, 155.1, 153.9, 148.5, 142.0, 139.6, 137.3, 136.2, 130.7, 130.6, 130.0, 127.8, 124.1, 122.3, 121.8, 121.4, 112.0, 77.0, 76.7, 71.4, 55.9, 55.1, 54.8, 42.0, 39.4, 37.5, 36.4, 34.9, 31.6, 29.3, 29.0, 24.2, 21.8, 20.2, 16.1, 13.6 ppm. HRMS (ESI+) 640.2971 *m/z* $[M+H]^+$ ($C_{34}H_{43}ClN_3O_7$ requires 640.2790).

6.6 SYNTHESIS OF METHYLATED CrpTE SUBSTRATE

The successful capture of a CrpTE crystal structure was not successful using wild type enzyme, so a substrate hindered in its ability to undergo cyclization was prepared as described in Scheme 6.2. When substrate **102**

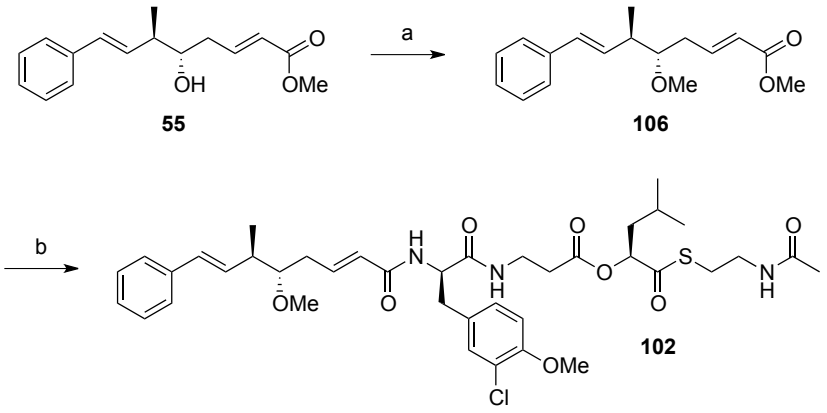

Scheme 6.2: Preparation of a methylated CrpTE substrate blocked in cyclization. *Reaction conditions:* (a) Ag_2O, MeI, THF, 23 °C, 24 h; (b) LiOH, MeOH/THF/H_2O, 23 °C; then EDC, HOBt, DIPEA, units DCB-SNAc, 23 °C, 18 h.

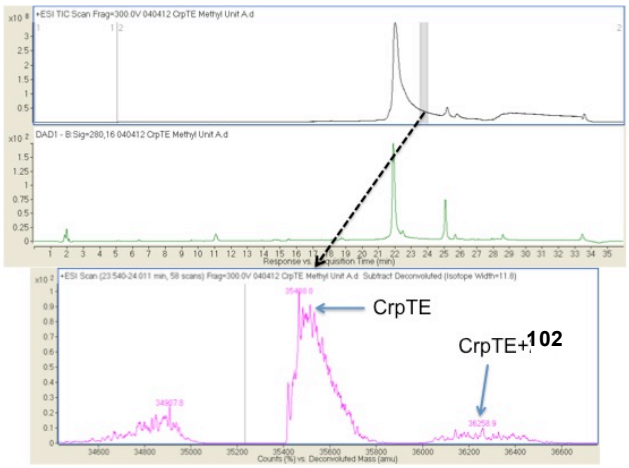

Figure 6.1: LC-QTOF-MS analysis of CrpTE acylation with methylated unit A substrate. *Reaction conditions*: 30 uM CrpTE, 50 uM **102**, 50 mM sodium phosphate, pH 7.0, 5% DMSO, 23 °C, 4 h. Top panel is MS trace of CrpTE with analyzed inset; bottom panel is extracted spectrum of inset showing WT CrpTE and acylated CrpTE.

was incubated with CrpTE at room temperature over 4 h, only a trace amount of the acyl-CrpTE complex was observed by LC-QTOF-MS (Figure 6.1). Clearly hydrolysis of the substrate dominated when cyclization was blocked, but we were encouraged by the observation that CrpTE could still accept substrates disfavoring catalytic turnover.

6.7 CrpTE Expression, Purification, and Enzymatic Reaction

The expression and purification of CrpTE was carried out as previously reported by Beck et al. as the pET28b construct in *E. coli* strain BL21 (DE3).[4] One liter cultures of 2XYT media containing 50 µg/mL kanamycin were inoculated with 1% (v/v) of an LB starter culture and grown to OD_{600} of 0.6-0.8 at 37 °C and 160 rpm. Overexpression was induced by the addition of 100 µM IPTG at 30 °C for approximately 16 h. CrpTE was purified on Ni agarose resin to >95% purity. Purified protein aliquots were stored in 100 mM sodium phosphate buffer, pH 7.8, snap frozen in liquid nitrogen, and stored at -80 °C until needed.

Small-scale CrpTE reactions were conducted in 1.7 mL Eppendorf tubes containing 100 µM purified CrpTE, 500 µM substrate (at 50 mM in DMSO), 5% (v/v) DMSO, and 50 mM sodium phosphate buffer, pH 7.0 in 100

µL total volume. Reaction components were combined, adding CrpTE last, then shaken by inversion, briefly centrifuged to settle the contents, and incubated at 28 °C overnight. After incubation, reactions were extracted with EtOAc (2 x 200 µL) and the organics were combined in a clean 1.7 mL Eppendorf tube and dried under a stream of nitrogen. The residue was resuspended in LC-MS grade ACN and briefly centrifuged for analysis by LC-QTOF-MS using a Phenomenex Synergi 4u HydroRP (100 x 2.0 mm, 4 µm) column under the following conditions: mobile phase (A) deionized water + 0.1% formic acid (FA), (B) acetonitrile + 0.1% FA; 0-2 min 10% B, 2-17 min 10-100% B, 17-18 min 100% B, 18-19 min 100-10% B; flow rate, 0.3 mL/min.

For large-scale reactions, it is recommended to charge 20 mL SPE tubes equipped with a bottom frit with 500-750 µM SNAc-thioester substrate, 20% (v/v) diglyme, 1% methyl β-cyclodextrin, 1 mL purified CrpTE, and enough 100 mM sodium phosphate buffer, pH 7.0 to make 5 mL total volume. The SPE tubes are then capped and agitated in an upright position on an orbital shaker at 250 rpm at room temperature. After 16 h, reactions are diluted with EtOAc (10 mL), shaken vigorously, and filtered through a compressed plug of celite. The filtrate is then transferred to a separatory funnel and diluted with water and EtOAc. The organic layer is washed with brine and then dried with Na_2SO_4, after which solvent removal under vacuum provides a residue for purification.

Compound **88** was acquired from W. Seufert and analyzed by ^{1}H NMR and HRMS to confirm identity and purity.

6.8 CrpE Expression, Purification, and Enzymatic Reaction

Soluble, active CrpE was grown in *E. coli* BL21 (DE3) containing the CrpE gene on a pSJ8 plasmid and the pGro7 chaperone plasmid. One liter TB cultures containing 50 µg/mL ampicillin and 25 µg/mL chloramphenicol were seeded with 1% (v/v) LB starter cultures and supplemented with 0.5 mM $Fe(NH_4)_2(SO_4)_2$ and 1 mM thiamine. Cells were grown to an OD_{600} of 0.6 at

37 °C, 160 rpm, supplied 2 mM 5-ALA, and acclimated to 18 °C over 1 h. Cultures were then induced with 1.0 g/L arabinose and 100 µM IPTG, and incubated at 18 °C, 160 rpm for 18 h. The resulting cell pellet was lysed by sonication and soluble protein was purified on amylose resin to afford CrpE at 14 µM with the GroEL chaperone (Figure 6.1). The functional concentration of CrpE was measured by diluting 500 µL of purified enzyme with 2.5 mL water and sparging with CO for 30 sec. The UV-Vis spectrum of 800 µL of the diluted CrpE in a cuvette was then recorded from 380 to 550 nm, followed by the addition of ~10 mg of sodium dithionite. A series of UV-Vis measurements were then recorded over 5 min to catch the transition to 450 nm.

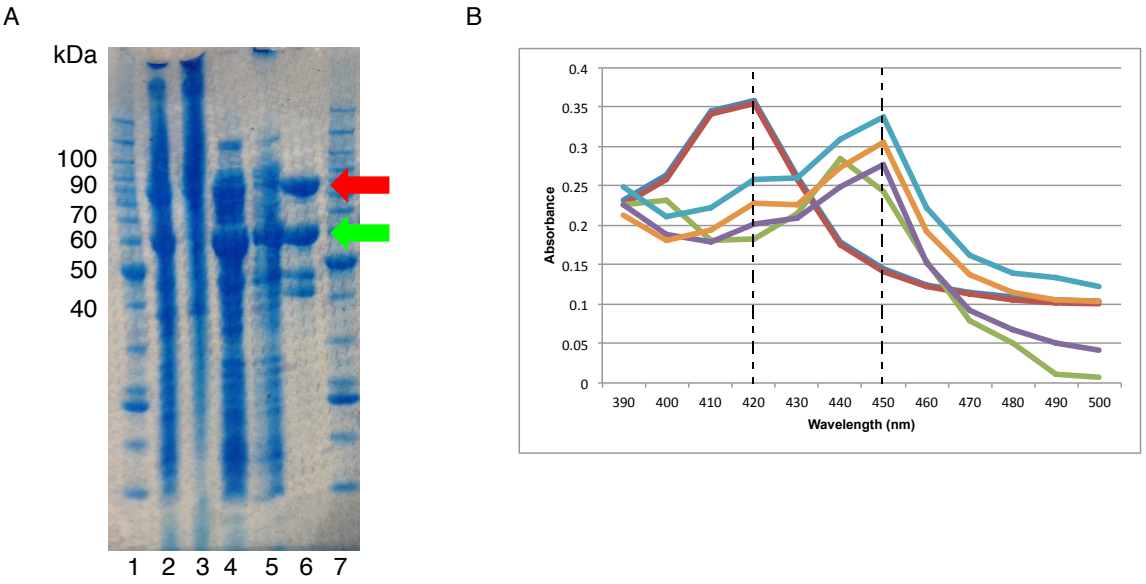

Figure 6.2: Purification and Functional Analysis of CrpE. A) SDS-PAGE gel of CrpE purification. Lane 1, Invitrogen Benchmark™ protein ladder; lane 2, whole cell protein after induction; lane 3, insoluble lysate pellet; lane 4, lysate soluble fraction; lane 5, resin flow-through; lane 6, purified MBP-CrpE (red) and GroEL (green); lane 7, Invitrogen Benchmark™ protein ladder. B) CO binding assay of CrpE functionality observing the shift from 420 to 450 nm upon reduction of the heme.

A typical CrpE reaction in a 1.7 mL Eppendorf tube contained 100 µg/mL spinach ferredoxin, 0.2 unit/mL ferredoxin reductase, 1.4 mM NADPH, 10 mM glucose-6-phosphate, 8 units/mL glucose-6-phosphate dehydrogenase, 5 µM substrate (in DMSO), and 5% (v/v) DMSO in 100 µL of 50 mM sodium phosphate, pH 6.4. Reaction components were mixed by inversion and centrifuged briefly to settle the contents. The purified CrpE was

then *added last* to a final concentration of 0.2 µM. Reactions were incubated for 4 h at room temperature and then extracted with EtOAc (2 x 200 µL). The combined organics were transferred to a clean Eppendorf tube and dried under a stream of nitrogen. The resulting residue was dissolved in LC-MS grade ACN and briefly centrifuged for analysis by LC-QTOF-MS using a Phenomenex Synergi 4u HydroRP (100 x 2.0 mm, 4 µm) column under the following conditions: mobile phase (A) deionized water + 0.1% formic acid (FA), (B) acetonitrile + 0.1% FA; 0-2 min 10% B, 2-17 min 10-100% B, 17-18 min 100% B, 18-19 min 100-10% B; flow rate, 0.3 mL/min

Cryptophycin 4 was obtained from W. Seufert and analyzed by ^{1}H NMR and HRMS to confirm identity and purity.

LITERATURE REFERENCES

1 Seufert, W., Beck, Z. Q. & Sherman, D. H. Enzymatic Release and Macrolactonization of Cryptophycins from a Safety-Catch Solid Support. *Andew. Chem. Int. Ed.* **46**, 9298-9300 (2007).

2 Ahn, Y. M., Yang, K. & Georg, G. I. A Convenient Method for the Efficient Removal of Ruthenium Byproducts Generated During Olefin Metathesis Reactions. *Org. Lett.* **3**, 1411-1413 (2001).

3 Ding, Y., Seufert, W. H., Beck, Z. Q. & Sherman, D. H. Analysis of the Cryptophycin P450 Epoxidase Reveals Substrate Tolerance and Cooperativity. *J. Am. Chem. Soc.* **130**, 5492-5498 (2008).

4 Beck, Z. Q., Aldrich, C. C., Magarvey, N. A., Georg, G. I. & Sherman, D. H. Chemoenzymatic Synthesis of Cryptophycin/Arenastatin Natural Products. *Biochemistry* **44**, 13457-13466 (2005).

Appendix A

^{1}H, ^{13}C, and ^{19}F NMR Spectra of All New Compounds

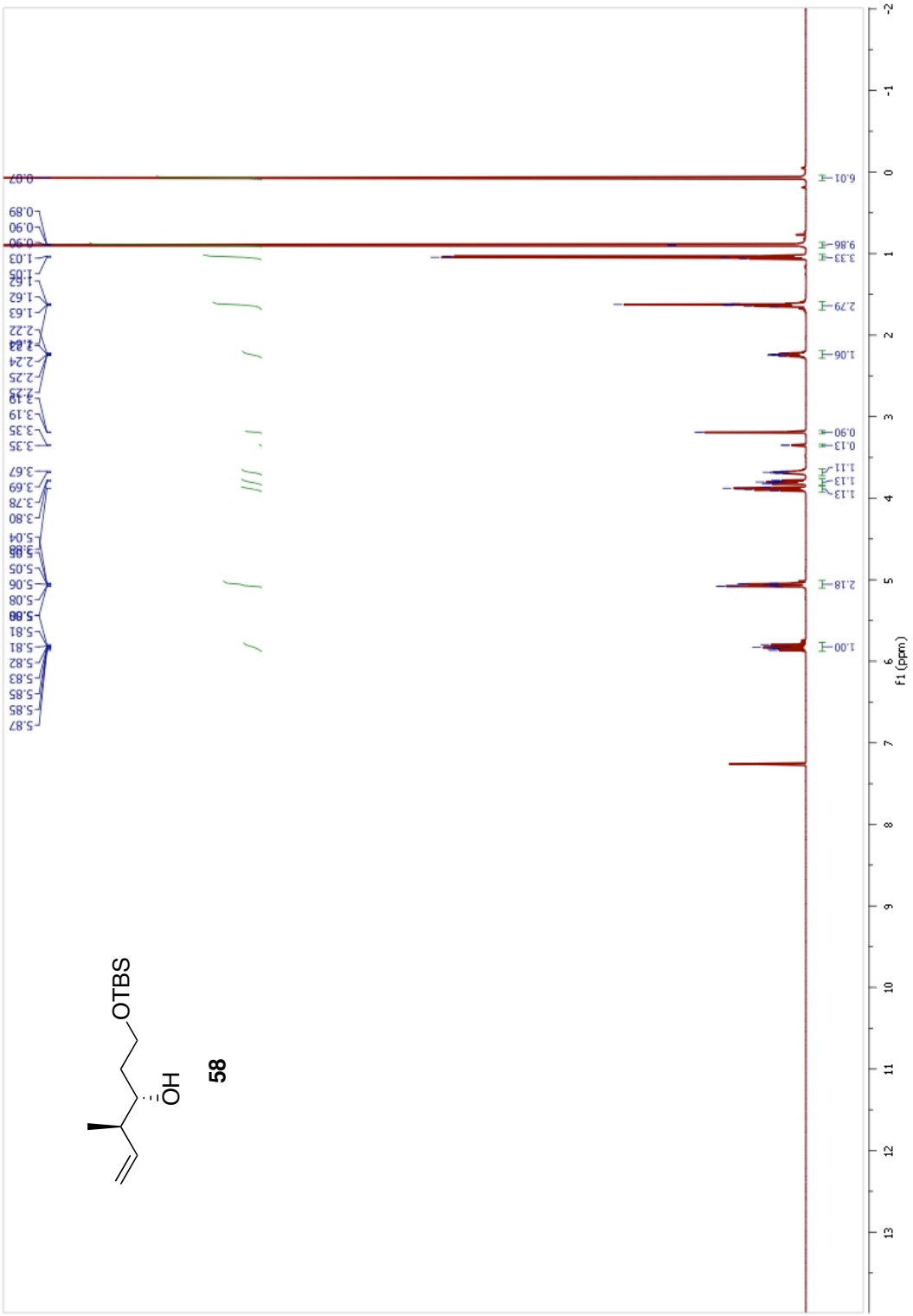

^{1}H NMR Spectrum of Compound 58

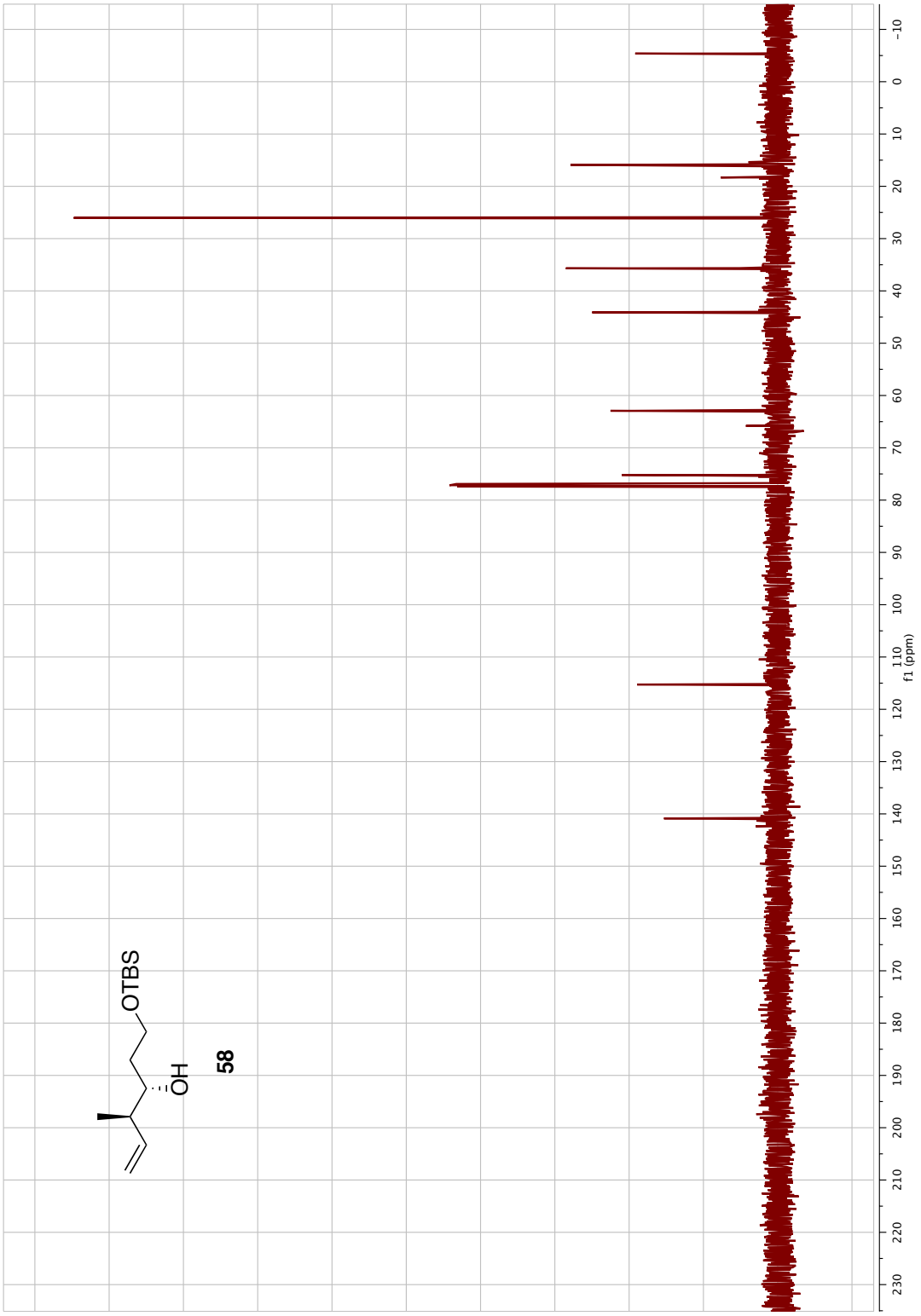

^{13}C NMR Spectrum of Compound 58

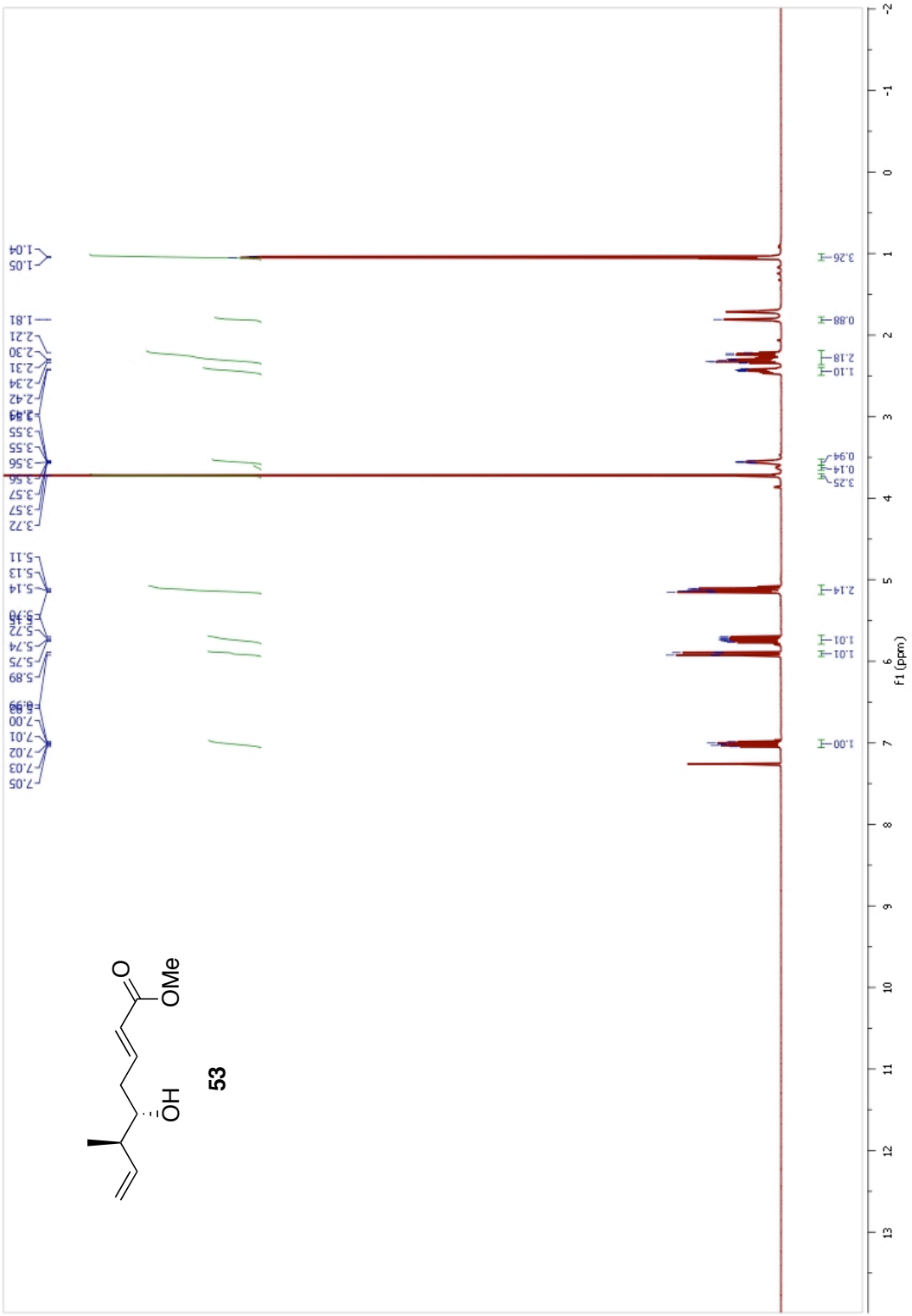

^{1}H NMR Spectrum of Compound 53

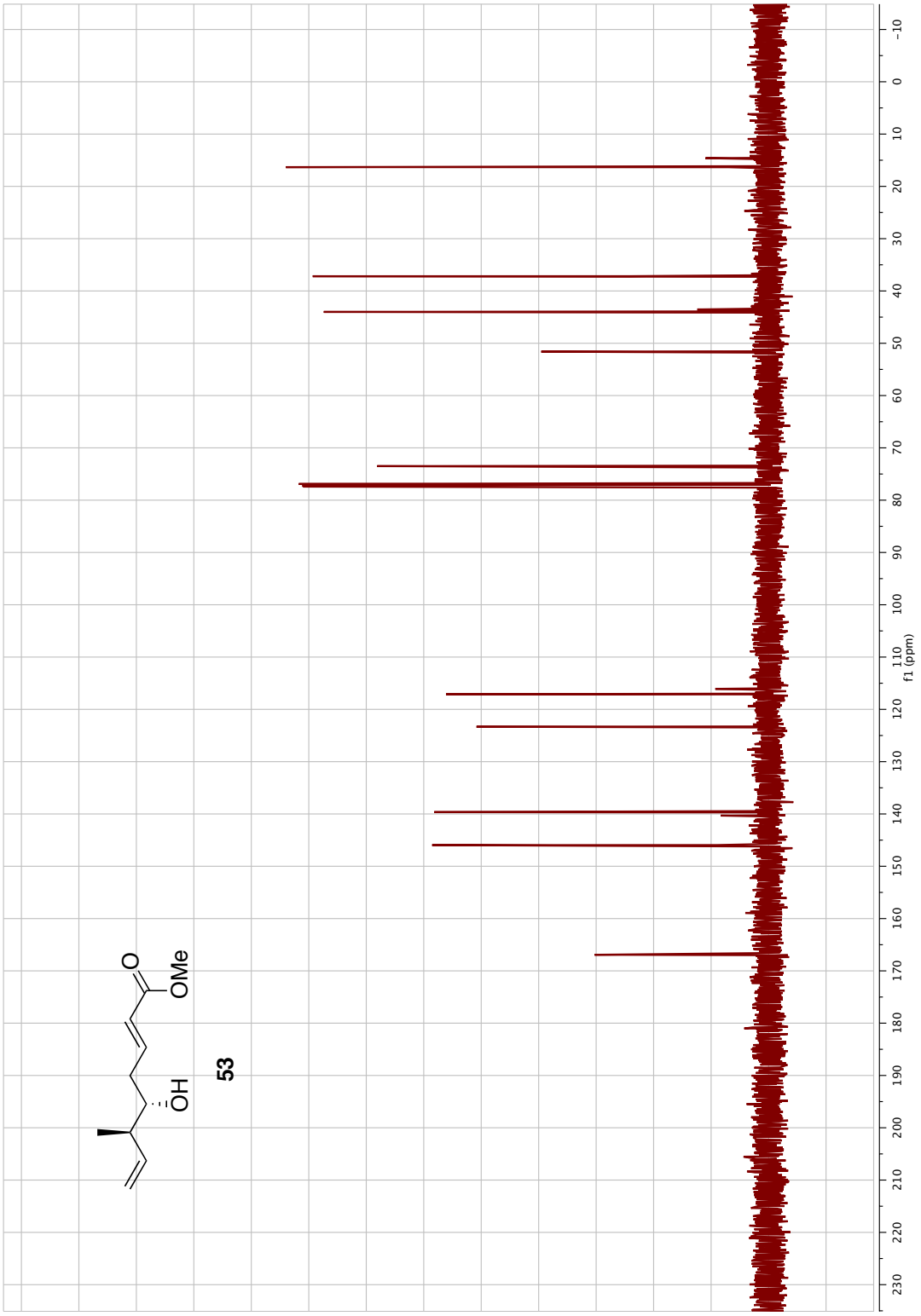

^{13}C NMR Spectrum of Compound 53

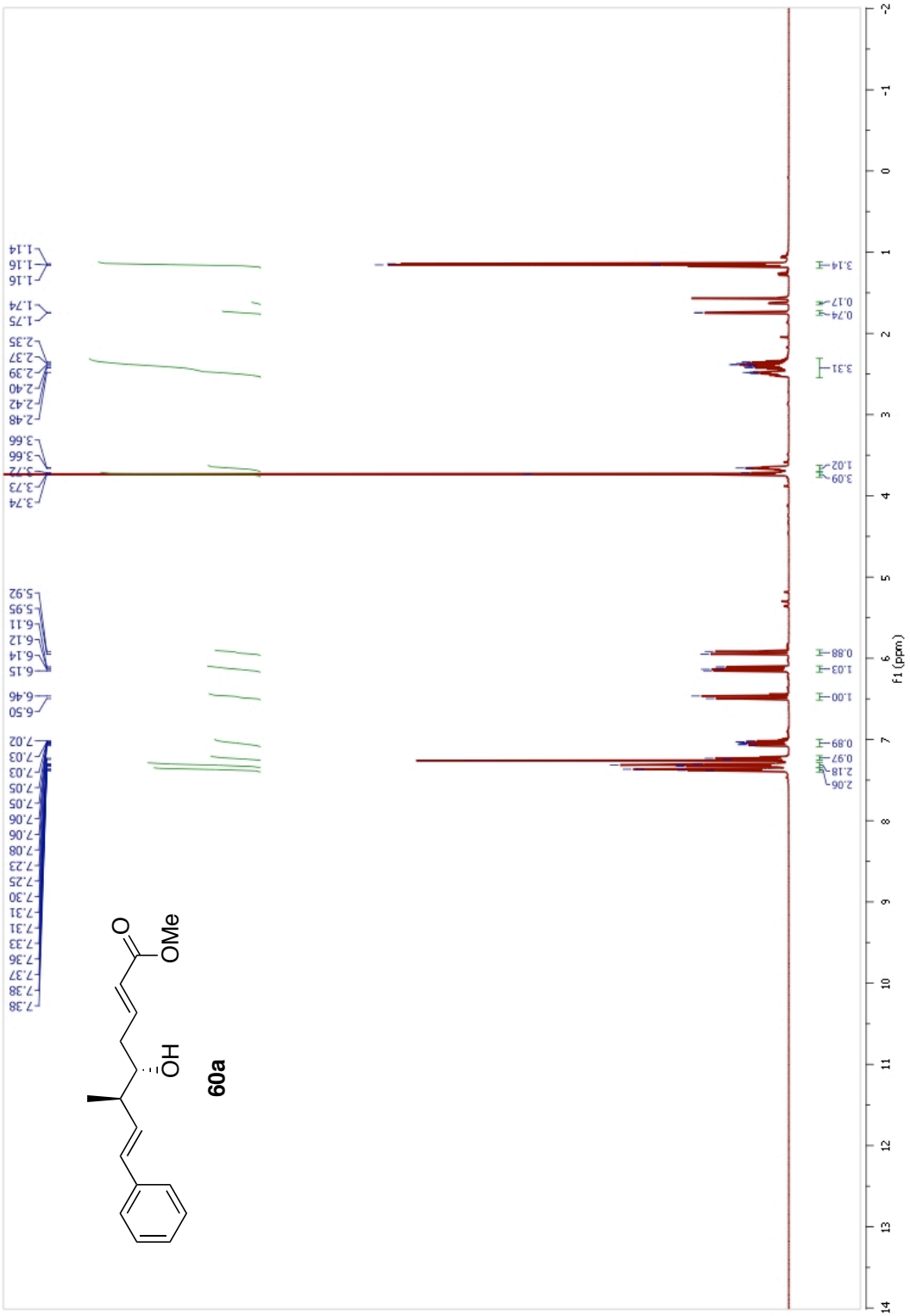

^{1}H NMR Spectrum of Compound 60a

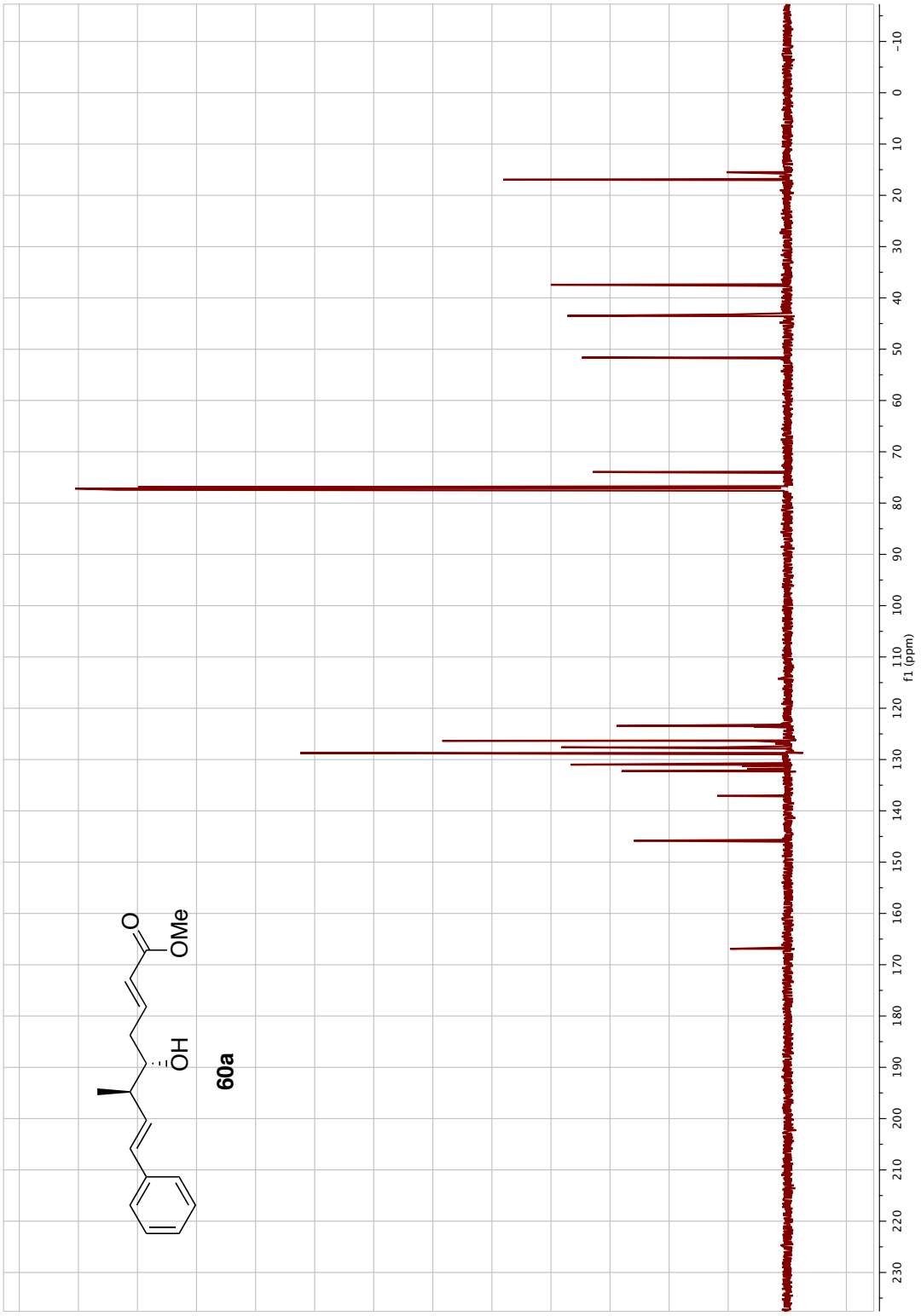

^{13}C NMR Spectrum of Compound 60a

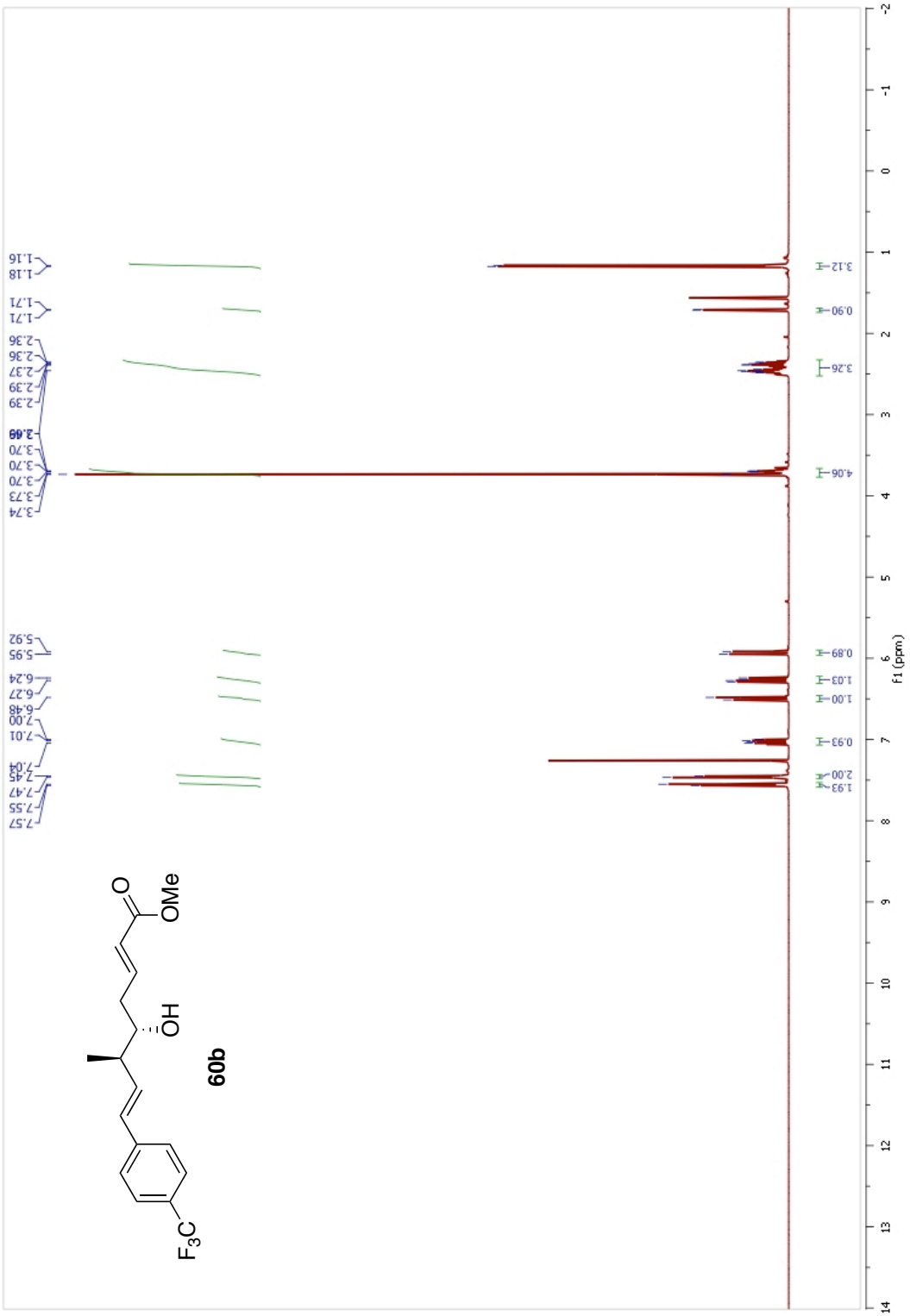

^{1}H NMR Spectrum of Compound 60b

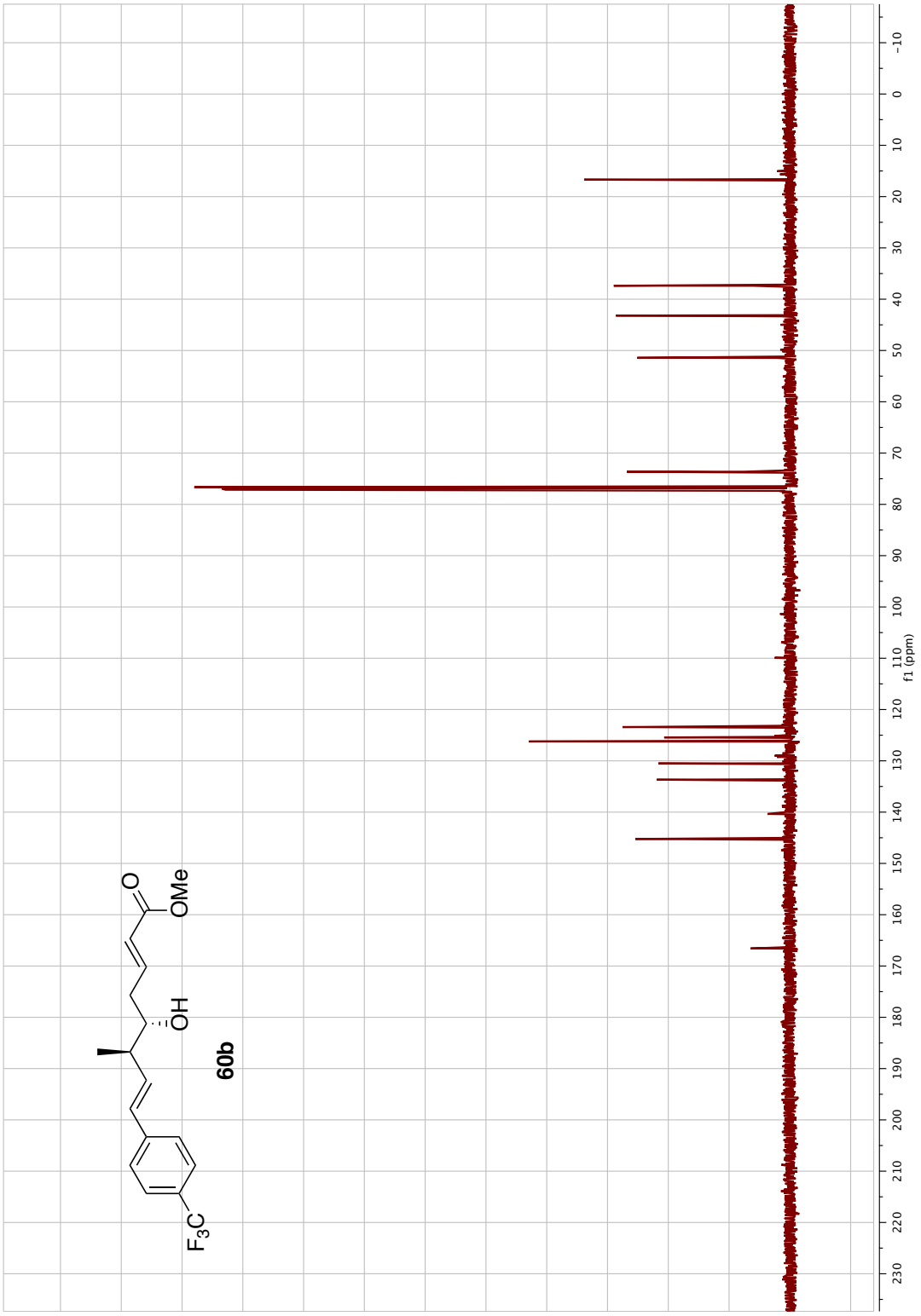

^{13}C NMR Spectrum of Compound 60b

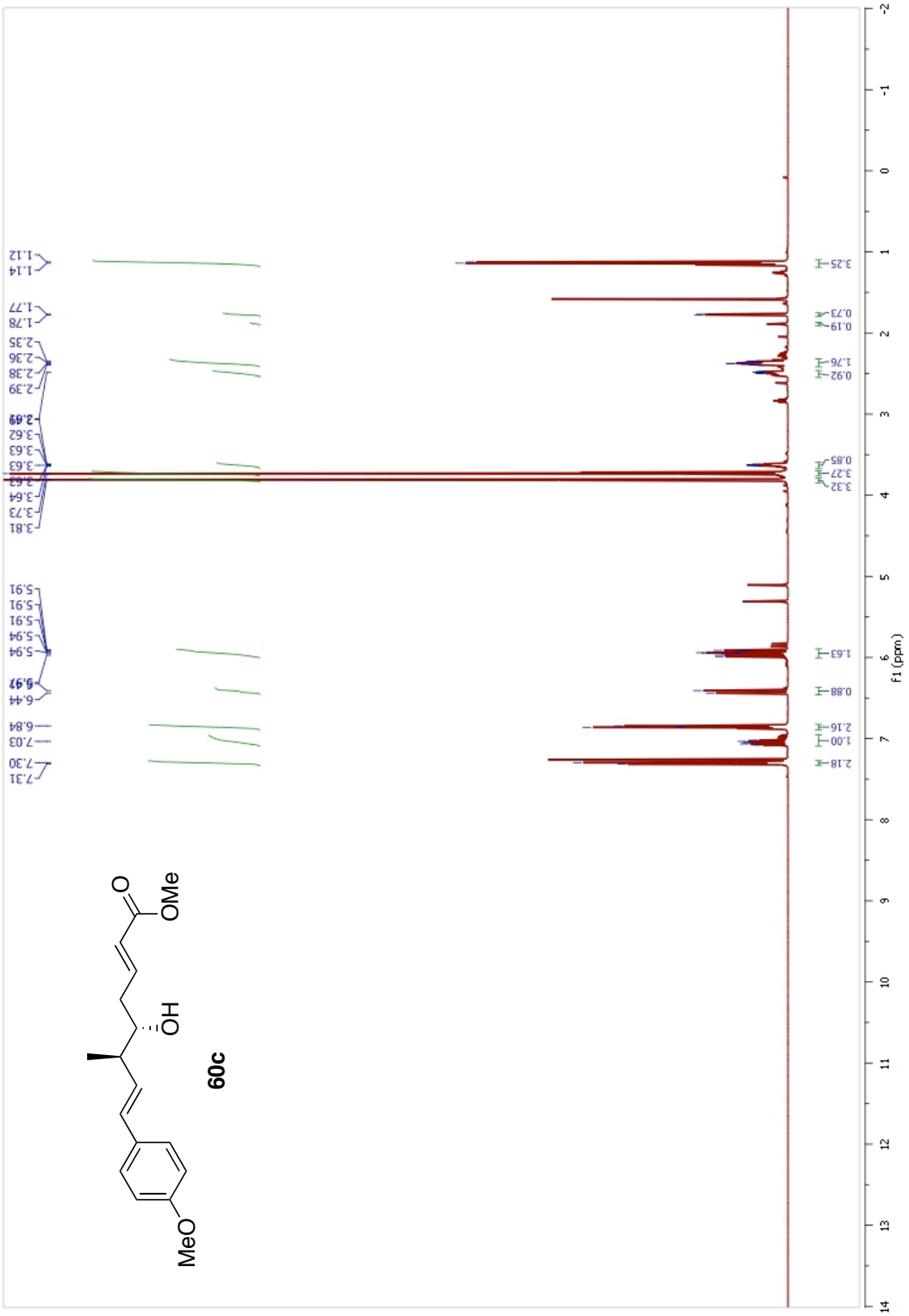

^{1}H NMR Spectrum of Compound 60c

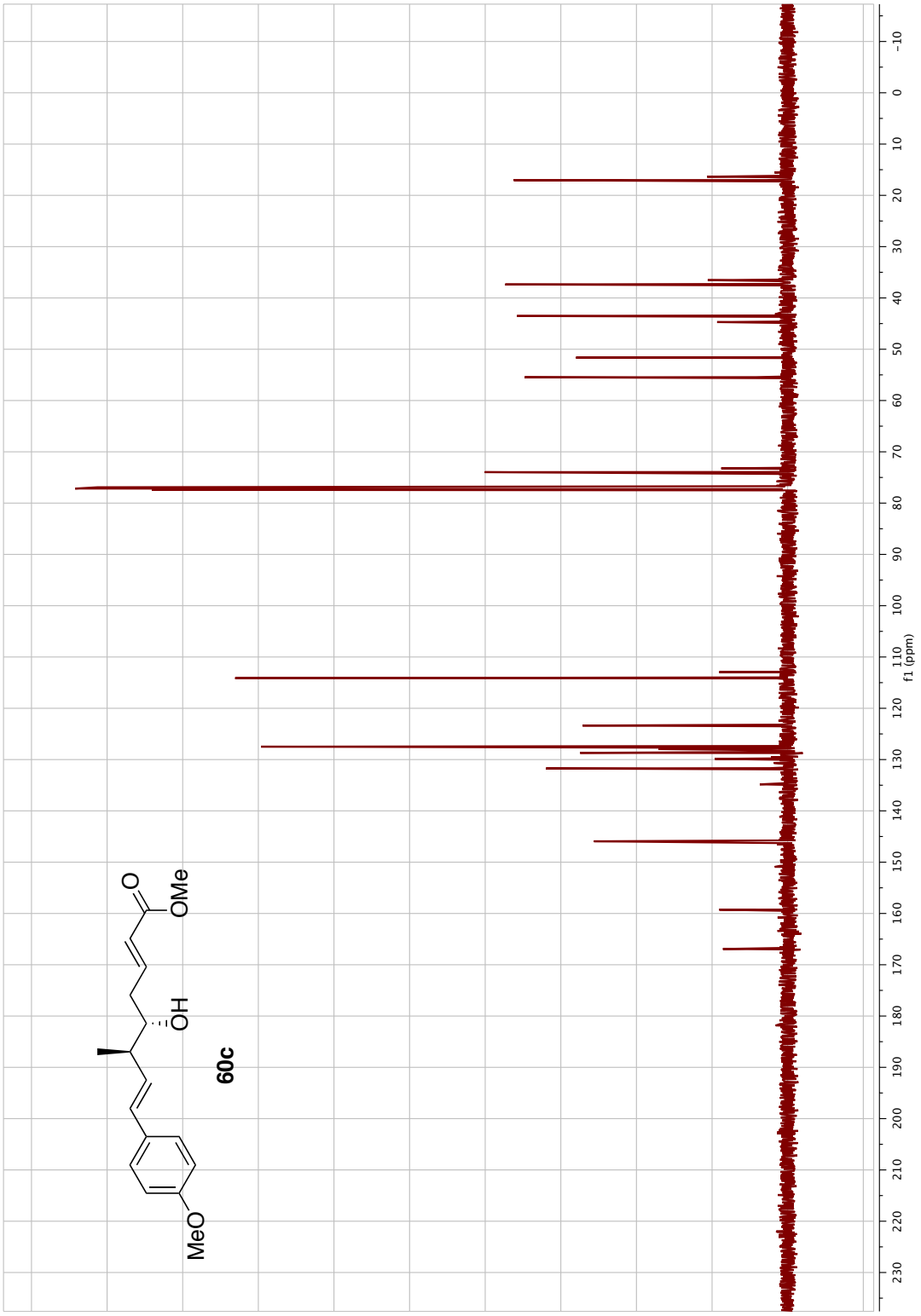

^{13}C NMR Spectrum of Compound 60c

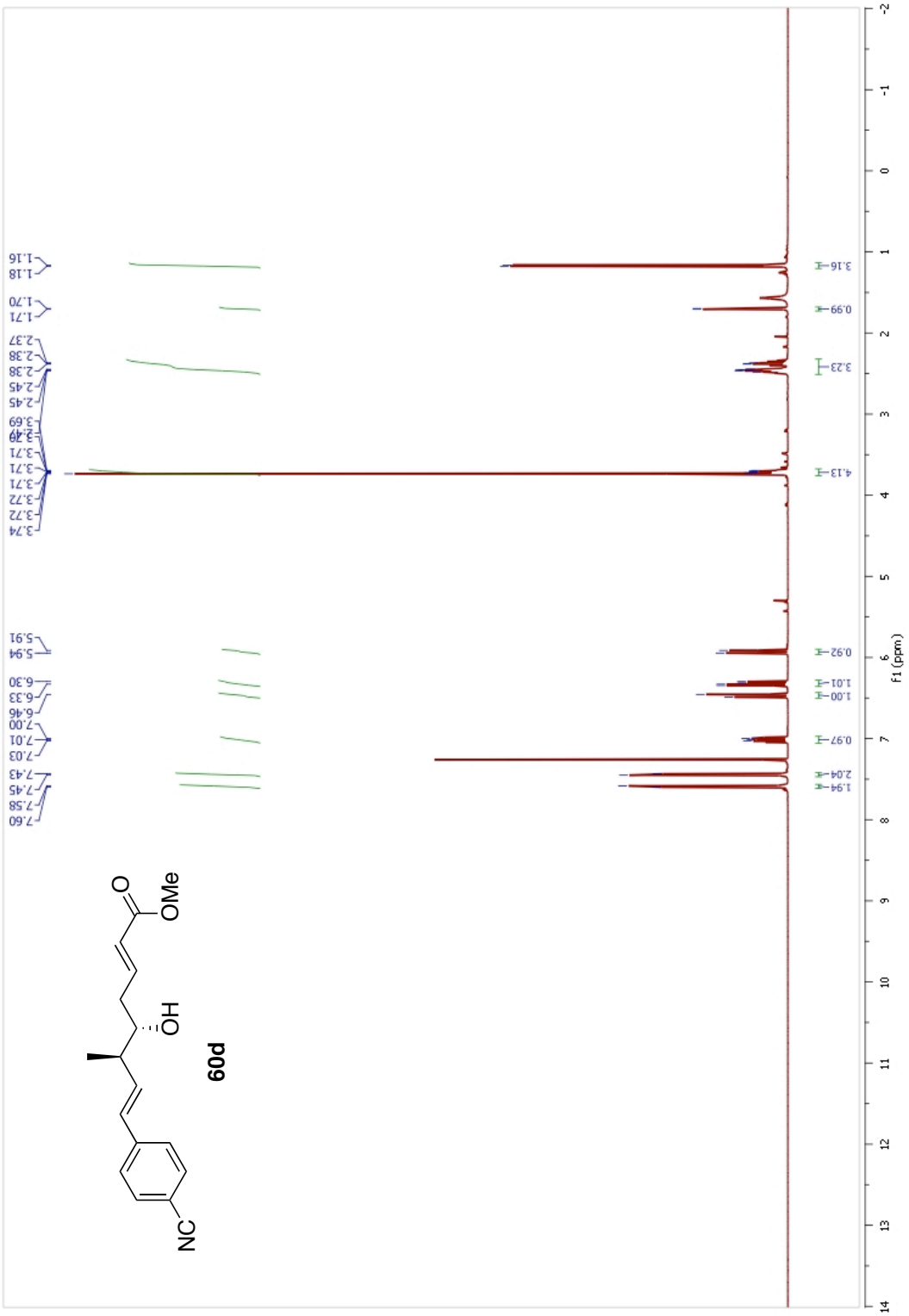

[1]H NMR Spectrum of Compound 60d

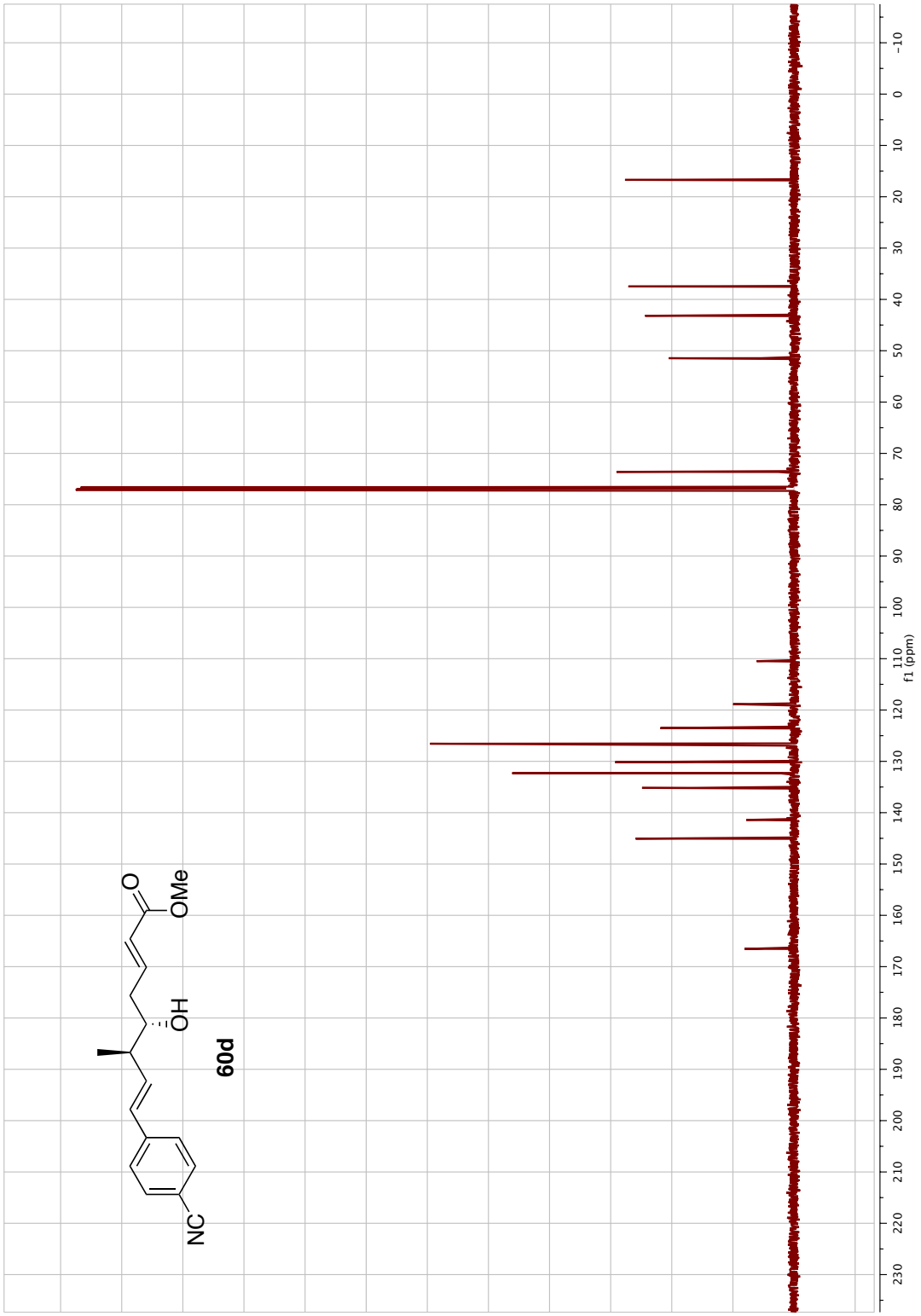

^{13}C NMR Spectrum of Compound 60d

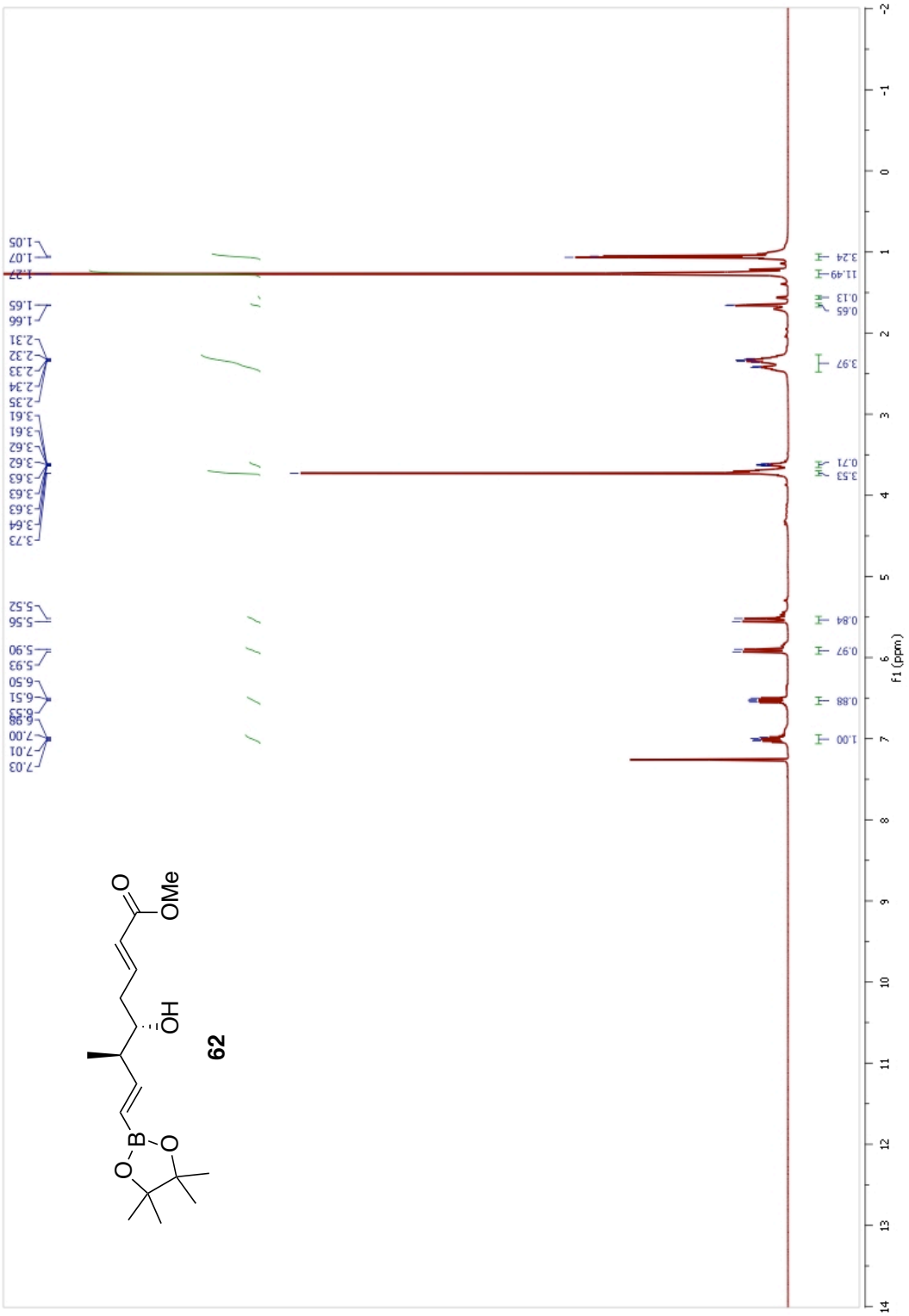

^{1}H NMR Spectrum of Compound 62

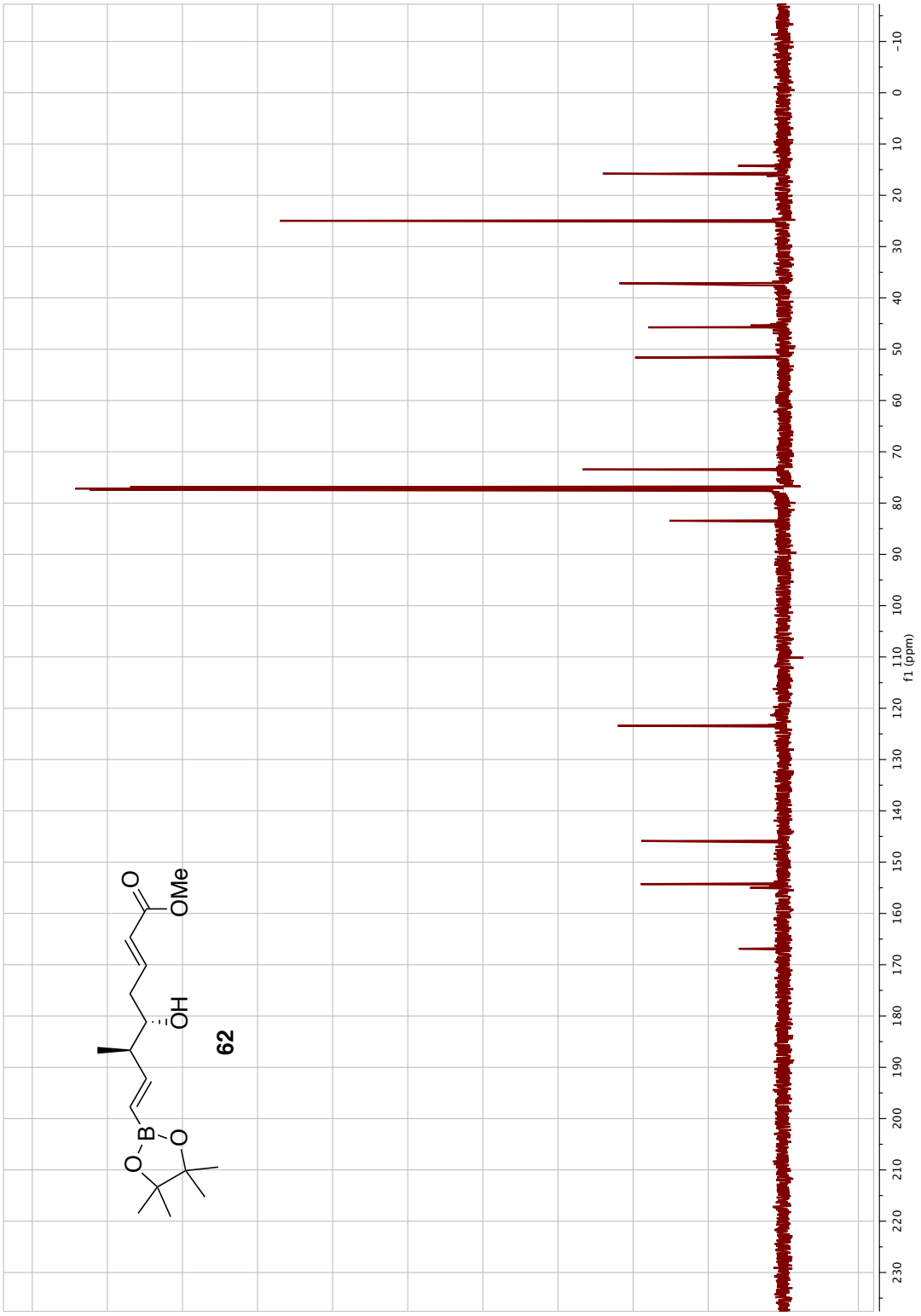

^{13}C NMR Spectrum of Compound 62

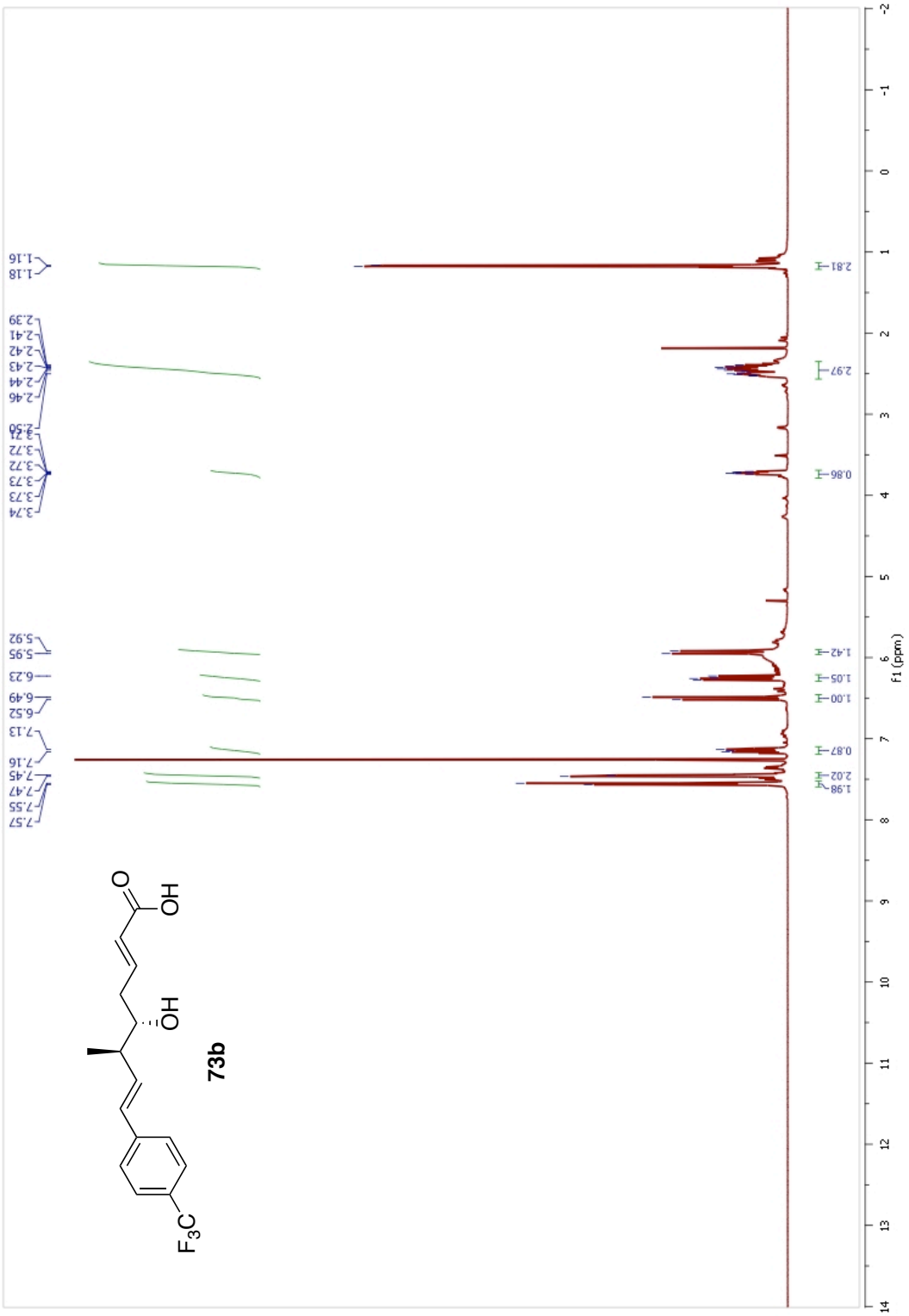

^{1}H NMR Spectrum of Compound 73b

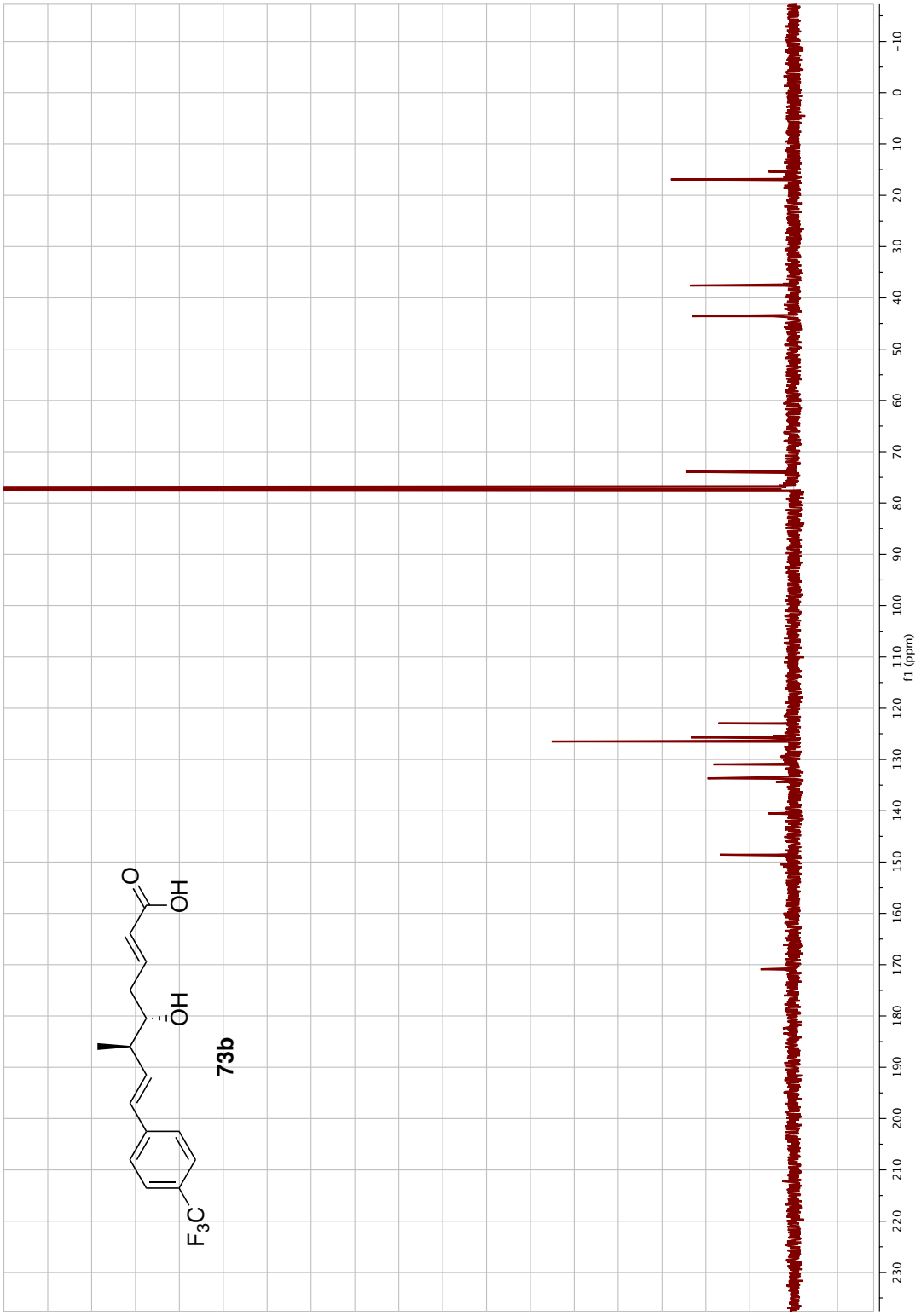

^{13}C NMR Spectrum of Compound 73b

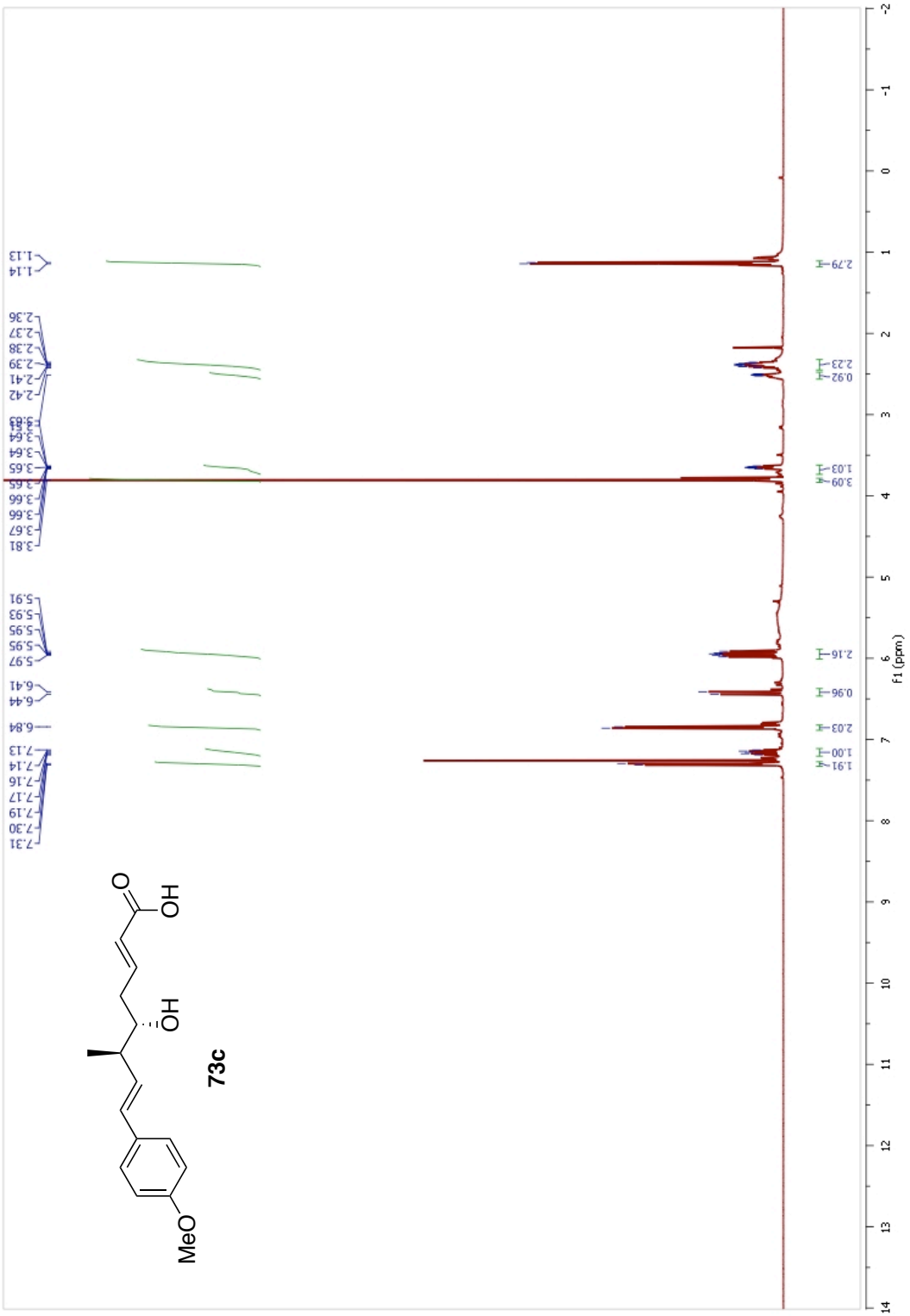

^{1}H NMR Spectrum of Compound 73c

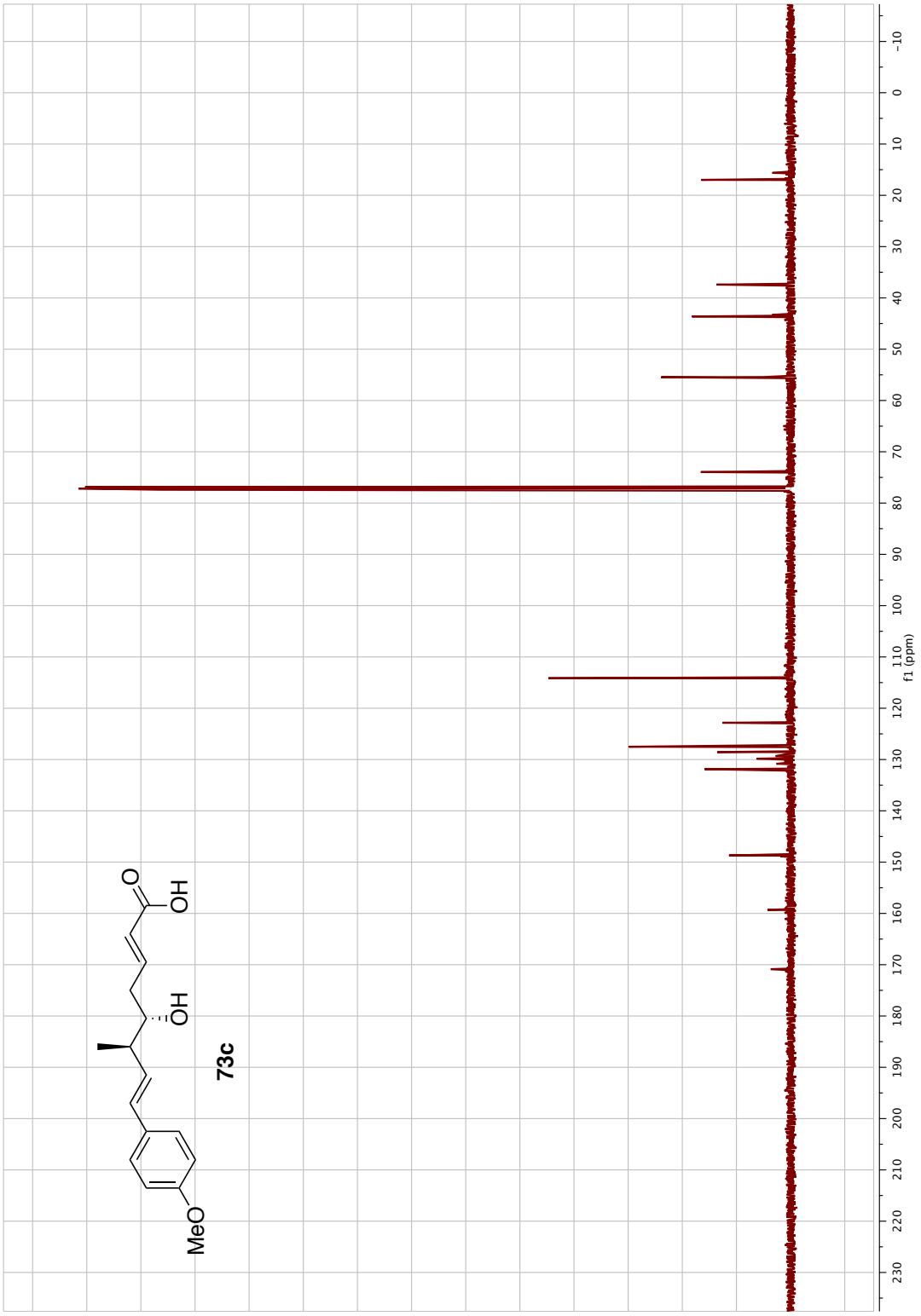

^{13}C NMR Spectrum of Compound 73c

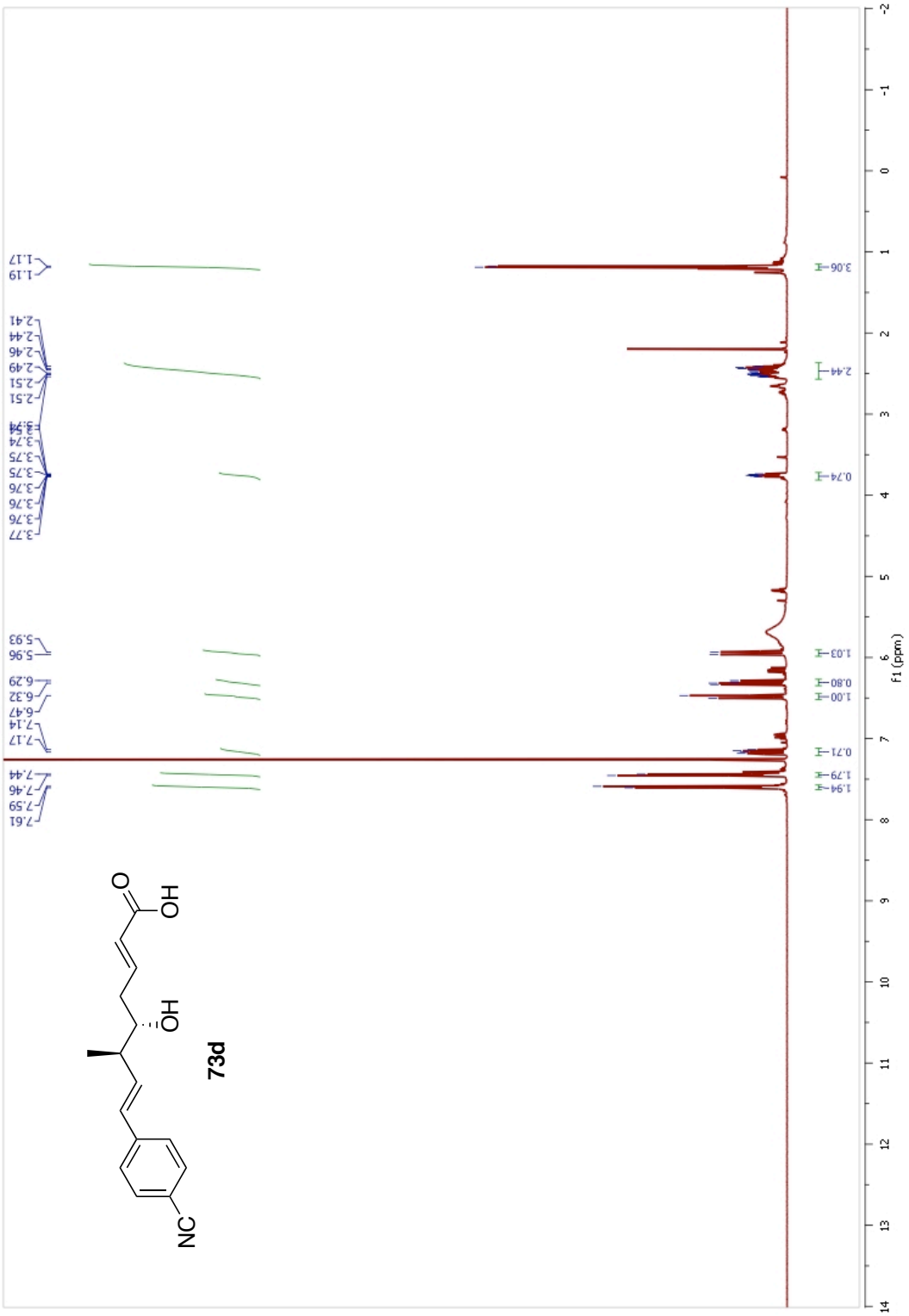

^{1}H NMR Spectrum of Compound 73d

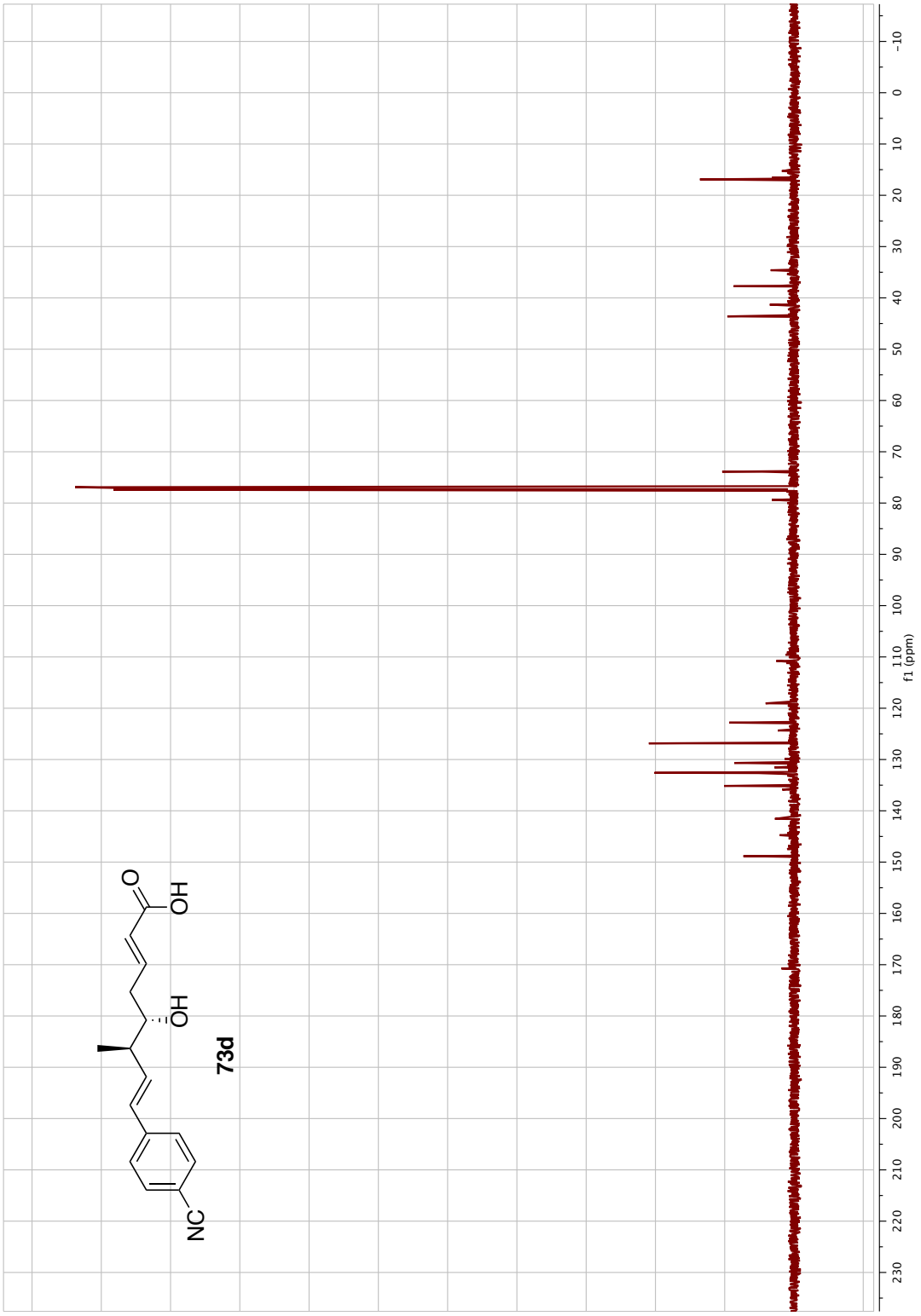

^{13}C NMR Spectrum of Compound 73d

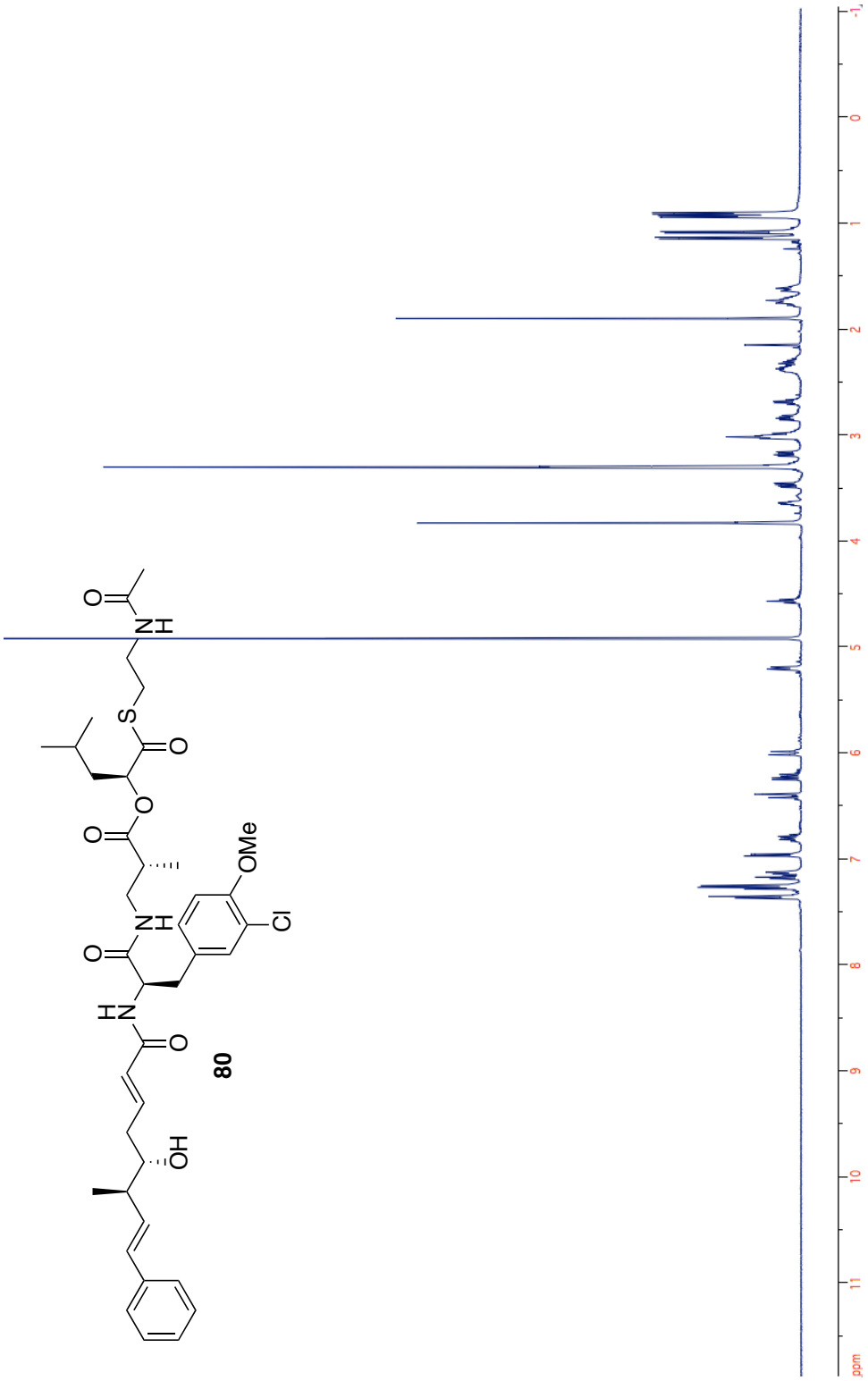

^{1}H NMR Spectrum of Compound 80

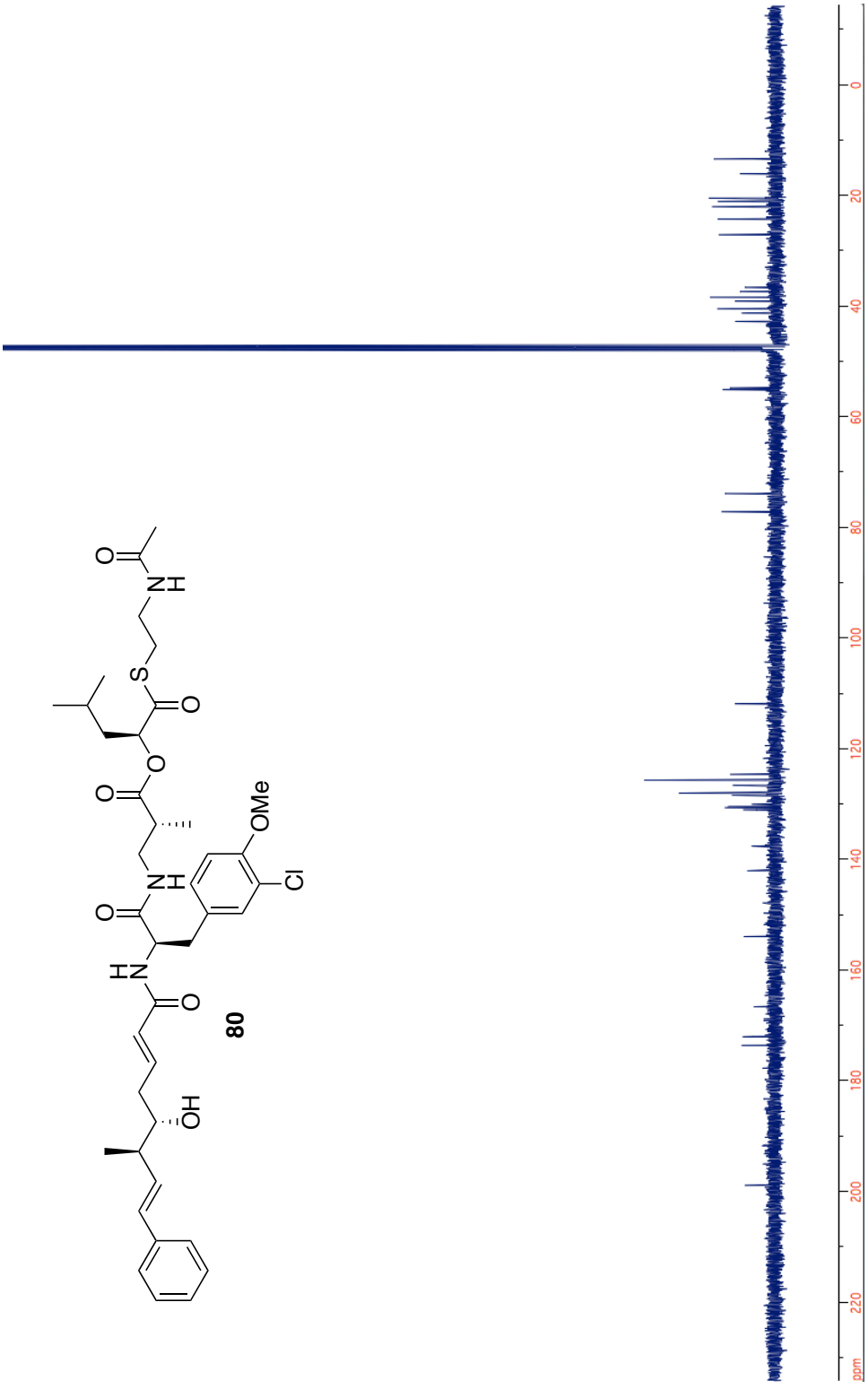

^{13}C NMR Spectrum of Compound 80

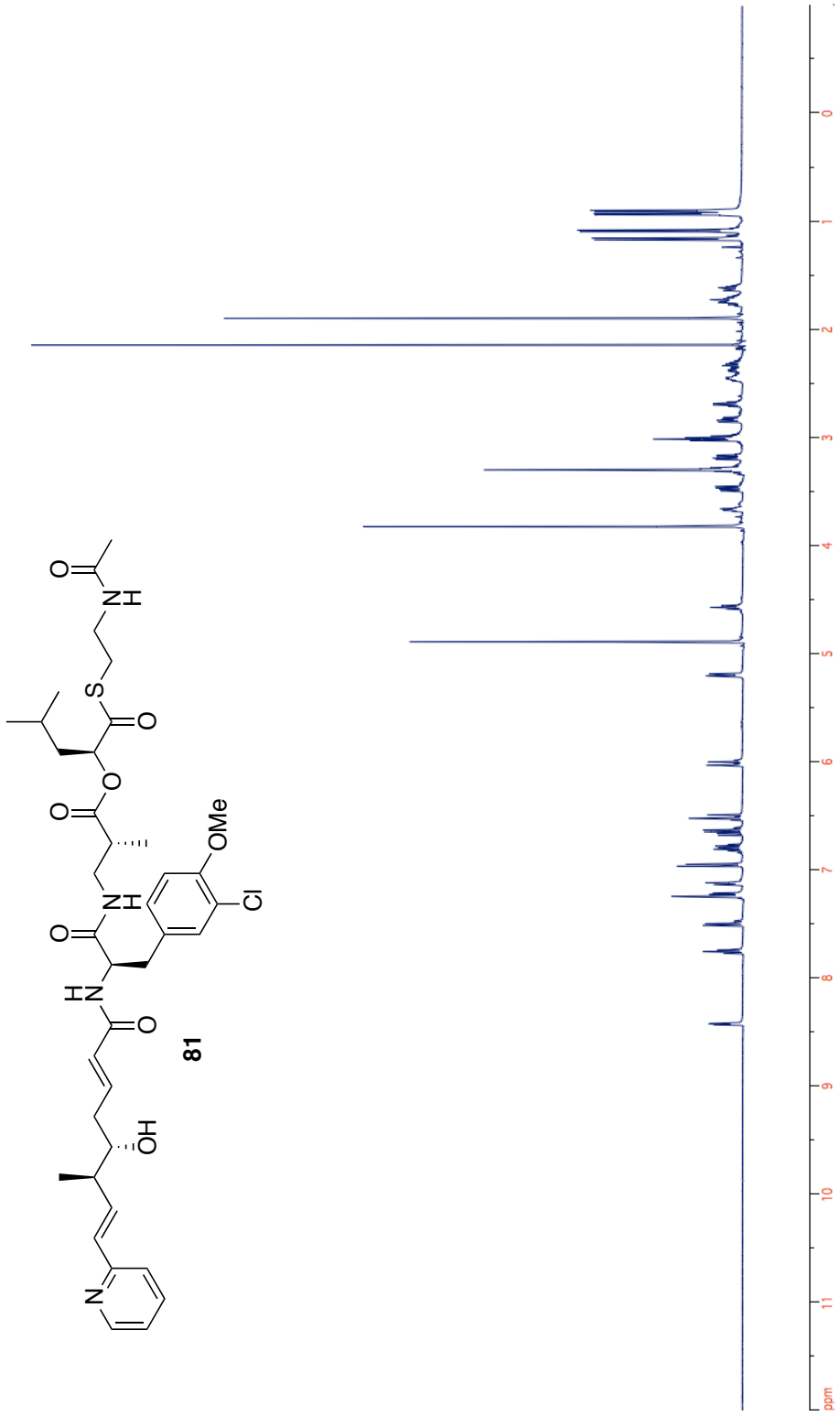

^{1}H NMR Spectrum of Compound 81

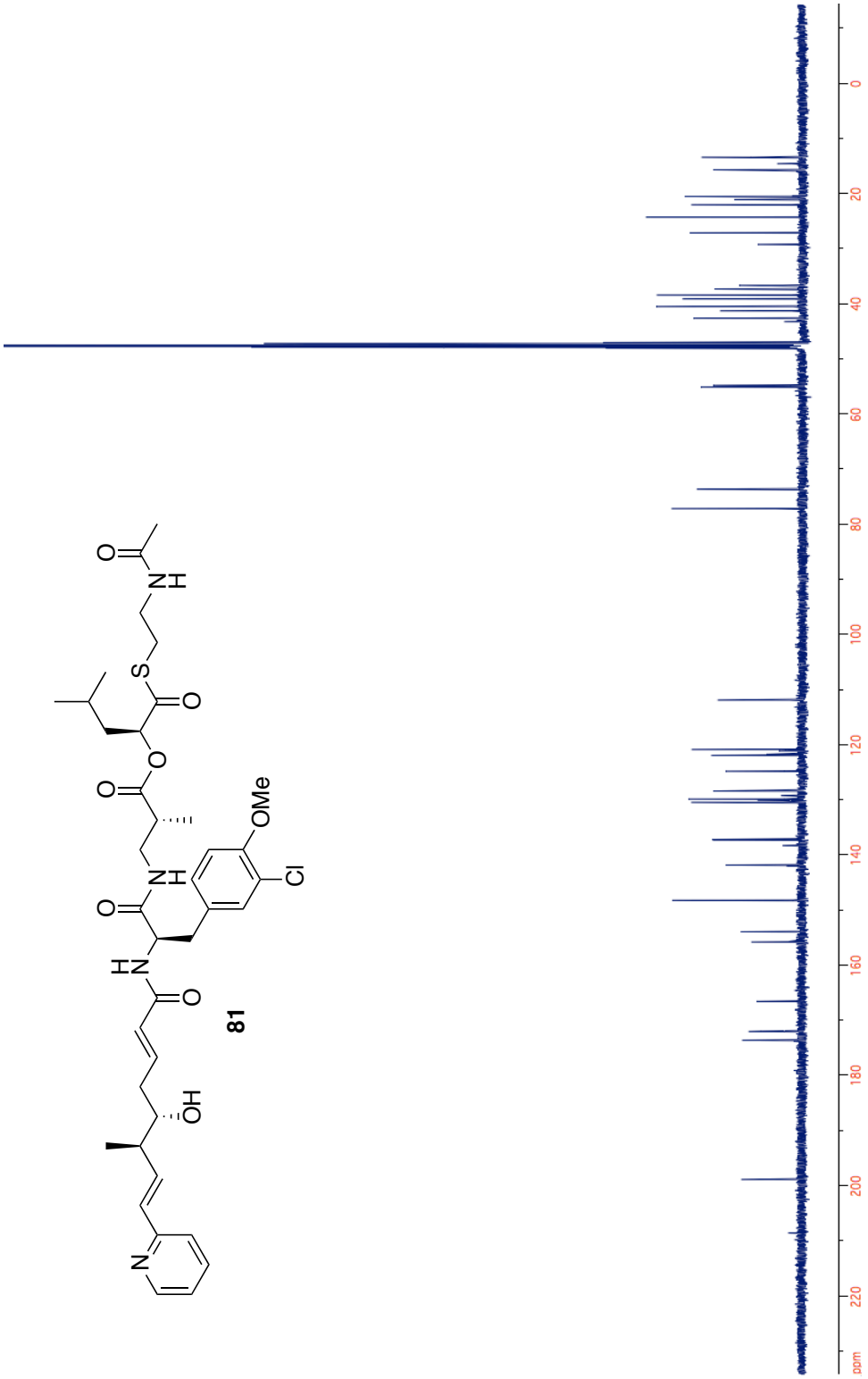

^{13}C NMR Spectrum of Compound 81

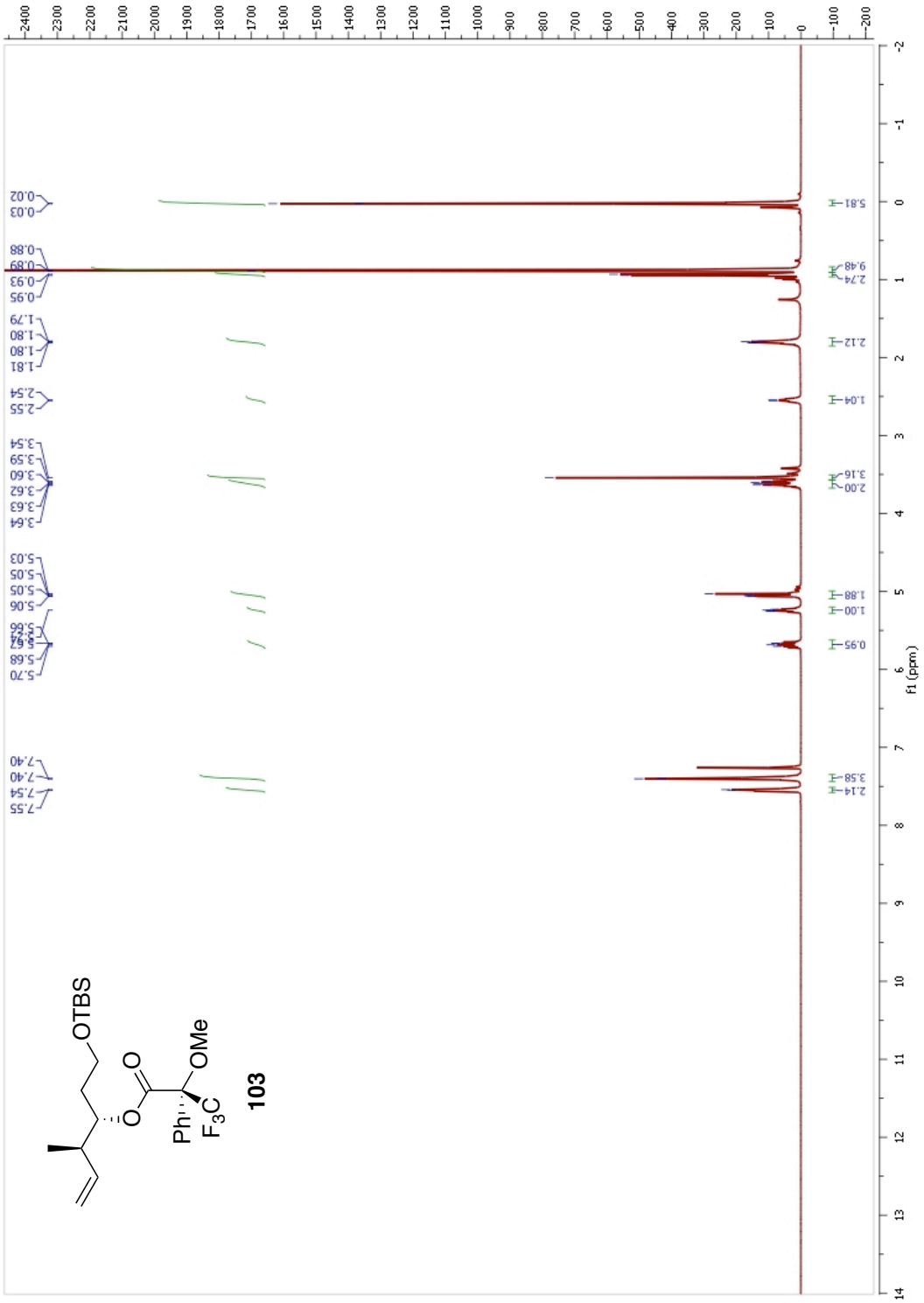

^{1}H NMR Spectrum of Compound 103

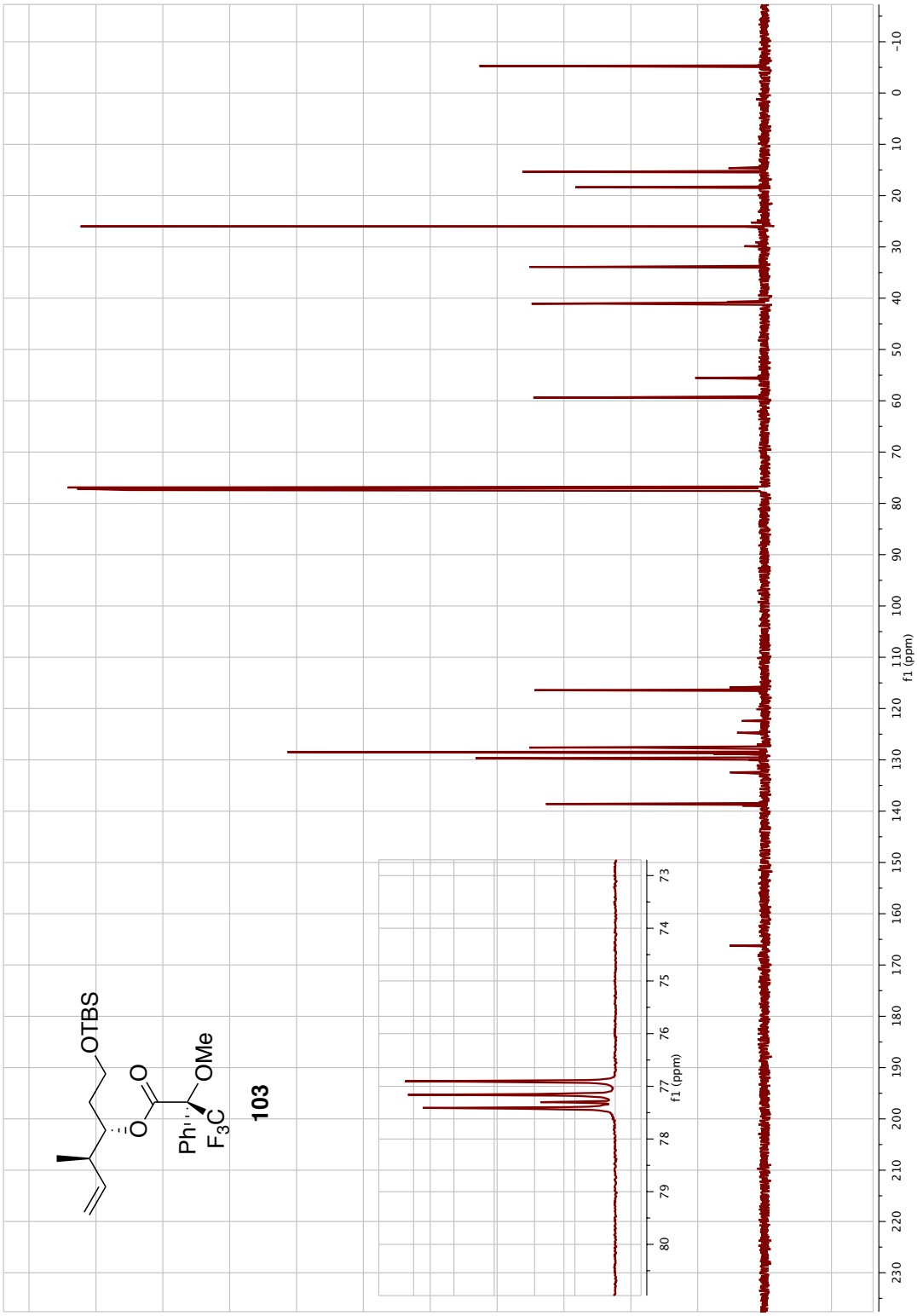

^{13}C NMR Spectrum of Compound 103

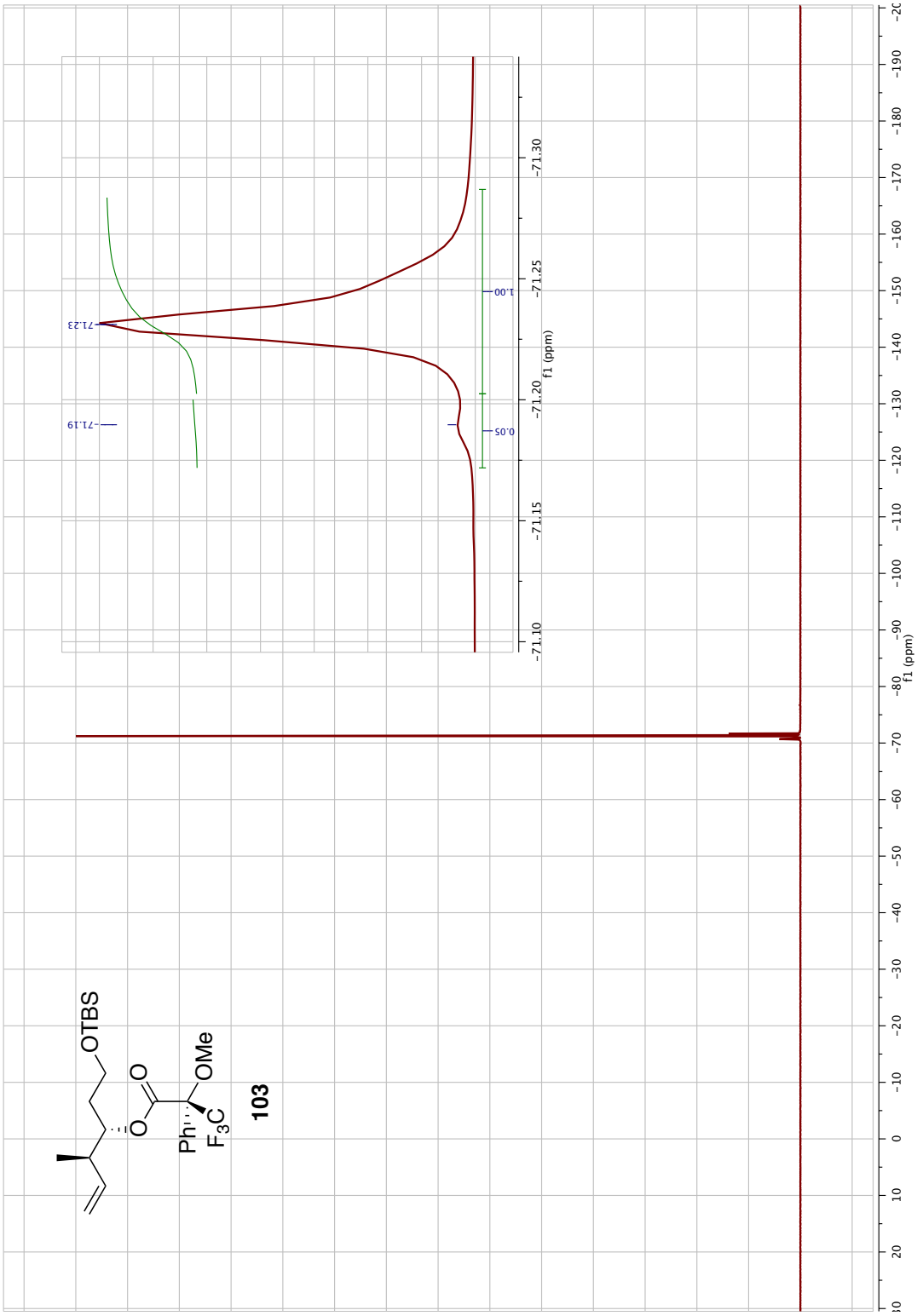

^{19}F NMR Spectrum of Compound 103

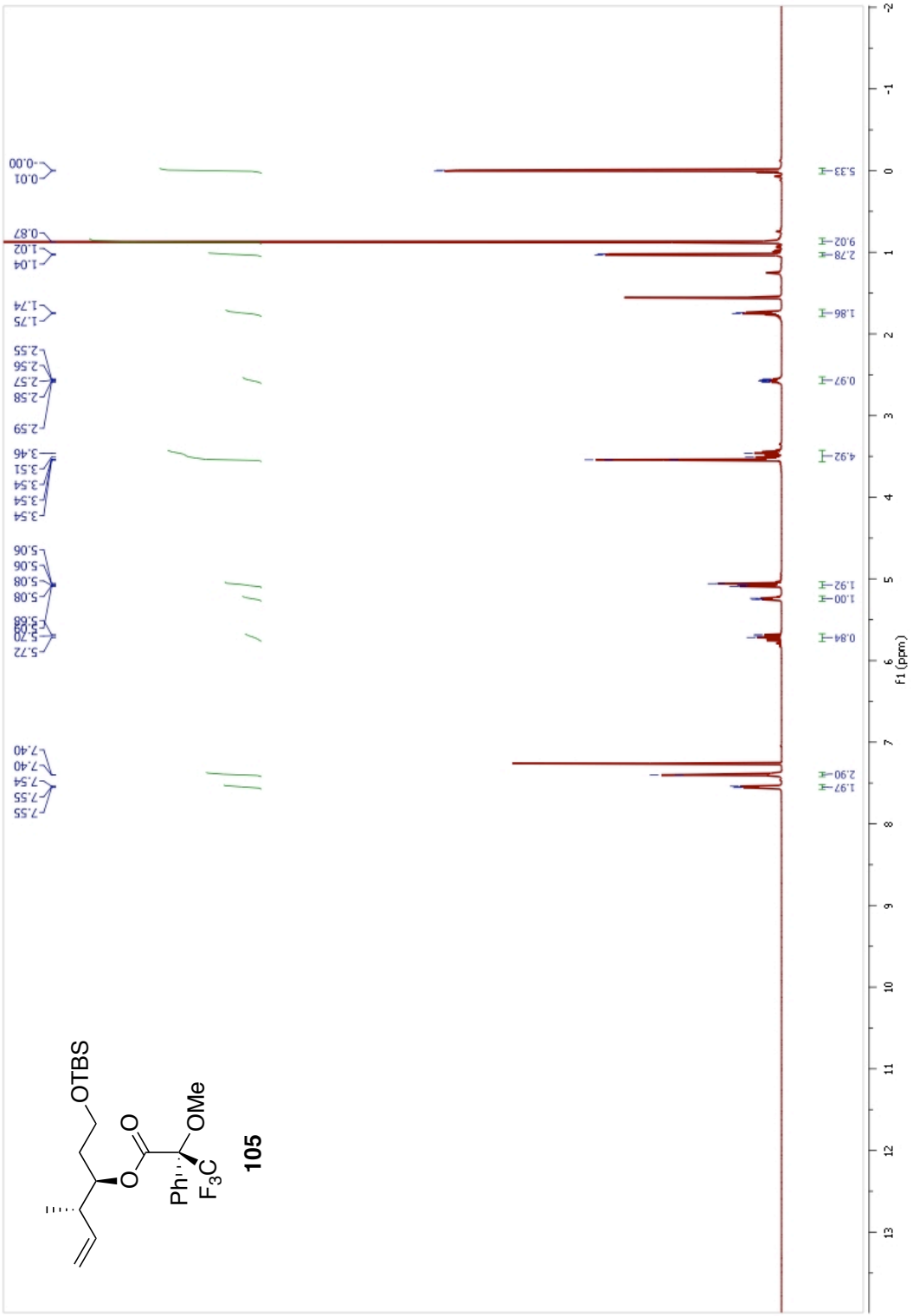

^{1}H NMR Spectrum of Compound 105

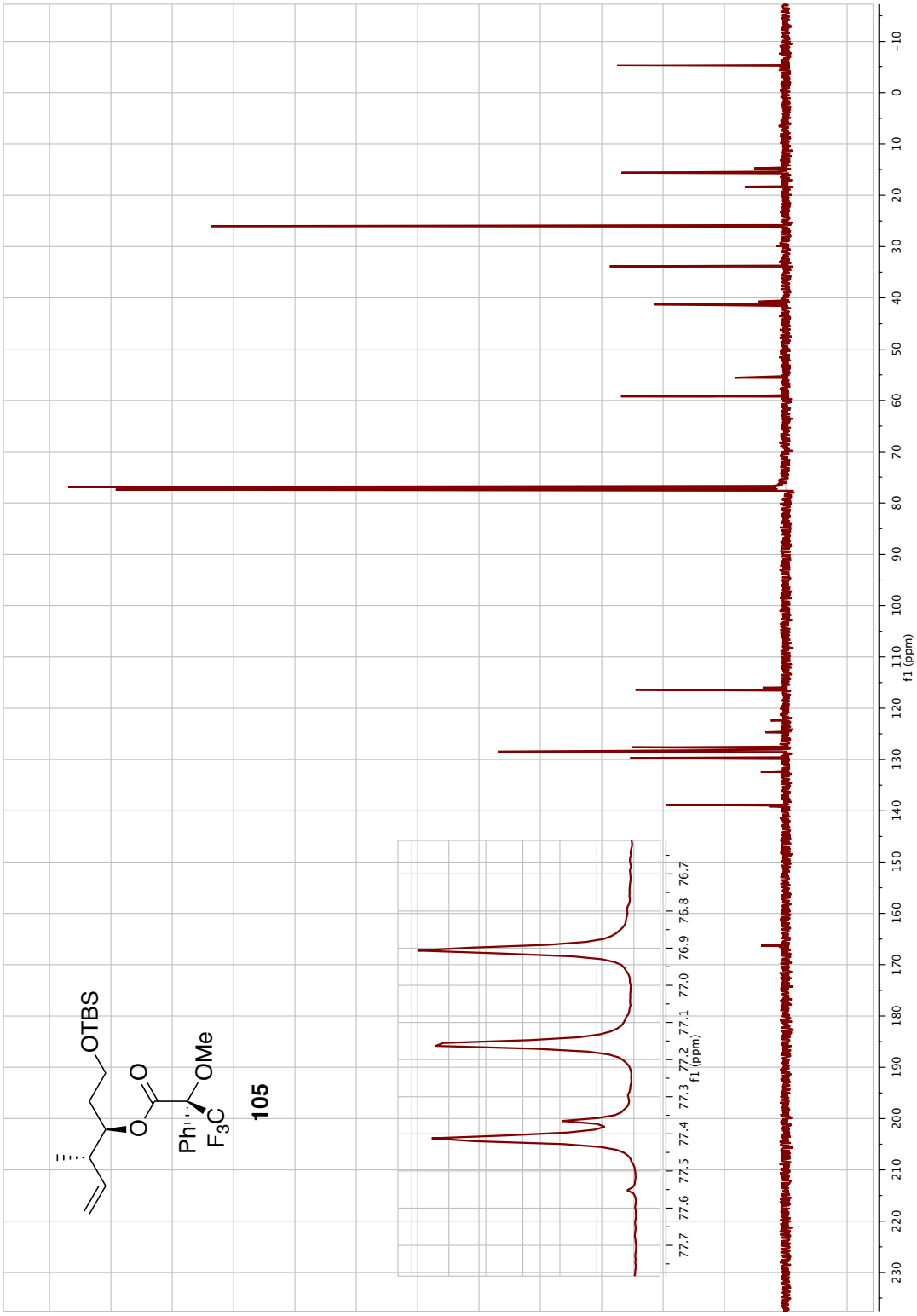

^{13}C NMR Spectrum of Compound 105

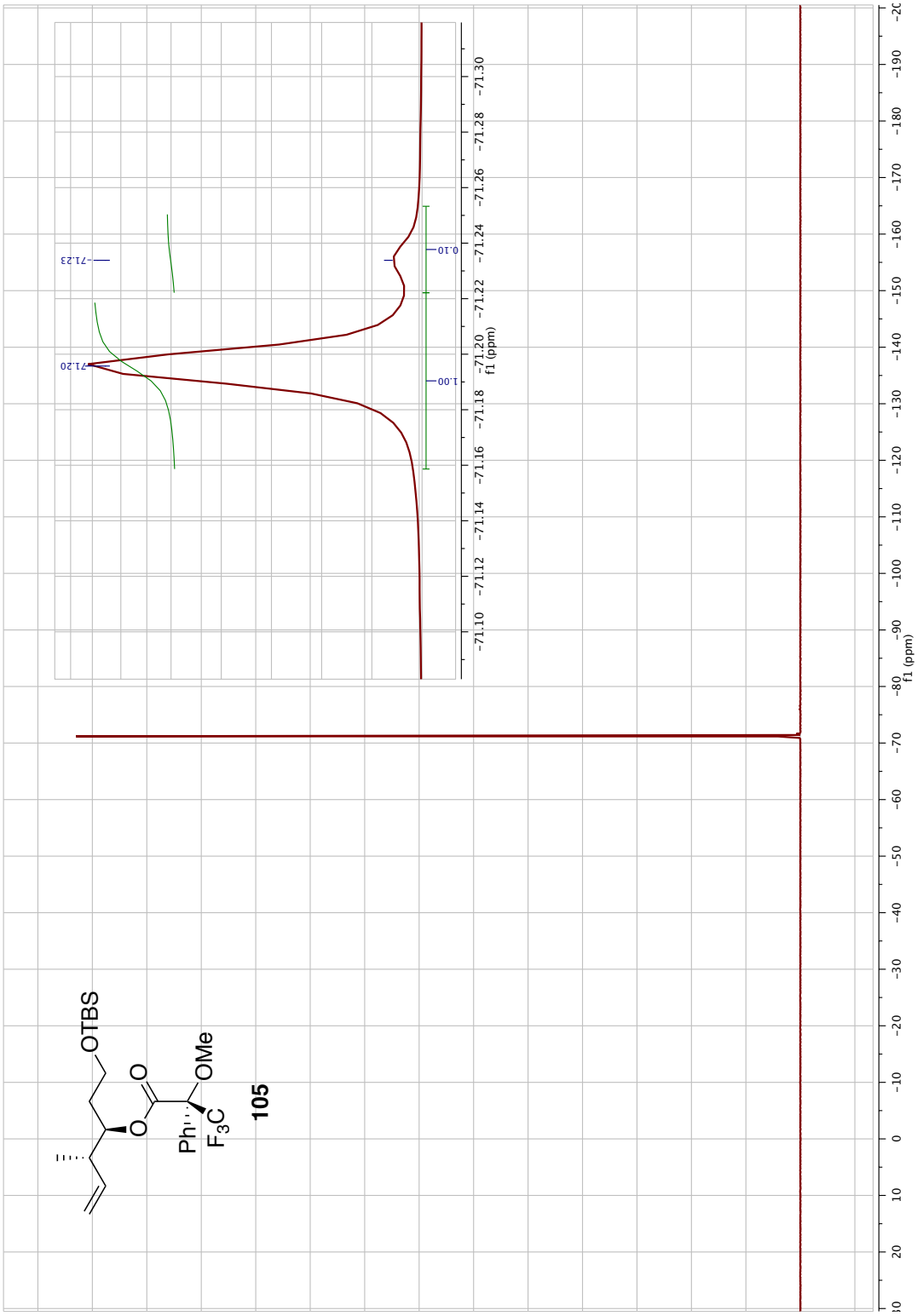

^{19}F NMR Spectrum of Compound 105

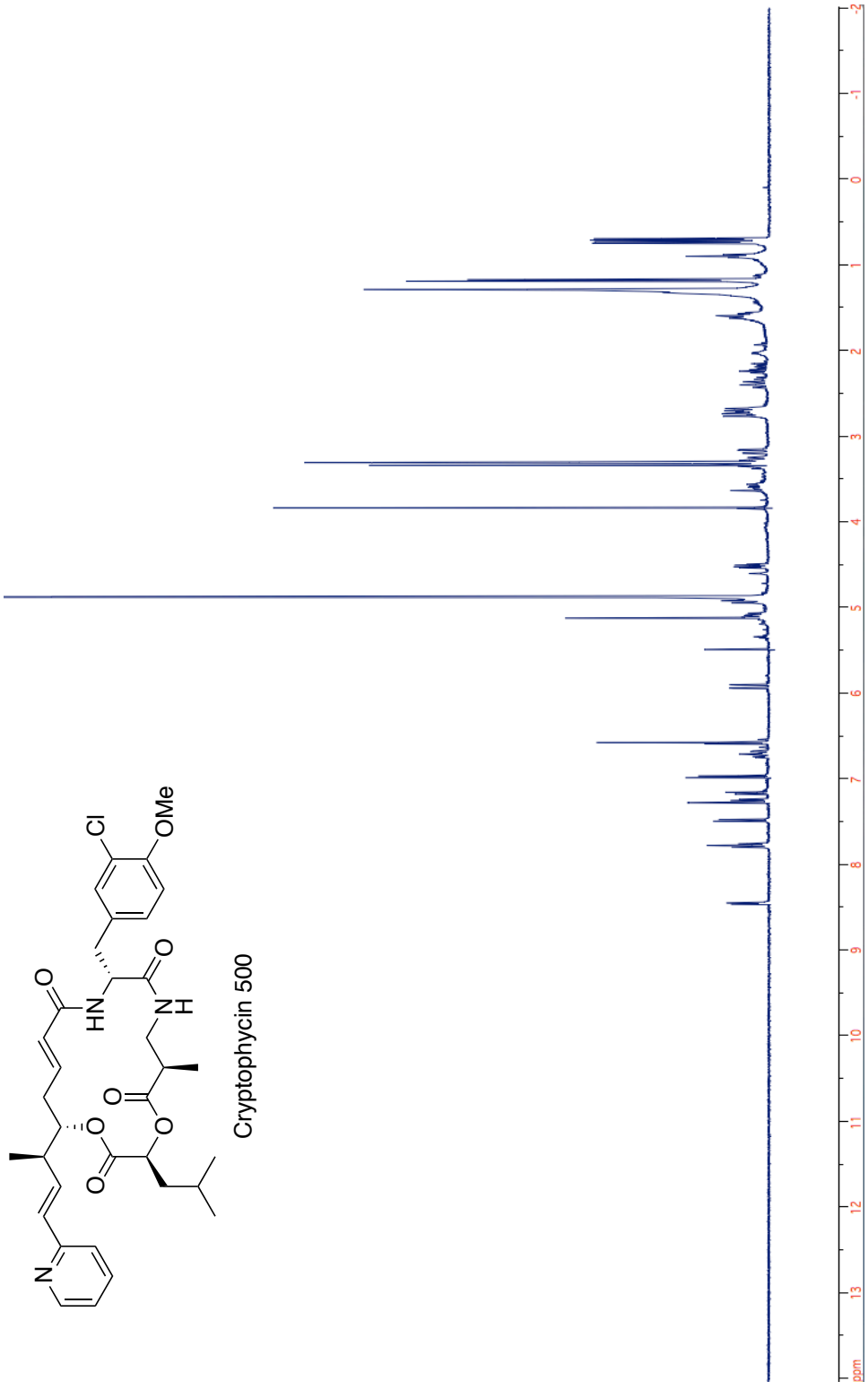

^{1}H NMR Spectrum of Cryptophycin 500

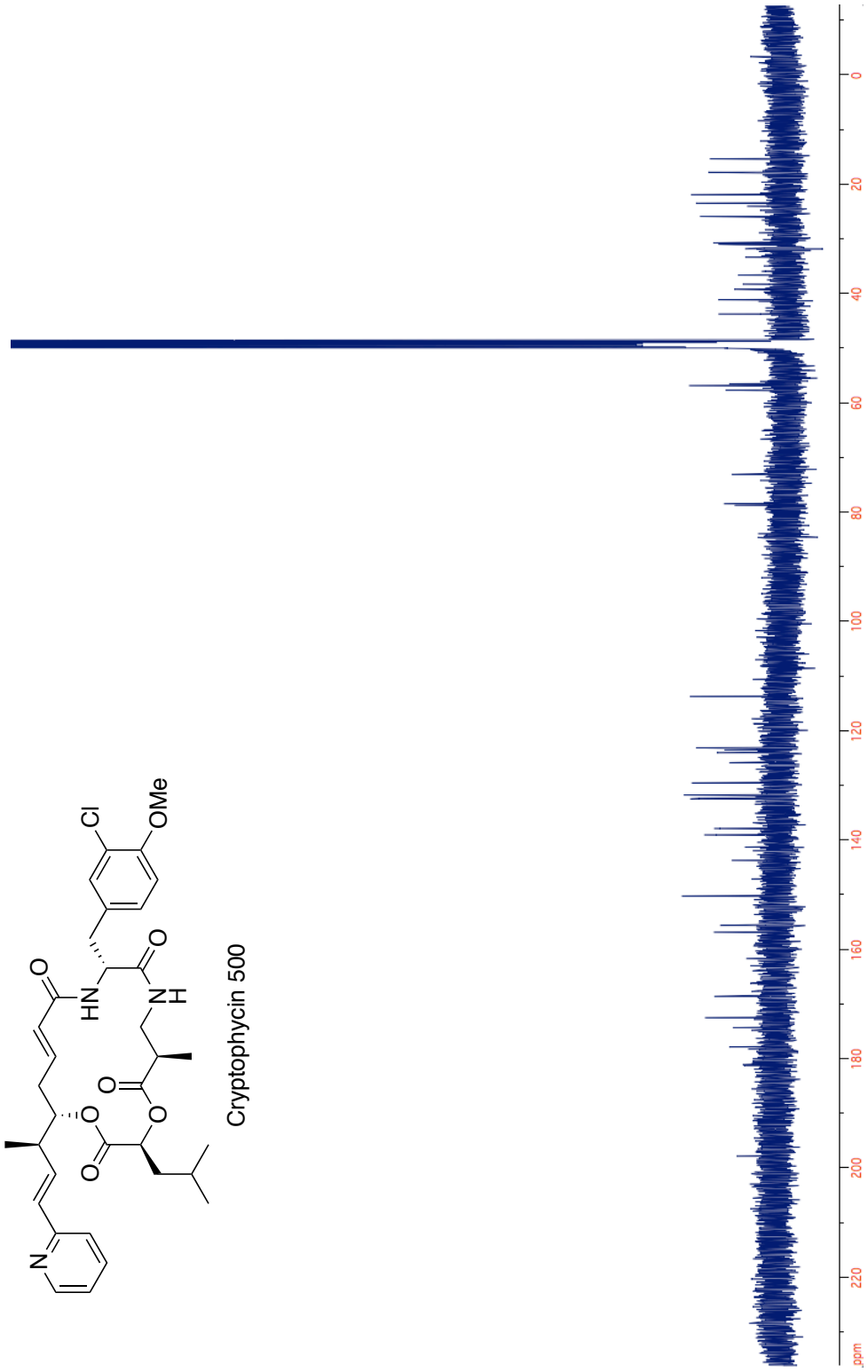

^{13}C NMR Spectrum of Cryptophycin 500